UNIVERSITE SULTAN MOULAY SLIMANE
Faculté des Sciences et Techniques
Béni-Mellal

Centre d'Études Doctorales : Sciences et Techniques
Formation Doctorale : Ressources Naturelles, Environnement et Santé (RNES)

THÈSE

Présentée par

Nourddine AJERMOUN

Pour l'obtention du grade de

DOCTEUR

Discipline: Chimie Physique

Spécialité: Electrochimie Analytique

Elaboration des électrodes à base d'argent pour la détermination des pesticides néonicotinoïdes: Applications dans l'eau et les plantes agricoles

---

Soutenue publiquement le 23/11/ 2022 devant la commission d'examen :

Pr. M. Bakasse	Faculté des Sciences, El jadida, Maroc	Présidente
Pr. M. El Mahi	Ecole Nationale Supérieure d'Arts et Métiers, Rabat, Maroc	Rapporteur
Pr. A. Loukili	Centre Régional des Métiers de L'éducation et de la Formation, Rabat-Salé-Kenitra, Maroc	Rapporteur
Pr. M. Siniti	Faculté des Sciences, El jadida, Maroc	Rapporteur
Pr. A. Farahi	Faculté Polydisciplinaire, Khouribga, Maroc	Examinateur
Pr. S. Lahrich	Faculté Polydisciplinaire, Khouribga, Maroc	Examinatrice
Pr. S. Saqrane	Faculté Polydisciplinaire, Khouribga, Maroc	Co-directrice de thèse
Pr. M. A. El Mhammedi	Faculté Polydisciplinaire, Khouribga, Maroc	Directeur de thèse

SULTAN MOULAY SLIMANE UNIVERSITY

Faculty of Sciences and Techniques

Beni-Mellal

Center for Doctoral Studies: Sciences and Techniques
Doctoral Training: Natural Resources, Environment and Health (NREH)

THESIS

Presented by

Nourddine AJERMOUN

To obtain the degree of

DOCTOR

Discipline: Physical Chemistry

Speciality: Analytical Electrochemistry

Development of silver-based electrodes for the determination of neonicotinoid pesticides: Applications in water and agricultural plants

---

Public defense on November 23, 2022:

Pr. M. Bakasse	Faculty of Sciences, El jadida, Morocco	President
Pr. M. El Mahi	National Superior School of Arts and Crafts, Rabat, Morocco	Reviewer
Pr. A. Loukili	Regional Center for Education and Training, Rabat-Sale-Kenitra, Morocco	Reviewer
Pr. M. Siniti	Faculty of Sciences, El jadida, Morocco	Reviewer
Pr. A. Farahi	Polydisciplinary Faculty, Khouribga, Morocco	Examiner
Pr. S. Lahrich	Polydisciplinary Faculty, Khouribga, Morocco	Examiner
Pr. S. Saqrane	Polydisciplinary Faculty, Khouribga, Morocco	Co-Supervisor
Pr. M. A. El Mhammedi	Polydisciplinary Faculty, Khouribga, Morocco	Supervisor

"The highest education is that which does not merely give us information but makes our life in harmony with all existence."

Rabindranath Tagore

Dedicated to my father,

grandfather

and

family

Acknowledgments

First and foremost, I would like to pay sincere gratitude to my thesis director **Pr**. **Moulay. Abderrahim El Mhammedi** for accepting me in his group, continuous support, patience, vast knowledge, immense experience and guidance during my PhD thesis. His optimism and dedication to science are impressive and I must thank him for his continuous and endless support and also for all the fruitful scientific and non-scientific discussions also, priceless lessons in science and life.

I would like to express my sincere gratitude and deepest appreciation to my co-supervisor, **Pr. Sana Saqrane**, for her valuable advice, support, discussion, patience and ideas. I appreciate all she has done for me and the gratitude to drive the research for a new aspect of biological science.

My special thanks go to **Pr. Abdelfettah Farahi**, who encouraged me to pursue new academic career in Khouribga and gives valuable advices and help in future career plans. I greatly appreciate his kindness and generosity. Also, has guided me patiently at all the times regarding experimental and theoretical aspects for the work. I would also like to thank **Pr. Sara Lahrich** for her help and guidance in the research lab, for her support and encouraging ideas.

I would also like to thank members of jury for the thesis defence professors**: Mohammed El Mahi, Abdechahid Loukili, Mostapha Siniti, Mina Bakasse, Abdelfettah Farahi and Sara Lahrich** for taking time out of their busy schedules to evaluate my research work. Their suggestions and critical opinions will help me to improve quality of this work.

My Colleagues and friends in the lab had been a great source of fun, encouragement and support during this thesis. I would like to specially thank **Asmae Hrioua, Sara Aghris, Dr. A. Loudiki, Dr. F. Laghrib** among many others. I cannot forget the interesting talks, the coffee and lunch breaks, and the parties we had.

I would like to mention the most important people in my life, my father my mother, my brothers, and sister, who have been at my support through all life's ups and downs. I would also like to thank my grandfather, and grandmother for making me the person I am today.

I would also thank all my past teachers and all the well-wishers, who have influenced my life and taught me about it.

Résumé

Les insecticides de la famille des néonicotinoïdes ont été découverts en 1980 et mis sur le marché depuis les années 1990. Depuis, leur utilisation s'est extrêmement répandue dans le monde, notamment en réponse à la résistance croissante des organismes ravageurs aux insecticides utilisés. Sous ces dénominations, on trouve les substances actives : thiaméthoxam et imidaclopride. Leur caractère systémique leur confère la possibilité d'être présent dans la totalité de la plante durant toute sa vie.

La question des impacts de thiaméthoxam et imidaclopride sur la santé s'impose au regard de la contamination généralisée de notre environnement, des plantes, eaux et de l'imprégnation de l'alimentation. La présence de ces résidus pose donc un problème de sécurité alimentaire pour les consommateurs. Bien que la réglementation impose une teneur maximale en résidus sur la base d'études toxicologiques, les consommateurs deviennent aussi plus exigeants et souhaitent, qu'ils ont à leur disposition des produits de bonne qualité.

L'évaluation du risque de contamination des organes végétaux consommés demande une bonne caractérisation des transferts de ces produits à l'intérieur de la plante. Cependant, les niveaux auxquels ces composés doivent être déterminés sont de plus en plus faibles. Il est donc devenu nécessaire de développer des méthodes analytiques capables de détecter et de quantifier ces insecticides à de faibles teneurs.

Les résidus de néonicotinoïdes sont souvent analysés par chromatographie qui nécessite des traitements préalables. En revanche, l'analyse par voie électrochimique, s'avère bien adaptée aux propriétés physico-chimiques de thiamethoxam et d'imidaclopride. Ainsi, couplée à des capteurs électrochimiques, cette méthode s'est imposée comme un outil analytique de choix pour l'analyse de résidus de néonicotinoïdes étudiés.

Ce travail de thèse avait comme objectif le développement des capteurs électrochimiques à base d'argent pour l'analyse de résidus de thiaméthoxam et d'imidaclopride. La nouvelle approche adoptée a permis de réduire considérablement la taille d'argent par des procédés variés allant de l'imprégnation par voie solide, l'électrodéposition ainsi que par voie colloïdale pour la synthèse des nanoparticules d'argent stabilisées par un gel de chitosane.

Ces capteurs ont montré une efficacité considérable pour la détection et la quantification de résidus de thiaméthoxam et d'imidaclopride dans les eaux et les aliments. Ils ont été appréciés pour l'évaluation de l'écotoxicité de ces néonicotinoïdes dans les plantes biotests respectivement ; *Zea mays* et l'haricot *Phaseolus vulgaris L.* En effet, ces capteurs ont permis la détection et par conséquent, le suivi de transfert de ces insecticides à travers les différents tissues de plantes et d'expliquer, notamment, les anomalies observées sur les coupes histologiques, la mort cellulaire et l'inhibition de la germination et de la croissance des plantes d'une manière générale.

Mots-clés : Néonicotinoïdes; thiaméthoxame; imidaclopride; écotoxicité; analyse; capteur électrochimique.

Abstract

Insecticides from the neonicotinoid family were discovered in 1980 and have been on the market since the 1990s. Since then, their use has become extremely widespread throughout the world, particularly in response to the growing resistance of pest organisms to the insecticides used. Under these names, we find the active substances: thiamethoxam and imidacloprid. Their systemic nature gives them the possibility of being present in the entire plant throughout its life. The question of the impacts of thiamethoxam and imidacloprid on health is essential given the widespread contamination of our environment, plants, water and the impregnation of food. Therefore, the presence of these residues poses a food safety problem for consumers. Although the regulations impose a maximum residue content based on toxicological studies, consumers are also becoming more demanding and wish that they have good quality products at their disposal.

Assessing the risk of contamination of plant organs consumed requires a good characterization of the transfers of these products within the plant. However, the levels at which these compounds need to be determined are getting lower. It has therefore become necessary to develop analytical methods capable of detecting and quantifying these insecticides at low levels.

Neonicotinoid residues are often analyzed by chromatography which requires prior treatment. On the other hand, electrochemical analysis proves to be well suited to the physicochemical properties of thiamethoxam and imidacloprid. Thus, coupled with electrochemical sensors, this method has established itself as an analytical tool of choice for the analysis of studied neonicotinoid residues.

This thesis work aimed to develop silver-based electrochemical sensors for the analysis of thiamethoxam and imidacloprid residues. The new approach adopted has made it possible to considerably reduce the size of silver through various processes ranging from impregnation by the solid way, to electrodeposition as well as by the colloidal way for the synthesis of silver nanoparticles stabilized by a chitosan gel.

These sensors have shown considerable efficiency for the detection and quantification of thiamethoxam and imidacloprid residues in water and food. They were appreciated for the evaluation of the ecotoxicity of these neonicotinoids in biotest plants respectively; *Zea mays* and the bean *Phaseolus vulgaris L*. Indeed, these sensors have allowed the detection and therefore the monitoring of the translocation of these insecticides through the different plant tissues and to explain, in particular, the anomalies observed in the histological sections, cell death and overall inhibition of plant germination and growth.

Keywords: Neonicotinoids; thiamethoxam; imidacloprid; ecotoxicity; analysis; electrochemical sensors.

ABBREVIATIONS

Ag/AgCl	Silver / silver chloride
Ag@GrCE	Graphite carbon modified electrodeposited silver particles electrode.
Ag-CPE	Silver imprinted graphite carbon electrode
AgNDs	Silver nanodendrites
Ag-NHS	Silver nanohemisphere
Ag-NPs	Silver nanoparticles
Ag-NW	Silver nanowires
Au	Gold electrode
B-R	Britton-Robinson buffer
CHI	Chitosan
CHI-AgNPs	Chitosan stabilised silver nanoparticles
CMEs	Chemically modified electrodes
CNT	Carbon nanotubes
CPE	Carbon paste electrode
CV	Cyclic voltammetry
DPV	Differential pulse voltammetry
ECS	Electrochemical sensors
EDX	Energy dispersive x-Ray
EPA	Environmental Protection Agency
ESA	Electroactive surface area
ET	Heterogeneous electron transfer
FFTCAV	Fast Fourier transform Coulometric Admittance Voltammetry
FT-IR	Fourier transform infrared spectroscopy
FWHM	Full Width Half Maximum
GCE	Glassy carbon electrode
GrCE	Graphite carbon electrode
Hg	Mercury electrode
HMDE	Hanging mercury drop electrode
HPLC	High performance chromatography
LC50	Lethal concentration.
LOD	Limit of detection
LOQ	Limit of quantification
MFE	Mercury film electrode

MIP	Molecularly imprinted polymer
MSE	Metallic silver electrode
MWCNT	Multiwalled carbon nanotubes
nAChRs	Nicotinic acetylcholine receptors
NEOs	Neonicotinoid
ORR	Oxygen reduction reaction
Pt:	Platinum electrode
rGO	Reduced graphene oxide
RHE	Reversible hydrogen electrode
ROS	Reactive oxygens species
RSD	Relative standard deviation
SDS	Sodium dodecyl sulphate
SEM	Scanning electron microscopy
SERS	Surface enhanced raman scattering
SWV	Square wave voltammetry
TMX	Thiamethoxam
UVA	Ultraviolet active
W-H	Williamson-Hall
XPS	X-ray Photoelectron Spectroscopy
XRD	X-Ray diffraction
β-CD	β-cyclodextrin
ΔEp	Peak-to-peak separation

LIST OF FIGURES

CHAPTER I:

CHAPTER II:

CHAPTER III:

CHAPTER IV:

CHAPTER V:

LIST OF TABLES

CHAPTER V:

CONTENTS

CHAPTER III: Impregnation of silver particles on graphite for thiamethoxam analysis

CHAPTER IV: Chitosan-stabilized silver nanoparticles for the detection of thiamethoxam in plant tissues

CHAPTER V: Phytotoxic effect of the insecticide imidacloprid in plant *of Phaseolus vulgaris L.* and its electrochemical analysis

INTRODUCTION

Pesticides, also called phytosanitary products, are chemical substances used for the growth, protection and conservation of plants. From the end of the Second World War, these products were widely used in the agricultural sector not only to increase production yields but also in order to protect plants throughout their development [1, 2]. Pesticides include insecticides, herbicides, fungicides, nematicides, plant growth regulators and others are envisioned to kill or control the growth of pests, such as insects, rodents, or certain kinds of animals that can harm crops, resulting in increased agricultural yield and quality. These compounds are commonly grouped on the basis of their pesticidal actions, or on the basis of their chemical nature or mode/period of action [3, 4]. Despite their well-known utility, particularly for agricultural output and pathogen control, pesticides are today regarded one of the most dangerous types of compounds that could cause health risks to human being and affects whole ecosystem [5, 6]. In particular, insecticides are regarded to be one of the major stressors influencing stream macro-invertebrates, as well as basic ecosystem activities [7].

Neonicotinoids are the most widely used class of insecticides globally for the management of insect pests in more than 120 countries [8]. They are used in a wide range of applications, including veterinary medicine, urban landscaping, and crop protection in various agricultural systems. They can be applied by multiple methods as foliar sprays to aboveground plants, as root drenches to the soil or as trunk injections to tree. Among these most used neonicotinoid insecticides in Morocco: thiamethoxam (TMX) and imidacloprid (IMD). These compounds are used in agriculture to control insect pests, such as *Zea mays* and bean *Phaseolus vulgaris* plants [9]. However, the relationship to food has evolved, food must be a source of good health for the body. Indeed, the food is more praised for its nutritional qualities than for its taste. In the same way, the individual is more concerned about the environment, we become sensitive to the problems of pollution, and these concerns are also found in political discourse. Thus, the consumer wonders about the TMX and IMD residues found in food and in the environment, and their impacts on human health. Indeed, the massive use of these compounds has raised concerns about their residues. These residues are potentially harmful to human health and can be found in different compartments of the environment [10, 11]. According to the Food and Agriculture Organization of the United Nations (FAO), neonicotinoids have been assessed as "*moderately hazardous to humans* [12]". Therefore, the residual persistence of TMX and IMD neonicotinoids, after any application, must be determined for the environment and public safety. In this context, and to properly assess the ecotoxicity, it appears of crucial interest to be able to detect and quantify the thiamethoxam and imidacloprid present in the environment in particular

2

water, plant, food and food industries. Therefore, eco-toxicological studies need reliable and easy-to-use analytical methods to respond to these major challenges in terms of public health. While many techniques such as chromatography or spectrometry are already available, they all require complex and expensive equipment and skilled operators [13–15]. In addition, analysis times are often extended by sample preparation phases which may include separation and purification steps. Electrochemistry then arises as an alternative of choice to offer less expensive measurement methods that combine simplicity, speed, sensitivity and specificity [16, 17].

Chemically modified graphite electrodes appear precisely as instruments capable of meeting these requirements. In general, their use is simple and they can easily be used for real-time measurements. To this end, the modification of the electrodes attracts more and more the interest of researchers for the determination of thiamethoxam and imidacloprid because of their low cost, their sensitivity and their reliability of the measurements, as well as their ease of use [18–21].

The work of the thesis is part of this logic and aims to assess, on the one hand, the toxicity of thiamethoxam and imidacloprid insecticides by studying their effects on *Zea* mays and bean *Phaseolus vulgaris* plants respectively, and to on the other hand to develop new silver-based electrochemical sensors capable of detecting thiamethoxam and imidacloprid neonicotinoids bioaccumulated in *Zea* mays and bean *Phaseolus vulgaris* plants as well as which persist in the environment, in particular in water and food. It should be noted that metallic silver has interesting catalytic properties allowing them ease of reduction and high sensitivity in terms of the reduction of thiamethoxam and imidacloprid with a relatively cheaper cost than that of other noble materials.

Thus, this present work proposes a reflection built from elements of the scientific bibliography on pesticides, and their consequences on human health: initially, we will question ourselves on the definition of thiamethoxam and imidacloprid neonicotinoids, their modes of action, and we will see that, although these products are extremely widespread in our environment, toxicity and ecotoxicity studies, supposed to guarantee the health safety of the user and the consumer by developing of new electrochemical sensors.

This thesis manuscript is structured around the following five chapters:

First, we will give an overview of the impact of neonicotinoid pesticides on the different environmental compartments. Additionally, we will attempt to illustrate human exposure to neonicotinoids throughout biomonitoring and health effects. Then the focus is on the electrochemical detection methods of neonicotinoid pesticides which are used recently as well

as the strategies used for the remediation of these chemicals into less toxic or neutral compounds.

The second chapter describes the electrocatalytic effect of silver electrode for the reduction of thiamethoxam, as well as presents a procedure for the electrochemical determination of thiamethoxam in seedlings of *Zea mays*, after its exposure in the laboratory conditions. This chapter also focuses on the evaluation of the insecticidal effect of thiamethoxam on the seedling growth and its bioaccumulation in seeds and seedlings of *Zea mays* using square wave voltammetry.

The third chapter is dedicated to the impregnation of silver particles on the carbon surface by two methods in particular the solid way and the electrodeposition. The morphology, distribution and size of the synthesized materials were characterized by X-ray diffraction (XRD) and scanning electron microscopy (SEM). In addition, the catalytic efficiency of the materials obtained for the reduction of thiamethoxam was evaluated using cyclic voltammetry (CV), square wave voltammetry (SWV), Tafel curves and by chronoamperometry.

The fourth chapter deals with the synthesis and characterization of silver nanoparticles stabilized by chitosan. The synthesized composite nanomaterials were used to facilitate and amplify the signal of graphite electrode in the detection of thiamethoxam. These sensors were used successively to evaluate the bioaccumulation of thiamethoxam in various plant in particular in extracts tissues of *Zea* mays and bean *Phaseolus vulgaris*.

The fifth chapter discusses the toxicological effect of IMD on bean plants (*Phaseolus vulgaris L*) when used at high concentrations. To this end, bean plants were exposed to increasing concentrations of IMD and subsequently the different plant tissues were subjected to various analyses. To do this, the detection of imidacloprid was carried out by square voltammetry. The effect of imidacloprid was also evaluated on germination, seedlings and photosynthetic pigments of beans.

References

[1] Chen, Y.; Yu, K.; Hassan, M.; Xu, C.; Zhang, B.; Gin, K.Y.-H. and He, Y.: Occurrence, distribution and risk assessment of pesticides in a river-reservoir system, *Ecotoxicology and Environmental Safety*, **166** (2018), pp. 320–327.

[2] Mascarelli, A.: Growing up with pesticides2013.

[3] McKnight, U.S.; Rasmussen, J.J.; Kronvang, B.; Binning, P.J. and Bjerg, P.L.: Sources, occurrence and predicted aquatic impact of legacy and contemporary pesticides in streams, *Environmental Pollution*, **200** (2015), pp. 64–76.

[4] Tiryaki, O. and Temur, C.: The fate of pesticide in the environment, J*ournal of Biological and Environmental Sciences*, **4** (2010), no. 10, pp. 29–38.

[5] Matsukawa, M.; Ito, K.; Kawakita, K. and Tanaka, T.: Current status of pesticide use among rice farmers in Cambodia, *Applied entomology and zoology*, **51** (2016), no. 4, pp. 571–579.

[6] Ge, J.; Cui, K.; Yan, H.; Li, Y.; Chai, Y.; Liu, X.; Cheng, J. and Yu, X.: Uptake and translocation of imidacloprid, thiamethoxam and difenoconazole in rice plants, *Environmental Pollution*, **226** (2017), pp. 479–485.

[7] Peters, K.; Bundschuh, M. and Schäfer, R.B.: Review on the effects of toxicants on freshwater ecosystem functions, *Environmental pollution*, **180** (2013), pp. 324–329.

[8] Jeschke, P.; Nauen, R.; Schindler, M. and Elbert, A.: Overview of the status and global strategy for neonicotinoids, *Journal of agricultural and food chemistry*, **59** (2011), no. 7, pp. 2897–2908.

[9] Schreinemachers, P. and Tipraqsa, P.: Agricultural pesticides and land use intensification in high, middle and low income countries, *Food policy*, **37** (2012), no. 6, pp. 616–626.

[10] Fang, Q.; Shi, Y.; Cao, H.; Tong, Z.; Xiao, J.; Liao, M.; Wu, X. and Hua, R.: Degradation Dynamics and Dietary Risk Assessments of Two Neonicotinoid Insecticides during Lonicera japonica Planting, Drying, and Tea Brewing Processes, *Journal of Agricultural and Food Chemistry*, **65** (2017), no. 8, pp. 1483–1488.

[11] Watanabe, E.; Miyake, S. and Yogo, Y.: Review of Enzyme-Linked Immunosorbent Assays (ELISAs) for Analyses of Neonicotinoid Insecticides in Agro-environments, *Journal of Agricultural and Food Chemistry*, **61** (2013), no. 51, pp. 12459–12472.

[12] FAO SPECIFICATIONS AND EVALUATIONS FOR … / fao-specifications-and-evaluations-for.pdf / PDF4PRO, PDF4PRO, https://pdf4pro.com/amp/view/fao-specifications-and-evaluations-for-41c4eb.html, accessed 19 February 2022.

[13] Liu, H.; Song, J.; Zhang, S.; Qu, L.; Zhao, Y.; Wu, Y. and Liu, H.: Analysis of residues of imidacloprid in tobacco by high-performance liquid chromatography with liquid–liquid partition cleanup, *Pest Management Science: formerly Pesticide Science*, **61** (2005), no. 5, pp. 511–514.

[14] Di Muccio, A.; Fidente, P.; Barbini, D.A.; Dommarco, R.; Seccia, S. and Morrica, P.: Application of solid-phase extraction and liquid chromatography-mass spectrometry to the determination of neonicotinoid pesticide residues in fruit and vegetables, *Journal of Chromatography*. A, **1108** (2006), no. 1, pp. 1–6.

[15] Fidente, P.; Seccia, S.; Vanni, F. and Morrica, P.: Analysis of nicotinoid insecticides residues in honey by solid matrix partition clean-up and liquid chromatography–electrospray mass spectrometry, *Journal of Chromatography* A, **1094** (2005), no. 1, pp. 175–178.

[16] Chorti, P.; Fischer, J.; Vyskocil, V.; Economou, A. and Barek, J.: Voltammetric Determination of Insecticide Thiamethoxam on Silver Solid Amalgam Electrode, *Electrochimica Acta*, **140** (2014), pp. 5–10.

[17] Gajdar, J.; Horakova, E.; Barek, J.; Fischer, J. and Vyskocil, V.: Recent applications of mercury electrodes for monitoring of pesticides: A critical review, *Electroanalysis*, **28** (2016), no. 11, pp. 2659–2671.

[18] Kumaravel, A. and Chandrasekaran, M.: Nanosilver/surfactant modified glassy carbon electrode for the sensing of thiamethoxam, *Sensors and Actuators B: Chemical*, **174** (2012), pp. 380–388.

[19] Norouzi, P.; Ghaheri, N.; Aghazadeh, M.; Mofidi, Z. and Larijani, B.: Sensitive Electrochemical Measurement of Thiamethoxam on Nanocomposite Coated Carbon Paste Using FFT Coulometric Admittance Voltammetry and Flow Injection Analysis, *Int. J. Electrochem. Sci*, **12** (2017), pp. 8847–8859.

[20] Urbanová, V.; Bakandritsos, A.; Jakubec, P.; Szambó, T. and Zbořil, R.: A facile graphene oxide based sensor for electrochemical detection of neonicotinoids, *Biosensors and Bioelectronics*, **89** (2017), pp. 532–537.

[21] Oliveira, A.E.F.; Bettio, G.B. and Pereira, A.C.: An Electrochemical Sensor Based on Electropolymerization of ß-Cyclodextrin and Reduced Graphene Oxide on a Glassy Carbon Electrode for Determination of Neonicotinoids, *Electroanalysis*, **30** (2018), no. 9, pp. 1918–1928.

Chapter I

Literature review

I. Introduction

Neonicotinoids represent a relatively new class of insecticides that have quickly become the most widely used class [1] in the world for a variety of urban and agricultural uses [2, 3]. Industry crop scientists consider the discovery of neonicotinoid insecticides a milestone in agrochemical research that resulted in the most rapidly-growing class of insecticides since the commercialization of pyrethroids [4]. The word neonicotinoid means "new nicotine-like insecticide" [5, 6]. Historically, neonicotinoid insecticides were viewed as ideal replacements for some insecticides (e.g., organophosphates and carbamates) due in part to both their perceived low risk to the environment and to non-target organisms. Within the agricultural sector, neonicotinoids are preferred over other insecticides for several reasons including their: (1) flexibility of application (e.g., spray, injections, or seed treatments) [7–12]; (2) broad-spectrum insect toxicity; (3) perceived low acute toxicity to non-target aquatic and terrestrial organisms [13], and (4) high potency for insects [2, 7, 12, 14–17]. The neonicotinoids have significant toxicity to insects but low toxicity to mammals, birds and other higher organisms. However, more recent in vitro, in vivo, and ecological field studies indicate that the neonicotinoid insecticides can have adverse effects on vertebrate and invertebrate species, as well as mammals [18]. The potential toxic effects of neonicotinoids include mainly reproductive toxicology, neurotoxicity, hepatotoxicity/ hepatocarcinogenicity, immunotoxicity, genetic toxicity [19]. Studies on rats and mice show also that neonicotinoid pesticides may pose potential reproductive health risks to humans, especially to children and professional populations, as well as may adversely affect the developing brain [19–21]. Emerging contaminants, including neonicotinoid insecticides, are by definition currently not included in (inter)national routine monitoring programs, thus relevant data/parameters about their fate, behavior and ecotoxicological effects are often scarce and not well understood. However, these data are necessary to undertake further legal actions to assess associated risk to protect terrestrial and aquatic ecosystems and human health. Therefore, the requirement to systematically discover the possible health effects of these compounds so as to minimize their toxicological side effects has risen sharply. Many detection methods have been engaged in order to identify even the trace amounts of these pesticides so as to govern their exposure to peoples. To make neonicotinoid insecticides in environment manageable we need to determine the associated risk to humans and ecosystems, which in turn requires to critically review the current state of the art about processes, parameters, and phenomena influencing their fate in soil-water systems in order to reveal existing knowledge gaps. The purpose of this chapter is to give an insight into the impact of neonicotinoid pesticides on the environment. Also, attempts to

illustrate human exposure to neonicotinoids throughout biomonitoring and health effects. As well as, their detection electrochemical methods which are being used recently along with the strategies that are used for remediation of these chemicals into less toxic or neutral compounds.

II. Use, efficacy and economic evaluation of neonicotinoids

Neonicotinoid insecticides are one of the most widely used groups of pesticide to control agricultural and domestic insects (e.g., plant hoppers, thrips, some micro-lepidoptera, and other coleopteran pests) [22]. They are currently registered in over 120 countries as insecticides marketed, representing 25 % of the global insecticide sales in 2014 with a global market value of $3.7 billion US dollars (USD) [1, 23]. They are employed for a variety of agricultural and non-agricultural applications such as agent for crop protection, urban landscaping and veterinary medicine [24]. Several application methods can be applied to use these chemicals including soil drench, seed treatments, foliar application by aerial or ground spray equipment, chemigation and truck injection trees [25]. They are used in commercial products ranging from trade formulation for agricultural products such as cucurbit vegetables, grapes, leafy vegetables, fruiting vegetables and nut trees to oral formulation for dog and cats [26]. Furthermore, the majority of NEOs are most commonly utilised as seed/soil treatment in agricultural system, comprising 80% of the seed treatment global market in 2008 [1]. Clothianidin or thiamethoxam coated seeds are applied to approximately 80% of corn (maize) seeds in north America, making it the largest market for seed treatment. This market is anticipated to reach $ 10 billion USD per year by 2025, with use in China growing by 14%. In the United States, the usage of treated seeds has increased threefold in the last decade, with a particularly significant increase in use from 2003 to 2011 as a pre-emptive insecticide used as a seed coating for row crops including soybeans, corn (maize), wheat, and cotton [27].

Though the use of pesticides has offered substantial economic benefits by enhancing the production and yield of food and fibbers and the prevention of vector-borne diseases. But their use has adversely affected the health of human populations and the environment.

III. Impact of neonicotinoids on soil

The widespread application of neonicotinoid insecticides led to the occurrence of its residues in soil, water, and various environmental samples (atmospheric dust, vegetable and living plants and organisms [28–30]). The long-term persistence of NEOs in both soil and water poses serious threat not only to the environment but also to human health. A number of research studies have shown that NEOs persist in soils for several years after planting treated seeds and

can accumulate in the soil after repeated applications. Only 2 to 20% of the active ingredient in NEOs applied as seed treatments or granules is absorbed by the crop [31]. Between 80 and 98% of the active component is left in the environment, and able to accumulate in soil, be lost as dust during planting, or be transferred to surface and/or groundwater (Figure 1) [32, 33]. In soil, these drugs may affect the microbial activities and have impact on microbial population [34]. Soil biological properties are involved in organic matter decomposition, nutrient cycling and pesticides degradation. Therefore, can sensitively reflect the change of the soil quality, also are crucial to ecosystem functioning. On the other hand, soil biological properties are used as indicators of its quality than physical chemical properties, as they often show a faster response to an environmental impact. In recent years, the soil microbial biomass and enzyme activities are frequently recommended for evaluating the effect of pesticides on soil environment and characterizing the change and dynamics of its quality [35].
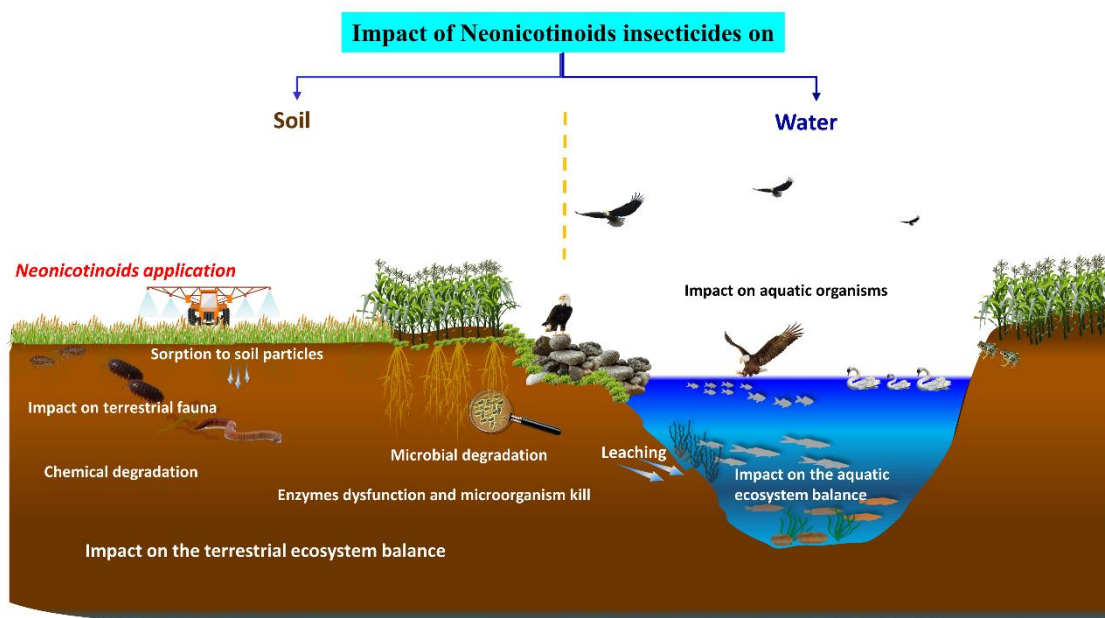
Figure 1: Fate and impacts of neonicotinoids on soil and aquatic life.

IV. Impact of neonicotinoids on water

NEOs are highly water-soluble chemicals that have been found in surface water (rivers, streams, irrigation channels and puddled water) and groundwater around the world [36, 37]. In addition, they also have long half-lives in soil and water, where they are resistant to hydrolysis at neutral or acidic pH and under anaerobic conditions; although some of them are subject to rapid photodegradation under favourable conditions. For example, imidacloprid insecticide is highly soluble in water with a solubility of up 610 mg/L and can persist in natural water for

more than one year in temperature between 18 °C and 25 °C [38, 39], potentially causing downstream effects. In fact, recent studies indicate that have negative impacts on aquatic arthropods [40].

Considering the frequency of detection of NEOs in aquatic systems, many recent findings have examined at the possible lethal and sublethal effects of NEOs on aquatic species [12, 41] (Figure 1). Aquatic insects are typically more responsive on NEOs than other aquatic species such as fish, crustaceans, molluscs etc., which is reasonable considering their mode of action [12]. NEOs have also been demonstrated to decrease feeding rates, mobility, fecundity, developmental rates, and growth in aquatic insects, in addition to their effects on mortality [42–44].

The most frequently assessed toxicity endpoint for NEOs was mortality, being reported in roughly 70% of studies, generally as mean lethal concentration (LC50). Imidacloprid formulation (Admire®) had 48-h LC50 values between 103 and 45 μg/L in Mosquito species *Aedes aegypti* and *Aedes taeniorhynchus* [45]. Same Mayfly (*Epeorus longimanus*) larvae were acutely sensitive to Admire® as well. The reported 24-h LC50s were 2.1μg/L for both early instar and late instar larvae [46, 47]. Similarly, mayfly, *Cloeon dipterum* and *Caenis horaria* were susceptible to long exposure of imidacloprid insecticide, with reported 28-d LC50s of 0.2 and 0.3μg/L, respectively [48]. In other hand, sublethal indicators are considered to be more sensitive endpoints for low toxicant concentrations, as expected in field conditions. Exposure to sublethal NEOs concentrations triggers a stress response in susceptible organisms, resulting in sublethal effects including immobilization, altered brain function and behavior in aquatic insects. Another important finding was that immobilization of *Cloeon. dipterum* and *Caenis. horaria* occurred at a concentration of 0.1g/L in both species during the course of a 28-day experiment [48], demonstrating a very high sensitivity to chronic exposure to imidacloprid. Other sublethal effects observed in chironomids such as immobilization, change in burrowing behavior and growth inhibition under imidacloprid application at concentration between 0.3 and 12.9 μg/L [49], indicating that chironomids are susceptible to imidacloprid insecticide. Following exposure to 4 μg/L of technical imidacloprid for 48-h, Overmayer et *al.* reported significant changes in behavior and muscle control of blackfly larvae *simulum vittatum* [50]. In addition to aquatic insect, NEOs insecticides affect negatively crustaceans and molluscs. Acute toxicity of NEOs to the most sensitive crustaceans is typically in low μg/L range.

In aquatic ecosystem, fish are generally less sensitive to NEOs insecticides than others aquatic species such as insects or crustaceans, as indicated by the geomean LC50 value of 60 μg/L published by sanchez-Bayo and goka [51, 52]. Recently, Vignet, C. et *al.* investigated and

compared the effects of imidacloprid on development and behavior of two fish model species: Zebrafish (*danio rerio)* and Japanese medaka (*Oryzias latipes*) [53]. In both species, imidacloprid showed sublethal effects, but the effects were much stronger in medaka with deformities and lesions. For example, in flounder (*Paralichthys olivaceus*) gill cells, the most sensitive effects endpoints were found, with cytotoxicity IC50s (median inhibitory doses) ranging from 38.5 to 41.9g/L of technical imidacloprid [54]. Not only mentioned aquatic species but also other organisms such as algae/macrophytes and amphibians have been evaluated for sensitivity towards NEOs. For instance, Amphibian had an estimated LC50 for NEOs of 162.8 µg/L [52]. For algae, the species *Desmodesmus subspicatus* was the most often studied. For macrophyte species, *Lemna gibba* and *Selenastrum carpricornutum* exhibited high levels of tolerance clothianidin at concentration around 100 µg/L [55]. Based on the available data, it is difficult to make a complete assessment of the risk posed by NEOs to aquatic organisms. for example, the half-life of NEOs is generally in the range of hours to days, so exposure would be acute rather than chronic.

V. Impact of neonicotinoids on plants.

The NEOs insecticides are commonly used in seed treatment (such as seed dressing or film coating) and soil treatment (via broadcast application, mechanical integration, soil drench, or soil injection) and are also directly applied to plant foliage for crop protection. Therefore, can lead to demolition of micro-fauna and flora of soil and water [56, 57]. These insecticides influence or kill plants in variety of mechanism, such as the inhibition of biological processes (photosynthesis, mitosis, cell division, enzyme function, root growth, or leaf formation); interfering with the production of pigments, proteins or DNA; destroying cell membranes or promoting uncontrolled growth (Figure 2) [58]. The abiotic stress was studied trough physiological effect of thiamethoxam on *zea mays* and found that *Zea mays* was sensitive to this insecticide and that germination and growth inhibition were dose dependent [59]. Also, it was found that different classes of insecticide (including thiamethoxam, lambda-cyhalothrin cum thiamethoxam, fenitrothion and etofenprox) influence on soybean physiologic and metabolic actions such as germination, early growth, and antioxidant activities, implying that yield and nutrient content also may be altered [60].
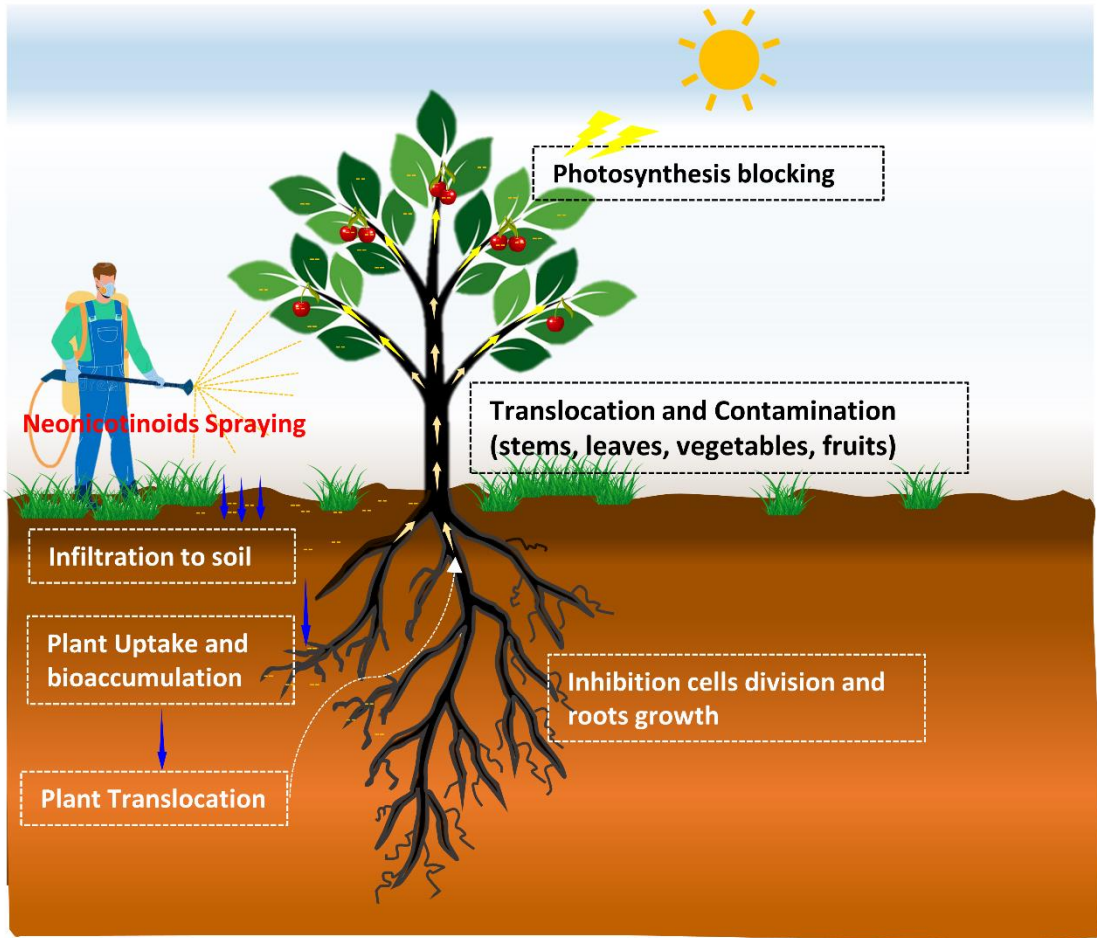
Figure 2: Plants responses to neonicotinoids impacts.

Plant root exudates consist of low molecular weight organic metabolites (i. e. organic acids, sugars, amino acids, lipids, nucleotides and secondary metabolites) and high molecular weight substances especially mucilages and proteins. The chemical components in root exudates, as well as their abundances, vary depending on plant species, growth phases, and cultivation conditions [61]. Plants could regulate the composition of root exudates in exposure to different biotic and abiotic stressors in order to mitigate the detrimental impacts of severe environmental conditions [62]. Li, X. et *al.* studied the effect of dinotefuran insecticide on root exudates of *Brassica rapa var. chinensis* by analysis of the metabolic profiling of plant root exudates, physiological activities of plant tissues and uptake behaviours of dinotefuran in plants [63]. The results show that dinotefuran is readily absorbed by plant roots and then accumulates in vegetable shoots, inducing oxidative stress in plant tissues even at low doses. Recently, insecticide-induced oxidative stress has attracted the attention of researchers. Reactive oxygen species (ROS) were produced during the metabolism of insecticides such as malathion and

13

imidacloprid, causing oxidative damage [64]. Furthermore, ROS are very susceptible molecules that alter protein, lipid, and nucleic acid degradation [65]. In recent time, Shahid, M. et *al.* evaluated the toxicological potential of imidacloprid and thiamethoxam on chickpea as test crop [66]. The results indicate that the tested insecticides retard the biological, physiological and enzymatic activities and induced the cellular death by oxidative stress in chickpea. Another important finding, used RNA-Seq to explore how these two neonicotinoids (imidacloprid and thiamethoxam) modify gene expression in soybean thereby lowering plant resistance [67]. As a result, the both insecticides treatment downregulated genes involved in plant-pathogen interaction, phytohormone pathways, phenylpropanoid pathway, and cell wall biosynthesis. The imidacloprid effects on the anabolism and release of C6-green leaf volatiles (GLV) in tea plants were investigated [68]. It's can reduce GLV emission by repressing a crucial GLVs synthesis-related gene, influencing plant indirect defence.

Given their systemic and persistence properties, NEOs insecticides can be taken up by roots and then translocated to almost every tissue of the plants, and thus, could not be removed from fruits or vegetables by peeling or washing.

VI. Human exposure levels and health effects of neonicotinoids

1) Human exposure

Despite widespread use of NEOs, there have been relatively few published studies addressing the risks of human exposure. Diet or consumption of contaminated agricultural products is believed to be a potential source of human exposure to NEOs. Since NEOs absorbed by plant, they are difficult to remove from food, and have been determined in honey, fruits, vegetables, cereals, grape berries, and tea leaves [69–73].

In China, a total of 528 composite dietary samples were analysed to study the dietary exposure of the Chinese adult populations to ten NEOs [74]. Imidacloprid and acetamiprid were the most frequently detected NEOs in the majority of the analysed samples (70%). As well as, vegetables were the primary contributor of dietary exposure, although exposure via cereals, beverages and water must be addressed [74]. NEOs residues were found in foods that are commonly consumed in cafeterias in the United States (USCC) and by group of Chinese elementary school children living in Hangzhou, China (HZC) [72]. The data indicate that NEOs are ubiquitous in the food samples tested for the USCC and HZC experiments. About 79 and 65 % of fruits and vegetables, respectively, contained more than one neonicotinoid, while approximately 62 and 38 % of fruits and vegetables, respectively, contained more than three NEOs. Thiamethoxam was the most commonly identified NEO in fruits and vegetables taken from these two congressional

cafeterias, with 53% detection, followed by imidacloprid with 52% detection [72]. In the same way, at least one NEO was detected in every fruit and vegetable samples (excluding nectarines and tomatoes) and 90% of honey samples, according to Chen et *al.* [75]. More than one NEO was determined in 72 % of fruits, 45% of vegetables and 50% of honey samples, with individual NEO concentration ranging from 0.1 to 100 ng/g. Recently in China, a total of 693 honey samples from both *Apis melifera* and *Apis cerana*, were analysed for five NEOs, including Thiamethoxam imidacloprid, acetamiprid, clothianidin and thiacloprid [76]. The 40.8% of the samples contained at least one of the five NEOs tested, and the average neonicotinoid concentrations detected in all contaminated samples were between 5.42 and 23.9 µg/kg. Also, acetamiprid and imidacloprid were the most frequently detected NEO, and based on the ranking of residual risk, presented a medium risk for consumers.

The hydrophilic nature of NEOs, unlike other insecticides, could result in significant exposure through ingestion of contaminated drinking water. This is especially common if the water sources are near farmlands where NEOs are often used through direct spraying, sowing neonicotinoid-treated seeds, or irrigation. Wan et *al*. determined NEOs residues including (acetamiprid, imidacloprid, thiamethoxam, dinotefuran, clothianidin, nitenpyram, thiacloprid, flonicamid, imidaclothiz, sulfoxaflor) in 20 raw water samples, 20 finished water samples and 165 tap water samples which collected during 2018 [77]. They reported that NEOs were found in all raw water samples with a median sum concentration of 27.7 ng/L. Moreover, in all tap water samples, at least three NEOs were detected with the highest sum concentration of 96.2 ng/L [77]. Also, it is interesting to note that in all tested group, infant could be the most sensitive to NEOs exposure via water ingestion compared to other age groups. These results are on accord with an Australia study indicating that 93% of water samples collected from rivers contained at least two NEOs with levels about 0.06 – 4.5µg/L [78].

2) Risk evaluation

In recent time, in order to evaluate the human exposure to NEOs, several scientists have started to investigate methods to identify the concentrations of these chemicals and their metabolites in biological samples such as human urine, serum and human hair. In the United States, a representative sample of general population 3 year of age and older from 2015-2016, National Health and Nutrition Examination Survey (NHANES) was investigated to quantify the urinary concentration of NEOs and two metabolites [79]. Suggesting that metabolites are better biomarkers of background exposure than the parent compounds with rate detection were 35% (N-desmethyl-acetamiprid), 20% (5-hydroxy imidacloprid), 8% (clothianidin), 4%

(imidacloprid) and < 0.5% (acetamiprid, thiacloprid). Moreover, compared to other age group and ethnic group, young children (3-5 years old) and Asians may experience higher exposure to NEOs. The reason for mentioned differences between age and ethnic groups remain unknown [79]. More recently, a Chinese study found that NEOs and metabolites were frequently detected in paired urine samples (81%-98%) and indoor dust samples (75%- 95%). The most abundant chemical detected in urine was 5-Hydroxy-imidacloprid, while N-desmethyl acetamiprid was predominant in indoor dust samples, accounting for 56% and 37 % respectively [80]. Additionally, evidence that proximity to farms increases exposure to NEOs has also highlighted by studies that investigate or compared human living around sprayed area and humans living in urban versus rural landscapes. In Japan, urine specimens of 46 children (23 males and 23 females) were collected before, during and after insecticide spraying events. seven NEOs were determined in urine samples. In Greece, a study of imidacloprid exposure in urine and hair compared concentrations between urban (n = 26) and rural (n =32) populations. As results, rural peoples engaged in agriculture were more likely to have a positive detection of target chemical in their hair than urban residents [81]. Moreover, the serum can be exploited as a matrix to assess human exposure to NEOs and their metabolites, but studies on serum concentration of these chemicals are still limited.

Ingestion (e.g., water, food), inhalation (e.g., dust), and cutaneous exposure, as well as occupational and residential use, have all been linked to human exposure to NEOs. However, methods for determining damage and evaluating risk from NEOs in environmental and human biological samples are remaining in the research stage and also deserve further investigation.

3) Health effects

Recent epidemiological evidence revealed increasing amounts of NEOs detected in human samples, and highlighted human health concerns. The majority of this evidence is limited to case reports, which cover a range of observed human health effects from neurological to hematological and cardiovascular effects after acute, high-exposure scenarios (Figure 3). Human population studies have reported that environmental exposure to NEOs is associated with adverse cardiovascular, respiratory and neurological endpoints such as memory loss and finger tremor [82–94]. Following acute exposure to NEOs, a study revealed two fatalities and eight patients with major effects (severe symptoms that necessitated intubation and critical care) as result of imidacloprid exposure [84]. This finding was based on examination of 70 poisoning cases reported to the Taiwan National Poison Centre, 46 of which were cases of NEOs ingestion alone. The other cases were exposed to various class of pesticide and/or ethanol. Two of the

critically ill individuals died of respiratory failure [84]. Also, due to limited number of severe/fatal poisoning, no significant association between severity and volume of ingestion, route of exposure and intent of exposure was indicated. Consistent with the report case from Sri-Lanka [85], the majority of patient with inhalation and dermal poisoning had only mild symptoms such as headache, nausea, vomiting, abdominal pain, and diarrhoea. Similarly, Forrester reported a serious outcome rate of 2.9%, suggesting NEOs might differ in their levels of toxicity to humans. Ocular, dermal, gastrointestinal and neurological were the most commonly effects observed [95]. Moreover, a number of case reports have revealed different poisoning effects including shortness of breath, coma, low blood pressure and dilated pupils, as a result of acute exposure and are presented in table 1.
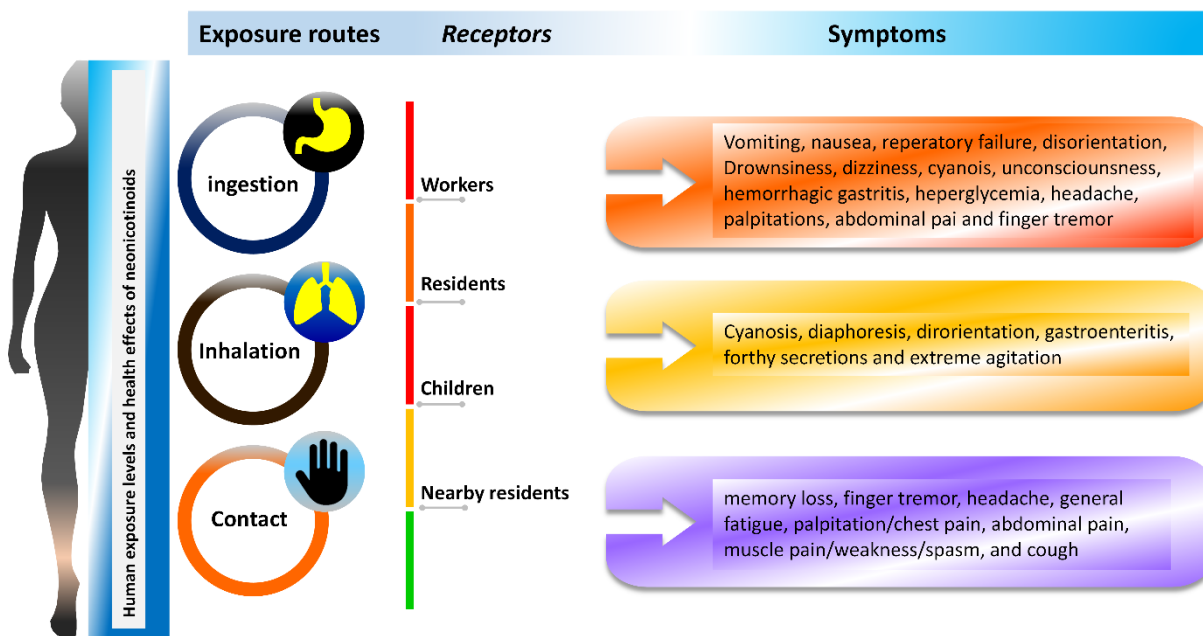
Figure 3: Impacts of neonicotinoids on human health.

In Japan, subacute intoxication has been documented as a result of eating certain fruits, vegetables, and tea [96]. As well as, finger tremor, fever, decreased short-term memory, general weariness, headache, palpitation/chest pain, abdominal pain, muscle soreness/muscle weakness/muscle spasm, and cough were among the symptoms described by six patients who ingested more than 500g/day of domestic fruits/vegetables and/or tea [96, 97]. Furthermore, some researchers focused on pesticide sprayers. Kourea et *al*. found that the frequency of NEOs application was related to the induction of oxidative damage to DNA in the entire blood of 80 pesticide sprayers [98].

Table 1: *Summary of research on neonicotinoids exposure and adverse human health effects.*

Type of Toxicity	Type of Neonicotinoid	Exposure Route	Symptoms /Presentation	Ref
Acute toxicity	Imidacloprid	Ingestion	Drowsiness, disorientation, dizziness, oral and gastroesophageal erosions, hemorrhagic gastritis, productive cough, fever, leukocytosis, and hyperglycemia.	[83]
			Mild-to-moderate severity, respiratory failure or coma and death.	[84]
			Cyanosis, apnea, and unconsciousness	[86]
			Disorientation, drowsiness, dizziness, and palpitations, respiratory effort was poor.	[87]
			Poor respiratory efforts	[89]
			Abdominal discomfort, vomiting	[99]
			Gastrointestinal symptoms, no corrosive injuries and neurological effects and symptoms mimicking cholinergic syndrome. Liver injury, moderate initial severity and death	[100]
			Disorientation, drowsiness, and increased salivation	[90]
			Diaphoretic and cyanosed, deterioration of renal function with progressive oligoanuria	[92]
			Drowsiness	[101]
			Severe nausea, vomiting, and altered level of consciousness	[102]
	Acetamiprid		Consciousness disturbance (GCS-8), hypotension, nausea, vomiting and hyperglycemia	[88]

			Nausea and muscle weakness, a single self-limiting seizure, tachycardia, hypotension, dyspnea, and thirst	[91]
			Nausea, vomiting, developed multiple episodes of generalized toniclonic seizures and unconscious with poor respiratory efforts	[103]
	Thiamethoxam		Nausea, vomiting, and abdominal pai	[104]
	Imidacloprid + alcohol		Mild disorientation, bradycardia, ventricular arrhythmia, and cardiopulmonary arrest	[93]
	Imidacloprid	Ingestion dermal	Nausea, vomiting, headache and diarrhoea, respiratory failure	[85]
	Imidacloprid	Inhalation	Symptoms of gastroenteritis	[94]
			Extreme agitation, frothy secretions, cyanosis, diaphoresis, and disorientation	[105]
Subacute toxicity	Imidacloprid, Nitenpyram, Acetamiprid, Thiacloprid	ingestion	Headache, general fatigue, finger tremor, and short time memory disturbance	[96]
Chronic toxicity	Acetamiprid, *N*-desmethyl-acetamiprid	-	Memory loss, finger tremor, headache, general fatigue, palpitation/chest pain, abdominal pain, muscle pain/weakness/spasm, and cough	[106]

19

	Imidacloprid, Desmethyl-acetamiprid	-	Farmers (both with and without chronic kidney disease with unknown etiology (CKDu)) living in CKDu-endemic areas in the NCR of Sri Lanka are exposed to lower neonicotinoid concentrations	[107]
	Imidacloprid	-	Weak positive association between autism spectrum disorders and prenatal imidacloprid exposure	[108]
			Significant link between residential proximity to agricultural use of Imidacloprid and tetralogy of fallot	[109]
		Ingestion	Significant association between residential proximity to agricultural use of imidacloprid and anencephaly	[110]

In Spain, the respiratory functions of 89 pesticide sprayers and 25 non-spraying control farmers were assessed and compared by Hernandez et *al.* [111]. The findings revealed a correlation between the use of NEOs and lung dysfunction (lower total lung capacity, residual volume and functional residual capacity). In addition, Marfo et *al.* reported an association between N-desmethyl-acetamiprid urinary concentration and increased prevalence of neurologic symptoms among symptomatic patients compared to 50 non-symptomatic volunteers [106].

Indeed, the limited research that has been conducted appears to indicate long-term potential for genotoxicity, cytotoxicity, impaired immune function, reproduction, and birth defects; as well as, acute health effects ranging from respiratory, cardiovascular and neurological symptoms.

VII. Remediation

Increased usage of pesticides, which have become an integral aspect of contemporary agriculture, has enabled greatly increased agricultural production. Their continued and excessive usage harms farms, creates significant soil pollution, and damages soil quality and the environment. NEOs pesticides easily find their way into the soil, water, and will therefore soon enter the bodies of plants and animals, and detected in food for human consumption. The ubiquitous NEOs are considered one of the most serious environmental pollutants. Their toxicity is well documented for its impairment of plant growth and human health. Hence, credible and efficient techniques used to remove these substances in soil and water are urgently needed to avoid unwanted outcomes. Adsorption, photocatalysis, reduction, and chemical oxidation are the most common techniques for remediating contaminated soils and water.

1) In soil

The effects and fate of pesticides residues in the soil are influence by farming practices, application of fertilizer, the soil type, surface and its pH value [112, 113]. Under environmental conditions, imidacloprid in soil can be degraded by microorganisms or through photolysis sunlight. Mahaparta et *al.* reported a non-significant dissipation of imidacloprid between sterile and non-sterile soils and its degradation will be faster under sunlight and at higher soil moisture [114]. The reduction of pesticide contaminants depends on the role of bacteria/fungi. Erguven et *al.* investigated the bioremediation performance of *Methylobacterium radiotolerans* and *Microbacterium arthrosphaerae* bacteria and their consortia to eliminate imidacloprid. In soil test units after 18 days, they found that the bacterial consortium is effective for the bioremediation of this insecticide at two volumes of 40 and 80 ml of the consortia [115]. Similarly, *Ochrobactrum thiophenivorans* and *Sphingomonas melonis* bacteria and consortia

21

were used by Erguven et *al.* to evaluate the bioremediation of imidacloprid. It was observed that each bacterium and their mixes had complete reduction rate for imidacloprid active ingredient after 14 days [116]. Recently, Wu et *al.* reported that *Rhodopseudomonas capsulata* (R. *capsulata*) remediate imidacloprid residue, improve soil fertility and improved the microbial community structure [117].

Many physicochemical methods have been applied to degrade acetamiprid neonicotinoids, including chemical decomposition, high-temperature incineration and landfilling. Under low nutrient stimuli, *ensifer adhaerens* CGMCC 6315 could degrade acetamiprid efficiently. This degradation was via nitrile hydratase pathway [118].

In recent years, the application of the photodegradation process to contaminants in the environment has attracted a lot of interest. It has several benefits, including high degradation efficiency, quick degradation, and used at large concentrations [119]. Li, Y et *al.* reported that ultraviolet B (UVB) played a crucial role in the photodegradation of clothianidin and thiamethoxam in soil, while visible and ultraviolet A (UVA) light had insignificant influence [120]. In addition, four possible photodegradation products of clothianidin and three of thiamethoxan were identified. Similarly, photodegradation phenomenon for clothianidin and acetamiprid was reported by Guptaa et *al.* [121]. For imidacloprid, ultraviolet active (UVA) light provides more efficient photodegradation than visible irradiation [122]. Indeed, the photodegradation rate of NEOs by monocromatic ultraviolet (UV) light (254 nm) is constant depending on the pH value, the properties of the specific compounds, and the presence or absence of free radical scavenging agent [123].

Phytoremediation utilizes plants to purify or improve polluted soil and water and to mineralize compounds into non-toxic end products through biochemical processes initiated by plants [124]. Differences in phytoremediation potential among plants are due to the complexity of plant physiology and biochemistry, and hence phytoremediation performance is primarily dependent on the proper selection of plant species [125].

2) In water

In general, NEOs are less persistent in water than in soil, but imidacloprid, clothianidin and thiamethoxam are still able to contaminate both surface and ground water, and accumulate in the food chain. Thus, remediation of NEOs pollution in water bodies is of crucial importance. Significant efforts have been focused on the development of methods for treating these substances, including conventional physical techniques (adsorption and filtration with developed membrane materials and adsorbent), and physico-chemical strategies like

electrocatalytic degradation [126] and photocatalytic degradation [127, 128]. Furthermore, chemical selective oxidation methods investigated using powerful oxidant for in situ environmental remediation and for water /wastewater treatment [129, 130]. Recently, a chemical remediation of imidacloprid whit permanganate was investigated in aqueous solution [131].

Due to its cost-effective, environmentally sustainable, and promising bioremediation potential, constructed wetlands are one of the most often employed mitigation strategies to reduce pesticide input into water bodies [132, 133]. Wetland plants have a high development rate and a large root system, making them essential components of constructed wetlands [134]. According to Main et *al.,* in prairie wetlands, plant communities appear to be significant drivers of NEOs abundance and concentration [135]. Additionally, in planted wetland systems, imidacloprid, thiamethoxam and acetamiprid were more readily removed, while *C. alternifolius* and *C. papyrus* were the most effective species in removing NEOs. These findings seem to be consistent with other research which detected and quantified the residues of NEOs in different wetland plants species.

The microbial biodegradation of NEOs is considered to be the most effective and ecologically friendly in situ repair pathway [136]. Numerous microbes that degrade NEOs have been isolated and identified. Bacillus, Mycobacterium, *Pseudoxanthomonas*, *Rhodococcus*, *Actinomycetes*, and *Stenotrophomonas* are among the bacteria that have been discovered [136, 137]. Guo et *al*. isolated an oligotrophic bacterium (*Hymenobacter latericoloratus* CGMCC 16346) from a water environment, this bacterium can survive in apotrophic surface water for a long period on a 1/10,000 diluted nutrient medium and degrade imidacloprid [138]. The isolation or development of certain bacteria is important for the sustainability of biologically mediated environmental degradation of NEOs. However, none of the single bacterial isolates appeared able to completely mineralize NEOs insecticides including imidacloprid, thiamethoxam, thiacloprid, and clothianidin.

Despite their effective performance to degrade or eliminate the NEOs in soil and surface /groundwater, the remediation strategies of NEOs can lead to toxic degraded-intermediates, which more toxic than their parent compounds. However, it is then necessary to develop alternatives to NEOs that satisfy certain criteria.

VIII. Electroanalysis of NOEs insecticides

For the detection of traces residues of NOEs insecticides throughout the year, an appropriate methodology and sampling regime is required. Numerous methods have been introduced for

this purpose, which can be categorized as chromatographic method, spectroscopic method and electrochemical methods. In this chapter, we focus just on recent progress in electrochemical sensors and biosensors for NOEs determination in different matrices.

1) Electrochemical sensors for NOEs determination

Widely developed electrochemical sensors (ECS) are considered as alternative to traditional methods for detecting organic, inorganic and biological analytes, due to their fast response time, simplicity and low cost. An electrochemical sensor is composed of two principal constituents as shown in figure 4; the first one corresponds to the sensing surface that reacts with the desired analyte. The second constituent is the transducer which transforms this reaction into a readable electronic signal. The development of ECS would be very promising and beneficial. For instance, neonicotinoid Insecticide TMX is an electrochemically active molecule due to its nitro-group reduction. Various models of electrochemical sensors have been developed to improve the sensor performance to enhance electrochemical reduction signal. Also, several techniques as voltammetry, amperometry and were used for TMX detection (Figure 5). A wide range of materials (metals, metal oxides, alloys, amalgams and their composites) have been used to detect NOEs residues in various matrices, due to their good conductivity, large surface area and high catalytic properties.

i) Metal and amalgams metal

The first metal electrode investigated for detect of NOEs is mercury electrode using direct current and differential pulse polarography, based on the reduction behaviour of target molecule. A pH >5, the differential pulse polarography (DPP) method offers the sensitive trace level determination of NOEs providing an adequate recovery and reproducibility [139]. The bismuth film modified glassy carbon electrode was employed for the rapid and simple voltammetric detection of NOEs. Moreover, the reduction mechanism of this film electrode and that of mercury film electrode (MFE) are compared, and the results show that the electrochemical reaction is the same at both electrodes [140]. Also, the potato and maize samples were used to investigate the analytical applicability of film modified glassy carbon substrate. Before each measurement, potato and maize samples were treated due of the matrix complexity [140]. The results proved that the bismuth film electrode is potentially interesting, useful and inexpensive tool for the determination of NOE, showing a comparable analytical applicability to that of MFE. Furthermore, considering its nontoxic metal character, it could be applied as a convenient environmentally friendly method [140].
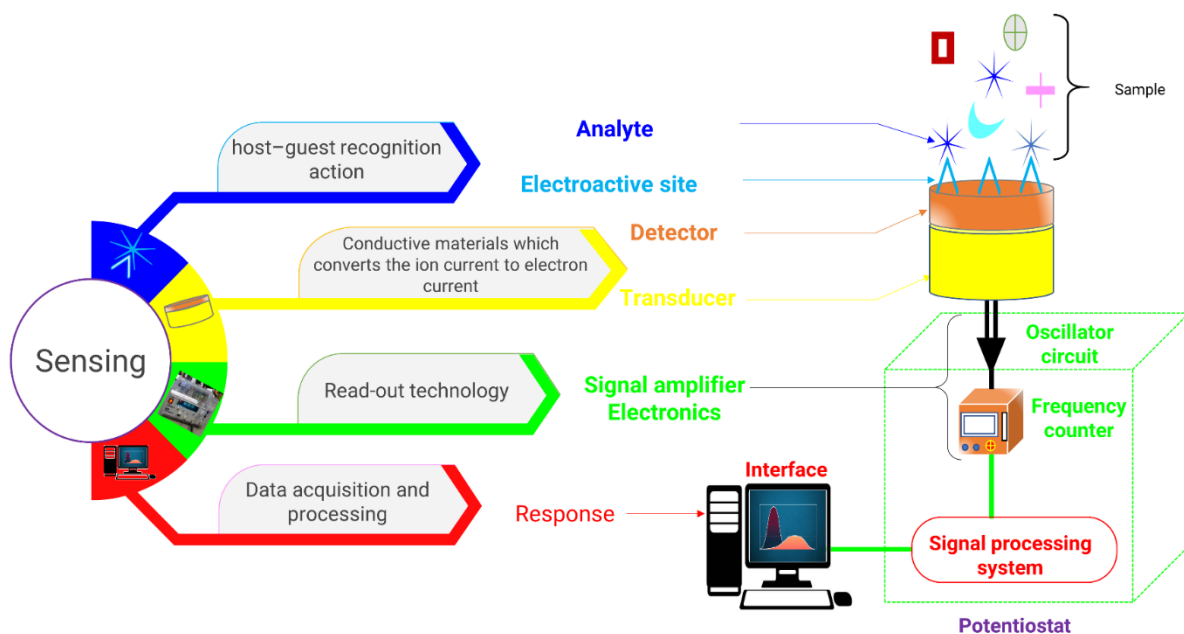
Figure 4: Illustration of the components of electrochemical sensors.

Electrochemical methods used for thiamethoxam determination
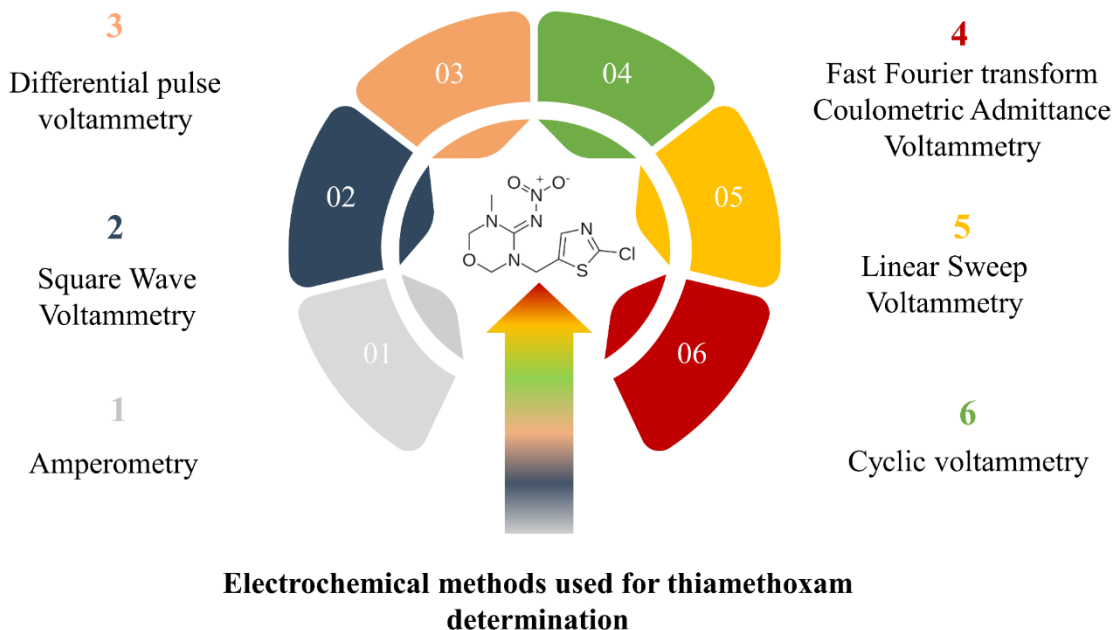
Figure 5: Electrochemical techniques used for NEOs detection.

For the most promising alternative to mercury electrode, due to concerns about its toxicity, we find the metal solid amalgam such as renewable silver amalgam-film electrode (Hg(Ag)FE),

which introduced for first time to determine organic compound of B_1 vitamin using square wave voltammetry (SWV) [141, 142]. This electrode has been subsequently developed by Marie Putek et *al*. for the voltammetric determination of NOE by comparing its analytical performance against the hanging mercury drop electrode (HMDE) [143]. The voltammetric method (Hg(Ag)FE) was found to be the most sensitive for NOE determination. This sensitivity depends considerably on the state of electrode surface and supporting electrolyte pH. Moreover, the proposed procedure was found to be sensitive and advantageous for sensing NOEs in river water and honey samples [143].

Chorti et *al*. used a non-toxic mercury meniscus modified silver solid amalgam electrode (m-AgSAE) for the determination of NOE using direct differential pulse voltammetry (DPV) [144]. This electrode demonstrated the lowest determination limit and confirmed a good applicability for the direct measurements in real samples, such as drinking and river water. Moreover, m-AgSAE exhibits a higher sensitivity in comparison with amalgam film electrode.

Recently, a method of the electrocatalytic detection of NOE at metallic silver electrode was developed by Ajermoun et al. [145]. The electrocatalytic activity of silver toward NOE was compared with other electrodes such as glassy carbon and carbon paste electrode using cyclic voltammetry, Tafel plots and electrochemical impedance spectroscopy. The silver electrode showed a significant electrocatalytic activity compared to other electrodes. At the same time, it has excellent applicability and sensitivity for determination of target molecule in real samples such as tomato and orange juices without separation using solid phase extraction, with the limit of detection about 12.4 and 34.8 µmol L^{-1} and limit of quantification (LOQ) of 41.3 and 115.9 µmol L^{-1}, respectively [145]. Moreover, a consideration is given to the presence of electrochemically active interferents, which generally pose a problem as they can distort the results. Metallic silver electrode was tested for determination of TMX in presence of several organic compounds including 4-nitroaniline, 2-nitroanaline, 4-nitrophenole and 2,4-dinitrophenylhydrazine (DNPH). This electrode showed a suitable selectivity towards these compounds. As a continuation of previous study and to exploit these results, the bioaccumulation of NOE in zea mays plant was followed using metallic silver electrode. After 10 days of treatment of this plant, NOE analysis was realized in the extract of different part of plant (roots, stems and leaves). The acceptable detection and quantification limits were obtained [59].

ii) Metallic nanoparticle

During electrochemical measurements of organic and biological compounds (pesticides, dyes, pharmaceutical products and emerging pollutants…) on the solid and bare electrode, a problem in producing reproducible electrochemical signal is always present. This may be due to the adsorption of the reduction products of target molecules at electrode. To minimise this problem, the idea of modifying electrode active surface area was introduced to invent and to develop new chemically modified electrodes with much better characteristics and advantages. In order, to enhance the performance of the electrodes to sensing pesticides residues, many chemical modifications have been reported in literature [146–148]. In fact, the use of nanomaterials and nanocomposites materials for the preparation of electrodes can grant several advantages in electrochemical response, such as a great surface area with nanoscales features that provide catalytic properties with improvement of selectivity and sensitivity related to NOE reduction. Silver nanoparticles exhibit a superior catalytic activity and high reactivity compared to others metal nanoparticles and improve enhancement factor for surface enhanced Raman spectroscopy. Silver nanoparticles have appropriate plasmon resonance frequencies and absorption characteristics to achieve effective enhancement with visible excitation [149–151], also silver nanoparticles were used for metal fluorescence because of their ability to significantly enhance the intensity of fluorophore emission [152, 153]. Kumaravel and Chandradekaran developed a novel nanosilver/SDS modified glassy carbon electrode for electrochemical sensing of NOEs [154], employing cyclic voltammetry, differential pulse voltammetry and amperometry. The sodium dodecyl sulphate (SDS) is an anionic surfactant with a negative sulphate group at end, which plays an important role in the formation and size control of silver nanoparticles on the electrode surface. The sodium dodecyl sulphate SDS reacts with surface of glassy carbon which is highly hydrophobic in nature, then the adsorption of the surfactant takes place on the surface of electrode. For differential pulse voltammetry, a linear range of $0.1 – 9$ µmol L^{-1} and a LOQ of 0.1 µmol L^{-1} were found. This LOQ is not low enough to quantify NOE. When amperometric method was used, linear range from 5 to 25 µmol L^{-1} and LOQ of 2.94 µmol L^{-1} were mentioned; this result may be due to the adsorption of the reactant/product molecules on the electrode surface [154] (Figure 6). This proposed modified electrode shows better electrocatalytic activity toward NOE reduction and lower limit of detection (0.04 µmol L^{-1}) compared with other electrodes reported in literature. In addition, the recovery rate in potato sample is in good agreement with the HPLC method. In the same context of the metal-nanoparticles, carbon nanotubes (CNT) are increasingly used as transducer materials and have considerably improved the sensors electrochemical response due to their

large surface area, electronic and optical properties. The mixture with nanoparticles and polymer were used to construct modified electrodes.
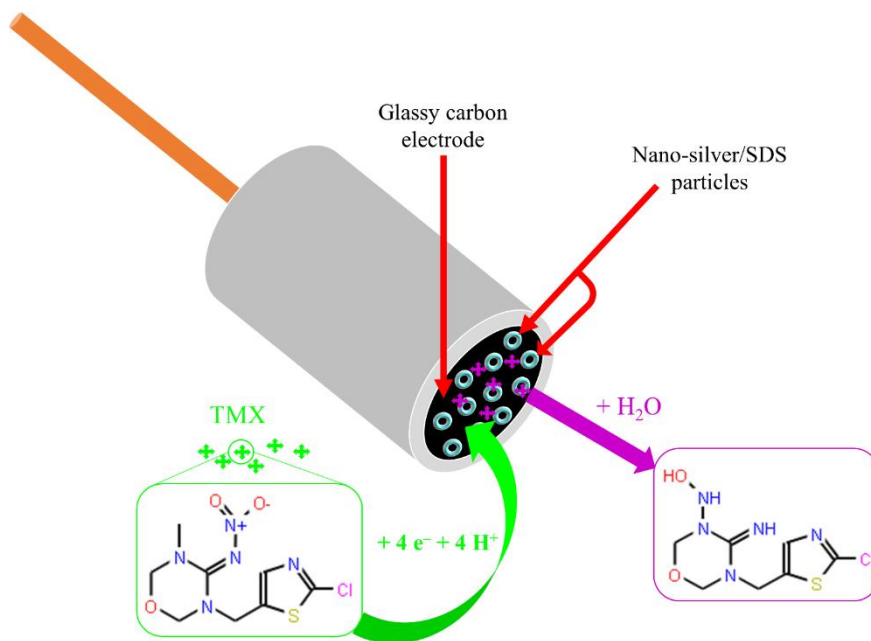
Figure 6: *Describe the mechanism of electrochemical detection and the processes adsorption of the NEOs at electrode surface.*

Parviz Norouzi et *al*. developed a nanocomposite application of new electrode for NOE determination [155]; consists to casting mixture of chitosan, multi-walled carbon nanotube, reduced graphene nanosheets and gold nanoparticles on a carbon paste ionic liquid electrode (CHI-MWCNT/AuNP/RGNS/CILE) using Fast Fourier transform Coulometric Admittance Voltammetry (FFTCAV). The developed electrode exhibits an excellent and reproducible sensitivity due to its large surface area and fast electron transfer provided through graphene and gold nanoparticles, with a LOD 1.62×10^{-12} mol L^{-1}. The nanocomposite electrode also poses relatively long-term stability for ninety days. Recently, another nanocomposite electrode developed by Shangxing Chen and co-works [156], consists of a voltammetric sensing platform, which can be used for application in stripping analysis of TMX neonicotinoid in agricultural and environmental samples. This technology based on thick-walled Moso biochar combined with carbonate minerals dolomite modified glassy carbon electrode (BC-DM / GCE) [156]. This electrode showed a good stability and sensitivity to NOE in a wide linear range from $0.5 - 35$ µg mL^{-1} with the LOD of 0.22 µg mL^{-1}. Furthermore, good recovery results were

obtained in all samples (rice, pear, red soil, spinach, river water, lake water tap water and farmland water), indicating that the prepared modified nanocomposite electrode was suitable for the detection analyte in environmental real samples. Moreover, the electrode selectivity was tested against many pesticides and metal ions, for tenfold amount, most interfering substance were Cu^{2+} ions with the RDS of 2.56%.

Recently, a free metal carbon nanomaterial was investigated for electrochemical sensing applications, based on graphitic carbon nitride, which is a stable layered material of carbon nitride framework. The latter reveals structural similarity to graphene (2D layer), with tris-triazine building units connected with planar amino groups in each layer and weak van der Waals force between layers. Due to its unique properties (including stability, semiconductivity, unique electronic structure, and easy preparation), it has received much research attention for a wide range of applications in various fields, such as hydrogen storage, oxygen reduction reaction [157, 158], photocatalytic organics degradation [159, 160], water splitting [161, 162] and electrochemical sensing [163–165].

Jaysiva Ganesamurthi et *al*. investigated a robust method based on cobalt oxide nanoparticles decorated graphitic carbon nitride nanocomposite (Co_3O_4@g-C_3N_4/SPCE) for the determination of NOE [166]. The composition and crystalline structure were determined out by XPS, FT-IR, XRD and FSEM. The electrocatalytic activity of the Co_3O_4@g-C_3N_4/SPCE toward NOE was studied using cyclic voltammetry and differential pulse voltammetry. The selectivity of proposed electrode was investigated in the presence of nitro-aromatic pesticides (such as methyl-parathion, parathion and fenitrothion), and the variation range of recovery received in term of current intensity was from -0.004% to -5.8%, revealing an excellent selectivity toward NOE analyte.

iii) Carbon

For first investigation of electrochemical methods to detect TMX neonicotinoid, in 2004, Valeria Guzsvany et *al.* developed a simple voltammetric method employing glassy carbon electrode. The method displayed a limit of detection for NOE about 29.1 µmol L^{-1} and performed to well assess the accuracy of results in potato sample [167].

Graphene is the basic building block for graphitic materials of all other interesting dimensionalities (0D Fullerenes, 1D nanotube, 3D graphite), it consists essentially of a planar monolayer of carbon atoms tightly packed into a two dimensional (2D) hexagonal lattice [168, 169]. Graphene is attracting enormous interest due to its numerous unexpected properties, showing good electrical conductivity, high specific surface area and high-speed electron

mobility and high value of its Young's modulus. In electrochemical field, graphene and graphene nanocomposite based sensors have proved its successful application, especially, chemically reduced graphene oxide, commonly, has significant structural defects [170, 171] and functional groups [172] have beneficial electrochemical applications [173–176]. For NOEs insecticides, Veronika Urbanová et *al*. demonstrated the applicability of graphene oxide modified electrode for the determination of NOEs (TMX and imidacloprid). The proposed modified electrode exhibits an excellent electrocatalytic activity compared to other electrodes reported previously with satisfactory detection limits. It also demonstrated good applicability toward determination of TMX with detection limit of 8.3 µmol L^{-1}. Also, the sensor analytical utility was successfully tested and the recovery rate found to be around 98 % and 95 % in the spiked water and honey samples, respectively [177]. Ana Elisa Ferreira Oliveira et *al*. proposed an electrochemical modified electrode based on glassy carbon modified with reduced graphene oxide and β-cyclodextrin (GCE/rGO/ β-CD) as an alternative in the analysis of NOEs insecticides (such as imidacloprid, clothianidine and thiamethoxam) in real honey samples. They mentioned that the β-CD can form an inclusion complex with the target molecule (NOE), increasing the sensitivity when the analyte is included in the cavity of β-CD, due to hydrophobic character. The proposed electrochemical approach showed high sensitivity and conductivity characteristics of extreme importance in the sensor's construction. Furthermore, three real samples were used to test analytical ability of sensor such as honey, pollen and beeswax. However, only determination in honey sample was performed without any pretreatment, making the method fast and simple [178].

iv) Molecularly imprinted polymer MIP

Molecularly imprinted polymer is synthesized through the technology of molecular imprinting via copolymerization of an appropriate monomer and cross-linker in the presence of analyte template. MIP extensively used as specific recognition and selective adsorbent of the analyte molecule in the design of sensor, due to their high thermal stability, easy preparation, great reusability, favourable selectivity and possibility of miniaturization [179, 180]. The principal of this approach is mainly based on the change in electrochemical signal resulting from the interaction of the target molecule with the cavity, depending to its shape, charge and functionality. Many different methods have been utilized to product molecularly imprinted electrochemical sensors, such as electrochemical polymerization, self-assembly, in situ polymerization and sol-gel technique. Tianjiao Xie and co-works developed a facile method for the preparation of molecularly imprinted polymer based on graphene for the sensing of NOEs

residue [181]. The innovation of this research lies in the selection of 4-vinylbenzoic acid (VBA) as a functional monomer. VBA structurally contains alkenyl group and hydroxyl group, so it can react with the template molecule and cross-linking agent, and can be immobilized on the graphene surface through π-π interaction. However, it can provide an ultra-thin printing film by reducing the addition step involving the alkenyl modifier, which makes the preparation process much easier. The proposed sensors showed good sensitivity and binding capacity for NOE, also good reproducibility and reusability. Furthermore, the analytical applicability of MIP-GN/GCE was applied to the determination of TMX neonicotinoid in brow rice samples with satisfactory results. Various type sensors and their features for the determination of NOEs insecticides are shown in the table 2. Thereafter, analytical performance parameters of the utilized electrodes for TMX neonicotinoid detection are detailed and materials applied in electrode modification for its detection are illustrated in the (Figure 7).
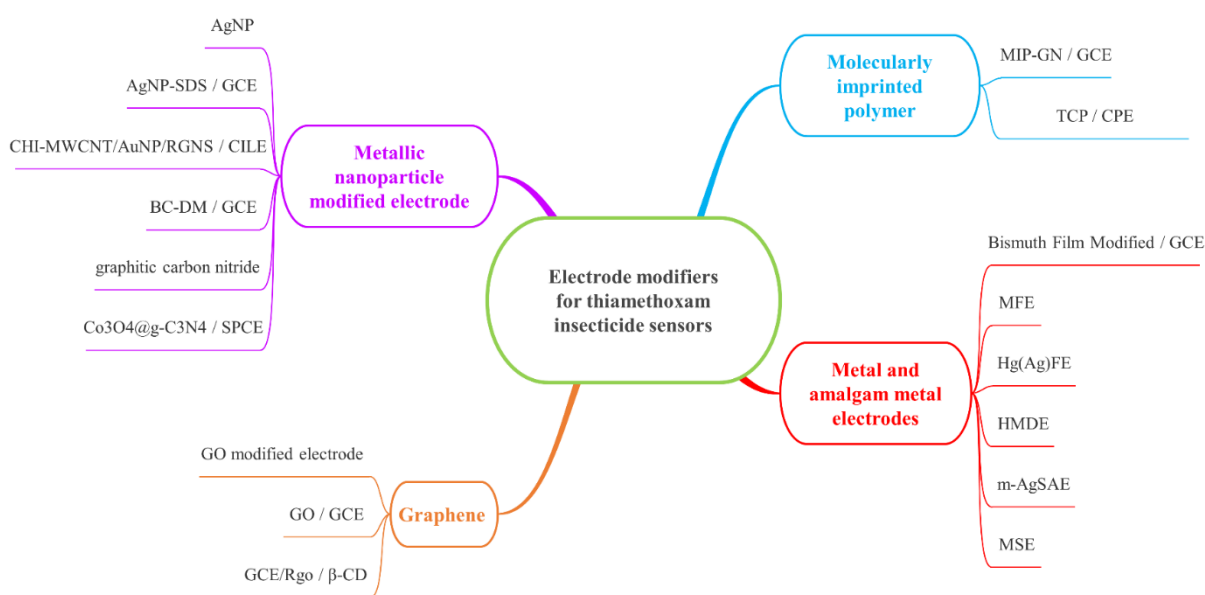
Figure 7: Schematic illustration of materials applied in electrode modification for NEOs detection.

31

Table 2: Summary of the analytical performance data of the electrochemical sensors for NEOs insecticides.

Electrodes	Electrochemical methods	Linear range (μmol L^{-1})	Limit of detection (μmol L^{-1})	Real samples	Refs
Dropping mercury electrode (DME)	Differential Pulse Polarography (DPP)	0.11 – 1.60	0.032	Potato - maize	[139]
Bismuth Film Modified Glassy Carbon Electrode BiFE	Differential Pulse Voltammetry DPV	2.64 – 154	1.300	Potato - maize	[140]
Mercury Film Electrode	Differential Pulse Voltammetry DPV	4.32 – 154	0.890		
Silver Amalgam-Film Electrode Hg(Ag)FE Hanging Mercury Drop Electrode HMDE	Square Wave Voltammetry (SWV)	2.39 – 265 3.12 – 170	0.860 0.860	Honey	[143]
Silver Solid Amalgam Electrode m-AgSAE	Differential Pulse Voltammetry (DPV)	-	-	Drinking - river water	[144]
Metallic Silver Electrode (MSE)	Square Wave Voltammetry SWV	10 – 100	5.490	Tomato - orange juices	[145]
Metallic Silver Electrode (MSE)	Square Wave Voltammetry SWV	50 – 1000	9.580	Zea mays	[59]
Nanosilver/SDS /GCE	Differential Pulse Voltammetry DPV Cyclic Voltammetry (CV) Amperpmetry	0.10 – 9	0.100 4.700 0.880	Potato	[154]
CHI-MWCNT/AuNP/RGNS/CILE	Fast Fourier transform Coulometric Admittance Voltammetry (FFTCAV)	0.05×10^{-3} – 35×10^{-3}	6.2×10^{-6}	–	[155]

DM-BC/GCE	Differential Pulse Voltammetry (DPV)	1.74 – 120	0.750	Spinach River water Rice Pear Red soil Farmland water Lake water Tap water	[156]
Glassy Carbon Electrode (GCE)	Cyclic Voltammetry (CV)	95.90 – 1714	29.100	Potato	[167]
Graphen Oxide Galssy Carbon Electrode GO/GCE	Square Wave Voltammetry (SWV)	10 – 200	8.300	River water honey	[177]
GCE/rGO/β-CD	Square Wave Voltammetry (SWV)	-	7.450	Honey, pollen beeswax	[178]
MIP-GN/GCE	Linear Sweep Voltammetry (LSV)	0.50 – 20	0.040	Brown rice	[181]
β-CD-rGO/GCE	Linear Sweep Voltammetry (LSV)	-	0.270	Brown rice	[182]
Tricresyl Phosphate- Carbon Paste Electrode TCP-CPE	Differential Pulse Voltammetry DPV	12.70 – 142	_	River water	[183]

IX. Conclusion

This chapter comprehensively summarized the effect of neonicotinoid insecticides on the soils, water body and human health. Neonicotinoids are the most widely used pesticides in agricultural sectors due to their effective insecticidal properties. its long-term persistence in soil and water poses serious threat not only to the environment but also to human health.

Neonicotinoids application significantly affect the soil bacterial abundance in the short term, which reduced the microbial diversity and changed the bacterial community structure, this impact depends on insecticides concentration and soil type. While, undergoing biological and physicochemical transformations and impacting microbial development, enzymatic activity and soil fertility. Furthermore, the potential for leaching or run-off from fields could pose serious risks to aquatic ecosystems.

Because neonicotinoids are commonly applied, widespread human exposure to these insecticides can be suggested. Ingestion (e.g., water, food), inhalation (e.g., dust), and cutaneous exposure, as well as occupational and residential use, have all been linked to human exposure to neonicotinoids. In addition, the ingestion exposure appears to be the most dominated route of exposure to evaluate the impact of these chemicals on human health. Furthermore, the present evidence from epidemiological studies suggests that neonicotinoids cause acute health effects to human health ranging from respiratory, cardiovascular and neurological symptoms.

For the remediation of neonicotinoids from the environment, various strategies have been introduced and applied in recent decades, mainly physicochemical degradation and biodegradation.

Electroanalytical methods offer advantages for determination of neonicotinoid residues due to its characteristics including low cost, ease of use, wide dynamic range, and high sensitivity compared to other analytical methods. However, there are limited papers concerning usage of advanced material and nanomaterial throughout modified electrochemical sensors manufacturing for sensing these insecticides.

References

[1]   Jeschke, P.; Nauen, R.; Schindler, M. and Elbert, A.: Overview of the status and global strategy for neonicotinoids, Journal of agricultural and food chemistry, **59** (2011), no. 7, pp. 2897–2908.

[2]   Tomizawa, M. and Casida, J.E.: NEONICOTINOID INSECTICIDE TOXICOLOGY: Mechanisms of Selective Action, Annual Review of Pharmacology and Toxicology, **45** (2005), no. 1, pp. 247–268.

[3]   Hladik, M.L.; Main, A.R. and Goulson, D.: Environmental risks and challenges associated with neonicotinoid insecticides2018.

[4]   Jeschke, P. and Nauen, R.: Neonicotinoids—from zero to hero in insecticide chemistry, Pest Management Science, **64** (2008), no. 11, pp. 1084–1098.

[5]   Shivanandappa, T. and Rajashekar, Y.: Mode of Action of Plant-Derived Natural Insecticides, Advances in Plant Biopesticides, Springer India, New Delhi, 2014, pp. 323–345.

[6]   Yamamoto, I. and Casida, J.E.: Nicotinoid insecticides and the nicotinic acetylcholine receptor, (1999).

[7]   Simon-Delso, N.; Amaral-Rogers, V.; Belzunces, L.P.; Bonmatin, J.M.; Chagnon, M.; Downs, C.; Furlan, L.; Gibbons, D.W.; Giorio, C.; Girolami, V.; Goulson, D.; Kreutzweiser, D.P.; Krupke, C.H.; Liess, M.; Long, E.; McField, M.; Mineau, P.; Mitchell, E.A.D.; Morrissey, C.A.; Noome, D.A.; Pisa, L.; Settele, J.; Stark, J.D.; Tapparo, A.; Van Dyck, H.; Van Praagh, J.; Van der Sluijs, J.P.; Whitehorn, P.R. and Wiemers, M.: Systemic insecticides (neonicotinoids and fipronil): trends, uses, mode of action and metabolites, Environmental Science and Pollution Research, **22** (2015), no. 1, pp. 5–34.

[8]   Uneme, H.: Chemistry of Clothianidin and Related Compounds, Journal of Agricultural and Food Chemistry, **59** (2011), no. 7, pp. 2932–2937.

[9]   Cappaert, D.; McCullough, D.G.; Poland, T.M. and Siegert, N.W.: Emerald ash borer in North America: a research and regulatory challenge, American Entomologist. 51 (3): 152-165., **51** (2005), no. 3.

[10]   Struger, J. and Fletcher, T.: Occurrence of lawn care and agricultural pesticides in the Don River and Humber River watersheds (1998–2002), Journal of Great Lakes Research, **33** (2007), no. 4, pp. 887–905.

[11] McCurdy, J.D.; Held, D.W.; Gunn, J.M. and Barickman, T.C.: Dew from Warm-Season Turfgrasses as a Possible Route for Pollinator Exposure to Lawn-Applied Imidacloprid, Crop, Forage & Turfgrass Management, **3** (2017), no. 1, pp. 1–6.

[12] Anderson, J.C.; Dubetz, C. and Palace, V.P.: Neonicotinoids in the Canadian aquatic environment: a literature review on current use products with a focus on fate, exposure, and biological effects, Science of the Total Environment, **505** (2015), pp. 409–422.

[13] Lewis, K.A.; Tzilivakis, J.; Warner, D.J. and Green, A.: An international database for pesticide risk assessments and management, Human and Ecological Risk Assessment: An International Journal, **22** (2016), no. 4, pp. 1050–1064.

[14] Tomizawa, M. and Casida, J.E.: Selective Toxicity of Neonicotinoids Attributable to Specificity of Insect and Mammalian Nicotinic Receptors, Annual Review of Entomology, **48** (2003), no. 1, pp. 339–364.

[15] Tomizawa, M. and Casida, J.E.: Minor structural changes in nicotinoid insecticides confer differential subtype selectivity for mammalian nicotinic acetylcholine receptors, British Journal of Pharmacology, **127** (1999), no. 1, pp. 115–122.

[16] Lansdell, S.J. and Millar, N.S.: The influence of nicotinic receptor subunit composition upon agonist, α–bungarotoxin and insecticide (imidacloprid) binding affinity, Neuropharmacology, **39** (2000), no. 4, pp. 671–679.

[17] Tomizawa, M. and Casida, J.E.: Imidacloprid, thiacloprid, and their imine derivatives up-regulate the α4β2 nicotinic acetylcholine receptor in M10 cells, Toxicology and applied pharmacology, **169** (2000), no. 1, pp. 114–120.

[18] Cimino, A.M.; Boyles, A.L.; Thayer, K.A. and Perry, M.J.: Effects of neonicotinoid pesticide exposure on human health: a systematic review, Environmental health perspectives, **125** (2017), no. 2, pp. 155–162.

[19] Han, W.; Tian, Y. and Shen, X.: Human exposure to neonicotinoid insecticides and the evaluation of their potential toxicity: an overview, Chemosphere, **192** (2018), pp. 59–65.

[20] Bal, R.; Türk, G.; Tuzcu, M.; Yilmaz, O.; Kuloglu, T.; Gundogdu, R.; Gür, S.; Agca, A.; Ulas, M. and Çambay, Z.: Assessment of imidacloprid toxicity on reproductive organ system of adult male rats, Journal of Environmental Science and Health, Part B, **47** (2012), no. 5, pp. 434–444.

[21] Kimura-Kuroda, J.; Komuta, Y.; Kuroda, Y.; Hayashi, M. and Kawano, H.: Nicotine-like effects of the neonicotinoid insecticides acetamiprid and imidacloprid on cerebellar neurons from neonatal rats, PLoS One, **7** (2012), no. 2, p. e32432.

[22] Fauser, A.; Sandrock, C.; Neumann, P. and Sadd, B.M.: Neonicotinoids override a parasite exposure impact on hibernation success of a key bumblebee pollinator, Ecological Entomology, **42** (2017), no. 3, pp. 306–314.

[23] Gerwick, B.C. and Sparks, T.C.: Natural products for pest control: an analysis of their role, value and future, Pest Management Science, **70** (2014), no. 8, pp. 1169–1185.

[24] Zhou, Y.; Lu, X.; Yu, B.; Wang, D.; Zhao, C.; Yang, Q.; Zhang, Q.; Tan, Y.; Wang, X. and Guo, J.: Comparison of neonicotinoid residues in soils of different land use types, Science of The Total Environment, **782** (2021), p. 146803.

[25] Bonmatin, J.-M.; Giorio, C.; Girolami, V.; Goulson, D.; Kreutzweiser, D.P.; Krupke, C.; Liess, M.; Long, E.; Marzaro, M.; Mitchell, E.A.D.; Noome, D.A.; Simon-Delso, N. and Tapparo, A.: Environmental fate and exposure; neonicotinoids and fipronil, Environmental Science and Pollution Research, **22** (2015), no. 1, pp. 35–67.

[26] Codling, G.; Al Naggar, Y.; Giesy, J.P. and Robertson, A.J.: Concentrations of neonicotinoid insecticides in honey, pollen and honey bees (Apis mellifera L.) in central Saskatchewan, Canada, Chemosphere, **144** (2016), pp. 2321–2328.

[27] Tooker, J.F.; Douglas, M.R. and Krupke, C.H.: Neonicotinoid seed treatments: limitations and compatibility with integrated pest management, Agricultural & Environmental Letters, **2** (2017), no. 1, pp. ael2017-08.

[28] Limay-Rios, V.; Forero, L.G.; Xue, Y.; Smith, J.; Baute, T. and Schaafsma, A.: Neonicotinoid insecticide residues in soil dust and associated parent soil in fields with a history of seed treatment use on crops in southwestern Ontario, Environmental Toxicology and Chemistry, **35** (2016), no. 2, pp. 303–310.

[29] Watanabe, E.; Kobara, Y.; Baba, K. and Eun, H.: Determination of seven neonicotinoid insecticides in cucumber and eggplant by water-based extraction and high-performance liquid chromatography, Analytical Letters, **48** (2015), no. 2, pp. 213–220.

[30] Regan, K.; Ordosch, D.; Glover, K.D.; Tilmon, K.J. and Szczepaniec, A.: Effects of a pyrethroid and two neonicotinoid insecticides on population dynamics of key pests of soybean and abundance of their natural enemies, Crop Protection, **98** (2017), pp. 24–32.

[31] Sánchez-Bayo, F.: The trouble with neonicotinoids, Science, **346** (2014), no. 6211, pp. 806–807.

[32] Tapparo, A.; Marton, D.; Giorio, C.; Zanella, A.; Soldà, L.; Marzaro, M.; Vivan, L. and Girolami, V.: Assessment of the environmental exposure of honeybees to particulate matter containing neonicotinoid insecticides coming from corn coated seeds, Environmental science & technology, **46** (2012), no. 5, pp. 2592–2599.

[33] Van Dijk, T.C.; Van Staalduinen, M.A. and Van der Sluijs, J.P.: Macro-invertebrate decline in surface water polluted with imidacloprid, PloS one, **8** (2013), no. 5, p. e62374.

[34] Klose, S.; Acosta-Martínez, V. and Ajwa, H.A.: Microbial community composition and enzyme activities in a sandy loam soil after fumigation with methyl bromide or alternative biocides, Soil Biology and Biochemistry, **38** (2006), no. 6, pp. 1243–1254.

[35] Pose-Juan, E.; Igual, J.M.; Sánchez-Martín, M.J. and Rodríguez-Cruz, M.S.: Influence of herbicide triasulfuron on soil microbial community in an unamended soil and a soil amended with organic residues, Frontiers in microbiology, **8** (2017), p. 378.

[36] Hladik, M.L.; Corsi, S.R.; Kolpin, D.W.; Baldwin, A.K.; Blackwell, B.R. and Cavallin, J.E.: Year-round presence of neonicotinoid insecticides in tributaries to the Great Lakes, USA, Environmental Pollution, **235** (2018), pp. 1022–1029.

[37] Zhang, C.; Tian, D.; Yi, X.; Zhang, T.; Ruan, J.; Wu, R.; Chen, C.; Huang, M. and Ying, G.: Occurrence, distribution and seasonal variation of five neonicotinoid insecticides in surface water and sediment of the Pearl Rivers, South China, Chemosphere, **217** (2019), pp. 437–446.

[38] Tišler, T.; Jemec, A.; Mozetič, B. and Trebše, P.: Hazard identification of imidacloprid to aquatic environment, Chemosphere, **76** (2009), no. 7, pp. 907–914.

[39] Thuyet, D.Q.; Watanabe, H. and Ok, J.: Effect of pH on the degradation of imidacloprid and fipronil in paddy water, Journal of Pesticide Science, (2013), pp. D12-080.

[40] Butcherine, P.; Benkendorff, K.; Kelaher, B. and Barkla, B.J.: The risk of neonicotinoid exposure to shrimp aquaculture, Chemosphere, **217** (2019), pp. 329–348.

[41] Pisa, L.W.; Amaral-Rogers, V.; Belzunces, L.P.; Bonmatin, J.-M.; Downs, C.A.; Goulson, D.; Kreutzweiser, D.P.; Krupke, C.; Liess, M. and McField, M.: Effects of neonicotinoids and fipronil on non-target invertebrates, Environmental Science and Pollution Research, **22** (2015), no. 1, pp. 68–102.

[42] Kreutzweiser, D.; Good, K.; Chartrand, D.; Scarr, T. and Thompson, D.: Non-target effects on aquatic decomposer organisms of imidacloprid as a systemic insecticide to control emerald ash borer in riparian trees, Ecotoxicology and Environmental Safety, **68** (2007), no. 3, pp. 315–325.

[43] Böttger, R.; Feibicke, M.; Schaller, J. and Dudel, G.: Effects of low-dosed imidacloprid pulses on the functional role of the caged amphipod Gammarus roeseli in stream mesocosms, Ecotoxicology and environmental safety, **93** (2013), pp. 93–100.

[44] Colombo, V.; Mohr, S.; Berghahn, R. and Pettigrove, V.J.: Structural changes in a macrozoobenthos assemblage after imidacloprid pulses in aquatic field-based

microcosms, Archives of environmental contamination and toxicology, **65** (2013), no. 4, pp. 683–692.

[45] Song, M.Y.; Stark, J.D. and Brown, J.J.: Comparative toxicity of four insecticides, including imidacloprid and tebufenozide, to four aquatic arthropods, Environmental Toxicology and Chemistry: An International Journal, **16** (1997), no. 12, pp. 2494–2500.

[46] Alexander, A.C.; Culp, J.M.; Baird, D.J. and Cessna, A.J.: Nutrient–insecticide interactions decouple density-dependent predation pressure in aquatic insects, Freshwater Biology, **61** (2016), no. 12, pp. 2090–2101.

[47] Alexander, A.C.; Culp, J.M.; Liber, K. and Cessna, A.J.: Effects of insecticide exposure on feeding inhibition in mayflies and oligochaetes, Environmental Toxicology and Chemistry: An International Journal, **26** (2007), no. 8, pp. 1726–1732.

[48] Roessink, I.; Merga, L.B.; Zweers, H.J. and Van den Brink, P.J.: The neonicotinoid imidacloprid shows high chronic toxicity to mayfly nymphs, Environmental toxicology and chemistry, **32** (2013), no. 5, pp. 1096–1100.

[49] Azevedo-Pereira, H.; Lemos, M.F.L. and Soares, A.M.: Effects of imidacloprid exposure on Chironomus riparius Meigen larvae: linking acetylcholinesterase activity to behaviour, Ecotoxicology and environmental safety, **74** (2011), no. 5, pp. 1210–1215.

[50] Overmyer, J.P.; Mason, B.N. and Armbrust, K.L.: Acute toxicity of imidacloprid and fipronil to a nontarget aquatic insect, Simulium vittatum Zetterstedt cytospecies IS-7, Bulletin of environmental contamination and toxicology, **74** (2005), no. 5, pp. 872–879.

[51] Sánchez-Bayo, F.; Goka, K. and Hayasaka, D.: Contamination of the aquatic environment with neonicotinoids and its implication for ecosystems, Frontiers in Environmental Science, **4** (2016), p. 71.

[52] Sánchez-Bayo, F.: Insecticides mode of action in relation to their toxicity to non-target organisms, J. Environ. Anal. Toxicol. S, **4** (2012), pp. S4-002.

[53] Vignet, C.; Cappello, T.; Fu, Q.; Lajoie, K.; De Marco, G.; Clérandeau, C.; Mottaz, H.; Maisano, M.; Hollender, J. and Schirmer, K.: Imidacloprid induces adverse effects on fish early life stages that are more severe in Japanese medaka (Oryzias latipes) than in zebrafish (Danio rerio), Chemosphere, **225** (2019), pp. 470–478.

[54] Su, F.; Zhang, S.; Li, H. and Guo, H.: In vitro acute cytotoxicity of neonicotinoid insecticide imidacloprid to gill cell line of flounder Paralichthy olivaceus, Chinese Journal of Oceanology and Limnology, **25** (2007), no. 2, pp. 209–214.

[55] Finnegan, M.C.; Baxter, L.R.; Maul, J.D.; Hanson, M.L. and Hoekstra, P.F.: Comprehensive characterization of the acute and chronic toxicity of the neonicotinoid

insecticide thiamethoxam to a suite of aquatic primary producers, invertebrates, and fish, Environmental toxicology and chemistry, **36** (2017), no. 10, pp. 2838–2848.

[56] Cardone, A.: Imidacloprid induces morphological and molecular damages on testis of lizard (Podarcis sicula), Ecotoxicology, **24** (2015), no. 1, pp. 94–105.

[57] Martinez, R.S.; Di Marzio, W.D. and Sáenz, M.E.: Genotoxic effects of commercial formulations of Chlorpyrifos and Tebuconazole on green algae, Ecotoxicology, **24** (2015), no. 1, pp. 45–54.

[58] Yang, X.; Lu, M.; Wang, Y.; Wang, Y.; Liu, Z. and Chen, S.: Response Mechanism of Plants to Drought Stress, Horticulturae, **7** (2021), no. 3, p. 50.

[59] Ajermoun, N.; Lahrich, S.; Bouarab, L.; Bakasse, M.; Saqrane, S. and El Mhammedi, M.A.: Physiological effects of thiamethoxam on Zea mays and its electrochemical detection using a silver electrode, Journal of the Science of Food and Agriculture, **100** (2020), no. 5, pp. 2090–2098.

[60] Dhungana, S.K.; Kim, I.-D.; Kwak, H.-S. and Shin, D.-H.: Unraveling the effect of structurally different classes of insecticide on germination and early plant growth of soybean [Glycine max (L.) Merr.], Pesticide biochemistry and physiology, **130** (2016), pp. 39–43.

[61] Pétriacq, P.; Williams, A.; Cotton, A.; McFarlane, A.E.; Rolfe, S.A. and Ton, J.: Metabolite profiling of non-sterile rhizosphere soil, The Plant Journal, **92** (2017), no. 1, pp. 147–162.

[62] Wang, Y.; Ren, W.; Li, Y.; Xu, Y.; Teng, Y.; Christie, P. and Luo, Y.: Nontargeted metabolomic analysis to unravel the impact of di (2-ethylhexyl) phthalate stress on root exudates of alfalfa (Medicago sativa), Science of the Total Environment, **646** (2019), pp. 212–219.

[63] Li, X.; Zhang, M.; Li, Y.; Yu, X. and Nie, J.: Effect of neonicotinoid dinotefuran on root exudates of Brassica rapa var. chinensis, Chemosphere, **266** (2021), p. 129020.

[64] Toumi, H.; Boumaiza, M.; Millet, M.; Radetski, C.M.; Camara, B.I.; Felten, V. and Ferard, J.-F.: Investigation of differences in sensitivity between 3 strains of Daphnia magna (crustacean Cladocera) exposed to malathion (organophosphorous pesticide), Journal of Environmental Science and Health, Part B, **50** (2015), no. 1, pp. 34–44.

[65] Yilmaz, S.; Kaya, E. and Kisacam, M.A.: The effect on oxidative stress of aflatoxin and protective effect of lycopene on aflatoxin damage, Aflatoxin-Control, Analysis, Detection and Health Risks, **30** (2017), pp. 67–90.

[66] Shahid, M.; Khan, M.S.; Ahmed, B.; Syed, A. and Bahkali, A.H.: Physiological disruption, structural deformation and low grain yield induced by neonicotinoid insecticides in chickpea: A long term phytotoxicity investigation, Chemosphere, **262** (2021), p. 128388.

[67] Wulff, J.A.; Kiani, M.; Regan, K.; Eubanks, M.D. and Szczepaniec, A.: Neonicotinoid insecticides alter the transcriptome of soybean and decrease plant resistance, International journal of molecular sciences, **20** (2019), no. 3, p. 783.

[68] Zhou, Q.; Cheng, X.; Wang, S.; Liu, S. and Wei, C.: Effects of chemical insecticide Imidacloprid on the release of C 6 green leaf volatiles in tea plants (Camellia sinensis), Scientific reports, **9** (2019), no. 1, pp. 1–6.

[69] Arora, P.K.; Jyot, G.; Singh, B.; Battu, R.S.; Singh, B. and Aulakh, P.S.: Persistence of imidacloprid on grape leaves, grape berries and soil, Bulletin of environmental contamination and toxicology, **82** (2009), no. 2, pp. 239–242.

[70] Chauzat, M.-P.; Carpentier, P.; Martel, A.-C.; Bougeard, S.; Cougoule, N.; Porta, P.; Lachaize, J.; Madec, F.; Aubert, M. and Faucon, J.-P.: Influence of pesticide residues on honey bee (Hymenoptera: Apidae) colony health in France, Environmental Entomology, **38** (2009), no. 3, pp. 514–523.

[71] Kapoor, U.; Srivastava, M.K.; Srivastava, A.K.; Patel, D.K.; Garg, V. and Srivastava, L.P.: Analysis of imidacloprid residues in fruits, vegetables, cereals, fruit juices, and baby foods, and daily intake estimation in and around Lucknow, India, Environmental toxicology and chemistry, **32** (2013), no. 3, pp. 723–727.

[72] Lu, C.; Chang, C.-H.; Palmer, C.; Zhao, M. and Zhang, Q.: Neonicotinoid residues in fruits and vegetables: an integrated dietary exposure assessment approach, Environmental science & technology, **52** (2018), no. 5, pp. 3175–3184.

[73] Ikenaka, Y.; Fujioka, K.; Kawakami, T.; Ichise, T.; Bortey-Sam, N.; Nakayama, S.M.; Mizukawa, H.; Taira, K.; Takahashi, K. and Kato, K.: Contamination by neonicotinoid insecticides and their metabolites in Sri Lankan black tea leaves and Japanese green tea leaves, Toxicology reports, **5** (2018), pp. 744–749.

[74] Chen, D.; Liu, Z.; Barrett, H.; Han, J.; Lv, B.; Li, Y.; Li, J.; Zhao, Y. and Wu, Y.: Nationwide biomonitoring of neonicotinoid insecticides in breast milk and health risk assessment to nursing infants in the Chinese population, Journal of Agricultural and Food Chemistry, **68** (2020), no. 47, pp. 13906–13915.

[75] Chen, M.; Tao, L.; McLean, J. and Lu, C.: Quantitative analysis of neonicotinoid insecticide residues in foods: implication for dietary exposures, Journal of agricultural and food chemistry, **62** (2014), no. 26, pp. 6082–6090.

[76] Wang, X.; Goulson, D.; Chen, L.; Zhang, J.; Zhao, W.; Jin, Y.; Yang, S.; Li, Y. and Zhou, J.: Occurrence of neonicotinoids in Chinese apiculture and a corresponding risk exposure assessment, Environmental science & technology, **54** (2020), no. 8, pp. 5021–5030.

[77] Wan, Y.; Wang, Y.; Xia, W.; He, Z. and Xu, S.: Neonicotinoids in raw, finished, and tap water from Wuhan, Central China: Assessment of human exposure potential, Science of The Total Environment, **675** (2019), pp. 513–519.

[78] Sánchez-Bayo, F. and Hyne, R.V.: Detection and analysis of neonicotinoids in river waters–development of a passive sampler for three commonly used insecticides, Chemosphere, **99** (2014), pp. 143–151.

[79] Ospina, M.; Wong, L.-Y.; Baker, S.E.; Serafim, A.B.; Morales-Agudelo, P. and Calafat, A.M.: Exposure to neonicotinoid insecticides in the US general population: Data from the 2015–2016 national health and nutrition examination survey, Environmental research, **176** (2019), p. 108555.

[80] Zhang, H.; Shen, K.; Wu, R.; Li, Z.; Wang, X.; Wang, D.; Zhan, M.; Xu, W.; Gao, Y. and Lu, L.: Occurrence and distribution of neonicotinoids and characteristic metabolites in paired urine and indoor dust from young adults: Implications for human exposure, Environmental Research, **199** (2021), p. 111175.

[81] Kavvalakis, M.P.; Tzatzarakis, M.N.; Theodoropoulou, E.P.; Barbounis, E.G.; Tsakalof, A.K. and Tsatsakis, A.M.: Development and application of LC–APCI–MS method for biomonitoring of animal and human exposure to imidacloprid, Chemosphere, **93** (2013), no. 10, pp. 2612–2620.

[82] Lin, P.-C.; Lin, H.-J.; Liao, Y.-Y.; Guo, H.-R. and Chen, K.-T.: Acute poisoning with neonicotinoid insecticides: a case report and literature review, Basic & clinical pharmacology & toxicology, **112** (2013), no. 4, pp. 282–286.

[83] Wu, I.-W.; Lin, J.-L. and Cheng, E.-T.: Acute poisoning with the neonicotinoid insecticide imidacloprid in N-methyl pyrrolidone, Journal of Toxicology: Clinical Toxicology, **39** (2001), no. 6, pp. 617–621.

[84] Phua, D.H.; Lin, C.C.; Wu, M.-L.; Deng, J.-F. and Yang, C.-C.: Neonicotinoid insecticides: an emerging cause of acute pesticide poisoning, Clinical toxicology, **47** (2009), no. 4, pp. 336–341.

[85] Mohamed, F.; Gawarammana, I.; Robertson, T.A.; Roberts, M.S.; Palangasinghe, C.; Zawahir, S.; Jayamanne, S.; Kandasamy, J.; Eddleston, M. and Buckley, N.A.: Acute human self-poisoning with imidacloprid compound: a neonicotinoid insecticide, PLoS One, **4** (2009), no. 4, p. e5127.

[86] Huang, N.-C.; Lin, S.-L.; Chou, C.-H.; Hung, Y.-M.; Chung, H.-M. and Huang, S.-T.: Fatal ventricular fibrillation in a patient with acute imidacloprid poisoning, The American journal of emergency medicine, **24** (2006), no. 7, pp. 883–885.

[87] Shadnia, S. and Moghaddam, H.H.: Fatal intoxication with imidacloprid insecticide, The American journal of emergency medicine, **26** (2008), no. 5, pp. 634-e1.

[88] Todani, M.; Kaneko, T.; Hayashida, H.; Kaneda, K.; Tsuruta, R.; Kasaoka, S. and Maekawa, T.: Acute poisoning with neonicotinoid insecticide acetamiprid, Chudoku kenkyu: Chudoku Kenkyukai jun kikanshi= The Japanese journal of toxicology, **21** (2008), no. 4, pp. 387–390.

[89] Panigrahi, A.K.; Subrahmanyam, D.K.S. and Mukku, K.K.: Imidacloprid poisoning: a case report, The American journal of emergency medicine, **27** (2009), no. 2, pp. 256-e5.

[90] Karatas, A.D.: Severe central nervous system depression in a patient with acute imidacloprid poisoning, The American journal of emergency medicine, **27** (2009), no. 9, pp. 1171-e5.

[91] Imamura, T.; Yanagawa, Y.; Nishikawa, K.; Matsumoto, N. and Sakamoto, T.: Two cases of acute poisoning with acetamiprid in humans, Clinical toxicology, **48** (2010), no. 8, pp. 851–853.

[92] Iyyadurai, R.; George, I.A. and Peter, J.V.: Imidacloprid poisoning—newer insecticide and fatal toxicity, Journal of medical toxicology, **6** (2010), no. 1, pp. 77–78.

[93] Yeh, I.-J.; Lin, T.-J. and Hwang, D.-Y.: Acute multiple organ failure with imidacloprid and alcohol ingestion, The American journal of emergency medicine, **28** (2010), no. 2, pp. 255-e1.

[94] Chwaluk, P.: Acute inhalation imidacloprid poisoning–a case report, Przeglad lekarski, **67** (2010), no. 8, pp. 619–620.

[95] Forrester, M.B.: Neonicotinoid insecticide exposures reported to six poison centers in Texas, Human & experimental toxicology, **33** (2014), no. 6, pp. 568–573.

[96] Taira, K.; Aoyama, Y.; Kawakami, T.; Kamata, M. and Aoi, T.: Detection of chloropyridinyl neonicotinoid insecticide metabolite 6-chloronicotinic acid in the urine: six cases with subacute nicotinic symptoms, Chudoku kenkyu: Chudoku Kenkyukai jun kikanshi= The Japanese journal of toxicology, **24** (2011), no. 3, pp. 222–230.

[97] Taira, K.: Human neonicotinoids exposure in Japan, Jpn. J. Clin. Ecol, **23** (2014), pp. 14–24.

[98] Koureas, M.; Tsezou, A.; Tsakalof, A.; Orfanidou, T. and Hadjichristodoulou, C.: Increased levels of oxidative DNA damage in pesticide sprayers in Thessaly Region (Greece). Implications of pesticide exposure, Science of the Total Environment, **496** (2014), pp. 358–364.

[99] Mundhe, S.A.; Birajdar, S.V.; Chavan, S.S. and Pawar, N.R.: Imidacloprid poisoning: An emerging cause of potentially fatal poisoning, Indian journal of critical care medicine: peer-reviewed, official publication of Indian Society of Critical Care Medicine, **21** (2017), no. 11, p. 786.

[100] Sriapha, C.; Trakulsrichai, S.; Tongpoo, A.; Pradoo, A.; Rittilert, P. and Wananukul, W.: Acute Imidacloprid Poisoning in Thailand, Therapeutics and Clinical Risk Management, **16** (2020), p. 1081.

[101] David, D.; George, I.A. and Peter, J.V.: Toxicology of the newer neonicotinoid insecticides: imidacloprid poisoning in a human, Clinical toxicology, **45** (2007), no. 5, pp. 485–486.

[102] Pirasath, S.; Senthuran, R.; Athirayan, C.; Gevakaran, M.; Guruparan, M. and Gnanathasan, A.: Acute poisoning with acetamiprid: a case report, Journal of medical case reports, **15** (2021), no. 1, pp. 1–5.

[103] Vinod, K.V.; Srikant, S.; Thiruvikramaprakash, G. and Dutta, T.K.: A fatal case of thiacloprid poisoning, The American journal of emergency medicine, **33** (2015), no. 2, pp. 310-e5.

[104] Ramanathan, S.; Sanjeevi, G.; Narayanan, B. and Kurien, A.A.: Thiamethoxam, a Neonicotinoid Poisoning Causing Acute Kidney Injury via a Novel Mechanism, Kidney International Reports, **5** (2020), no. 7, pp. 1111–1113.

[105] Agarwal, R. and Srinivas, R.: Severe neuropsychiatric manifestations and rhabdomyolysis in a patient with imidacloprid poisoning., The American journal of emergency medicine, **25** (2007), no. 7, pp. 844–845.

[106] Marfo, J.T.; Fujioka, K.; Ikenaka, Y.; Nakayama, S.M.; Mizukawa, H.; Aoyama, Y.; Ishizuka, M. and Taira, K.: Relationship between urinary N-desmethyl-acetamiprid and typical symptoms including neurological findings: a prevalence case-control study, PloS one, **10** (2015), no. 11, p. e0142172.

[107] Kabata, R.; Nanayakkara, S.; STMLD, S.; Harada, K.H.; Chandrajith, R.; Hitomi, T.; Abeysekera, T.; Takasuga, T. and Koizumi, A.: Neonicotinoid concentrations in urine

from chronic kidney disease patients in the North Central Region of Sri Lanka, Journal of occupational health, (2015), pp. 15–0140.

[108] Keil, A.P.; Daniels, J.L. and Hertz-Picciotto, I.: Autism spectrum disorder, flea and tick medication, and adjustments for exposure misclassification: the CHARGE (CHildhood Autism Risks from Genetics and Environment) case–control study, Environmental Health, **13** (2014), no. 1, pp. 1–10.

[109] Carmichael, S.L.; Yang, W.; Roberts, E.; Kegley, S.E.; Padula, A.M.; English, P.B.; Lammer, E.J. and Shaw, G.M.: Residential agricultural pesticide exposures and risk of selected congenital heart defects among offspring in the San Joaquin Valley of California, Environmental research, **135** (2014), pp. 133–138.

[110] Yang, W.; Carmichael, S.L.; Roberts, E.M.; Kegley, S.E.; Padula, A.M.; English, P.B. and Shaw, G.M.: Residential agricultural pesticide exposures and risk of neural tube defects and orofacial clefts among offspring in the San Joaquin Valley of California, American journal of epidemiology, **179** (2014), no. 6, pp. 740–748.

[111] Hernández, A.F.; Casado, I.; Pena, G.; Gil, F.; Villanueva, E. and Pla, A.: Low level of exposure to pesticides leads to lung dysfunction in occupationally exposed subjects, Inhalation toxicology, **20** (2008), no. 9, pp. 839–849.

[112] Bhatt, P.; Huang, Y.; Zhan, H. and Chen, S.: Insight into microbial applications for the biodegradation of pyrethroid insecticides, Frontiers in microbiology, **10** (2019), p. 1778.

[113] Huang, Y.; Lin, Z.; Zhang, W.; Pang, S.; Bhatt, P.; Rene, E.R.; Kumar, A.J. and Chen, S.: New insights into the microbial degradation of D-cyphenothrin in contaminated water/soil environments, Microorganisms, **8** (2020), no. 4, p. 473.

[114] Mahapatra, B.; Adak, T.; Patil, N.K.; Pandi, G.G.P.; Gowda, G.B.; Yadav, M.K.; Mohapatra, S.D.; Rath, P.C.; Munda, S. and Jena, M.: Effect of abiotic factors on degradation of imidacloprid, Bulletin of environmental contamination and toxicology, **99** (2017), no. 4, pp. 475–480.

[115] Erguven, G.O. and Yildirim, N.: The evaluation of imidacloprid remediation in soil media by two bacterial strains, Current microbiology, **76** (2019), no. 12, pp. 1461–1466.

[116] Erguven, G.O. and Demirci, U.: Statistical evaluation of the bioremediation performance of Ochrobactrum thiophenivorans and Sphingomonas melonis bacteria on Imidacloprid insecticide in artificial agricultural field, Journal of Environmental Health Science and Engineering, **18** (2020), no. 2, p. 395.

[117] Wu, P.; Zhang, X.; Niu, T.; Wang, Y.; Liu, R. and Zhang, Y.: The imidacloprid remediation, soil fertility enhancement and microbial community change in soil by

Rhodopseudomonas capsulata using effluent as carbon source, Environmental Pollution, **267** (2020), p. 114254.

[118] Tang, H.; Li, J.; Hu, H. and Xu, P.: A newly isolated strain of Stenotrophomonas sp. hydrolyzes acetamiprid, a synthetic insecticide, Process Biochemistry, **47** (2012), no. 12, pp. 1820–1825.

[119] Rajabi, H.R.; Arjmand, H.; Kazemdehdashti, H. and Farsi, M.: A comparison investigation on photocatalytic activity performance and adsorption efficiency for the removal of cationic dye: quantum dots vs. magnetic nanoparticles, Journal of environmental chemical engineering, **4** (2016), no. 3, pp. 2830–2840.

[120] Li, Y.; Li, Y.; Liu, Y. and Ward, T.J.: Photodegradation of clothianidin and thiamethoxam in agricultural soils, Environmental Science and Pollution Research, **25** (2018), no. 31, pp. 31318–31325.

[121] Gupta, S.; Gajbhiye, V.T. and Gupta, R.K.: Effect of light on the degradation of two neonicotinoids viz acetamiprid and thiacloprid in soil, Bulletin of environmental contamination and toxicology, **81** (2008), no. 2, pp. 185–189.

[122] Banić, N.D.; Abramović, B.F.; Šojić, D.V.; Krstić, J.B.; Finčur, N.L. and Bočković, I.P.: Efficiency of neonicotinoids photocatalytic degradation by using annular slurry reactor, Chemical Engineering Journal, **286** (2016), pp. 184–190.

[123] Acero, J.L.; Real, F.J.; Benitez, F.J. and Matamoros, E.: Degradation of neonicotinoids by UV irradiation: Kinetics and effect of real water constituents, Separation and Purification Technology, **211** (2019), pp. 218–226.

[124] Meagher, R.B.: Phytoremediation of toxic elemental and organic pollutants, Current opinion in plant biology, **3** (2000), no. 2, pp. 153–162.

[125] Vangronsveld, J.; Herzig, R.; Weyens, N.; Boulet, J.; Adriaensen, K.; Ruttens, A.; Thewys, T.; Vassilev, A.; Meers, E. and Nehnevajova, E.: Phytoremediation of contaminated soils and groundwater: lessons from the field, Environmental Science and Pollution Research, **16** (2009), no. 7, pp. 765–794.

[126] Zhang, Y.; He, P.; Zhou, L.; Dong, F.; Yang, D.; Lei, H.; Du, L.; Jia, L. and Zhou, S.: Optimized terbium doped Ti/PbO2 dimensional stable anode as a strong tool for electrocatalytic degradation of imidacloprid waste water, Ecotoxicology and environmental safety, **188** (2020), p. 109921.

[127] Rózsa, G.; Náfrádi, M.; Alapi, T.; Schrantz, K.; Szabó, L.; Wojnárovits, L.; Takács, E. and Tungler, A.: Photocatalytic, photolytic and radiolytic elimination of imidacloprid

from aqueous solution: reaction mechanism, efficiency and economic considerations, Applied Catalysis B: Environmental, **250** (2019), pp. 429–439.

[128] Yin, K.; Deng, Y.; Liu, C.; He, Q.; Wei, Y.; Chen, S.; Liu, T. and Luo, S.: Kinetics, pathways and toxicity evaluation of neonicotinoid insecticides degradation via UV/chlorine process, Chemical Engineering Journal, **346** (2018), pp. 298–306.

[129] Xu, K.; Ben, W.; Ling, W.; Zhang, Y.; Qu, J. and Qiang, Z.: Impact of humic acid on the degradation of levofloxacin by aqueous permanganate: Kinetics and mechanism, Water research, **123** (2017), pp. 67–74.

[130] Yang, J.-F.; He, M.; Wu, T.-F.; Hao, A.-P.; Zhang, S.-B.; Chen, Y.-D.; Zhou, S.-B.; Zhen, L.-Y.; Wang, R. and Yuan, Z.-L.: Sulfadiazine oxidation by permanganate: Kinetics, mechanistic investigation and toxicity evaluation, Chemical Engineering Journal, **349** (2018), pp. 56–65.

[131] Jiang, X.; Song, D.; Wang, D.; Zhang, R.; Fang, Q.; Sun, H. and Kong, F.: Eliminating imidacloprid and its toxicity by permanganate via highly selective partial oxidation, Ecotoxicology and environmental safety, **191** (2020), p. 110234.

[132] Vymazal, J. and Březinová, T.: The use of constructed wetlands for removal of pesticides from agricultural runoff and drainage: a review, Environment international, **75** (2015), pp. 11–20.

[133] Pilon-Smits, E.: Phytoremediation, Annu. Rev. Plant Biol., **56** (2005), pp. 15–39.

[134] Brix, H.: Do macrophytes play a role in constructed treatment wetlands?, Water science and technology, **35** (1997), no. 5, pp. 11–17.

[135] Main, A.R.; Michel, N.L.; Headley, J.V.; Peru, K.M. and Morrissey, C.A.: Ecological and landscape drivers of neonicotinoid insecticide detections and concentrations in Canada's prairie wetlands, Environmental science & technology, **49** (2015), no. 14, pp. 8367–8376.

[136] Hamada, A.; Wahl, G.D.; Nesterov, A.; Nakao, T.; Kawashima, M. and Banba, S.: Differential metabolism of imidacloprid and dinotefuran by Bemisia tabaci CYP6CM1 variants, Pesticide biochemistry and physiology, **159** (2019), pp. 27–33.

[137] Zhang, P.; Ren, C.; Sun, H. and Min, L.: Sorption, desorption and degradation of neonicotinoids in four agricultural soils and their effects on soil microorganisms, Science of the Total Environment, **615** (2018), pp. 59–69.

[138] Guo, L.; Dai, Z.; Guo, J.; Yang, W.; Ge, F. and Dai, Y.: Oligotrophic bacterium Hymenobacter latericoloratus CGMCC 16346 degrades the neonicotinoid imidacloprid in surface water, Amb Express, **10** (2020), no. 1, pp. 1–13.

[139] Guzsvány, V.; Kádár, M.; Gaál, F.; Tóth, K. and Bjelica, L.: Rapid Differential Pulse Polarographic Determination of Thiamethoxam in Commercial Formulations and some Real Samples, Microchimica Acta, **154** (2006), no. 3, pp. 321–328.

[140] Guzsvány, V.; Kádár, M.; Gaál, F.; Bjelica, L. and Tóth, K.: Bismuth Film Electrode for the Cathodic Electrochemical Determination of Thiamethoxam, Electroanalysis, **18** (2006), nos. 13–14, pp. 1363–1371.

[141] Baś, B.; Jakubowska, M. and Górski, Ł.: Application of renewable silver amalgam annular band electrode to voltammetric determination of vitamins C, B1 and B2, Talanta, **84** (2011), no. 4, pp. 1032–1037.

[142] Danhel, A. and Barek, J.: Amalgam Electrodes in Organic Electrochemistry, Current Organic Chemistry, **15** (2011), no. 17, pp. 2957–2969.

[143] Putek, M.; Guzsvány, V.; Tasić, B.; Zarębski, J. and Bobrowski, A.: Renewable Silver-Amalgam Film Electrode for Rapid Square-Wave Voltammetric Determination of Thiamethoxam Insecticide in Selected Samples, Electroanalysis, **24** (2012), no. 12, pp. 2258–2266.

[144] Chorti, P.; Fischer, J.; Vyskocil, V.; Economou, A. and Barek, J.: Voltammetric Determination of Insecticide Thiamethoxam on Silver Solid Amalgam Electrode, Electrochimica Acta, **140** (2014), pp. 5–10.

[145] Ajermoun, N.; Farahi, A.; Lahrich, S.; Bakasse, M.; Saqrane, S. and El Mhammedi, M.A.: Electrocatalytic activity of the metallic silver electrode for thiamethoxam reduction: application for the detection of a neonicotinoid in tomato and orange samples, Journal of the Science of Food and Agriculture, **99** (2019), no. 9, pp. 4407–4413.

[146] Navaratne, A. and Susantha, N.: An Electroanalytical Sensor for the Detection of Gramoxone (Paraquat), Analytical Letters, **33** (2000), no. 8, pp. 1491–1499.

[147] Manisankar, P.; Vedhi, C. and Selvanathan, G.: Electrochemical determination of methyl parathion using a modified electrode, Toxicological & Environmental Chemistry, **85** (2003), nos. 4–6, pp. 233–241.

[148] Brett, C.M.A.: Electrochemical sensors for environmental monitoring. Strategy and examples, Pure and Applied Chemistry, **73** (2001), no. 12, pp. 1969–1977.

[149] Furno, F.; Morley, K.S.; Wong, B.; Sharp, B.L.; Arnold, P.L.; Howdle, S.M.; Bayston, R.; Brown, P.D.; Winship, P.D. and Reid, H.J.: Silver nanoparticles and polymeric medical devices: a new approach to prevention of infection?, Journal of Antimicrobial Chemotherapy, **54** (2004), no. 6, pp. 1019–1024.

[150] Mao, C.F. and Vannice, M.A.: Formaldehyde Oxidation over Ag Catalysts, Journal of Catalysis, **154** (1995), no. 2, pp. 230–244.

[151] Hu, J.; Zhao, B.; Xu, W.; Li, B. and Fan, Y.: Surface-enhanced Raman spectroscopy study on the structure changes of 4-mercaptopyridine adsorbed on silver substrates and silver colloids, Spectrochimica Acta Part A: Molecular and Biomolecular Spectroscopy, **58** (2002), no. 13, pp. 2827–2834.

[152] Jia, H.; Zeng, J.; Song, W.; An, J. and Zhao, B.: Preparation of silver nanoparticles by photo-reduction for surface-enhanced Raman scattering, Thin Solid Films, **496** (2006), no. 2, pp. 281–287.

[153] Aslan, K.; Holley, P. and Geddes, C.D.: Metal-enhanced fluorescence from silver nanoparticle-deposited polycarbonate substrates, Journal of Materials Chemistry, **16** (2006), no. 27, pp. 2846–2852.

[154] Kumaravel, A. and Chandrasekaran, M.: Nanosilver/surfactant modified glassy carbon electrode for the sensing of thiamethoxam, Sensors and Actuators B: Chemical, **174** (2012), pp. 380–388.

[155] Norouzi, P.; Ghaheri, N.; Aghazadeh, M.; Mofidi, Z. and Larijani, B.: Sensitive Electrochemical Measurement of Thiamethoxam on Nanocomposite Coated Carbon Paste Using FFT Coulometric Admittance Voltammetry and Flow Injection Analysis, Int. J. Electrochem. Sci, **12** (2017), pp. 8847–8859.

[156] Chen, S.; Li, L.; Wen, Y.; Yang, G.; Liu, G.; Yi, Y.; Shang, Q.; Yang, X. and Cai, S.: Voltammetric analysis of thiamethoxam based on inexpensive thick-walled moso bamboo biochar nanocomposites, Int. J. Electrochem. Sci, **14** (2019), pp. 10848–10861.

[157] Huang, H.; Yang, S.; Vajtai, R.; Wang, X. and Ajayan, P.M.: Pt-decorated 3D architectures built from graphene and graphitic carbon nitride nanosheets as efficient methanol oxidation catalysts, Advanced Materials, **26** (2014), no. 30, pp. 5160–5165.

[158] Ma, T.Y.; Dai, S.; Jaroniec, M. and Qiao, S.Z.: Graphitic carbon nitride nanosheet–carbon nanotube three-dimensional porous composites as high-performance oxygen evolution electrocatalysts, Angewandte Chemie, **126** (2014), no. 28, pp. 7409–7413.

[159] Li, Y.; Zhang, H.; Liu, P.; Wang, D.; Li, Y. and Zhao, H.: Cross-linked g-C3N4/rGO nanocomposites with tunable band structure and enhanced visible light photocatalytic activity, Small, **9** (2013), no. 19, pp. 3336–3344.

[160] Zhu, Y.-P.; Li, M.; Liu, Y.-L.; Ren, T.-Z. and Yuan, Z.-Y.: Carbon-doped ZnO hybridized homogeneously with graphitic carbon nitride nanocomposites for

photocatalysis, The Journal of Physical Chemistry C, **118** (2014), no. 20, pp. 10963–10971.

[161] Hou, Y.; Zuo, F.; Dagg, A.P.; Liu, J. and Feng, P.: Branched WO3 nanosheet array with layered C3N4 heterojunctions and CoOx nanoparticles as a flexible photoanode for efficient photoelectrochemical water oxidation, Advanced materials, **26** (2014), no. 29, pp. 5043–5049.

[162] Zhang, J.; Zhang, M.; Yang, C. and Wang, X.: Nanospherical carbon nitride frameworks with sharp edges accelerating charge collection and separation at a soft photocatalytic interface, Advanced Materials, **26** (2014), no. 24, pp. 4121–4126.

[163] Cheng, C.; Huang, Y.; Wang, J.; Zheng, B.; Yuan, H. and Xiao, D.: Anodic electrogenerated chemiluminescence behavior of graphite-like carbon nitride and its sensing for rutin, Analytical chemistry, **85** (2013), no. 5, pp. 2601–2605.

[164] Zhuang, J.; Lai, W.; Xu, M.; Zhou, Q. and Tang, D.: Plasmonic AuNP/g-C3N4 nanohybrid-based photoelectrochemical sensing platform for ultrasensitive monitoring of polynucleotide kinase activity accompanying DNAzyme-catalyzed precipitation amplification, ACS Applied Materials & Interfaces, **7** (2015), no. 15, pp. 8330–8338.

[165] Zou, J.; Wu, S.; Liu, Y.; Sun, Y.; Cao, Y.; Hsu, J.-P.; Wee, A.T.S. and Jiang, J.: An ultrasensitive electrochemical sensor based on 2D g-C3N4/CuO nanocomposites for dopamine detection, Carbon, **130** (2018), pp. 652–663.

[166] Ganesamurthi, J.; Keerthi, M.; Chen, S.-M. and Shanmugam, R.: Electrochemical detection of thiamethoxam in food samples based on Co3O4 Nanoparticle@Graphitic carbon nitride composite, Ecotoxicology and Environmental Safety, **189** (2020), p. 110035.

[167] Guzsvány, V.J.; Gaál, F.F.; Bjelica, L.J. and Ökrész, S.N.: Voltammetric determination of imidacloprid and thiamethoxam, Journal of the Serbian Chemical Society, **70** (2005), no. 5, pp. 735–743.

[168] Shao, Y.; Wang, J.; Wu, H.; Liu, J.; Aksay, I.A. and Lin, Y.: Graphene based electrochemical sensors and biosensors: a review, Electroanalysis: An International Journal Devoted to Fundamental and Practical Aspects of Electroanalysis, **22** (2010), no. 10, pp. 1027–1036.

[169] Geim, A.K. and Novoselov, K.S.: The rise of graphene, Nanoscience and technology: a collection of reviews from nature journals, World Scientific, 2010, pp. 11–19.

[170] Park, S. and Ruoff, R.S.: Chemical methods for the production of graphenes, Nature nanotechnology, **4** (2009), no. 4, pp. 217–224.

[171] Schniepp, H.C.; Li, J.-L.; McAllister, M.J.; Sai, H.; Herrera-Alonso, M.; Adamson, D.H.; Prud'homme, R.K.; Car, R.; Saville, D.A. and Aksay, I.A.: Functionalized single graphene sheets derived from splitting graphite oxide, The journal of physical chemistry B, **110** (2006), no. 17, pp. 8535–8539.

[172] Stankovich, S.; Dikin, D.A.; Piner, R.D.; Kohlhaas, K.A.; Kleinhammes, A.; Jia, Y.; Wu, Y.; Nguyen, S.T. and Ruoff, R.S.: Synthesis of graphene-based nanosheets via chemical reduction of exfoliated graphite oxide, carbon, **45** (2007), no. 7, pp. 1558–1565.

[173] McCreery, R.L.: Advanced carbon electrode materials for molecular electrochemistry, Chemical reviews, **108** (2008), no. 7, pp. 2646–2687.

[174] Banks, C.E.; Davies, T.J.; Wildgoose, G.G. and Compton, R.G.: Electrocatalysis at graphite and carbon nanotube modified electrodes: edge-plane sites and tube ends are the reactive sites, Chemical Communications, (2005), no. 7, pp. 829–841.

[175] Dumitrescu, I.; Unwin, P.R. and Macpherson, J.V.: Electrochemistry at carbon nanotubes: perspective and issues, Chemical Communications, (2009), no. 45, pp. 6886–6901.

[176] Wang, J.: Carbon-nanotube based electrochemical biosensors: A review, Electroanalysis: An International Journal Devoted to Fundamental and Practical Aspects of Electroanalysis, **17** (2005), no. 1, pp. 7–14.

[177] Urbanová, V.; Bakandritsos, A.; Jakubec, P.; Szambó, T. and Zbořil, R.: A facile graphene oxide based sensor for electrochemical detection of neonicotinoids, Biosensors and Bioelectronics, **89** (2017), pp. 532–537.

[178] Oliveira, A.E.F.; Bettio, G.B. and Pereira, A.C.: An Electrochemical Sensor Based on Electropolymerization of ß-Cyclodextrin and Reduced Graphene Oxide on a Glassy Carbon Electrode for Determination of Neonicotinoids, Electroanalysis, **30** (2018), no. 9, pp. 1918–1928.

[179] Yang, Y.; Cao, Y.; Wang, X.; Fang, G. and Wang, S.: Prussian blue mediated amplification combined with signal enhancement of ordered mesoporous carbon for ultrasensitive and specific quantification of metolcarb by a three-dimensional molecularly imprinted electrochemical sensor, Biosensors and Bioelectronics, **64** (2015), pp. 247–254.

[180] Yola, M.L.; Eren, T. and Atar, N.: A sensitive molecular imprinted electrochemical sensor based on gold nanoparticles decorated graphene oxide: application to selective determination of tyrosine in milk, Sensors and Actuators B: Chemical, **210** (2015), pp. 149–157.

[181] Xie, T.; Zhang, M.; Chen, P.; Zhao, H.; Yang, X.; Yao, L.; Zhang, H.; Dong, A.; Wang, J. and Wang, Z.: A facile molecularly imprinted electrochemical sensor based on graphene: application to the selective determination of thiamethoxam in grain, RSC Advances, **7** (2017), no. 62, pp. 38884–38894.

[182] Zhai, X.; Zhang, H.; Zhang, M.; Yang, X.; Gu, C.; Zhou, G.; Zhao, H.; Wang, Z.; Dong, A. and Wang, J.: A rapid electrochemical monitoring platform for sensitive determination of thiamethoxam based on β–cyclodextrin-graphene composite, Environmental Toxicology and Chemistry, **36** (2017), no. 8, pp. 1991–1997.

[183] Papp, Z.J.; Guzsvány, V.J.; Kubiak, S.; Bobrowski, A. and Bjelica, L.J.: Voltammetric determination of the neonicotinoid insecticide thiamethoxam using a tricresyl phosphate-based carbon paste electrode, Journal of the Serbian Chemical Society, **75** (2010), no. 5, pp. 681–687.

Chapter II

Physiological effect of thiamethoxam on Zea mays and its electrochemical detection

I. Introduction

The intensive action to protect crops from the use of many organic pesticides has increased in recent years. These compounds can be natural or they can be synthetically produced. They may belong to any one of the several pesticide classes in particular: organochlorines, carbamates, organophosphates, pyrethroids, and neonicotinoids. The great attention was placed on neonicotinoid insecticides, such as acetamiprid, imidacloprid, thiacloprid, and thiamethoxam, as these all act on the insect nicotinic (acetylcholine) receptor (nAChR) [1, 2]. Actually, neonicotinoid insecticides are widely used in agriculture and the seed coating is used all over the world to ensure a broad range pest control in several crops, including corn (*Zea mays* L.) [3] in Ontario with over 99 % of maize (corn), 60–80 % of soybean, 95 % of dry bean, 25 % of winter wheat and 100 % of canola crop areas planted with a neonicotinoid seed treatment in 2013 [4]. Neonicotinoids are water-soluble compounds and systemically translocate to plant tissues protecting young plants from root-eating insects and, after emergence, also from sucking insects – such as leafhoppers and aphids – responsible for the transmission of plant viruses. Among these molecules, we focus on thiamethoxam (3- (2-chlorin-1,3-thiazol-5-ylmethyl) -5-methyl-1,3,5-oxadiazinane 4-ylidene (nitro) amine) broad spectrum of action at low concentrations [5–8]. It is the second-largest-selling neonicotinoid, and is registered for 115 crops, such as vegetables, potatoes, rice, cotton, fruits, tobacco and cereals [9]. Thiamethoxam (TMX) is a nitroguanidine neonicotinoid that acts agonistically on nicotinic acetylcholine receptors in the insect central nervous system [10]. Due to its intensive use, high water solubility (4.1 g L^{-1} at 25 °C) and stability, residues of TMX persisting in the environment have adverse effects [11]. As a result, there is an increasing need to develop a methodology for the determination of thiamethoxam in food, agricultural and environmental samples. The need for sensitive and selective detectors for this compound is of crucial importance. However, the high cost of conventional photometric and chromatographic methods [12–14] indicates a need for more sensitive and fast analytical techniques. To meet this need, electrochemistry arises as an alternative that combines simplicity, speed, sensitivity, and specificity, using modified electrodes [15–19]. The use of these electrodes has registered considerable momentum during the last two decades undergoing a not insignificant impulse notably in the field of electrocatalysis [18, 20, 21].

This chapter described the electrocatalytic effect of metallic silver electrode towards the reduction of TMX insecticide, as well as presented a procedure for the cathodic electrochemical determination of thiamethoxam in *Zea mays* seedling following exposure under laboratory conditions, and the evaluation of this insecticide effect on plant seedling growth. In addition,

this chapter focus on assessment of the bioaccumulation of thiamethoxam in *Zea mays* seeds and seedlings using square wave voltammetry (SWV) after optimization of the experimental conditions.

II. Experiment section

1) Chemicals reagents and instruments

Thiamethoxam, purchased from Syngenta International, was used to treat the maize seeds samples. A stock solution of 5.0×10^{-2} mol L^{-1} thiamethoxam was prepared. Experiments were carried out using TMX with several doses (5.0×10^{-4}, 1.0×10^{-3}, 5.0×10^{-3}, 3.4×10^{-2}, 5.0×10^{-2} mol L^{-1}). Sodium hydroxide, phosphoric acid, acetic and boric acid were purchased from Merck (Darmstadt, Germany), Fluka (St. Gallen, Switzerland), and Riedel de Haen (Seelze, Germany). All chemicals employed were of analytical reagent grade.

The electrochemical measurements were investigated using a potentiostat (model PGZ 100, Eco Chemie B.V, Utrecht, the Netherlands) electrochemical analyzer operated via voltamaster 4 software. The solution was transferred to the conventional three-electrode electrochemical cell to analyze the thiamethoxam accumulated in *Zea mays* plant using metallic silver as a working electrode, platinum wire and Ag/AgCl (saturated KCl) as auxiliary and reference electrodes respectively. The pH solution was controlled with a pH-meter (SensION™, (pH31)). All measurements were carried out at 25°C.

2) Germination and growth tests of *Zea mays* exposed to TMX

Seeds germination test was carried out in incubator (22 ± 2 °C) in dark under sterile conditions for five days. The seeds were disinfected with sodium hypochlorite solution 10 % **(v/v)** for ten min. Then, washed thoroughly with sterile distilled water. Twenty corn seeds are placed in each petri dish (diameter: 9 cm) between two layers of filter paper and regularly soaked with adequate treatment solutions during the experiment time. This experiment is repeated three times for each treatment. The exposure of the seeds was performed on five treatments (5.0×10^{-4}, 1.0×10^{-3}, 5.0×10^{-3}, 3.4×10^{-2}, 5.0×10^{-2} mol L^{-1}). In parallel, a control sample was prepared under the same conditions but soaked with only sterile distilled water. At the end of incubation (5 days), the rate of germination was determined and the seeds germinated were transferred in plastic pots (diameter 8 cm) containing a mixture of peat and 40 % sand, in order to follow the growth of seedlings. The experiment was carried out in a greenhouse with natural photoperiod and temperature in continuous exposure to different concentrations of TMX. At the end of the

experiment (10 days), TMX bioaccumulation and histological structure were evaluated and biometric parameters were measured: root and plant lengths.

3) Extraction and quantification of TMX in plant

Before starting the TMX determination in *Zea mays* plant, we will be presented a preliminary voltammetric study to specify the electrochemical reactivity of the silver electrode in the electrolytic solution containing only the TMX.

The extraction of TMX in the plant was carried out according to the method described by Gonçalves da Rocha et al., 2012 [22] using only water purified. We extracted TMX in 2g of seeds and of each part of the seedlings (roots, stems, and leaves) by grinding with 100 mL of ultra-pure water. The resulting residue was sonicated (3 kHz × 40 min) and centrifuged (4000 RPM × 10 min). After three extractions (100, 100 and 50 mL), the resulting aqueous phase was concentrated with a rotary evaporator at 80 °C, to about 5 mL of water. The concentrated volume was brought to 25 mL with water. To ensure the best conditions for the TMX analysis, the pH of the solution was controlled by adding the Britton-Robinson pH 10.4 buffer components. The solution was transferred to the electrochemical cell for thiamethoxam detection in *Zea mays* plant on the metallic silver electrode using SWV.

4) Histological test

In order to evaluate the effect of TMX on the structure of root tissues and to understand this effect on roots formation and development, a histological study was done through primary root cross-sections. After five days of germination, cross-sections were taken at the level of the piliferous zone. The green carmino of Mirande double coloration was used in the preparation of transversals. Briefly, the root cuts were washed by the sodium hypochlorite for ten minutes, in distilled water for 5 min and in acetic acid 1% (v/v) for 3 min. Then, they were colored with the green carmino for 5 min. The green carmine of Mirande is a mixture of two dyes: carmine alum (9/10) which colors the cell membranes in pink-red, and the iodine green that colors the lignified membrane in green. At the end of preparation, the cuts were rinsed with distilled water for 2 min. Finally, these histological root cuts were microscopically examined.

III. Results and discusion

A) Electrochemistry of thiamethoxam insecticide

1) Electrochemical behaviour of thiamethoxam

The TMX electro-reduction was assessed using its cyclic voltammograms (CVs) at GCE, CPE and MSE electrodes in BR buffer (pH 10.4) containing 1.0×10^{-3} mol L^{-1} of TMX in the range from 00 to -1600 mV at a scan rate of 50 mV s^{-1} (Figure 1). The electrochemical parameters toward TMX electro-reduction obtained from (CVs) are summarized in (Table 1). The peak potential of TMX reduction at metallic silver electrode (MSE) (-1164 mV) have been decreased slightly respect to glassy carbon electrode (GCE) (-1316 mV) and carbon paste electrode (CPE) (-1186 mV). While not only the more positive potential shift observed for these electrodes, but also the current of cathodic peak increased significantly, so it can be concluded that metallic silver electrode is more efficient for TMX electro-reduction.
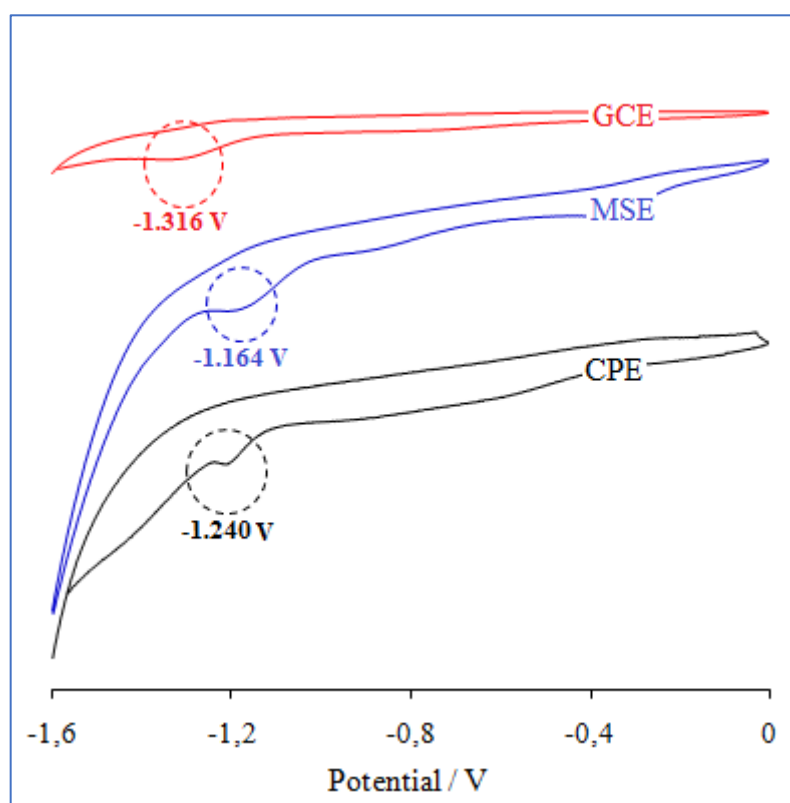
Figure 1: Cyclic voltammograms of the various electrodes in the potential range 00 to -1600 mV vs Ag/AgCl with a scan rate of 50 mV s-1, 1.0×10−3 mol L−1 of TMX in B-R buffer (pH 10.4).

Table 1: Electrochemical characterization of TMX electro-reduction.

electrode	E_p (V)	I_P (μA cm^{-2})
CPE	-1.240	10.9
GCE	-1.316	12.19
MSE	-1.164	31.09

To evaluate the kinetics of the electrodes, Tafel plots were considered using potentiodynamic pseudo-steady state polarization of 1.0×10^{-3} mol L^{-1} of TMX in BR buffer (pH 10.4) solution at a low scan rate of 20 mV. s^{-1} and shown in (Figure 2).
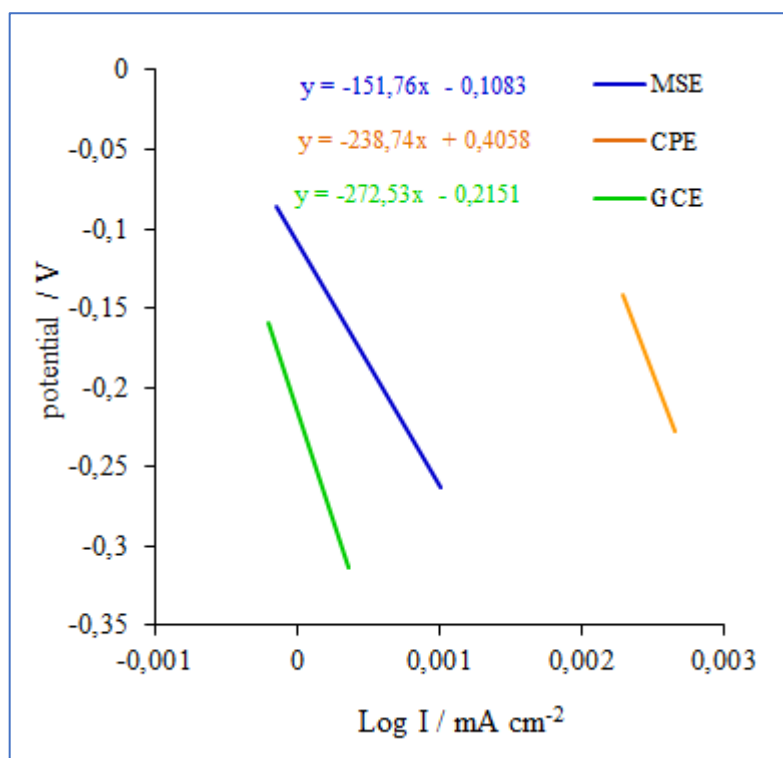
Figure 2: *Tafel plots for TMX reduction on the various electrodes at a scan rate of 20 mV s−1, 1.0×10−3 mol L−1 of TMX in B-R buffer (pH 10.4).*

Table 2: *Tafel slopes, exchange current densities, and charge transfer coefficients of various electrodes for TMX electro-reduction at a scan rate of 20 mV s−1.*

Electrode	Tafel slope (mV.dec^{-1})	a	i_0 (mA cm^{-2})	α
CPE	-238.74	0.404	1.0041	0.00025
GCE	-272.53	-0.2151	0.998	0.270
MSE	-151.76	-0.1083	0.998	0.536

The kinetic parameters, a, b, i_0, α values for TMX electro-reduction by the different three electrodes are reported in (Table 2). The kinetic parameters of TMX for three electrodes can be calculated by the following expressions [23]:

$$\eta = a + b \, log|i|$$

58

$$\log i_0 = -\frac{a}{b}$$

$$\alpha = -\frac{2.303RT}{bF}$$

Where η is the overpotential, i is the current density (mA cm^{-2}), a is the Tafel intercept and b is the Tafel slope. i_0 is the exchange current density, α is the charge transfer coefficient, F is the Faraday constant (96.487 A s mol^{-1}), R is the gas constant (8.314 J K^{-1} mol^{-1}), and T is the absolute temperature (K).

Tafel slope is an inherent property of electrocatalytic material. It is determined by the rate-limiting step of TMX electro-reduction. The determination and interpretation of Tafel slope are important for elucidation of the electrocatalytic activity of these electrodes towards TMX. The Tafel slope is -272.53, -229.04, and -151.76 mV.dec^{-1} for GCE, CPE and MSE, respectively. The Tafel slope of metallic silver electrode is smaller than that of other electrodes, which indicates that the step of TMX electro-reduction on metallic silver electrode is faster than other electrodes. The exchange current density is found from Tafel curve by extrapolating the linear fitted Tafel line where the over-potential equals zero. The exchange current density of GCE, CPE and MSE electrodes are 0.998, 1.004, and 0.998 (mA cm^{-2}), respectively. The charge transfer coefficient for metallic silver electrode is higher than that of other electrodes, which improved the electron-transfer rate between molecule and the electrode. The higher charge transfer coefficient of metallic silver electrode will lead to a faster increment of reaction rate with increasing overpotential. The higher charge transfer coefficient and lower Tafel slope observed on the metallic silver electrode is a sign of greater electrocatalytic activity.

Electro-catalytic activity of the electrodes toward TMX electro-reduction was also investigated by electrochemical impedance spectroscopy (EIS). The EIS experiments of the TMX in BR buffer (pH 10.38) have been performed and serve as initial insights into the electron transfer processes at the electrodes. Nyquist plots (imaginary values Z_{imag} versus real values Z_{real}) were obtained both at the open circuit potential and at overpotential value -1100 mV for the three electrodes (Figure 3). Lower charge-transfer resistance was observed on the metallic silver electrode, indicating the good conductivity of this electrode. These results illustrate the electrocatalytic activity of metallic silver electrode for TMX electro-reduction can be attributed to the high rate of electron transfer compared with other electrodes.
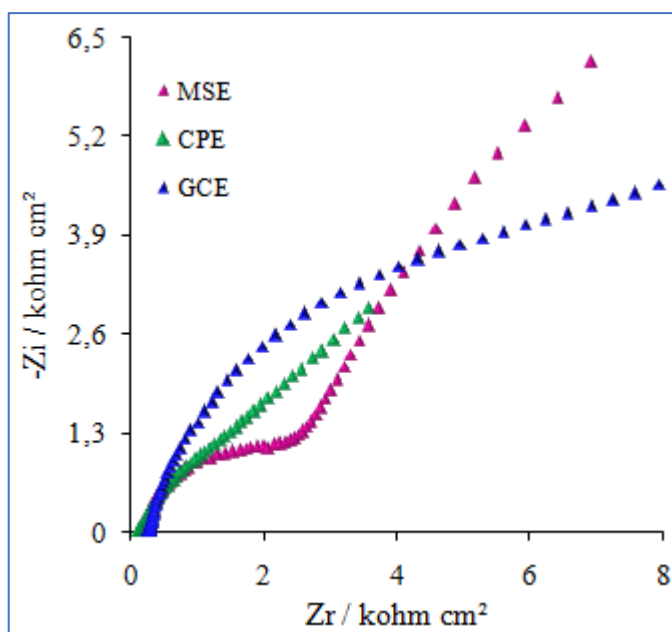
Figure 3: *EIS Nyquist plots obtained for MSE, GCE and CPE electrodes in B-R buffer (pH 10.4) containing 1.0 ×10−3 mol L−1 of TMX.*

The electroanalysis of TMX on the silver electrode was investigated, using square wave voltammetry, in electrolytic support containing TMX. Several electrolytes support have been tested to evaluate the electrochemical reduction of TMX in particular phosphate buffer solution (pH 7.0 and 8.0), acetate buffer (pH 4.0), hydrochloric acid and britton robinson buffer (pH 2.0 to pH 12.0). The best resolution is obtained using britton robinson (pH 10.4). Figure 4A shows a voltammogram of 1.0×10^{-3} mol L^{-1} of TMX, recorded in the potential ranging from 00 to -1500 mV in a britton-robinson (B-R) buffer (pH 10.4). No obvious redox peaks were observed (Blank) in the absence of TMX. While in the presence of TMX, a cathodic peak near the potential of -1196 mV was observed and is attributed to the reduction of the functional group (NO$_2$) of TMX [21].

In the literature, Kumaravel and Chandrasekaran, 2012 [18] reported that the nitro group of TMX is reduced to give the hydroxylamine functional group. Jan Fischer et *al.* 2011 [24] also reported that, in the alkaline media, the nitro functional group of nitroaromatic compounds could easily be transferred to the (NHOH) group corresponding to 4e-. With the same vision, it is thought that the same mechanism of electron transfer can be applied in the reduction of TMX. The recorded response depends on parameters of the square potential. Indeed, several parameters are taken into consideration, namely, the amplitude, the duration of the step and the duration of the pulse. All experiments are examined in a B-R buffer (pH 10.4) solution containing 1.0×10^{-3} mol L^{-1} TMX. Indeed, we find that the intensity of the cathodic current of

TMX varies with the parameters studied. The optimal response is obtained at 10 mV, 1 ms and 50 ms corresponds to the amplitude, the duration of the step and the duration of the pulse, respectively. The choice of these optimal values is based on peak intensity, background noise, and signal resolution.
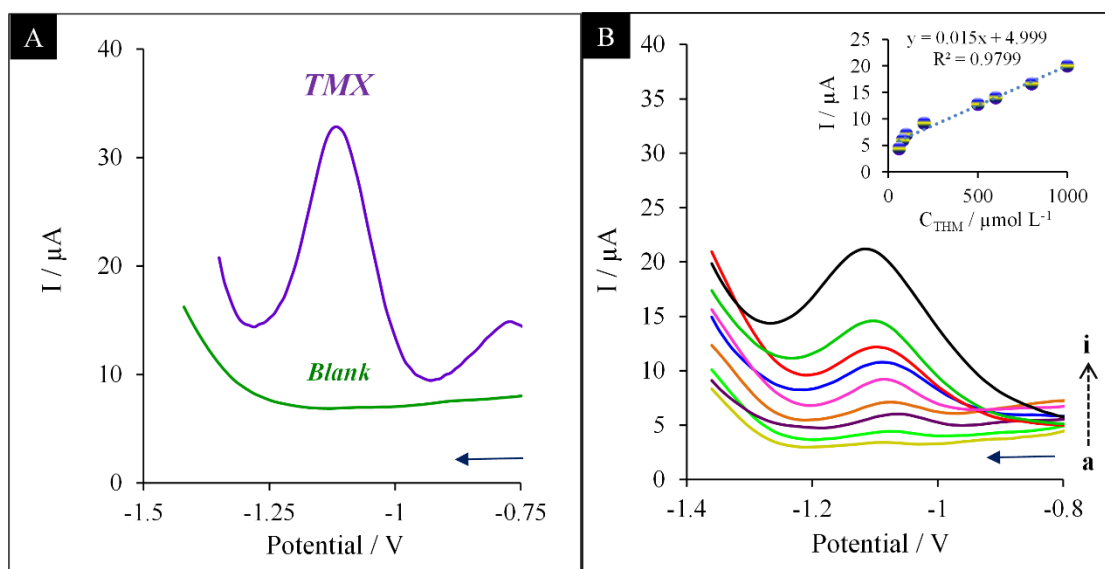
Figure 4: (A) Square wave voltammetric response of TMX 1.0×10-3 mol L-1 at metallic silver electrode in BR buffer pH 10.4. (B) Square-wave voltammetric response of various concentrations of TMX at metallic silver electrode in B-R buffer (pH 10.4): (a) 5.0×10-5 m.

After optimization of the square wave potential variables, we proceed by plotting the calibration curve. Figure 4B shows that the intensity of the current peak varies linearly with thiamethoxam in the concentration range from 5.0×10^{-5} to 1.0×10^{-3} mol L^{-1} according to equation 1: $I_{pc} = 15047$ [TMX] + 4.999 (R² = 0.97). The standard deviation (SD) is calculated after height measurements in the electrolytic solution in the absence of TMX according to the Miller et al. relation [25]. The calculated value of SD is used to calculate the detection limit (LOD, 3) using the signal-to-noise ratio equal to 3. Indeed, its value equal to 9.58×10^{-6} mol L^{-1}. The precision is 2.67 % for a solution containing 3.5×10^{-4} mol L^{-1} of TMX.

2) Calibration graphs of TMX in Zea mays seeds and seedlings

Under the optimized experimental electrochemical conditions, the SWV is applied for the determination of TMX in the extract of *Zea mays* seeds and seedling (roots, stems, and leaves). No trace is detected in the three samples of the *Zea mays* of the control (Figure 5). For this, we proceeded by the contamination of the plant by different concentrations of TMX. The results

show that, for all three samples of *Zea mays*, the intensity of the cathodic peak current increases linearly as the concentration of TMX increases in the range from 5.0×10^{-5} mol L^{-1} to 1.0×10^{-3} mol L^{-1}. The detection limits of TMX are 1.504×10^{-5}, 2.240×10^{-5} and 1.420×10^{-5} mol L^{-1} obtained respectively in roots, stems and leaves. The precision in the samples of the plant does not exceed 4.3 % in the plant samples contained 3.5×10^{-4} mol L^{-1} of the TMX.
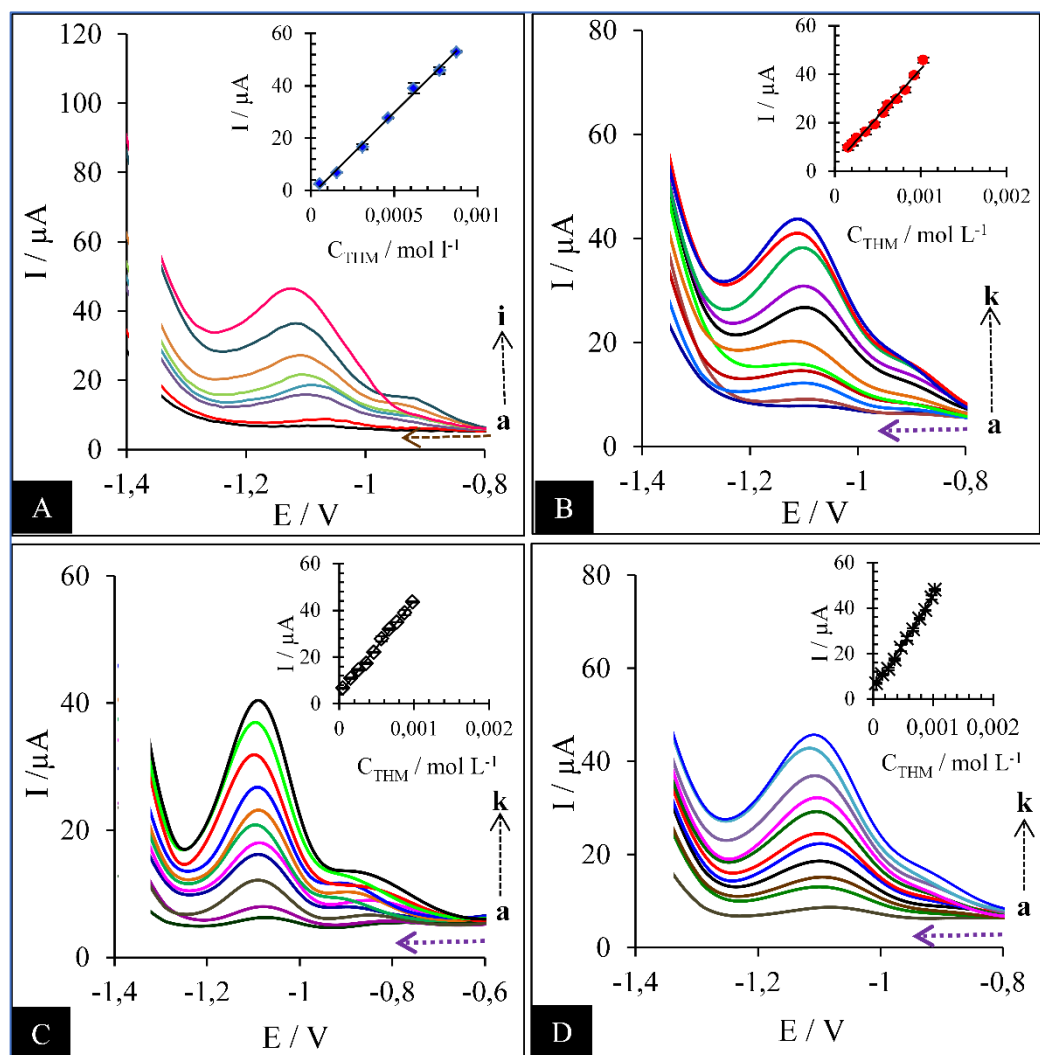
Figure 5: Calibration curves of TMX in (A) seeds, (B) roots, (C) stems and (D) leaves of Zea mays extract using SWV method at metallic silver electrode in the concentration range of 5.0×10−5 mol L-1 to 1.0×10−3 mol L−1 TMX. Inset shows the calibration graph.

B) Physiological effect of thiamethoxam on Zea mays

1) Thiamethoxam bioaccumulation in *Zea mays*

Neonicotinoids are crop protection agents used against sucking pests acting on receptor proteins of the insect nervous system. Many reports detail their insecticidal properties [26–29], but reports on bioaccumulation and its transfer into plant organs are minimal. In this context, we

will confirm the ability of *Zea mays* plant to accumulate the TMX in seeds and seedlings (roots, stem, and leaves) by metallic silver electrode using square-wave voltammetric method (Table 3). After 8 days of treatment, we find that thiamethoxam accumulated increases proportionally with the concentration of thiamethoxam contained in the treatment solutions. At the highest and intermediate concentrations (5.00×10^{-2} and 0.50×10^{-2} mol L^{-1}), values of 0.022×10^{-2} and 0.014×10^{-2} mol L^{-1} are detected respectively. These results show that the seeds of *Zea mays* can bioaccumulate TMX during the germination stage.

The SWV method was also applied for the determination of TMX in seedlings of the plant at the metallic silver electrode (MSE), under the optimized instrumental conditions. So, we observed that when the plants were exposed to the higher and intermediate concentrations, TMX was detected in all the organs and clearly indicating that they could be translocated within the plant. TMX accumulation was dose dependent, and the maximum level attained varied in each part of the plant (Table 3). Generally, the highest TMX content was in roots, then leaves and stem considered as a transitional organ of the TMX towards the aerial part of the plant. After exposure of *Zea mays* to the highest concentration (5.00×10^{-2} mol L^{-1}), TMX content was about 0.003×10^{-2} mol L^{-1} in the stem, 0.0047×10^{-2} mol L^{-1} in leaves and not determined in roots. After treatment with the lower concentration (0.05×10^{-2} mol L^{-1}), no TMX was detected in roots and stem, but a value of 0.0004×10^{-2} mol L^{-1} was appreciated in the leaves. Previously, it was reported that also imidacloprid can be transferred from soil to tomato plants and translocated in roots, shoots, leaves, and fruits by monitoring of radioactivity in plant [30]. In another study, it was shown that neonicotinoids, such as acetamiprid, thiacloprid, and imidacloprid were detected in cotton seed cake by solid-phase extraction technique using HPLC [14]. In a later study, TMX was also detected in the potato by voltammetry using a glassy carbon electrode. The experiments showed that the voltammetric response depends on the mode of electrode surface pretreatment and the polarization mode. The limits of detection and quantitation were 0.0085 mg/cm^3 and 0.028 mg/cm^3 respectively [31]. In comparison to our results, the applicability of the metallic silver electrode was confirmed for the direct measurements of TMX in *Zea mays*, which present the lower determination limits using SWV voltammetry in comparison with the glassy carbon. This method of silver electrode analysis has a high sensitivity to TMX and allows for detecting it in the plant even at low concentrations.

Table 3: TMX insecticide content in plant organs (seeds, roots, stem and leaves) of Zea mays, after 8 days of irrigation with TMX at various concentrations ((0.05-5.00)×10⁻² mol L⁻¹).

Concentration ($\times 10^{-2}$ mol L^{-1})	Thiamethoxam concentration in plant organ ($\times 10^{-2}$ mol L^{-1})			
	seeds	roots	stems	leaves
0.05	ND	ND	ND	0.0004
0.10	0.004	0.003	0.0009	0.0009
0.50	0.014	0.035	0.001	0.0022
3.40	0.017	0.021	0.002	0.0037
5.00	0.022	_	0.003	0.0047

2) Effects of TMX on germination and growth process

The treatment of *Zea mays* seeds with TMX induced an inhibitory effect on the germination process at the highest concentrations (Figure 6 and 7).
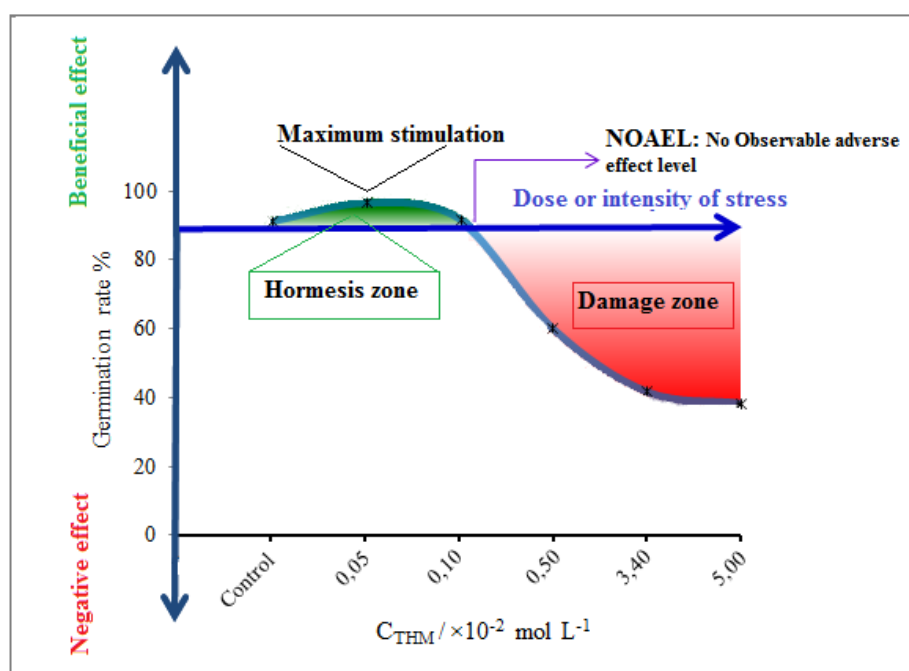
Figure 6: Experiment dose-response curve representing the hormesis effect in Zea mays.

At 5.0×10^{-3}, 3.4×10^{-2} and 5.0×10^{-2} mol L^{-1}, the rate of germination was 91.65, 41.66, and 38.33 % respectively. However, the result showed an important positive effect on seeds exposed to the lower concentrations (5.0×10^{-4} and 1.0×10^{-3} mol L^{-1}) in comparison to the control. So, the

maximum of the germination rate is obtained using 5.0×10^{-4} mol L^{-1} in treatment indicating that this dose of TMX could improve seeds germination of *Zea mays*.

A current spectrum is also recorded in the plant treated by different concentrations of thiamethoxam (Figure 7). We find that the current intensity increases proportionally with the concentration of TMX contained in the treating solutions. The recovery of the extraction of TMX from the seeds is decreased. This decrease is explained by the complexity of the plant matrix that may contain elements that can prevent the detection of TMX on the silver electrode.
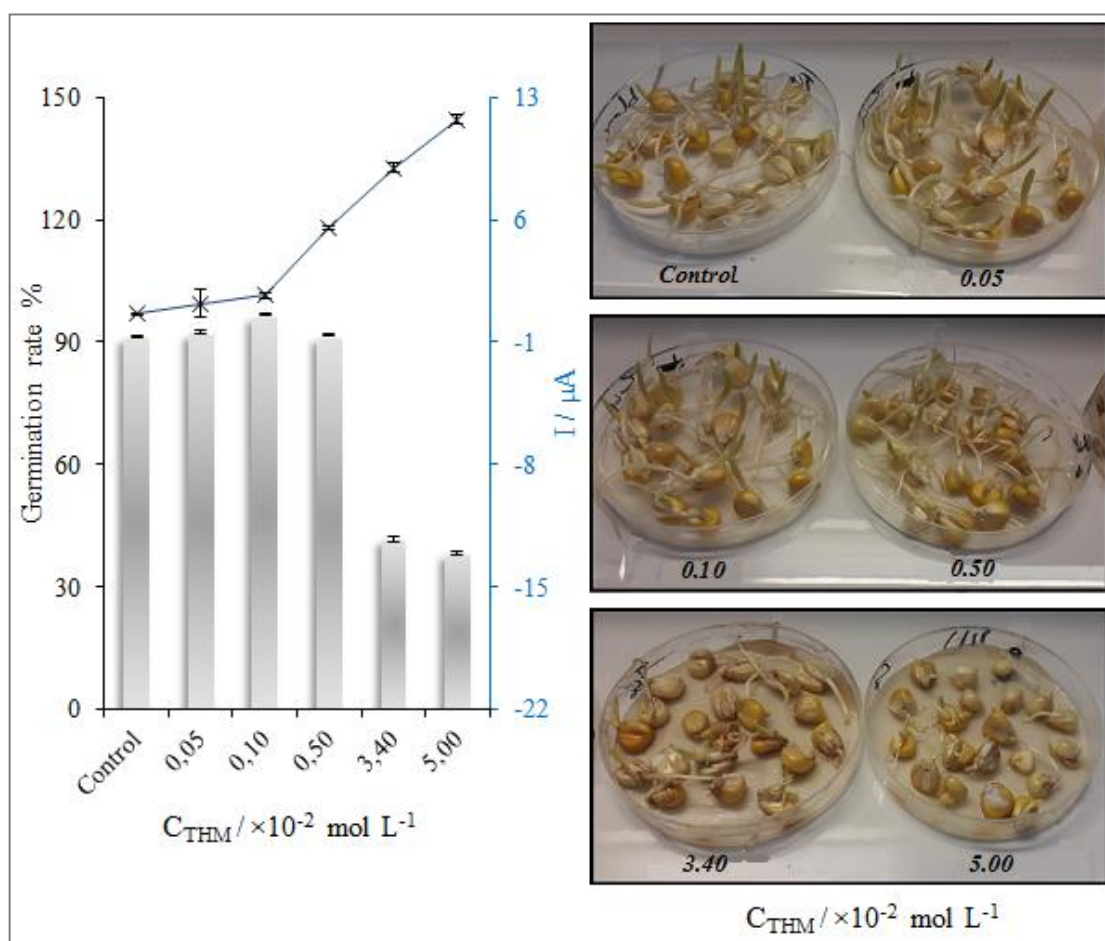
Figure 7: TMX effect on Zea mays germination rate, and the current response of treatment concentrations detected.

Semra Kilic et *al*. studied the inhibitory effects of chlorantraniliprole on the biological properties of maize seeds [32]. After seven days of the germination, the most devastating inhibitory effect on germination parameters of corn seed was the length of the coleoptile (90 %) at an insecticide concentration of 5.0×10^{-4} g Kg^{-1}. Dhanamanjuri et *al*. [33] studied the effect of different pesticides, in particular Captan, Bavistin, Domarck, Blitox and Sitara, on *Zea mays*

plant growth. The result, obtained for this study, indicates that recovery of seeds germination and biomass production were slightly influenced. The fungicide Bavistin (Carbendazim) at 1.0×10^{-3} g Kg^{-1} concentration was the best quantity of the treatments of *Zea mays* as compared to the reference.

To understand the performance and productivity of plants exposed to insecticides, the analysis of plant growth is a necessary step. With this vision, we studied the effect of TMX treatment on seedling growth of *Zea mays*. In figure 8, the effect of TMX is remarkable and similar to that observed in germination.
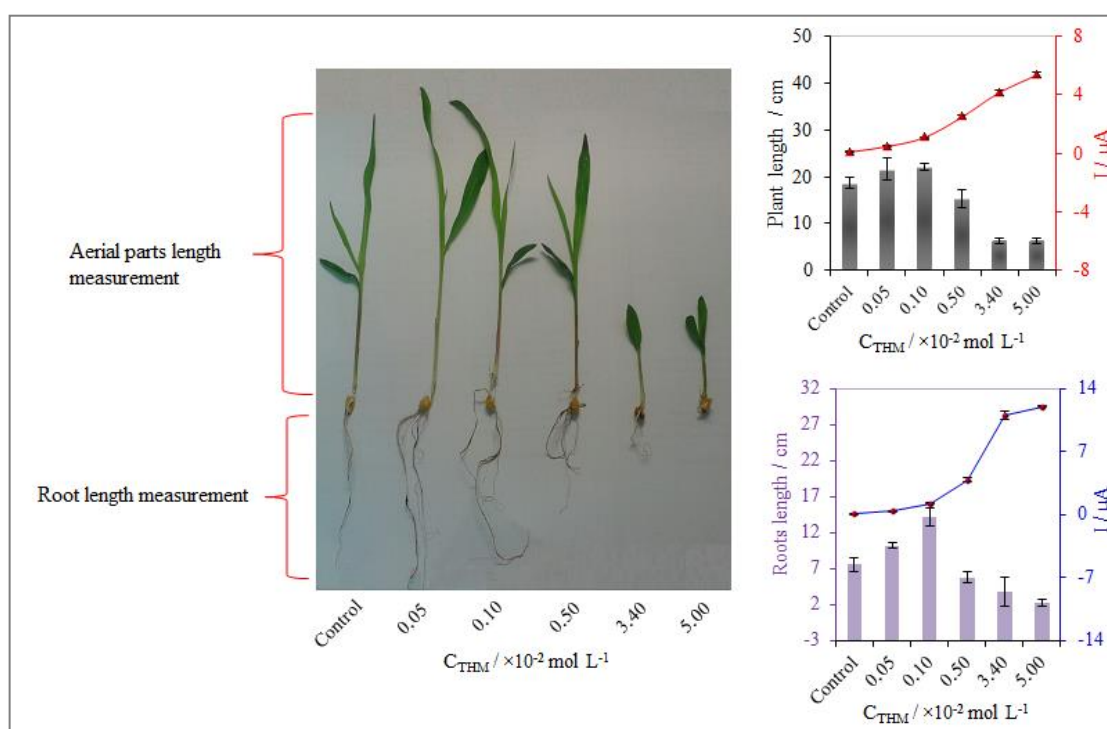
Figure 8: The effect of thiamethoxam insecticide on plant and roots lengths of Zea mays grown in peat with sand for 10 days, and the current response of various thiamethoxam concentration detected.

Indeed, the plant length of seedlings treated with 5.0×10^{-4} and 1.0×10^{-3} mol L^{-1} was 21.63 cm and 21.96 cm respectively and therefore lead to an increase with 16.10 % and 17.87 % respectively compared to those observed with the control. A negatively affect was observed when using 3.4×10^{-2} and 5.0×10^{-2} mol L^{-1} which cause a decrease in germination rates to 49.12 % and 69.07 %. The same phenomenon is observed on the roots by inhibiting the formation of primary and lateral roots and it was found that seedling growth was accelerated and inhibited at the lowest dose and the highest dose, respectively (Figure 8). The peak intensity of the electric current increase with increasing of the TMX quantity in treatment solution from 5.0×10^{-4} to

5.0×10^{-2} mol L^{-1}. The results of the electrochemical analysis are in perfect correlation with those of the bioaccumulation of TMX on the one hand and those of the effect on germination and growth on the other hand (Table 3 and Figure 6, 7 and 8).

The research team of Yasemin Coskun et al. showed also that maize growth was significantly inhibited by the increase of the concentration of pyriproxyfen, which is in agreement with previously published works with thiamethoxam and thiophanate-methyl on wheat seedlings [34]. However, it can be generally deduced that the insecticides used in *Zea mays* agriculture lead to the inhibition of plant growth. The TMX has the advantage of promoting growth at low concentrations. This result is explained by hormesis. This phenomenon is often dose dependant (Figure 6). The originality of our work is to prove experimentally the phenomenon of hormesis in maize treated by TMX. It may be observed at subtoxic doses of pesticides or other xenobiotics [35, 36]. Hormesis is a stimulatory or positive effect of low stress induced on the body by the activation of signaling and regulation pathways independently of cellular damage [35]. Several authors have shown, in some plant species, an increase in growth following the application of low doses of pesticides [37]. It can be observed, for example, an increase in the growth of mays, conventional soybean, *Eucalyptus grandis*, *Pinus L.* and *Commelia benghalensis* following the application of glyphosate. These results could be explained by the fact that low doses of glyphosate can stimulate photosynthesis, although the causes of this increase are not well characterized [38]. These results demonstrate the importance of considering the pollutant dose in studies.

It should be noted that low doses of pesticides could cause the same effects of high doses on plants because of their intensive use and thus their accumulation. Studies are therefore necessary to understand the mechanisms underlying these responses, by taking into account the simultaneous presence of many pollutants of different chemical classes, which leads to the complexity of environmental pollution.

3) Effect of TMX on the histological structure of the root in *Zea mays*

The results of the histological study showed that exposure to TMX induced a net histological modification of the primary root tissue of *Zea mays*. These cytological modifications were materialized by a change in the structure of primary root tissue and in cell size of hypoderm, and inhibition of absorbent root hairs formation (Figure 9). All these histological anomalies could explain the negative impact caused by TMX treatment on the growth and development of plant roots.
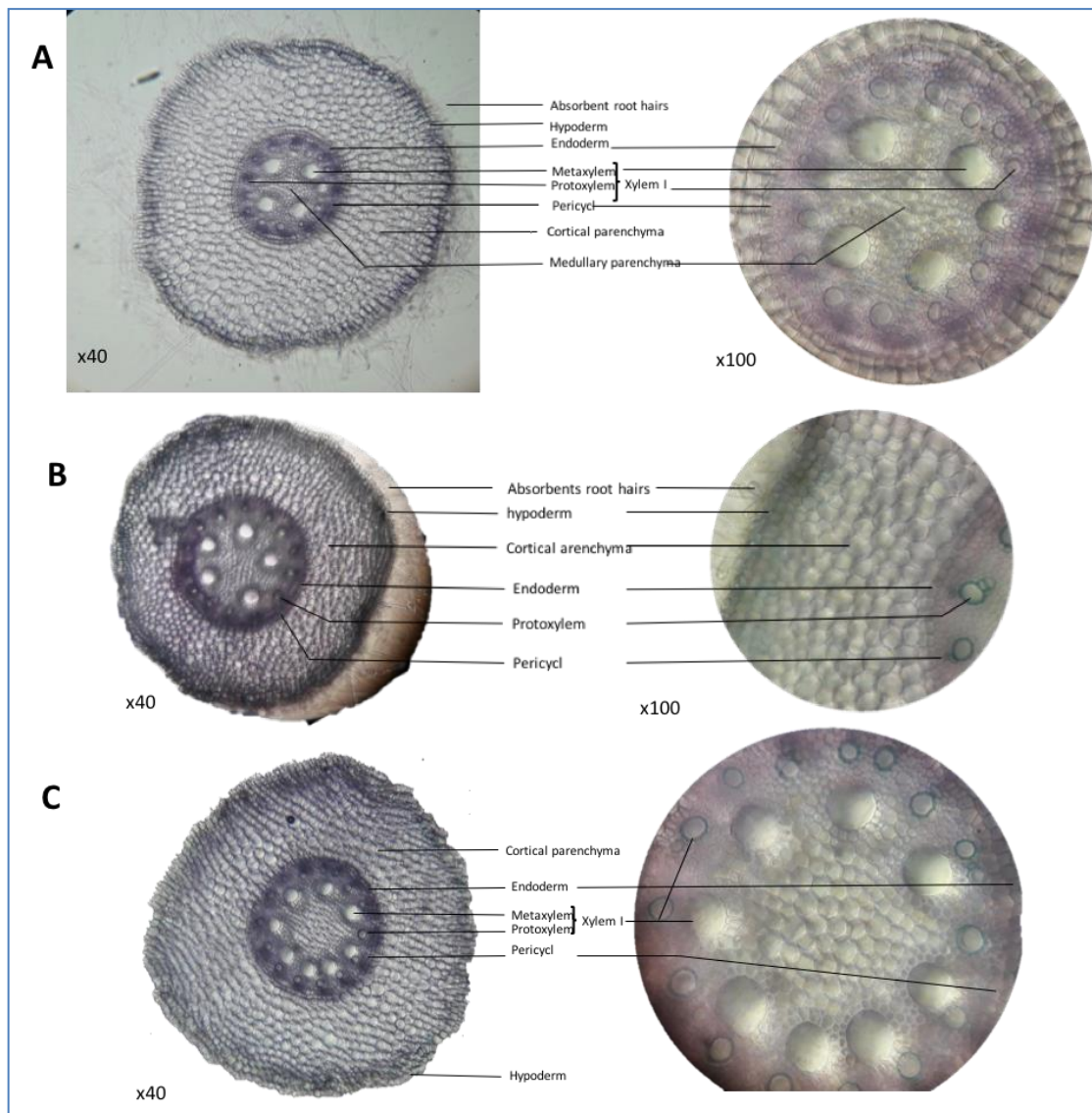
Figure 9: Transversal cross-sections of primary root of Zea mays showing histological changes induced by exposure to TMX treatment. (A) Control, (B) Exposed treatment at 1.0×10-3 mol L-1 dose, (C) Exposed treatment at 5.0×10-2 mol L-1 dose.

The result shows clearly the main histological difference between seedlings treated by TMX and no-treated ones. In comparison with the control, the root cuts observed by microscopy indicate that the effect was dose dependent. At $1.0×10^{-3}$ mol L^{-1} we observed (Figure 9B):

- ✓ Thick pericycle with slightly larger cells of green color (lignification)
- ✓ The presence of some absorbent root hairs more or less short compared to the control
- ✓ Presence of a hypodermis with a non-thick wall like that of the control
- ✓ Presence of 14 protoxylem and 6 meta xylem with 1/6 small 2 to 3 seated outer cells of cortical parenchyma of more or less small size with lignification tendency

However, at $5.0×10^{-2}$ mol L^{-1}, we observed (Figure 9C):

- ✓ Pericycle with rounded cells with a more or less green color (lignification)
- ✓ Absence of absorbent root hairs
- ✓ Presence of a more developed hypodermis with thick wall
- ✓ Presence of 14 protoxylems and 8 meta xylems all of the large size
- ✓ Cortical parenchyma cells smaller in size at 2 to 3 seated

Histological observation confirms this disorder, which is due to the bioaccumulation of TMX in roots transferred from the soil, and to the sharp decrease in the number of mitoses in the root meristem in the poisoned plant. It is probable that the inhibition of mitotic activity is the main cause of the decrease in root growth, and finally of the general growth of the plant [38]. This decrease in mitotic activity may be due in part to a decrease in the supply of sucrose to the root meristem, following blockage of starch degradation in leaf chloroplasts.

IV. Conclusion

To summarize, the electrochemical study of organic nitro-aromatic thiamethoxam was investigated using metallic silver electrode (MSE). The finding showed an excellent electrocatalytic performance of MSE toward target compound compared to other electrodes such as glassy carbon electrode and paste carbon electrode. In addition, The MSE was used for the determination of TMX the extract of the different part (roots, stems, and leaves) of plant Zea mays using square-wave voltammetry. The bioaccumulation of TMX in seedling growth was proved with the presence of the reduction peak. The current intensity of this peak varied linearly with the concentration of TMX bioaccumulated in seedling growth. The accumulation of TMX affects the structure of the Zea mays plant by modifying roots, stems, and leaves. The result was confirmed by the histological sections, which showed a change in cell size of Zea mays especially from the 1.0×10^{-3} mol L^{-1} concentration of TMX.

References

[1] Buckingham, S.; Lapied, B.; Corronc, H. and Sattelle, F.: Imidacloprid actions on insect neuronal acetylcholine receptors, Journal of Experimental Biology, **200** (1997), no. 21, pp. 2685–2692.

[2] Iwasa, T.; Motoyama, N.; Ambrose, J.T. and Roe, R.M.: Mechanism for the differential toxicity of neonicotinoid insecticides in the honey bee, Apis mellifera, Crop Protection, **23** (2004), no. 5, pp. 371–378.

[3] Elbert, A.; Haas, M.; Springer, B.; Thielert, W. and Nauen, R.: Applied aspects of neonicotinoid uses in crop protection, Pest Management Science: formerly Pesticide Science, **64** (2008), no. 11, pp. 1099–1105.

[4] Limay-Rios, V.; Forero, L.G.; Xue, Y.; Smith, J.; Baute, T. and Schaafsma, A.: Neonicotinoid insecticide residues in soil dust and associated parent soil in fields with a history of seed treatment use on crops in southwestern Ontario, Environmental Toxicology and Chemistry, **35** (2016), no. 2, pp. 303–310.

[5] Maienfisch, P.; Huerlimann, H.; Rindlisbacher, A.; Gsell, L.; Dettwiler, H.; Haettenschwiler, J.; Sieger, E. and Walti, M.: The discovery of thiamethoxam: a second-generation neonicotinoid, Pest Management Science, **57** (2001), no. 2, pp. 165–176.

[6] Maienfisch, P.; Angst, M.; Brandl, F.; Fischer, W.; Hofer, D.; Kayser, H.; Kobel, W.; Rindlisbacher, A.; Senn, R.; Steinemann, A. and Widmer, H.: Chemistry and biology of thiamethoxam: a second generation neonicotinoid, Pest Management Science, **57** (2001), no. 10, pp. 906–913.

[7] Pynenburg, G.M.; Sikkema, P.H. and Gillard, C.L.: Agronomic and economic assessment of intensive pest management of dry bean (Phaseolus vulgaris), Crop Protection, **30** (2011), no. 3, pp. 340–348.

[8] Sirchio, K. and Sutton, A.: Syngenta Professional Products Focuses Chemical Technology on New Applications to Enhance the Quality of Life, CHIMIA, **61** (2007), nos. 1–2, pp. 17–17.

[9] Jeschke, P.; Nauen, R.; Schindler, M. and Elbert, A.: Overview of the status and global strategy for neonicotinoids, Journal of agricultural and food chemistry, **59** (2011), no. 7, pp. 2897–2908.

[10] Tomizawa, M. and Casida, J.E.: NEONICOTINOID INSECTICIDE TOXICOLOGY: Mechanisms of Selective Action, Annual Review of Pharmacology and Toxicology, **45** (2005), no. 1, pp. 247–268.

[11] Gupta, S.; Gajbhiye, V.T. and Gupta, R.K.: Soil Dissipation and Leaching Behavior of a Neonicotinoid Insecticide Thiamethoxam, Bulletin of Environmental Contamination and Toxicology, **80** (2008), no. 5, pp. 431–437.

[12] Singh, S.B.; Foster, G.D. and Khan, S.U.: Microwave-Assisted Extraction for the Simultaneous Determination of Thiamethoxam, Imidacloprid, and Carbendazim Residues in Fresh and Cooked Vegetable Samples, Journal of Agricultural and Food Chemistry, **52** (2004), no. 1, pp. 105–109.

[13] Ying, G.-G. and Kookana, R.S.: Simultaneous Determination of Imidacloprid, Thiacloprid, and Thiamethoxam in Soil and Water by High-performance Liquid Chromatography with Diode-array Detection, Journal of Environmental Science and Health, Part B, **39** (2004), nos. 5–6, pp. 737–746.

[14] Mohan, C.; Kumar, Y.; Madan, J. and Saxena, N.: Multiresidue analysis of neonicotinoids by solid-phase extraction technique using high-performance liquid chromatography, Environmental Monitoring and Assessment, **165** (2010), no. 1, pp. 573–576.

[15] Guzsvány, V.J.; Gaál, F.F.; Bjelica, L.J. and Ökrész, S.N.: Voltammetric determination of imidacloprid and thiamethoxam, Journal of the Serbian Chemical Society, **70** (2005), no. 5, pp. 735–743.

[16] Guzsvány, V.; Kádár, M.; Gaál, F.; Tóth, K. and Bjelica, L.: Rapid Differential Pulse Polarographic Determination of Thiamethoxam in Commercial Formulations and some Real Samples, Microchimica Acta, **154** (2006), no. 3, pp. 321–328.

[17] Papp, Z.J.; Guzsvány, V.J.; Kubiak, S.; Bobrowski, A. and Bjelica, L.J.: Voltammetric determination of the neonicotinoid insecticide thiamethoxam using a tricresyl phosphate-based carbon paste electrode, Journal of the Serbian Chemical Society, **75** (2010), no. 5, pp. 681–687.

[18] Kumaravel, A. and Chandrasekaran, M.: Nanosilver/surfactant modified glassy carbon electrode for the sensing of thiamethoxam, Sensors and Actuators B: Chemical, **174** (2012), pp. 380–388.

[19] Guzsvány, V.; Kádár, M.; Gaál, F.; Bjelica, L. and Tóth, K.: Bismuth Film Electrode for the Cathodic Electrochemical Determination of Thiamethoxam, Electroanalysis, **18** (2006), nos. 13–14, pp. 1363–1371.

[20] Chorti, P.; Fischer, J.; Vyskocil, V.; Economou, A. and Barek, J.: Voltammetric Determination of Insecticide Thiamethoxam on Silver Solid Amalgam Electrode, Electrochimica Acta, **140** (2014), pp. 5–10.

[21] Ajermoun, N.; Farahi, A.; Lahrich, S.; Bakasse, M.; Saqrane, S. and El Mhammedi, M.A.: Electrocatalytic activity of the metallic silver electrode for thiamethoxam reduction: application for the detection of a neonicotinoid in tomato and orange samples, Journal of the Science of Food and Agriculture, **99** (2019), no. 9, pp. 4407–4413.

[22] Claudine, G. da R.; Francis, H.R.F. and Claudia, A.L.C.: Quantification of Thiamethoxam in Rhizomes and Leaves of the *Hedychium coronarium* and Water and Soil by High-Pressure Liquid Chromatography, American Journal of Analytical Chemistry, **2012** (2012).

[23] Ammar, H.B.; Brahim, M.B.; Abdelhédi, R. and Samet, Y.: Boron doped diamond sensor for sensitive determination of metronidazole: Mechanistic and analytical study by cyclic voltammetry and square wave voltammetry, Materials Science and Engineering: C, **59** (2016), pp. 604–610.

[24] Fischer, J.; Dejmkova, H. and Barek, J.: Electrochemistry of Pesticides and its Analytical Applications, Current Organic Chemistry, **15** (2011), no. 17, pp. 2923–2935.

[25] Miller, J.C. and Miller, J.N.: Basic statistical methods for analytical chemistry. Part I. Statistics of repeated measurements. A review, Analyst, **113** (1988), no. 9, pp. 1351–1356.

[26] Milosavljević, I.; Esser, A.D.; Murphy, K.M. and Crowder, D.W.: Effects of imidacloprid seed treatments on crop yields and economic returns of cereal crops, Crop Protection, **119** (2019), pp. 166–171.

[27] Berheim, E.H.; Jenks, J.A.; Lundgren, J.G.; Michel, E.S.; Grove, D. and Jensen, W.F.: Effects of Neonicotinoid Insecticides on Physiology and Reproductive Characteristics of Captive Female and Fawn White-tailed Deer, Scientific Reports, **9** (2019), no. 1, p. 4534.

[28] Del Pozo-Valdivia, A.I.; Reisig, D.D.; Arellano, C. and Heiniger, R.W.: A case for comprehensive analyses demonstrated by evaluating the yield benefits of neonicotinoid seed treatment in maize (Zea mays L.), Crop Protection, **110** (2018), pp. 171–182.

[29] Hladik, M.L.; Main, A.R. and Goulson, D.: Environmental risks and challenges associated with neonicotinoid insecticides2018.

[30] Alsayeda, H.; Pascal-Lorber, S.; Nallanthigal, C.; Debrauwer, L. and Laurent, F.: Transfer of the insecticide [14C] imidacloprid from soil to tomato plants, Environmental Chemistry Letters, **6** (2008), no. 4, pp. 229–234.

[31] Guzsvány, V.J.; Gaál, F.F.; Bjelica, L.J. and Ökrész, S.N.: Voltammetric determination of imidacloprid and thiamethoxam, Journal of the Serbian Chemical Society, **70** (2005), no. 5, pp. 735–743.

[32] Kilic, S.; Duran, R.E. and Coskun, Y.: Morphological and Physiological Responses of Maize (Zea mays L.) Seeds Grown under Increasing Concentrations of Chlorantraniliprole Insecticide, Polish Journal of Environmental Studies, **24** (2015), no. 3, pp. 1069–1075.

[33] Dhanamanjuri, W.; Thoudam, R. and Dutta, B.K.: Effect of Some Pesticides (Fungicides) on the Germination and Growth of Seeds/Seedlings of Some Crop Plants, (i.e. Cicer arietinum and Zea mays), (2013), p. 7.

[34] Belz, R.G. and Duke, S.O.: Herbicides and plant hormesis, Pest Management Science, **70** (2014), no. 5, pp. 698–707.

[35] Calabrese, E.J.; Bachmann, K.A.; Bailer, A.J.; Bolger, P.M.; Borak, J.; Cai, L.; Cedergreen, N.; Cherian, M.G.; Chiueh, C.C.; Clarkson, T.W.; Cook, R.R.; Diamond, D.M.; Doolittle, D.J.; Dorato, M.A.; Duke, S.O.; Feinendegen, L.; Gardner, D.E.; Hart, R.W.; Hastings, K.L.; Hayes, A.W.; Hoffmann, G.R.; Ives, J.A.; Jaworowski, Z.; Johnson, T.E.; Jonas, W.B.; Kaminski, N.E.; Keller, J.G.; Klaunig, J.E.; Knudsen, T.B.; Kozumbo, W.J.; Lettieri, T.; Liu, S.-Z.; Maisseu, A.; Maynard, K.I.; Masoro, E.J.; McClellan, R.O.; Mehendale, H.M.; Mothersill, C.; Newlin, D.B.; Nigg, H.N.; Oehme, F.W.; Phalen, R.F.; Philbert, M.A.; Rattan, S.I.S.; Riviere, J.E.; Rodricks, J.; Sapolsky, R.M.; Scott, B.R.; Seymour, C.; Sinclair, D.A.; Smith-Sonneborn, J.; Snow, E.T.; Spear, L.; Stevenson, D.E.; Thomas, Y.; Tubiana, M.; Williams, G.M. and Mattson, M.P.: Biological stress response terminology: Integrating the concepts of adaptive response and preconditioning stress within a hormetic dose–response framework, Toxicology and Applied Pharmacology, **222** (2007), no. 1, pp. 122–128.

[36] Velini, E.D.; Alves, E.; Godoy, M.C.; Meschede, D.K.; Souza, R.T. and Duke, S.O.: Glyphosate applied at low doses can stimulate plant growth, Pest Management Science, **64** (2008), no. 4, pp. 489–496.

[37] Cedergreen, N. and Olesen, C.F.: Can glyphosate stimulate photosynthesis?, Pesticide Biochemistry and Physiology, **96** (2010), no. 3, pp. 140–148.

[38] Çavuşoğlu, K.; Yalçin, E.; Türkmen, Z.; Yapar, K. and Sağir, S.: Physiological, anatomical, biochemical, and cytogenetic effects of thiamethoxam treatment on Allium cepa (amaryllidaceae) L., Environmental toxicology, **27** (2012), no. 11, pp. 635–643.

Chapter III

Impregnation of silver particles on graphite for thiamethoxam analysis

I. Introduction

Electrochemistry is essentially a surface and interface science that studies chemical reactions which take place at the interface of electrode and electrolyte. Electrodes are the key part in electrochemical measurements, thus modification of their size and surface structure offers possibilities to create novel electrochemical systems[1, 2]. Carbon and their variety has played for a long time an important role in solid electrode development, also favoured by its rich surface chemistry which has been exploited to influence surface reactivity[3, 4]. Due to its good electrical conductivity, a wide operable potential window in either aqueous or non-aqueous solutions, carbon-based materials exhibited a lower over potential and a wider useful electrochemical range [5–9]. The modification of carbon electrode has reached considerable attention in recent years because it offers a great opportunity to use various modifiers to the development of several types of electrodes and devices which aimed at improving the sensitivity of the analyses and lowering the detection and quantification limits [10–12].

Many reports were devoted to analysis the pesticides using carbon electrode [13–16]. Among these the neonicotinoids group which considered a new generation of insecticide widely used recently in agriculture. Zsigmond Papp, et *al.* investigated three kinds of modified carbon paste electrodes (CPEs) based on tricresyl phosphate, silicone oil, and *n*-tetradecane, for the detection of imidacloprid [17]. Valéria Guzsvány and co-workers applied a bismuth bulk modified carbon electrode for the determination of selected nitroguanidine neonicotinoid insecticides clothianidin, imidacloprid [18]. Herein we focused on thiamethoxam (*EZ*)-3-(2-chloro-1,3-thiazol-5-ylmethyl)-5-methyl-1,3,5-oxadiazinan-4-ylidene (nitro) amine, which considered a most water-soluble broad-spectrum insecticide, widely used for seed treatment, soil and foliar [19].

Recently, research works was studied the use of electrochemical methods for thiamethoxam analysis [20–24]. Indeed, Kumaravel et *al*. developed a nanosilver/SDS modified glassy carbon electrode as a sensing probe for the electrochemical determination of TMX with the limit of detection of 0.1 μmol L^{-1} [21]. The direct determination of TMX at a non-toxic mercury meniscus modified silver solid amalgam electrode (m-AgSAE) was reported by P. Chorti et *al.* [22], Veronika Urbanová prepared a glassy carbon electrode modified with graphene oxide for the electrochemical sensing of insecticides TMX and imidacloprid [23]. Maria Putek et *al.* present the use of a renewable silver-amalgam film electrode (Hg(Ag)FE) for the determination of the TMX [24].

In other hand, electrodes modified by metal particles have attracted attention of researchers for the sensing of pesticides due to their unusual physical and chemical properties [25, 26]

especially silver particles, based on their ability to support electrocatalytic activity, low toxicity, and high demand in sensor applications [27].

This chapter presented two preparation routes of carbon materials-based silver particles, which consist to the solid reaction under nitrogen flow and electrochemical deposition. The morphology, distribution and size of silver modified carbon materials were characterized by XRD, and SEM. In addition, the catalytic activity of silver particles impregnated and electrodeposited on graphite surface in reducing TMX was investigated. The reduction mechanism of TMX and effect of experimental conditions were studied using cyclic voltammetry, square wave voltammetry, Tafel plots and chronoamperometry.

II. Experimental

1) Chemicals and reagents

Thiamethoxam obtained from Syngenta international AG (Basel, Switzerland), silver nitrate ($AgNO_3$ p.a 98%), sodium hydroxide, phosphoric acid, acetic acid and boric acid were purchased from Merck (Darmstadt, Germany), Fluka (st.gallen, Switzerlan), Riedel de Haen (seelze, Germany) potassium ferrocyanide [$K_4(FeCN)_6$], potassium ferricyanide [$K_3(FeCN)_6$] were obtained from Loba Chem. These chemicals were used without any purification. Graphite was provided from carbon Lorraine (Lorraine, France ref 9900). The Britton-Robinson (B-R) buffers electrolytes (pH 10.4) were prepared in the laboratory by mixing 3.556 g of sodium hydroxide, 2.178 g of phosphoric acid, 1.334 g of acetic acid, 1.374 g of boric acid in 1 L of deionized water. A 1.0×10^{-3} mol L^{-1} stock solution was prepared by adding of the thiamethoxam mass in Britton-Robinson (B-R) buffers. Graphite was provided from carbon Lorraine (Lorraine, France ref 9900).

2) Instruments

Electrochemical measurements (cyclic voltammetry, linear sweeping voltammetry, chronoamperometry, square wave voltammetry and electrochemical impedance spectroscopy) were carried out by Voltalab potentiostat (model PGZ 100; Eco Chemie B.V, Utrecht, The Netherlands) operated by voltamaster 4 software as an electrochemical system data processing software, in conventional three electrodes connection including: silver modified graphite carbon (Ag@GrCE) as working electrode, Ag/AgCl/3M KCl reference electrode and platinum wire counter electrode.

The pH measurements were done using a (Radiometer, SENSION^{TM}, pH31, Leganes Spain) was employed for adjusting pH values.

X-ray diffractometer (XRD) spectra were performed by (XRD: Cu Ka radiation, XPERT-PRO), (Kcu = 1.5406 nm) produced at 30 kV and 25 mA. The diffraction angles were scanned between 10 and 80 with a step size of 0.02 per second and scan speed of 1°/min.

SEM images and EDX spectra of the prepared materials were obtained using the JOEL JSM-IT100 scanning electron microscope with FEG (field emission gun) system equipped with an energy dispersive X-ray analyzer at an accelerating voltage of 20 kV.

Fourier transform infrared (FT-IR) spectra of studied materials were performed in the frequency range of 400 to 4000 cm^{-1} by VORTEX 70 DTGS spectrometer using KBr pallet method. Dried Ag@GrC samples (1 mg) were mixed with KBr powder (100 mg) in an agate mortar. The mixture was pressed into a pellet under 10 tons load for 2–4 min, and the spectrum was recorded immediately. The signal from a pure KBr pellet was subtracted as the background.

III. Results and discussion

A) Impregnation of silver particles on graphite by solid reaction

1) Impregnation procedure

The modification graphite electrode was prepared by thoroughly mixing carbon graphite carbon powder and silver nitrate ($AgNO_3$) by different ratio by weight (w/w) in an agate mortar. The obtained powders were calcinated at different temperature (200, 300, 400, 500°C) for 12h in the kiln under nitrogen atmosphere. The resulting powders were mixed with paraffin oil a mortar by exhaustively hand mixing with a pestle and then incorporated into the cavity of working electrode (geometric surface area about 0.1295 cm^2). The external surface of electrode wase smoothed on a paper sheet. Electrical contact was established by a bar of carbon. The resulting electrode is hereby denoted as Ag-GrCE.

2) Characterization of synthesis powder

The formations of the silver nanoparticles on carbon heated at different temperatures were studied using X-ray diffraction profile (Figure 1a). For all characterized Ag-CP samples, the major characterization peaks (metallic silver nanoparticles) were found at 38.15, 44.27, 64.45 and 77.34° respectively corresponding to (111), (200), (220) and (311) orientation planes.

The XRD pattern showed that the silver particles have a crystalline and face-centred cubic (FCC) configuration in nature [28, 29]. The intensity of the diffraction peaks increased with increasing the calcination temperature from 200 to 400 °C, due to the crystallite size growth and better crystallization. The crystallite size of the silver nanoparticles was calculated by the Scherrer equation [30]:

$$D = k\lambda/\beta \cos\theta \qquad\qquad\qquad (1)$$

Where D = average crystallite size, K is shape constant, λ is wavelength of X-ray, β is Full Width Half Maximum (*FWHM*) of refection (in radians) located at 2θ and θ are angle of reflection (in radians) was used to relate the crystallite size to the line broadening.
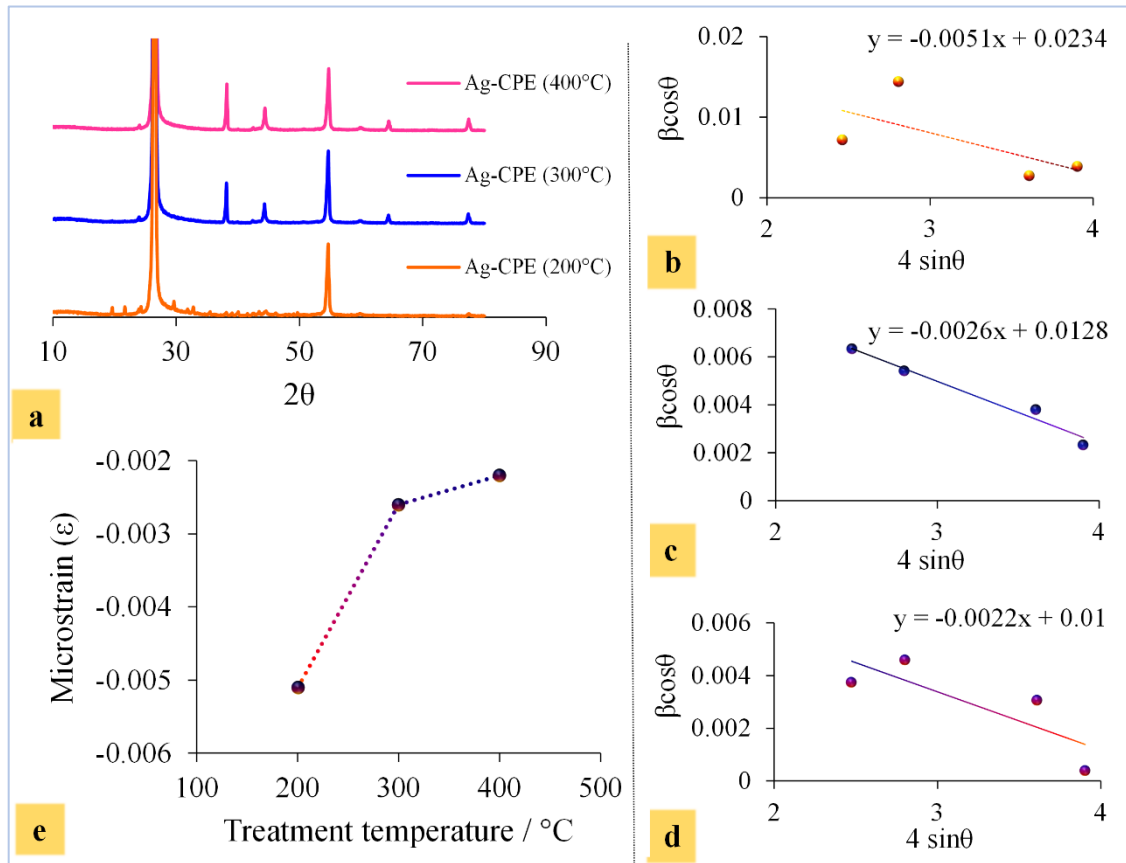
Figure 1: (**a**) *XRD pattern of modified Ag-CP heated at different temperature (200°C to 400°C) under nitrogen atmosphere,* (**b-d**) *W-H plots, (e) crystallite size-microstrain variation of Ag-CP with treatment thermal (200 to 400°C).*

Table 1 illustrates the average crystallite size calculated for the intense peaks of three samples carbon decorated silver particles (Ag-CP). The average crystallite size was found to be about 14, 16 and 42 nm, for Ag-CP (200 °C), Ag-CP (300 °C) and Ag-CP (400 °C) respectively. Silver crystallite size increases with increasing in treatment temperature, this indicates that our synthesized material is structured as nanocrystalline.

Samples	2θ of intense peak	hkl	FWHM (Degree)	FWHM (Radian)	Average cristallite size (nm)
Ag-CPE 200°C	37.95	111	0.524	0.00914089	14.1447882
	44.583	200	1.158	0.02021811	
	64.44	220	0.364	0.00634978	
	77.484	311	1.031	0.01800267	
Ag-CPE 300°C	38.156	111	0.462	0.00805933	16.5669403
	44.342	200	0.434	0.00757089	
	64.454	220	0.506	0.00882689	
	77.398	311	0.613	0.01069344	
Ag-CPE 400°C	38.212	111	0.273	0.00476233	42.0206948
	44.403	200	0.368	0.00641956	
	64.494	220	0.407	0.00709989	
	77.447	311	0.103	0.00179678	

The Williamson-Hall approach is method to measured lattice microstrain distribution in the sample and their effects on peak width. The scherrer equation depicts the line broadening (FWHM$_D$) of a bragg reflection in relationship with crystallite size [30]:

$$FWHM_{D} = k\lambda/D \cos\theta \qquad (2)$$

The lattice strain induced broadening (FWHMε) is given bay Stokes-Wilson formula as[31]:

$$FWHM\varepsilon = 4\varepsilon \sin\theta \qquad (3)$$

Where ε is microstrain. To assess the influence of the simultaneous contributions of crystallite size and strain on the widening of the line (β) when both approaches are operational, the W-H method is used [32] to evaluate the effect of thermal treatment over silver particles decorated graphite carbon:

$$FWHM_\beta = FWHM_D + FWHM\varepsilon \qquad (4)$$

$$\beta \cos\theta = \frac{\kappa\lambda}{D} + 4\varepsilon \sin\theta \qquad (5)$$

By drawing the straight line in the plot of $\beta\cos\theta$ vs $4\sin\theta$, the microstain and can be estimated from the slope figure 1b−d. Variations of microstain at various treatment temperatures were depicted in the figure 1e. The negative slopes were observed at all treatment temperature (200 °C to 400 °C) in the corresponding W-H plot, suggest the presence of compressive strain in the lattice, which can due to defects, and lattice mismatch. The sample heated at 300 °C reveal linearity plot (Figure 1c), on the other hand for others samples (200 °C and 400 °C) nonlinearity was observed (Figure 1b, d). This result demonstrated homogeneity in the nanoparticles size and the crystallinity order for sample heated at 300 °C. It was found that calcination temperature is an important factor in the synthesis of Ag nanoparticles on graphite with specific property as (catalytic property).

Furthermore, figure 2a−e depict the W-H plot of various carbon- silver weight ratio (20, 40, 50, 60, 80 wt%). The negative slopes were observed for different ratio of CP/Ag (20 to 80 wt%), shows good dispersion of Ag nanoparticles over carbon substrate surface area. Especially, for sample (60 wt% of Ag) exhibit an excellent homogeneity of particle size was demonstrated by good linearity of the $\beta\cos\theta$ versus $4\sin\theta$. It is interesting to note that the doping of higher amount of Ag and increase of temperature shifting the slope values from negative to positive.

Figure 3 depicts the nyquist plots of Ag−CPE prepared at different temperatures (200 °C to 400 °C) in the frequency range from 10^{-1} to 10^5 Hz measured at the open-circuit potential with an AC perturbation of 5 mV. However, for all modified electrodes, the arcs small at high frequency and the vertical lines at low frequency were observed, in term of charge transfer resistance (R_{ct}). The Ag-CPE (300 °C) presents lower R_{ct} than that of Ag-CPE (200 °C, 400 °C) (Table 2), which means that effective separation of electron–hole pairs and the fastest interfacial charge transfer to the electron donor/electron acceptor occurred by incorporation of silver nanoparticles on carbon with annealing temperature. The capacitive behavior of

electrochemical surface area (ECSA) is difficult to measure accurately, but this can be seen by calculating the double layer capacitances (C_{dl}) that is proportional to ECSA [33, 34].
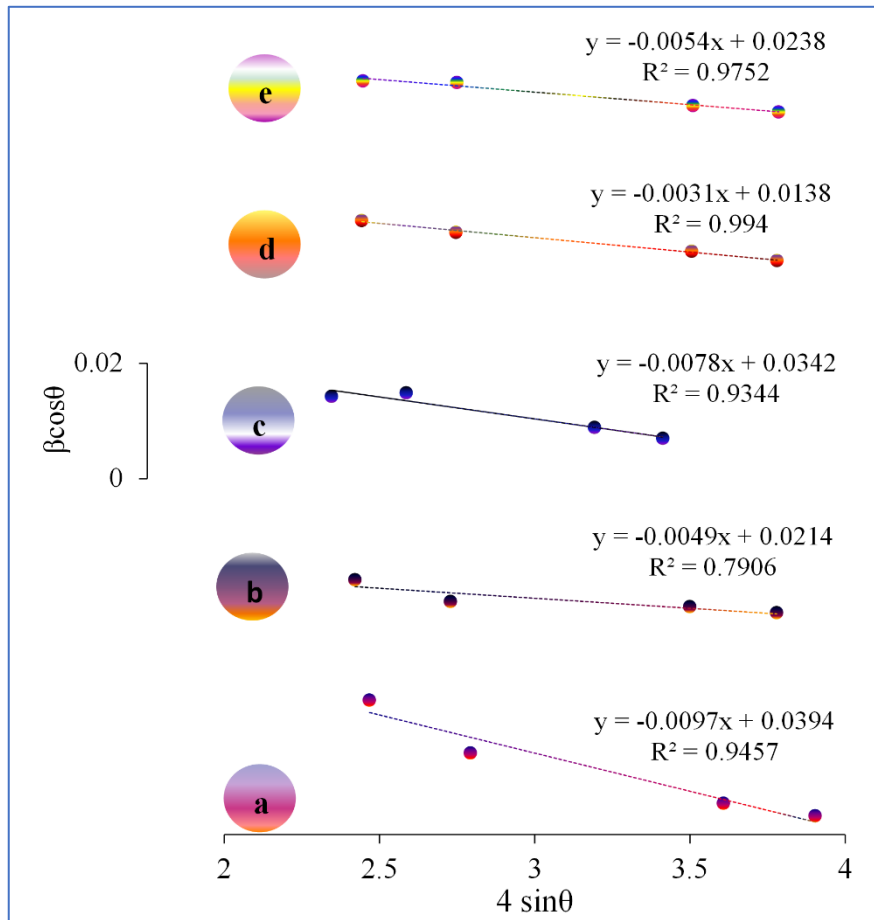
Figure 2: *W-H plots (**a-e**), crystallite size-microstrain variation of Ag-CP with carbon/silver weight rapport heated at 300 °C.*

Table 2: *EIS parameters of various Ag –CPE electrodes.*

Electrode	Rs (Ω cm^{-2})	Rc(Ω cm^{-2})	Cs(mF cm^{-2})	C_{dl}(mF cm^{-2})
Ag-CPE 200°C	41.19	118.4	8.48	38.1
Ag-CPE 300°C	40.50	69.49	10.26	57.8
Ag-CPE 400°C	41.79	77.82	1.83	48.1
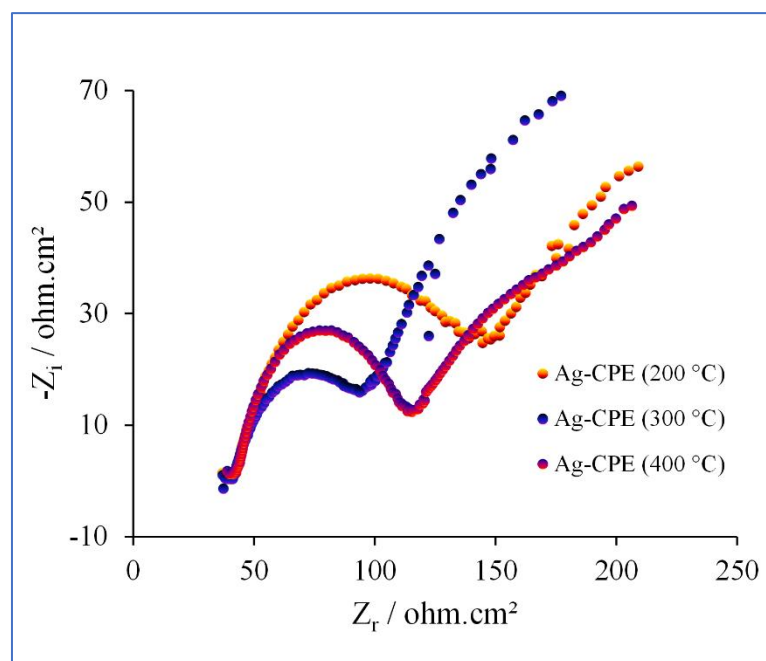
Figure 3: Nyquist plots of Ag−CPE prepared at different temperatures (200 to 400 °C) in 0.1 mol L-1 KCl solution containing equimolar concentration (5.0×10^{-3} mol L^{-1}) of $[FeCN6]^{3-/4-}$, Ag/CP = 60 %.

3) Catalytic effect of synthesis powder in reducing thiamethoxam

Electrochemistry investigation of TMX was performed out in Britton-Robinson buffer (B-R; pH = 10.4) containing TMX by cyclic voltammetry (CV). The latter were recorded between -100 and -1400 mV using different scan rate values depending on experimental purposes. The square wave voltammetric parameters include a pulse of 50 mV, a frequency of 25 Hz and amplitude modulation of 10 mV. The chronoamperometric tests were carried out at applied potential of -1000 mV and deposition time of 3 min. For the EIS measurement, the potential amplitude of ± 5 mV and frequency range of 0.01 to 10^5 Hz were adopted.

The overpotentials (η) were measured against Ag/AgCl electrode and corrected with respective to the reversible hydrogen electrode (RHE) according to the Nernst equation (E_{RHE}= $E_{Ag/AgCl}$+0.0591pH+0.198). Double layer capacitance C_{dl}, was estimated on the basic of CV tested between -400 to 700 mV with various scan rates from 20 to 100 mV.s^{-1}, C_{dl} was calculated by plotting the j= j_a-j_c against scan rate according to equation j=C_{dl}v [35, 36].

Figure 4 exhibits the square wave voltammetry (SWV) plots of the reduction of TMX at Ag−CPE prepared at different temperatures (from 200 °C to 400 °C) with Ag/CP = 60% under a flow of nitrogen. The modified electrodes Ag−CPE were demonstrated to have remarkable electro-catalytic activity towards TMX reduction as compared to unmodified graphite electrode (CPE). In addition, the current intensity of TMX reduction at Ag−CPE (200 °C) is 50.55 µA, at Ag−CPE (300 °C) is 34.98 µA, and at Ag−CPE (400 °C) is 22.46 µA. The higher peak current

was observed using Ag−CP heated at 300 °C, which might due to the interaction between active (111) facets of silver and nitro group of thiamethoxam. This electrode improved also the catalytic properties for the reduction of thiamethoxam.
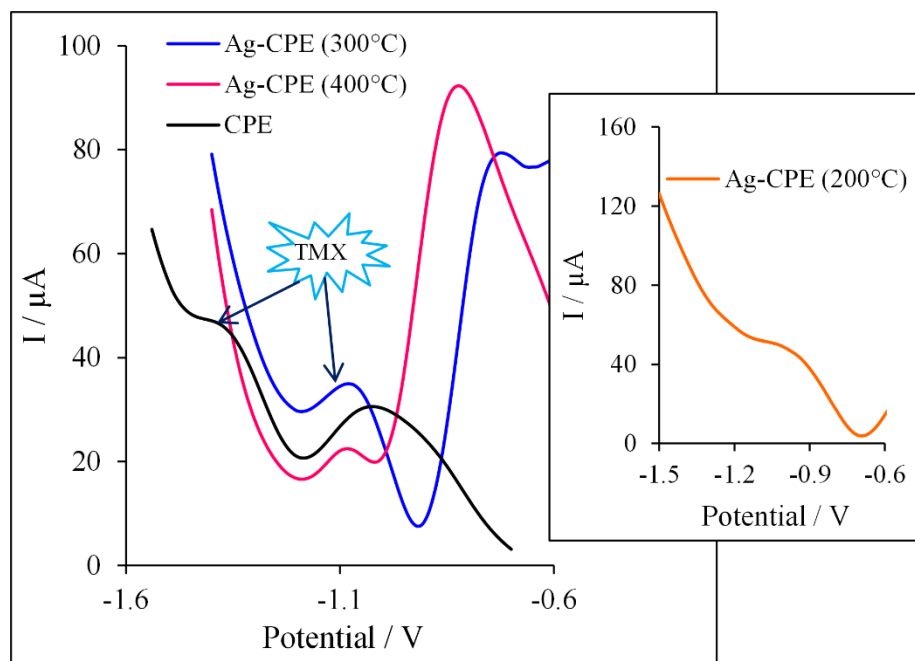
Figure 4: Square wave voltammetric plots of the reduction of TMX on unmodified electrode (CPE) and modified electrodes (Ag−CPE) prepared at different temperatures (200 °C to 400 °C).

The chronoamperometric measurements were employed to evaluate the effect of heated temperature of (Ag-CP) on the electroreduction of TMX. The figure 5 represents the current-time profiles obtained for three modified electrodes using a potential of -1000 mV. As seen, the behavior is typical of that expected for a mediated reduction. The current intensity of TMX at Ag−CPE (300 °C) is higher than that measured using others electrodes: Ag−CPE (200 °C) and Ag−CPE (400 °C), indicating that nanoparticles silver prepared at 300 °C show high catalytic performance to reduce TMX. This result confirms the previous results obtained by SWV.
The corresponding Tafel plots of Ag−CPE (200 °C), Ag−CPE (300 °C) and Ag−CPE (400 °C) are shown in figure 6. The fitted Tafel slope of the Ag−CPE (300 °C) was measured to be (-101.97 mV dec^{-1}), which is lower than Ag−CPE (200 °C) (-126.92 mV dec^{-1}) and Ag−CPE (400 °C) (-122.84 mV dec^{-1}), manifesting most favourable electroreduction of TMX while better reduction process was observed with Ag−CPE (300 °C) electrode.
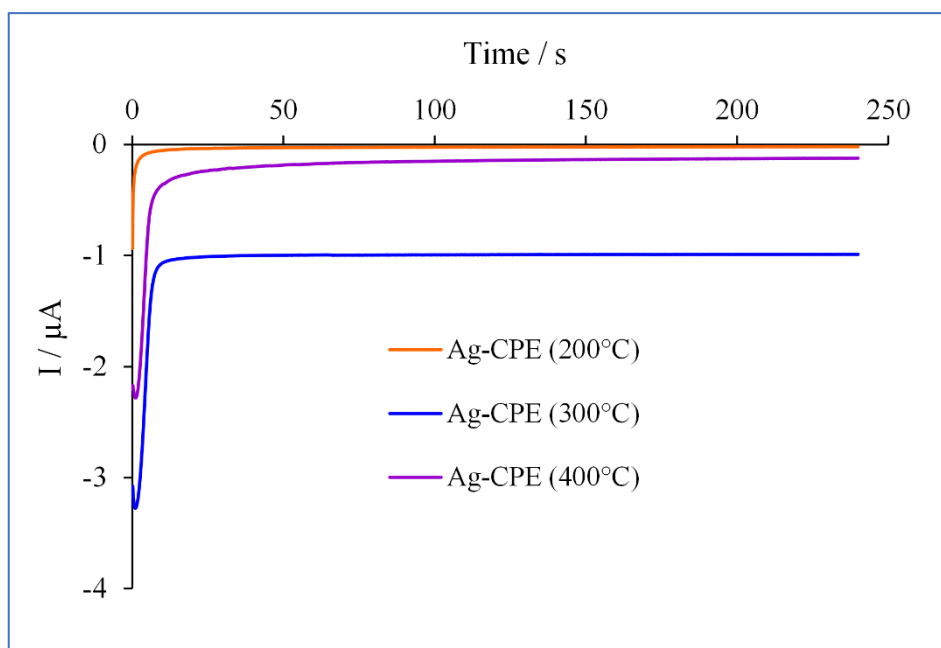
Figure 5*: Chronoamperogramms of thiamethoxam reduction (1.0×10^{-3} mol L^{-1}) with applied potential of -1000 mV at Ag-CPE prepared at different temperature, with Ag/CP = 60%.*
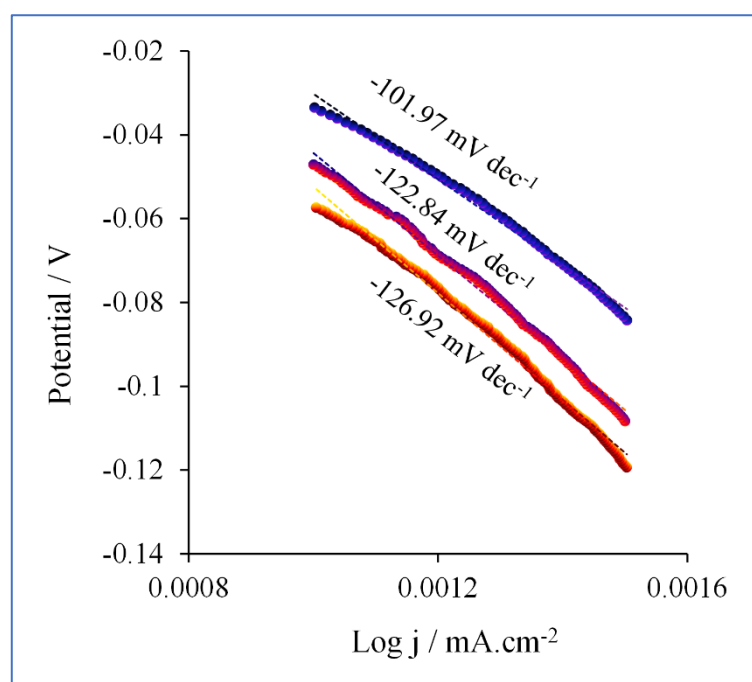
Figure 6*: Corresponding Tafel plots, of different Ag-CPE (200, 300 and 400 °C) in 1.0×10^{-3} mol L^{-1} TXM, Ag/CP = 60%.*

To better understand the mechanism of the electrocatalytic activity of Ag−CP heated at 300 °C, the Tafel plot relates the overpotential (η) as a function of logarithm of current density (j) was investigated by fitting the linear portion of the graph to Tafel equation (η= b logj + a), where b

85

corresponds to the Tafel slope value. To achieve a current density (j) of 10 mA cm^{-2}, Ag-CP treated at 300 °C requires a η_{10} of -101.74 mV, which obviously lower than those of Ag−CP treated under a nitrogen atmosphere at 200 °C (-122.76 mV) and 400 °C (-126.84 mV). The overpotential obtained with Ag-CPE (300 °C) is lower than those obtained with others electrode such as carbon paste electrode (CPE), metallic silver electrode (MSE) and glassy carbon electrode (GCE) (Table 3). This suggests a synergic enhancement between carbon and silver nanoparticles. The idea of modifying graphite by silver using a heat treatment, which shows good results with regard to the catalytic activity of TMX, inspired when see that the unmodified graphite electrode shows a poor activity comparing to metallic silver electrode which exhibits an acceptable catalytic activity toward TMX reduction. The remarkable activity of Ag−CPE can be attributed to *(i)* small sized, good homogeneity and high dispersion of active metal nanoparticles on graphite powder and *(ii)* synergic effect between host carbon and guest silver nanoparticles.

Table 3:Thiamethoxam reduction Tafel parameters of various electrodes.

Electrode	Tafel slope mV dec^{-1}	J_0 μA cm^{-2}	Overpotential j = 10 mA cm^{-2}	[Refs]
Ag-CPE 200°C	-122.84	1.20	-122.76	This work
Ag-CPE 300°C	-101.82	1.17	-101.74	This work
Ag-CPE 400°C	-126.92	1.19	-126.84	This work
MSE	-151.76	1.00	-151.87	[20]
GCE	-272.53	0.99	-272.12	[20]
CPE	-238.74	0.99	-238.95	[20]

4) Electrochemical behavior of thiamethoxam

The voltammetric behavior of the TMX at Ag−CPE (300 °C) was investigated in $1.0×10^{-3}$ mol L^{-1} B-R as supporting electrolyte. A single irreversible, reduction peak of the TMX was observed at quite negative potentials. The peak potential (E_p) and the peak current intensity (I_p) varied linearly with log (v) and log $v^{1/2}$, respectively. This result shows that TMX reduction was controlled by a diffusion process. The peak potential exhibited linear dependence with pH solutions in the range of pH ≤ 11.50: E_{pc}/V = -0.7683- 0.0326 pH (R^2= 0.983). According to the Nernst equation E = 0.0592m/n pH (n: number of electrons transferred, m: number of protons transferred), we find that the number of electrons transferred was twice as the number of protons transferred in electrochemical reduction of TMX [37].

The chronoamperometry was also employed to investigate TMX reduction at Ag−CPE (300 °C) (Figure 7A). Chronoamperometric measurements of thiamethoxam were done for various TMX concentrations. Generally, for an electroactive material (TMX in this case) with a diffusion coefficient of D, the current intensity for the electrochemical reaction (at mass transport limited rate) is described by the Cottrell equation [38]:

$$I = nFAD^{1/2}C_b^{-1/2}t^{-1/2} \tag{6}$$

Under diffusional process, a plot of I versus $t^{-1/2}$ will be linear and D value can be calculated (Figure 7B.) The mean value of the D was found to be $1.17 \times 10^{-6}\,\text{cm}^2\,\text{s}^{-1}$.
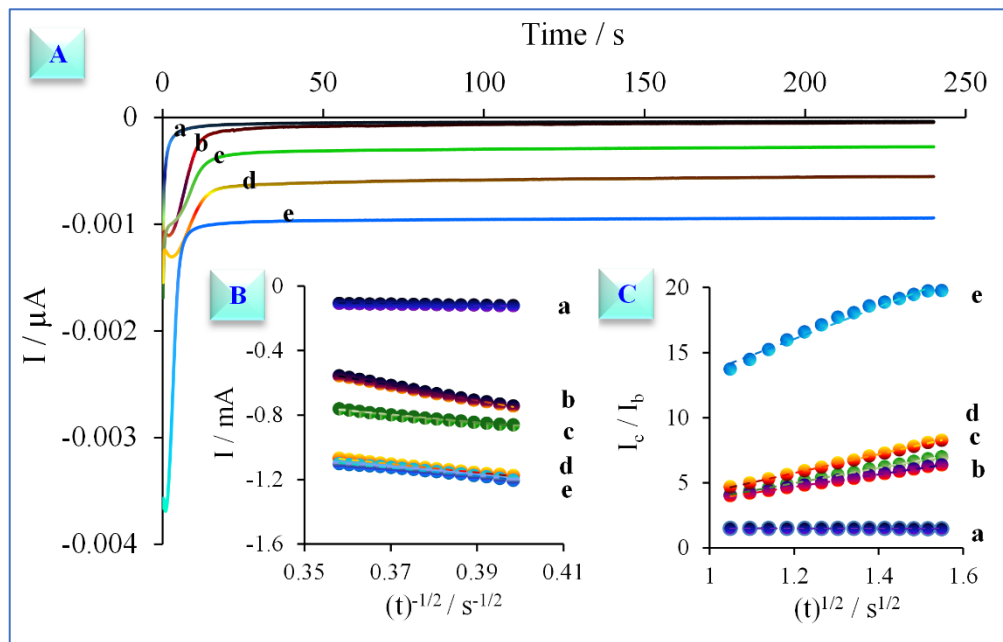
Figure 7: (A) Chronoamperometric measurements for various concentration of TMX (a) correspond to 1.0×10⁻⁵, (b) 5.0×10⁻⁵, (c) 1.0×10⁻⁴, (d) 5.0×10⁻⁴ and (e) 1.0×10⁻³mol L⁻¹ at Ag−CPE (300 °C) with applied potential of -1000 mV. (B): plots of I vs t⁻¹ᐟ² obtained from chronoamperogrammes, (C): plot of Iₒ / Iₗ vs t¹ᐟ² of Ag-CPE, Ag/CP =60%.

Chronoamperometry method can also be employed to evaluate the catalytic rate constant k, for the reaction between TMX and Ag−CPE (300 °C) according to Galus equation [39]:

$$I_C / I_L = \pi^{1/2}\gamma^{1/2} = \pi^{1/2}(kC_bt)^{1/2} \tag{7}$$

Where I_C is the catalytic current of TMX at Ag−CPE (300 °C), I_L is the limited current in the absence of TMX, $\gamma = kC_bt$, t is the time elapsed, and C_b is the bulk concentration of TMX.

Based on the slope of the I_C/I_L versus $t^{1/2}$ plot, k can be obtained for a given TMX concentration. From the values of the slopes (Figure 7C), the average value of k was found to be 6.7×10^4 mol^{-1} s^{-1}.

5) Thiamethoxam analysis in water

The square wave voltammetry was used for the determination of thiamethoxam. Indeed, the current intensity is sharper and more sensitive at low concentrations. It exhibited a linear relationship over the concentration range 1.0×10^{-4} to 1.0×10^{-3} mol L^{-1} of thiamethoxam (Figure 8). The linear regression equation was obtained to be $I_{pc}(\mu A) = 16132$ [TMX] + 2.9821 ($R^2 = 0.9894$). The limit of detection (LOD) was 3.6×10^{-5} mol L^{-1}, based on $3 \times SD_b/S$ were SD_b and S represent the standard deviation of the blank for eight repetition and slope of calibration curve respectively. The relative standard deviation (RSD) of the modified electrode for eight measurements was 2.015 %, suggesting that the precision and reproducibility of the proposed detection technique was quite promising (Table 4). High performance in the electrochemical process of the proposed electrode can be explained by the dispersion, homogeneity and nanoparticles size of the powder (Ag-CP) heated at 300 °C with carbon- silver weight ratio (60wt%). In addition, the current of TMX reduction obtained with Ag−CPE retained 83.17 % of its initial value after storage for 30 days in the standard conditions. The results suggested that Ag−CPE possessed acceptable storage stability.

Table 4: *Analytical characteristics obtained for TMX determination using square wave voltammetry technique.*

Characteristic	Value
Linear range / μmol L^{-1}	100 _ 1000
LOD / μmol L^{-1}	36.04
LOQ / μmol L^{-1}	120.13
Correlation coefficient (r)	0.98
Slope (μA L μmol^{-1})	16132
Intercept / μA	2.98
RSD (%)	2.02

The interferences remove is always a challenging work in electrochemical sensing field. So, a systematic study of interference of possible coexisting substances in real samples was performed to evaluate the selectivity of Ag-CPE in reducing TMX. The results indicated that 100-fold of 4-nitrophenol, 2-nitroaniline, 4-nitroaniline; 50-fold of 2,4-dinitrophenylhydrazine didn't interfere with the SWV signal of 5.0×10^{-4} mol L^{-1} TMX (peak current change $< \pm 5\%$). These results indicated that the modified electrode Ag−CPE heated at 300 °C showed excellent selectivity for TMX determination, and could be successfully employed for TMX analysis in real samples.
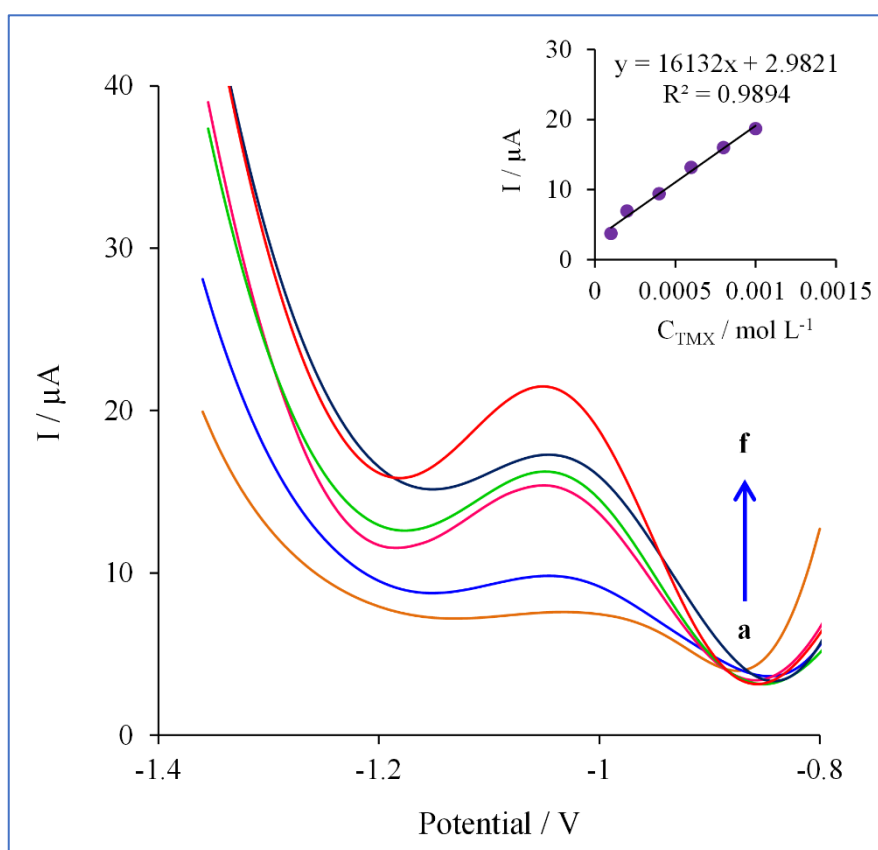
Figure 8: *SW voltammograms obtained at Ag-CPE (300°C) for different concentrations of thiamethoxam (a) 1.0×10^{-4}, (b) 2.0×10^{-4}, (c) 4.0×10^{-4}, (d) 6.0×10^{-4}, (e) 8.0×10^{-4} and (e) 1.0×10^{-3} mol L^{-1} insert calibration curve, Ag/CP = 60%.*

The performance of Ag−CPE heated at 300 °C was evaluated in the determination of thiamethoxam in wastewater and ground water samples. The detection of TMX was accomplished according to the procedure mentioned in the section of analytic performance. The recovery of TMX in the wastewater and groundwater samples were between (89.89 to 99.32

%) and (86.82 to 98.08 %) respectively, with the relative standard deviation (RSD) agreeable (3 measurements). The results (Table 5) indicated that the recovery of TMX on the modified electrode Ag−CPE was satisfactory.

Table 5:Recovery test of added samples.

Sample	Added concentration [$\times 10^2$ µmol L^{-1}]	Found concentration [$\times 10^2$ µmol L^{-1}]	Recovery [%]	RSD n=3 [%]
Wastewater	10	9.93	99.32	7.47
	5	4.49	89.93	1.40
Groundwater	10	9.80	98.68	2.76
	5	4.38	87.67	5.42

B) Electrodeposition of silver particles on graphite powder

1) Electrodeposition procedure and its efficiency for thiamethoxam sensing

Electrochemistry is a science of surfaces and interfaces that studies the chemical reactions that take place at the electrode-electrolyte interface. Electrodes are the main constituents in all electrochemical applications. The ability to modify their surface structure allows electrochemical systems to evolve. Electrodeposition is simple, controllable, low-cost and time-saving technique in comparison with other methods, such as physical and chemical vapour deposition, hydrogen plasma, hydrothermal and sonochemical methods. Also offer the advantage of being able to assembling nanostructured multi-component films. Various features of silver electrodeposition on electrode surface to control the composition and morphology of incorporated particles in the coatings were reported for electroanalytical applications, such as organic compound and heavy metal analysis, via different manufacture and flexibly design of silver electrodeposited. Majidi et *al.* introduced a novel electrochemical sensor based on AgNDs supported by graphene nanosheets modified GCE for imidacloprid determination [2]. Laghrib et *al.* determined para-nitroaniline and studied its electrocatalytic reduction using silver particles electrodeposited onto carbon-paste electrodes by cyclic voltammetry [40, 41]. An electrodeposition of silver amalgam particles (AgAPs) on basal-plane pyrolytic graphite electrode (bPGE), and prove on 4-nitrophenol [42]. Feng-Hsuan Cho et *al.* prepared silver dendrites (Ag-Ds) by electrodeposition on a glassy carbon electrode (GCE) and investigated its capability in sensing 4-nitrophenol, via surface enhanced raman scattering (SERS) using laser excitation at 633 nm [43]. Jia Bi has developed an electrodeposition approach to provide silver nanoflowers composed of many silver nanoleaves as sensitive surface enhanced raman

scattering sensing substrates [44]. In the same context, the results present by Joaquín Klug et al. showed direct interaction between the Myristoylated Alanine-Rich C Kinase Substrate (MARCKS) effector domain (ED) and Ag nanoparticles (AgNPs) electrochemicaly deposited on the silicon platform as surface enhanced raman scattring substrate [45]. Also, Mehdi Baghayeri and co-work adopted an electrochemically deposition of silver nanoparticles on the film of a metformin functionalized multi-walled carbon nanotube modified glassy carbon electrode (Met-MWCNT/GCE) for entacapone (ENT) determination [46]. Simultaneous electrochemical sensing of chloramphenicol and metronidazole are investigated by Haiyun Zhai et al. using electrodeposited silver nanoparticles/sulfonated functionalized graphene modified glassy carbon electrode (AgNPs/SF-GR/GCE) [47]. The same method was reported by Lorena Athie Goulart et al. for analysis of four phenolic compounds using a glassy carbon electrode (GCE) modified with electrodeposited silver nanoparticles onto multi-walled carbon nanotubes [48]. A glassy carbon electrode (GCE) modified by electrodeposited silver nanoparticles AgNPs as an electrochemical nanoaptasensor was used to determine trinitrotoluene [49]. Mercury ions were detected by silver nanoparticles as signal reporter selectively electrodeposited on glassy carbon electrode modified with DNA-based AuHg amalgam [50]. All these modifications were done in order to enhance the electrode sensitivity and others lead to high electrocatalytic activity. Tiwari et al. have investigated an electrodeposition technique, which provided a suitable route for the synthesis of silver coated nitrogen rich mesoporous carbon (Ag/NMC) composite for the electrocatalytic activity towards ORR (oxygen reduction reaction) [51]. Agnieszka Brzózka and co-works reported the elecrodeposition of silver nanohemisphere (Ag-NHS) and nanowire (Ag-NW) array into nanoporous aluminum oxide (AAO) templates where they compared their electrocatalytic properties against silver rod (Ag-bulk) electrode in an alkaline solution [52]. In our study, due to high importance of electrochemical deposition process, the chronoamperometry was employed to deposit silver particles onto graphite carbon. Indeed, the chronoamperometry was employed for the electrodeposition of silver particles on graphite electrode, in the electrolyte (volume 25 mL) of Britton-Robinson pH 2.0 containing 8.0×10^{-4} mol L^{-1} of silver nitrate. For this procedure, we use an electrode cavity (0.13 cm^2) and a graphite bar to finding the electrical contact. The prepared electrode carefully washed by distilled water and transferred into a cell (25 mL volume) containing thiamethoxam in Britton-Robinson pH 10.4. The square wave voltammetry was reported in the range from -400 mV to -1400 mV. This obtained modified electrode, denoted as Ag@GrCE, was used for thiamethoxam determination.

The electrocatalytic capacity of the Ag@GrCE toward electrocatalysis of TMX reduction was evaluated by cyclic voltammetry (CV) and square wave voltammetry (SWV). The cyclic voltammograms show a cathodic peak at -1186 mV and -1083 mV on graphite carbon electrode (GrCE) and graphite modified with electrodeposited silver particles (Ag@GrCE) respectively (Figure 9a). Under identical conditions, square wave voltammetry (SWV) confirms the same behavior of thiametoxam. In fact, a reduction peak is observed at -1186 mV and -1083 mV on GrCE and Ag@GrCE respectively (Figure 9b). Therefore, the Ag@GrCE presents great enhanced current response of the reduction peak, which due to the enhanced in surface conductivity with the presence of silver particles. Moreover, the peak potential shifted ~100 mV positively in the TMX reduction potential, which due to the electrocatalytic activity of silver particles [53].
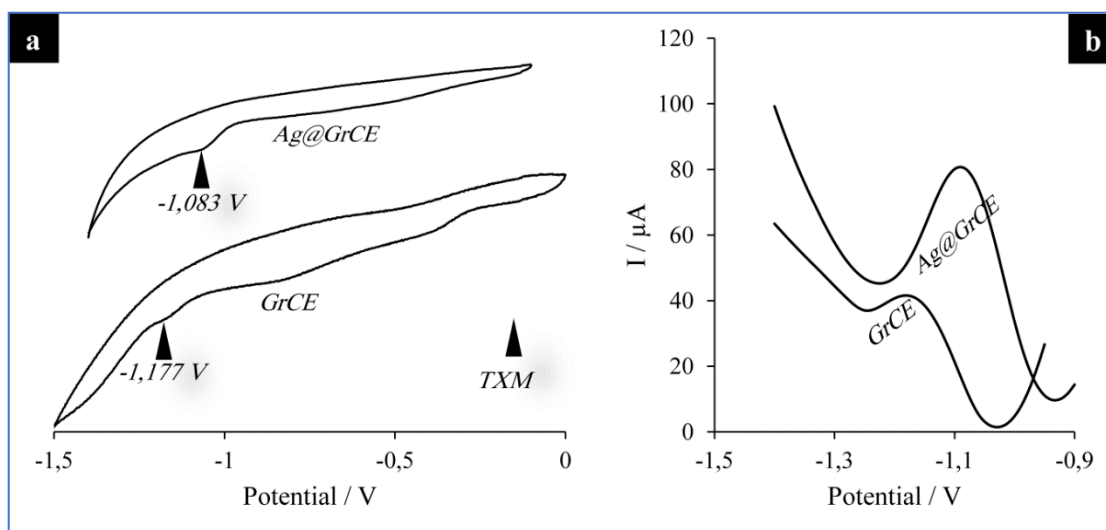
Figure 9: (a) Cyclic voltammetric response, (b) square wave voltammetric response of 1.0×10^{-3} mol L^{-1} TMX respectively at electrodeposited silver particles on graphite carbon electrode (Ag@GrCE) and graphite carbon electrode (GrCE) in R-B buffer pH 10.4.

2) Optimization of electrodeposition conditions

For deposit of the silver particles onto carbon with catalytic properties, it is essential to optimize the parameters influencing the detection of thiamethoxam by the SWV (deposition time, concentration of silver in electrolyte, solution pH and applying potential …). The effect of the deposition time of silver particles on the SWV response of TMX was investigated in a solution of B-R buffer (pH 10.4) containing 1.0×10^{-3} mol L^{-1} of TMX in the potential range from -0.4 to -1.4V. The maximum peak current was obtained with 4 min (Figure 10a), more this time, the peak current values decrease.

The applying potential is an important parameter in chronoamperometric measurements. For the right choice of this potential, several potentials were tested (Figure 10b) to have a good electrodeposition of silver particles on graphite surface. The Ag@GrCE electrode prepared at applied potential of -400 mV shows higher sensitivity toward TMX sensing.
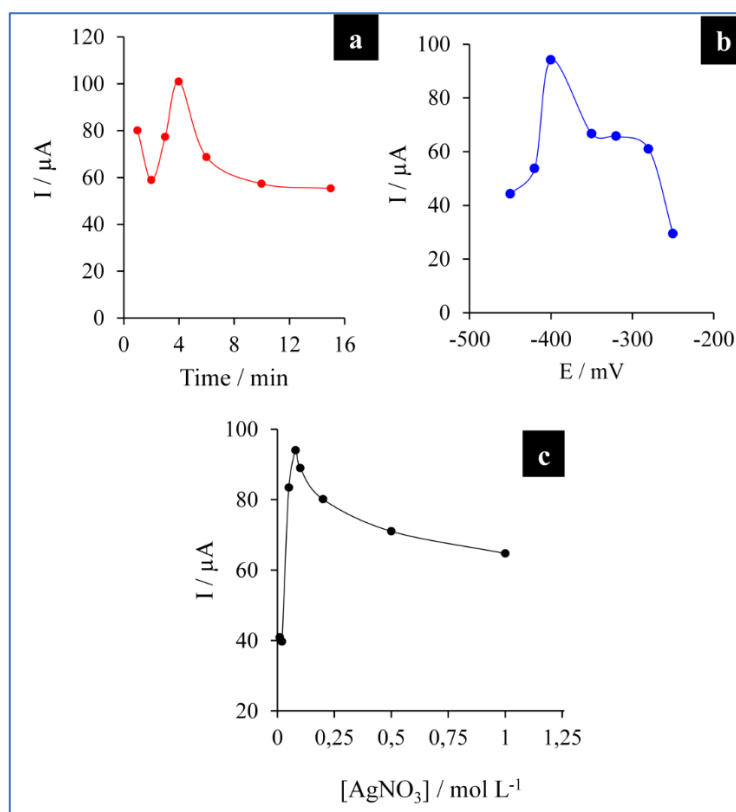
Figure 10: Influence of the experimental parameters, on chrononoamperometric electrodeposition: (a) the electrodeposition time, (b) the applying potential and (c) the amount of AgNO$_3$ on the reduction peak current of 1.0×10^{-3} mol L-1 TMX. Square wave voltammograms measurement were performed in B-R buffer (pH 10.4).

The amount of silver on the electrode surface is also necessary to assess the electrochemical determination of thiamethoxam. Therefore, it was optimized by varying the concentration of AgNO$_3$ in range from 1.0×10^{-4} to 1.0×10^{-3} mol L^{-1} of AgNO$_3$ in B-R buffer pH 2.0 with the evaluation of its effect on response of TMX. Under optimized parameters, applying potential of -400 mV for 4 min, the 8.0×10^{-4} mol L^{-1} of AgNO$_3$ shows the highest peak intensity. However, high concentration of AgNO$_3$ shows low response of TMX (Figure 10c). This behaviour was attributed to the formation of a large number of small clusters randomly distributed on the GrC electrode surface [54]. The electrodeposition parameters were as

follows: 4 min, 8.0×10^{-4} mol L^{-1}, pH 2.0 and -400 mV for deposition time, concentration of silver in electrolyte, solution pH and applying potential, respectively.

3) Physicochemical characterization of electrodeposit powder

The surface morphology of the Ag@GrCE was investigated by scanning electronic microscope (SEM). The image revealed that carbon had two-dimensional flat morphology exhibits a homogeneous and compact layer with small particles and full coverage (Figure 11a). To confirm the presence of the silver particles, the EDX was used. In EDX analysis, figure 11b shows the peaks in silver region confirming the presence of elemental silver [55]. To confirm this result, XRD pattern silver/ graphite were obtained as illustrate in figure 11c.
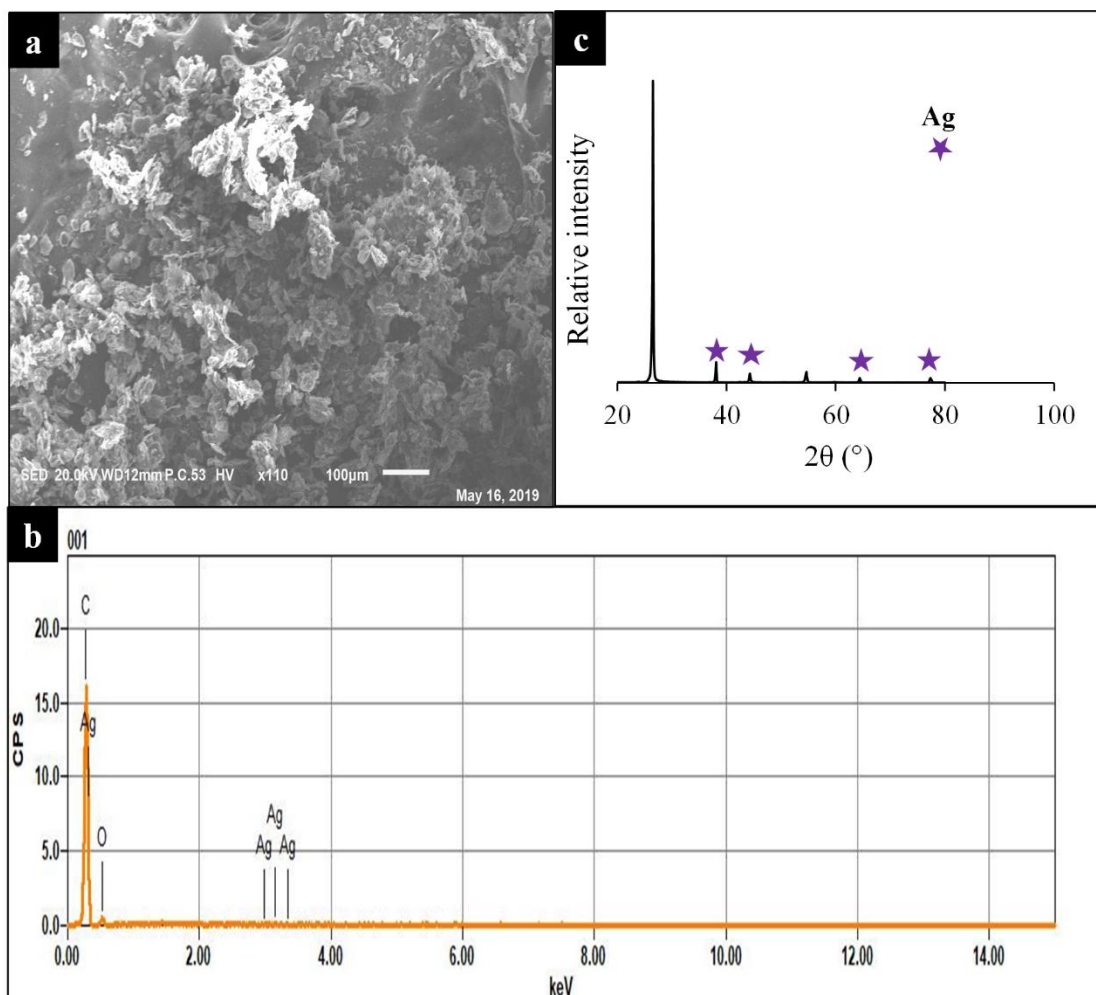
Figure 11: *(a) SEM image of Ag@GrCE (b) EDS spectrum of Ag@GrCE (c) XRD spectrum of the Ag@GrCE.*

The four diffraction peaks are observed at 2θ of 38.15, 44.19, 64.41 and 77.32, which can be designated respectively to diffraction from the planes (111), (200), (220) and (311) of the face centred structure of Ag(0), (JCPD, file No. 4-0183) [56].

The electroactive surface area (ESA) has been estimated using cyclic voltammetry of solution containing 1.0×10^{-2} mol L^{-1} of $[Fe(CN)_6]^{3-/4-}$ containing 0.1 mol L^{-1} KCl at different scan rates (ν) ranging from 0.005 V s^{-1} to 0.3 V s^{-1} according to Randles-Sevcik equation 8.

$$Ip = 2.69 \times 10^5 \times n^{3/2} \times A \times D^{1/2} \times C \times v^{1/2} \tag{8}$$

Both the peak currents (Ip) of the GrCE and Ag@GrCE were proportional to the square root of scan rate (Figure 12a-b). Considering $D = 7.6 \ 10^{-6}$ cm^2 s^{-1} and $n=1$ for a 1.0×10^{-2} mol L^{-1} of $[Fe(CN)_6]^{3-/4-}$ and from the slopes values of the straight lines. The ESA of GrCE and Ag@GrCE were obtained are 1.08×10^{-4} cm^2 and 2.25×10^{-4} cm^2 respectively. The electroactive surface area of Ag@GrCE increased approximately by 48.04% compared to the GrCE, demonstrating the enhancing conductivity of modified electrode.

To calculate the heterogeneous electron transfer (ET) rate k°, the Nicholson method was used from the peak-to-peak separation ΔEp of the cyclic voltammogram. As shown in Figure 12a-b, the ΔEp is increased with scan rate, indicating a quasi-reversible nature of reaction, using following equation 9 [57]:

$$\Psi = k°[\pi n D v F \ / \ RT]^{-1/2} \tag{9}$$

Where ψ is the dimensionless kinetic parameter, n is number of electrons transferred, D is the diffusion coefficient, F faradic constant, R the gas constant, T the temperature of solution and ν the scan rate. In practice, the kinetic parameter ψ is calculated from ΔEp for one step, one electron process at a set temperature 298 k, using an appropriate practical function (equation 10) [58]:

$$\Psi = (-0.628 + 0.021\Delta Ep) \ / \ (1-0.0071\Delta Ep) \tag{10}$$

The heterogeneous electron transfer (ET) rate constant $k°$ was determined from the slope of ψ-$[\pi n D F \ / \ RT]^{-1/2} v^{-0.5}$ dependence corresponding to equation 2 as shown in Figure 12a-b, while the operating curve determined according to this approach is limited to ΔEp occurred in the interval > 212 mV. A method devised by Kochi and Klinger permits the use of much large dEp for k° evaluation following equation 11 [59]:

$$K° = 2.18[D\alpha n\nu / RT]^{-1/2}Exp[-(\alpha^2 Nf / RT) \Delta Ep] \qquad (11)$$

The ET rate $k°$ was calculated to correspond to 8.84×10^{-4} cm s^{-1} and 1.09×10^{-3} cm.s^{-1} for both electrode GrCE and Ag@GrCE respectively using the above equations. The results suggesting that the electron transfer reaction was easily transferred on the surface modified silver particles. For explain the effect of electrodeposition potential onto formation of the silver particles, the surface properties of the different electrodes prepared were investigated using electrochemical impedance spectroscopy (EIS). Also, to evaluate the electron-transfer kinetic of the modified electrode by silver particles, solution of 0.1 mol L^{-1} KCl containing 1.0×10^{-2} mol L^{-1} of $[Fe(CN)_6]^{3-/4-}$ was used. The nyquist diagrams of Ag@GrCE prepared at different applied potentials (-300 mV, -400 mV and -500 mV) and GrCE were recorded in the range of 100 Hz to 100 MHz (Figure 12c). Indeed, the dielectric and insulating properties of the electrode/electrolyte interface depend on the charge transfer resistance R$_{ct}$, which corresponds to the diameter of the semicircle observed at high frequencies in Nyquist diagrams. All Ag@GrCE showed a higher electron transfer kinetic compared of unmodified electrode prepared GrCE (Figure 12c). The R$_{ct}$ of the Ag@GrCE (-400 mV) was measured to be (72.09 ohm cm^2), which is lower than Ag@GrCE (-300 mV; 120.3 ohm cm^2) and Ag@GrCE (-500 mV; 89.31 ohm cm^2). The Ag@GrCE (-400 mV) presented an excellent electronic property, forming a fast electron conduction pathway between the electrode and the electrochemical probe when compared with others electrodes.

Following EIS characterization and to investigate the functional groups of modified graphite, FT-IR measurements were recorded at the range 4000- 400 cm^{-1}. The spectra obtained for silver particles electrodeposited on graphite electrode applying various deposition potentials (-300, -400 and -500 mV) are given in figure 13. A broad band at 3444 cm^{-1} is attributed to the –O-H group into the external surface of graphite carbon. The two bands at 2921 and 2855 cm^{-1} in the higher frequency region of spectra correspond to C-H stretching mode, while the two shoulder peaks at 1632 and 1580 cm^{-1} can be ascribed to aromatic C=C and C-C or C-O groups, which exists on a sample of silver-graphite carbon (Ag@GrC) surface as functional groups prepared applying a potential of -500 mV.
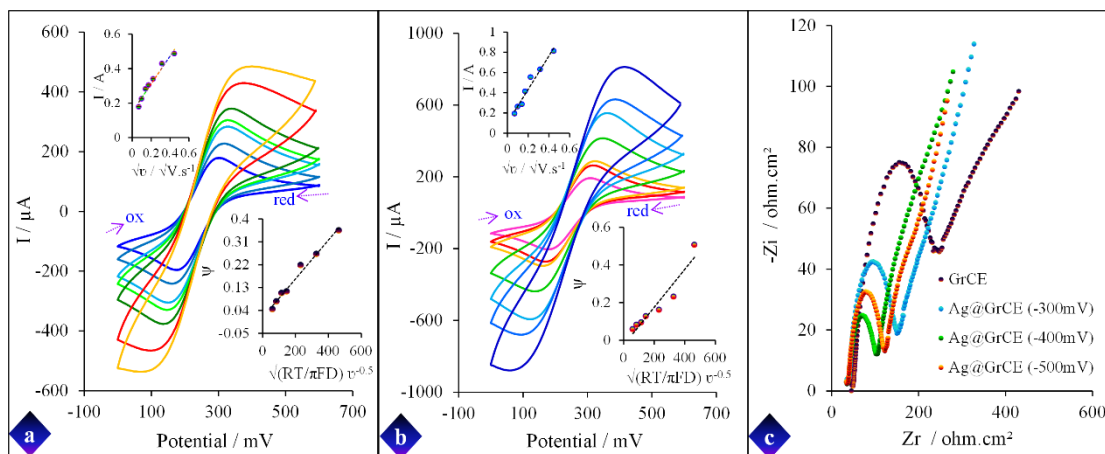
Figure 12: Cyclic voltammetry scan rate studies for [Fe(CN)6] $^{3-/4-}$ at (a) GrCE and (b) Ag@GrCE Inset: ψ versus [πDFnν/RT]$^{-1/2}$; and I_p (µA) versus $v^{1/2}$. (c) The Nyquist diagrams of the impedance (Z_{im} vs. Z_{re}) for Ag@GrCE prepared at different applied potentials (-300 mV, -400 mV and -500 mV) and GrCE, other condition: 0.01 mol L^{-1} K$_3$[Fe(CN)$_6$] and 0.1 mol L^{-1} KCl solutions.
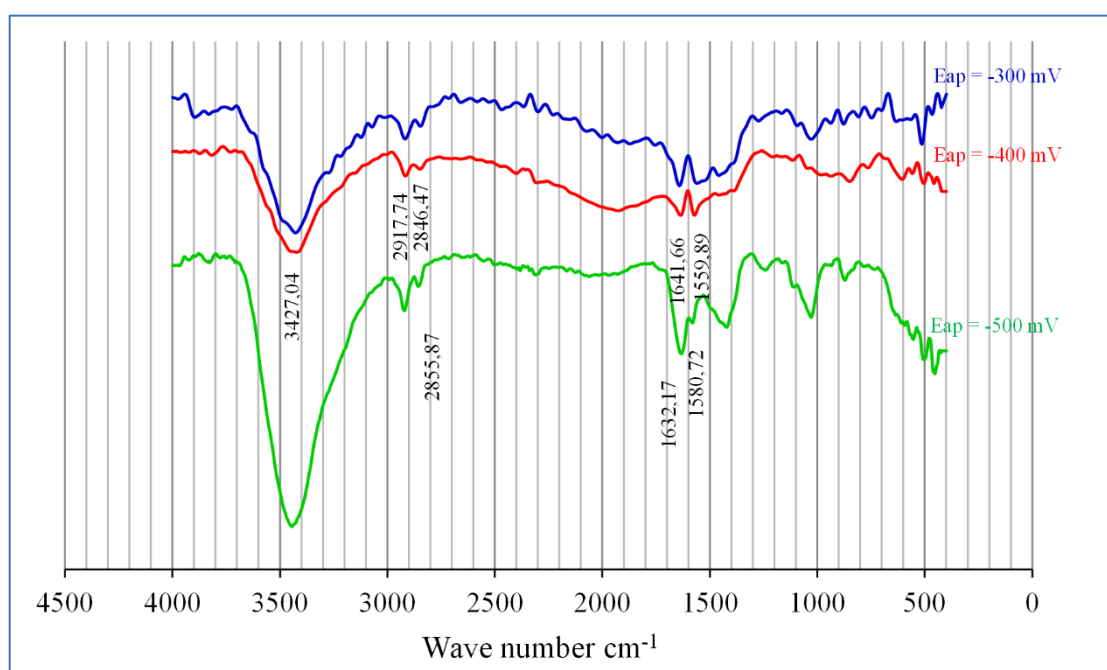
Figure 13: IR spectra of modified graphite carbon based on electrodeposited silver particles (Ag-GrC) prepared applying various potentials (-300, -400 and -500 mV).

The spectra of the Ag@GrC samples prepared applying -400 and -300 mV obtained are similar to that Ag@GrC prepared at -500mv surface, with the exception that all the bands shift to low wave numbers, which suggest that some changes of the environment of silver particle deposited on the surface of graphite carbon. No new covalent bonding between the graphite carbon and

97

Ag particles were formed. Which may be explained by silver particles immobilized and electron density of graphite carbon higher leading to weak O-H, C-H and C=C bands.

4) Reactional mechanism of thiamethoxam on electrodeposit powder

i) Scan rate effect

The electrochemical mechanism of electrode process studied by the relationship between the peak current and potential scan rate. The scan rate effect on the reduction of 5.0×10^{-2} mol L^{-1} thiamethoxam at the silver particles deposited onto graphite electrode was investigated by cyclic voltammetry. With the increase of the scan rate, the reduction peak currents of TMX enhanced and peak potentials shifted to more negative values of potential. There is no reverse peak obtained for all the cyclic voltammetric scans, which shows that TMX undergo irreversible reduction on electrodeposited silver particles modified graphite electrodes (Figure 14a).

The linear relationship between cathodic peak current of TMX (Ic) and scan rate (v) plot is shown in the inset of figure 14b, where the linear equation is $I_p = 0.0239 + 1.420\ v$, $R^2 = 0.966$. Moreover, a plot of the cathodic peak current versus the square root of scan rate ($v^{1/2}$) yielded a straight line in the range of 10 to 400 mV s^{-1} (Figure 14c) according to the equation I_p (μA) = $0.0267 + 1.17\ v^{1/2}$ ($V^{1/2}$ s$^{1/2}$) ($R^2 = 0.994$). To confirm the TMX reduction control process, we rely on the slope value of linear plot between log (scan rate) and log (peak current) (Figure 14d). This slope value was found to be about 0.55, which very close to theoretical value (0.5) for the diffusion-controlled reaction [60, 61].

Therefore, the result indicates that the electro-catalytic reduction of thiamethoxam at the Ag@GrCE was a typically diffusion-controlled electron transfer mechanism. As for an irreversible electrochemical reaction, the $E_{p,c}$ is determined by the following equation 12 [62].

$$Ep, c = E° - \frac{RT}{\alpha nF}\ln\left(\frac{\alpha nF}{RTK}\right) - \left(\frac{RT}{\alpha nF}\right)\ln(v) \tag{12}$$

$E°$ is formal redox potential, k is the standard heterogeneous rate constant of electron transfer, n is electron transfer number involved in rate determining step, v is scan rate, R is the gas constant, T is the absolute temperature, and F is the Faraday constant. According to the linear relationship of $E_{p,c}$ versus ln v, the value of αn is defined according the slope ($RT/\alpha nF$) of the fitted line to be -0.0353. Usually, α is simulated to be between 0.3 to 0.7 in totally irreversible electrode process [63–65], then, the value of the electron transfer number n must to be around 3, and α is 0.3. The reduction of aromatic nitro compound R-NO$_2$ to hydroxylamine R-NHOH

in aqueous media take place via four electrons. In alkaline medium, this reduction has been highlighted; essentially a 1e- reversible reduction is observed, followed by 3e- irreversible reduction [66–68]. In the present case, the studying peak correspond to second step three electrons and four-proton of nitro group TMX electro-reduction at Ag@GrCE in the alkaline media, because the 1e- reversible reduction of RNO_2^- is very small under these conditions, which can have illustrated as shown in scheme 1:
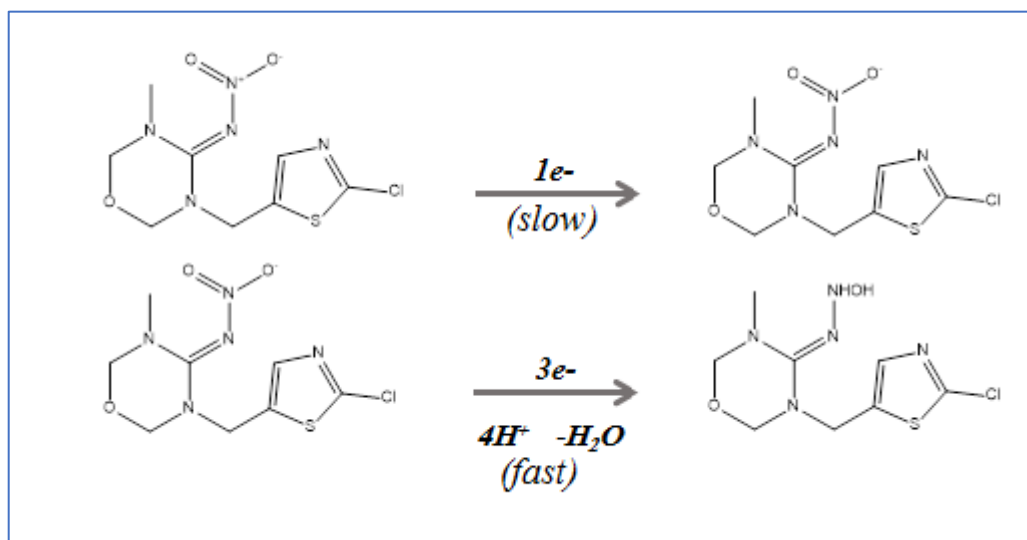
Scheme 1: *mechanism of electroreduction of organic nitro-group TMX in alkaline media.*
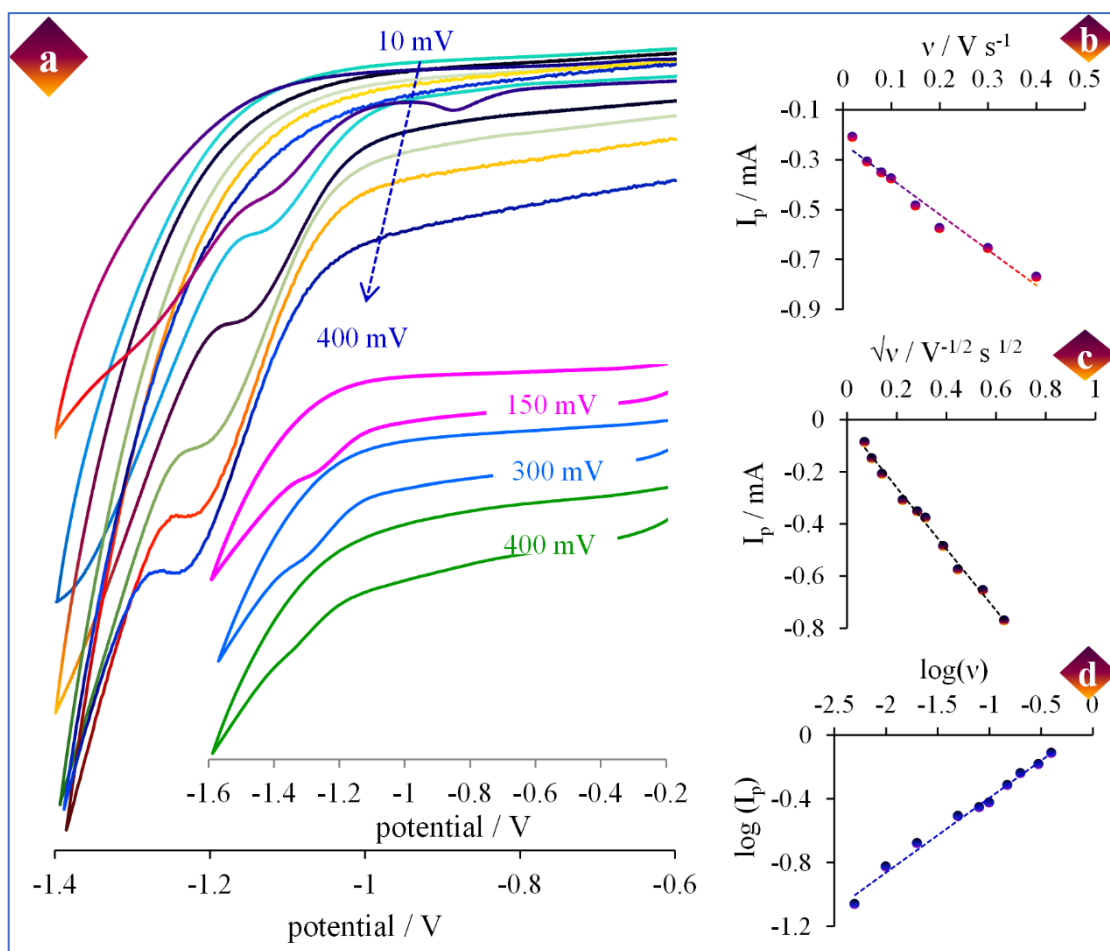
Figure 14: (a) Cyclic voltammograms recorded with carbon paste electrode modified electrodeposited silver particles in B-R buffer pH 10.4 containing 5.0×10⁻² mol L⁻¹ TMX at different scan rates. (b) The plot of cathodic peak current versus scan rate. (c) The I_c vs square root of scan rate. (d) The relationship between the logarithm of the peak currents versus the logarithm of scan rate.

Consequently, the electrochemical mechanism consists of a mixture of diffusion and adsorption-controlled processes depending on the scan rate [69–72]. The adsorption capacity (Γ) for the reduction of thiamethoxam was determined to be $3.76×10^{-2}$ mol cm⁻², from the slope of the linear plot of I_p vs scan rate following equation 13:

$$I_p = n^2F^2A\Gamma v/4RT \qquad (13)$$

Where *n* is the number of electrons involved in the reaction; *A* is the geometric surface area of the electrode (0.1256 cm²); *v* is scan rate; *R*, *F* and *T* have their normal meaning.

100

ii) Chronoamperometric study

Chronoamperometric method was used to evaluate the catalytic performance of proposed electrode toward the electro reduction of thiamethoxam (Figure 15).
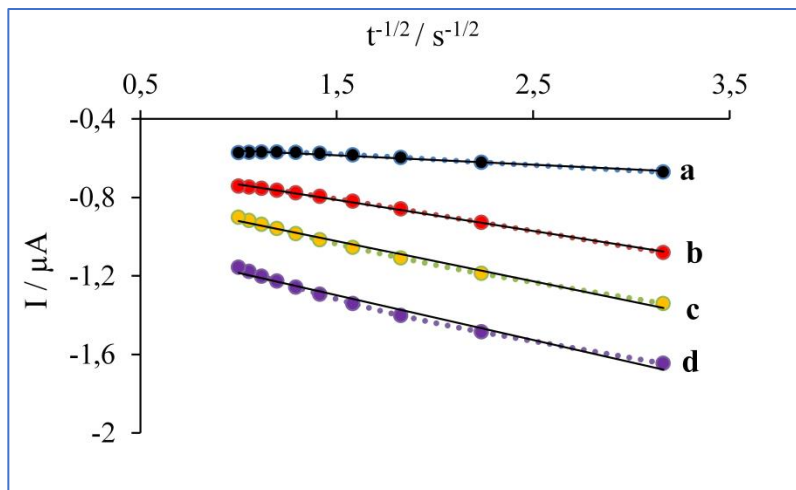
Figure 15*: The plots of Ic vs. $t^{-1/2}$ ($s^{-1/2}$) obtained from chronoamperograms of TMX concentrations (a) 1.0×10^{-5}, (b) 2.5×10^{-5}, (c) 2.5×10^{-4} and (d) 1.0×10^{-3} mol L^{-1} with a potential step at -1100 mV in BR buffer (pH 10.4).*

The diffusion coefficient (D) was found to be about 1.55×10^{-2} cm^2 s^{-1} from the slope of the I_c vs $t^{-1/2}$ plot for different TMX concentrations recorded at potential of -1100 mV, and employing the following Cottrell equation 14 [73]:

$$I=n.F.A.D^{1/2}.C.\pi^{-1/2}.t^{-1/2} \tag{14}$$

The rate constant of the electrocatalytic thiamethoxam reduction on Ag@GrCE was also determined using obtained chronoamperograms and the Galus equation 15 [74–76]:

$$I_c/I_b = \pi^{1/2} (k.C.t)^{1/2} \tag{15}$$

Where *C* is the concentration of thiamethoxam in bulk solution, *t* is elapsed time, *k* is catalytic rate constant, I_b and I_C are the currents in the absence and presence of thiamethoxam, respectively. Therefore, Galus plots were made between I_c/I_b and $t^{1/2}$ for various concentrations, the mean value of the rate constant (k) was obtained to be about 1.67×10^4 mol L^{-1} s^{-1}.

5) Thiamethoxam analysis in orange and tomato juices samples

Square wave voltammetry was recorded under optimum instrumental setting: pulse 50 mV, amplitude modulation 10 mV, pH solution (10.4) and duration 1 mint. Square wave voltammetry responses of various concentrations of thiamethoxam in B-R buffer at Ag@GrCE are shown in figure 16a. The cathodic peak current increased with increasing of TMX concentration ranging from 5.0×10^{-6} to 1.0×10^{-3} mol L^{-1}. The calibration plots illustrated good linear relationship between the peak current and the concentration of TMX (inset graph in figure 16a). The linear regression is depicted by following equation. $I_c(\mu A) = 57647[TMX] + 8.9179$ with correlation coefficient of 0.9804. The limit of detection (LOD) and quantification (LOQ) were determined to be 1.92×10^{-6} and 6.34×10^{-6} mol L^{-1} respectively, calculated by equations LOD= $3 \times \sigma/s$ and LOQ = $10 \times \sigma/s$ where σ is the standard deviation of the blank and s is the slope of the calibration curve [77]. This value of detection limit is lower than that reported for a sensor-based graphene oxide [23] and glassy carbon electrode [78].

For evaluating the repeatability of this electrode, the TMX detection was performed 8 times repeatedly with an identical electrode. The relative standard deviations were 2.46 % and 4.37 % for 5.0×10^{-4} mol L^{-1} and 8.0×10^{-5} mol L^{-1}, respectively, showing a satisfactory repeatability of the Ag@GrCE. The storage stability of the modified electrode was also evaluated by measuring square wave voltammetry responses after storing the modified electrode for 2 weeks. The peak current slightly decreased of 10 % of the original response, showing an acceptable stability of the Ag@GrCE.
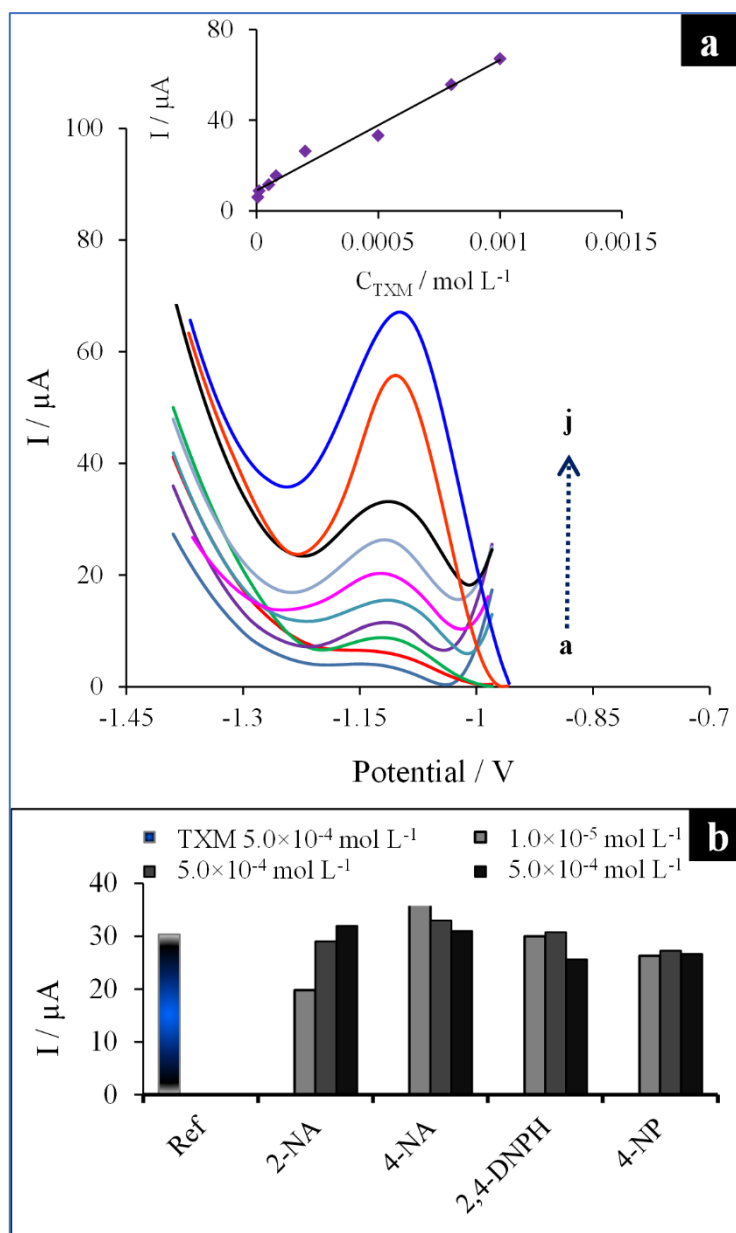
Figure 16: *(a) Responses of square-wave voltammetry to increasing concentration of TMX (a: 5.0×10-6, b: 8.0×10-6 c: 1.0×10-5, d: 2.0×10-5, e: 4.0×10-5, f: 8.0×10-5, g: 1.0×10-4, h: 2.0×10-4, i: 5.0×10-4, j: 8.0×10-4 mol L-1), with corresponding linear regression. All measurements were performed in B-R buffer (pH 10.4) with electrodeposited Ag-particles modified GrCE. (b) Interferences study of different concentrations of nitro-organic species (1.0×10^{-5}, 1.0×10^{-4} and 5.0×10^{-4} mol L^{-1}) on the reduction signal of 5.0×10^{-4} mol L^{-1} TMX.*

The selectivity of proposed electrode for the detection of thiamethoxam was examined in the presence of several nitro aromatics compounds (with different concentrations 1.0×10^{-5}, 1.0×10^{-4} and 5.0×10^{-4} mol L^{-1}) such as 4-nitrophenol (4-NP), 2-nitroaniline (2-NA), 4-nitroaniline (4-NA) and 2,4-dinitrophenylhydrazine (2,4-DNPH). Britton-robinson buffer solution (pH 10.4)

containing 5.0×10^{-4} mol L^{-1} TMX was used (Figure 16b). The presence of these species did not show significant change in cathodic current intensity of TMX. The signal change observed was less than 5%, which indicates that organic species did not interfere the detection of TMX. Therefore, the proposed electrochemical sensor presents good selectivity toward TMX.

In order to evaluate its practical application, the electrodeposited silver particles on graphite electrode was employed to analyze TMX in orange and tomato juices samples. To do experiment, 25 mL of juice samples containing B-R buffer (pH 10.4) were tested. The concentration of TMX was found is lower than the LOD. So, both orange and tomato juices were contaminated with three knowing amounts of TMX. The recovery factor ranged from 95.82% to 103.28% for juice tomato sample and between 90.17% and 97.001% for juice orange sample with coefficients of variation lower than 4.01% (Table 6). These values belong the range 70–130% that fixed by the Environmental Protection Agency (EPA) [79]. From these measurements, it is obvious that developed electrode can be suitable for analysis of TMX in real samples.

Table 6: Recovery test of in orange and tomato samples.

Sample	Added concentration [$\times 10^2$ µmol L^{-1}]	Found concentration [$\times 10^2$ µmol L^{-1}]	Recovery [%]	RSD n=3 [%]
	10	9.70	97.00	1.02
Orange juice	5	4.70	93.71	1.30
	1	0.91	90.17	3.30
	10	10.3	103.28	4.01
Tomato juice	5	4.37	92.07	0.91
	1	0.95	95.82	3.58

IV. Conclusion

In conclusion, a thermal solid reaction under nitrogen flow and electrodeposition process for the synthesis of silver particles modified graphite materials were discussed. The morphology and structured characterisation of prepared modified carbon materials revealed the formation of silver nanocrystalline and microparticles uniformly distributed on the carbon graphite material. Electrochemical measurement showed that silver microparticles modified graphite electrode shows enhanced current. In addition, the electrocatalytic activity of modified electrode was investigated for electroreduction of thiamethoxam insecticide. Furthermore,

under the best experimental conditions, the square wave voltammetry method was used to determine thiamethoxam with lower limit of detection in B-R buffer pH 10.4. Furthermore, the presented electrodes were successfully displayed excellent catalytic property toward thiamethoxam analysis in water samples and in orange and tomato juices. Finally, the analytical performance of as-prepared electrodes toward determining TMX in term of limit of detection was compared. It was found that the electrodeposition of silver shows a lower limit of detection than that obtained with silver impregnation, which reflect the improve of electrochemical sensing of our electrode as predicted.

Reference

[1] Li, S. ed.: Biosensor nanomaterials, Wiley-VCH, Weinheim, 2011.

[2] Majidi, M.R. and Ghaderi, S.: Facile fabrication and characterization of silver nanodendrimers supported by graphene nanosheets: A sensor for sensitive electrochemical determination of Imidacloprid, Journal of Electroanalytical Chemistry, **792** (2017), pp. 46–53.

[3] McCreery, R.L.: Carbon Electrodes: Structural Effects on Electron Transfer Kinetics, Electroanalytical Chemistry, CRC Press, 1991.

[4] McCreery, R.L.: Advanced carbon electrode materials for molecular electrochemistry, Chemical reviews, **108** (2008), no. 7, pp. 2646–2687.

[5] Chesney, D.J.: Laboratory Techniques in Electroanalytical Chemistry, 2nd Edition Edited by Peter T. Kissinger (Purdue University) and William R. Heineman (University of Cincinnati). Dekker: Monticello, NY. 1996. xxii + 986 pp. $79. ISBN 0-8247-9445-1., Journal of the American Chemical Society, **118** (1996), no. 44, pp. 10946–10946.

[6] Schumacher, P.D.; Fitzgerald, K.A.; Schenk, J.O. and Clark, S.B.: Preconcentration of f-Elements from Aqueous Solution Utilizing a Modified Carbon Paste Electrode, Analytical Chemistry, **83** (2011), no. 4, pp. 1388–1393.

[7] Švancara, I.; Vytřas, K.; Kalcher, K.; Walcarius, A. and Wang, J.: Carbon Paste Electrodes in Facts, Numbers, and Notes: A Review on the Occasion of the 50-Years Jubilee of Carbon Paste in Electrochemistry and Electroanalysis, Electroanalysis, **21** (2009), no. 1, pp. 7–28.

[8] Mazloum-Ardakani, M.; Rajabi, H. and Beitollahi, H.: Homogeneous and nanomolar detection of hydrazine by indigocarmine as a mediator at the surface of TiO2 nanoparticles modified carbon paste electrode, Chinese Chemical Letters, **23** (2012), no. 2, pp. 213–216.

[9] Karimi-Maleh, H.; Moazampour, M.; Ahmar, H.; Beitollahi, H. and Ensafi, A.A.: A sensitive nanocomposite-based electrochemical sensor for voltammetric simultaneous determination of isoproterenol, acetaminophen and tryptophan, Measurement, **51** (2014), pp. 91–99.

[10] Winiarski, J.P.; de Barros, M.R.; Magosso, H.A. and Jost, C.L.: Electrochemical reduction of sulfite based on gold nanoparticles/silsesquioxane-modified electrode, Electrochimica Acta, **251** (2017), pp. 522–531.

[11] Vanoni, C.R.; Winiarski, J.P.; Nagurniak, G.R.; Magosso, H.A. and Jost, C.L.: A Novel Electrochemical Sensor Based on Silsesquioxane/Nickel (II) Phthalocyanine for the

Determination of Sulfanilamide in Clinical and Drug Samples, Electroanalysis, **31** (2019), no. 5, pp. 867–875.

[12] Afkhami, A.; Madrakian, T.; Ghaedi, H. and Khanmohammadi, H.: Construction of a chemically modified electrode for the selective determination of nitrite and nitrate ions based on a new nanocomposite, Electrochimica Acta, **66** (2012), pp. 255–264.

[13] El Mhammedi, M.A.; Bakasse, M.; Bachirat, R. and Chtaini, A.: Square wave voltammetry for analytical determination of paraquat at carbon paste electrode modified with fluoroapatite, Food Chemistry, **110** (2008), no. 4, pp. 1001–1006.

[14] El Mhammedi, M.A.; Bakasse, M.; Najih, R. and Chtaini, A.: A carbon paste electrode modified with kaolin for the detection of diquat, Applied Clay Science, **43** (2009), no. 1, pp. 130–134.

[15] Farahi, A.; Achak, M.; El Gaini, L.; El Mhammedi, M.A. and Bakasse, M.: Silver particles-modified carbon paste electrodes for differential pulse voltammetric determination of paraquat in ambient water samples, Journal of the Association of Arab Universities for Basic and Applied Sciences, **19** (2016), no. 1, pp. 37–43.

[16] Farahi, A.; Achak, M.; El Gaini, L.; El Mhammedi, M.A. and Bakasse, M.: Electrochemical determination of paraquat in citric fruit based on electrodeposition of silver particles onto carbon paste electrode, Journal of Food and Drug Analysis, **23** (2015), no. 3, pp. 463–471.

[17] Papp, Z.; Švancara, I.; Guzsvány, V.; Vytřas, K. and Gaál, F.: Voltammetric determination of imidacloprid insecticide in selected samples using a carbon paste electrode, Microchimica Acta, **166** (2009), no. 1, pp. 169–175.

[18] Guzsvány, V.; Papp, Z.; Zbiljić, J.; Vajdle, O. and Rodić, M.: Bismuth Modified Carbon-Based Electrodes for the Determination of Selected Neonicotinoid Insecticides, Molecules, **16** (2011), no. 6, pp. 4451–4466.

[19] Pandey, G.; Dorrian, S.J.; Russell, R.J. and Oakeshott, J.G.: Biotransformation of the neonicotinoid insecticides imidacloprid and thiamethoxam by Pseudomonas sp. 1G, Biochemical and Biophysical Research Communications, **380** (2009), no. 3, pp. 710–714.

[20] Ajermoun, N.; Farahi, A.; Lahrich, S.; Bakasse, M.; Saqrane, S. and El Mhammedi, M.A.: Electrocatalytic activity of the metallic silver electrode for thiamethoxam reduction: application for the detection of a neonicotinoid in tomato and orange samples, Journal of the Science of Food and Agriculture, **99** (2019), no. 9, pp. 4407–4413.

[21] Kumaravel, A. and Chandrasekaran, M.: Nanosilver/surfactant modified glassy carbon electrode for the sensing of thiamethoxam, Sensors and Actuators B: Chemical, **174** (2012), pp. 380–388.

[22] Chorti, P.; Fischer, J.; Vyskocil, V.; Economou, A. and Barek, J.: Voltammetric Determination of Insecticide Thiamethoxam on Silver Solid Amalgam Electrode, Electrochimica Acta, **140** (2014), pp. 5–10.

[23] Urbanová, V.; Bakandritsos, A.; Jakubec, P.; Szambó, T. and Zbořil, R.: A facile graphene oxide based sensor for electrochemical detection of neonicotinoids, Biosensors and Bioelectronics, **89** (2017), pp. 532–537.

[24] Putek, M.; Guzsvány, V.; Tasić, B.; Zarębski, J. and Bobrowski, A.: Renewable Silver-Amalgam Film Electrode for Rapid Square-Wave Voltammetric Determination of Thiamethoxam Insecticide in Selected Samples, Electroanalysis, **24** (2012), no. 12, pp. 2258–2266.

[25] Hernández-Santos, D.; González-García, M.B. and García, A.C.: Metal-Nanoparticles Based Electroanalysis, Electroanalysis, **14** (2002), no. 18, pp. 1225–1235.

[26] Katz, E.; Willner, I. and Wang, J.: Electroanalytical and Bioelectroanalytical Systems Based on Metal and Semiconductor Nanoparticles, Electroanalysis, **16** (2004), nos. 1–2, pp. 19–44.

[27] Laghrib, F.; Lahrich, S.; Farahi, A.; Bakasse, M. and El Mhammedi, M.A.: Impregnation of silver in graphite carbon using solid reaction: Electrocatalysis and detection of 4-nitroaniline, Journal of Electroanalytical Chemistry, **823** (2018), pp. 26–31.

[28] Roy, K.; Sarkar, C.K. and Ghosh, C.K.: Photocatalytic activity of biogenic silver nanoparticles synthesized using potato (Solanum tuberosum) infusion, Spectrochimica Acta Part A: Molecular and Biomolecular Spectroscopy, **146** (2015), pp. 286–291.

[29] Sinha, T.; Ahmaruzzaman, M.; Sil, A.K. and Bhattacharjee, A.: Biomimetic synthesis of silver nanoparticles using the fish scales of Labeo rohita and their application as catalysts for the reduction of aromatic nitro compounds, Spectrochimica Acta Part A: Molecular and Biomolecular Spectroscopy, **131** (2014), pp. 413–423.

[30] Li, W.; Liu, J. and Yan, C.: Graphite–graphite oxide composite electrode for vanadium redox flow battery, Electrochimica Acta, **56** (2011), no. 14, pp. 5290–5294.

[31] Światowska, J.; Lair, V.; Pereira-Nabais, C.; Cote, G.; Marcus, P. and Chagnes, A.: XPS, XRD and SEM characterization of a thin ceria layer deposited onto graphite electrode for application in lithium-ion batteries, Applied Surface Science, **257** (2011), no. 21, pp. 9110–9119.

[32] Manikantan, J.; Ramalingam, H.B.; Shekar, B.C.; Murugan, B.; Kumar, R.R. and Santhoshi, J.S.: Physical and optical properties of HfO2 NPs – Synthesis and characterization in finding its feasibility in opto-electronic devices, Advanced Powder Technology, **28** (2017), no. 7, pp. 1636–1646.

[33] Stokes, A.R. and Wilson, A.J.C.: The diffraction of X rays by distorted crystal aggregates - I, Proceedings of the Physical Society, **56** (1944), no. 3, pp. 174–181.

[34] Terlan, B.; Levin, A.A.; Börrnert, F.; Simon, F.; Oschatz, M.; Schmidt, M.; Cardoso-Gil, R.; Lorenz, T.; Baburin, I.A.; Joswig, J.-O. and Eychmüller, A.: Effect of Surface Properties on the Microstructure, Thermal, and Colloidal Stability of VB2 Nanoparticles, Chemistry of Materials, **27** (2015), no. 14, pp. 5106–5115.

[35] Benck, J.D.; Chen, Z.; Kuritzky, L.Y.; Forman, A.J. and Jaramillo, T.F.: Amorphous Molybdenum Sulfide Catalysts for Electrochemical Hydrogen Production: Insights into the Origin of their Catalytic Activity, ACS Catalysis, **2** (2012), no. 9, pp. 1916–1923.

[36] Trasatti, S. and Petrii, O.A.: Real surface area measurements in electrochemistry, Journal of Electroanalytical Chemistry, **327** (1992), no. 1, pp. 353–376.

[37] Lukowski, M.A.; Daniel, A.S.; Meng, F.; Forticaux, A.; Li, L. and Jin, S.: Enhanced Hydrogen Evolution Catalysis from Chemically Exfoliated Metallic MoS2 Nanosheets, Journal of the American Chemical Society, **135** (2013), no. 28, pp. 10274–10277.

[38] Lukowski, M.A.; Daniel, A.S.; English, C.R.; Meng, F.; Forticaux, A.; Hamers, R.J. and Jin, S.: Highly active hydrogen evolution catalysis from metallic WS2 nanosheets, Energy & Environmental Science, **7** (2014), no. 8, pp. 2608–2613.

[39] Zhao, L.; Yang, J.; Ye, H.; Zhao, F. and Zeng, B.: Preparation of hydrophilic surface-imprinted ionic liquid polymer on multi-walled carbon nanotubes for the sensitive electrochemical determination of imidacloprid, RSC Advances, **7** (2017), no. 8, pp. 4704–4709.

[40] Laghrib, F.; Bakasse, M.; Lahrich, S. and El Mhammedi, M.A.: Electrochemical sensors for improved detection of paraquat in food samples: A review, Materials Science and Engineering: C, **107** (2020), p. 110349.

[41] Laghrib, F.; Ajermoun, N.; Hrioua, A.; Lahrich, S.; Farahi, A.; El Haimouti, A.; Bakasse, M. and El Mhammedi, M.A.: Investigation of voltammetric behavior of 4-nitroaniline based on electrodeposition of silver particles onto graphite electrode, Ionics, **25** (2019), no. 6, pp. 2813–2821.

[42] Sebest, P.; Fojt, L.; Ostatna, V.; Fojta, M. and Danhel, A.: Electrodeposited silver amalgam particles on pyrolytic graphite in (spectro)electrochemical detection of 4-

nitrophenol, DNA and green fluorescent protein, Bioelectrochemistry, **132** (2020), p. 107436.

[43] Cho, F.-H.; Kuo, S.-C. and Lai, Y.-H.: Surface-plasmon-induced azo coupling reaction between nitro compounds on dendritic silver monitored by surface-enhanced Raman spectroscopy, RSC Advances, **7** (2017), no. 17, pp. 10259–10265.

[44] Bi, J.: Electrodeposited silver nanoflowers as sensitive surface-enhanced Raman scattering sensing substrates, Materials Letters, **236** (2019), pp. 398–402.

[45] Klug, J.; Torresan, M.F.; Lurgo, F.; Borioli, G. and Lacconi, G.I.: A spectroscopic sensing platform for MARCKS protein monolayers, Journal of Colloid and Interface Science, **508** (2017), pp. 532–541.

[46] Baghayeri, M.; Tehrani, M.B.; Amiri, A.; Maleki, B. and Farhadi, S.: A novel way for detection of antiparkinsonism drug entacapone via electrodeposition of silver nanoparticles/functionalized multi-walled carbon nanotubes as an amperometric sensor, Materials Science and Engineering: C, **66** (2016), pp. 77–83.

[47] Zhai, H.; Liang, Z.; Chen, Z.; Wang, H.; Liu, Z.; Su, Z. and Zhou, Q.: Simultaneous detection of metronidazole and chloramphenicol by differential pulse stripping voltammetry using a silver nanoparticles/sulfonate functionalized graphene modified glassy carbon electrode, Electrochimica Acta, **171** (2015), pp. 105–113.

[48] Goulart, L.A.; Gonçalves, R.; Correa, A.A.; Pereira, E.C. and Mascaro, L.H.: Synergic effect of silver nanoparticles and carbon nanotubes on the simultaneous voltammetric determination of hydroquinone, catechol, bisphenol A and phenol, Microchimica Acta, **185** (2017), no. 1, p. 12.

[49] Roushani, M. and Shahdost-fard, F.: A glassy carbon electrode with electrodeposited silver nanoparticles for aptamer based voltammetric determination of trinitrotoluene using riboflavin as a redox probe, Microchimica Acta, **185** (2018), no. 12, p. 558.

[50] Tang, J.; Huang, Y.; Zhang, C.; Liu, H. and Tang, D.: DNA-based electrochemical determination of mercury(II) by exploiting the catalytic formation of gold amalgam and of silver nanoparticles, Microchimica Acta, **183** (2016), no. 6, pp. 1805–1812.

[51] Tiwari, A. and Nagaiah, T.C.: Dioxygen Reduction by Nitrogen-Rich Mesoporous Carbon bearing Electrodeposited Silver Particles, ChemCatChem, **8** (2016), no. 2, pp. 396–403.

[52] Wang, A.; Huang, Y.-F.; Sur, U.K.; Wu, D.-Y.; Ren, B.; Rondinini, S.; Amatore, C. and Tian, Z.-Q.: In Situ Identification of Intermediates of Benzyl Chloride Reduction at a Silver Electrode by SERS Coupled with DFT Calculations, Journal of the American Chemical Society, **132** (2010), no. 28, pp. 9534–9536.

[53] Kumaravel, A. and Chandrasekaran, M.: A novel nanosilver/nafion composite electrode for electrochemical sensing of methyl parathion and parathion, Journal of Electroanalytical Chemistry, **638** (2010), no. 2, pp. 231–235.

[54] Rezaei, B. and Damiri, S.: Electrodeposited silver nanodendrites electrode with strongly enhanced electrocatalytic activity, Talanta, **83** (2010), no. 1, pp. 197–204.

[55] Mitrikas, G.; Deligiannakis, Y.; Trapalis, C.C.; Boukos, N. and Kordas, G.: CW and Pulsed EPR Study of Silver Nanoparticles in a SiO2 Matrix, Journal of Sol-Gel Science and Technology, **13** (1998), no. 1, pp. 503–508.

[56] Swarthmore, P.A.: Joint Committee on Powder Diffraction Standards Diffraction Data File, JCPDS International Center for Diffraction Data, (1991).

[57] Nicholson, R.S.: Theory and Application of Cyclic Voltammetry for Measurement of Electrode Reaction Kinetics., Analytical Chemistry, **37** (1965), no. 11, pp. 1351–1355.

[58] Lavagnini, I.; Antiochia, R. and Magno, F.: An Extended Method for the Practical Evaluation of the Standard Rate Constant from Cyclic Voltammetric Data, Electroanalysis, **16** (2004), no. 6, pp. 505–506.

[59] Klingler, R.J. and Kochi, J.K.: Electron-transfer kinetics from cyclic voltammetry. Quantitative description of electrochemical reversibility, The Journal of Physical Chemistry, **85** (1981), no. 12, pp. 1731–1741.

[60] Laviron, E.; Roullier, L. and Degrand, C.: A multilayer model for the study of space distributed redox modified electrodes: Part II. Theory and application of linear potential sweep voltammetry for a simple reaction, Journal of Electroanalytical Chemistry and Interfacial Electrochemistry, **112** (1980), no. 1, pp. 11–23.

[61] Zhou, Y.; Tang, W.; Wang, J.; Zhang, G.; Chai, S.; Zhang, L. and Liu, T.: Selective determination of dopamine and uric acid using electrochemical sensor based on poly(alizarin yellow R) film-modified electrode, Analytical Methods, **6** (2014), no. 10, pp. 3474–3481.

[62] Laviron, E.: Adsorption, autoinhibition and autocatalysis in polarography and in linear potential sweep voltammetry, Journal of Electroanalytical Chemistry and Interfacial Electrochemistry, **52** (1974), no. 3, pp. 355–393.

[63] Bard, A.J. and Faulkner, L.R.: Electrochemical methods: fundamentals and applications, 2nd ed ed., Wiley, New York, 2001.

[64] Liu, S.-Q. and Ju, H.-X.: Renewable reagentless hydrogen peroxide sensor based on direct electron transfer of horseradish peroxidase immobilized on colloidal gold-modified electrode, Analytical Biochemistry, **307** (2002), no. 1, pp. 110–116.

[65] Liu, S.; Dai, Z.; Chen, H. and Ju, H.: Immobilization of hemoglobin on zirconium dioxide nanoparticles for preparation of a novel hydrogen peroxide biosensor, Biosensors and Bioelectronics, **19** (2004), no. 9, pp. 963–969.

[66] Laviron, E.; Vallat, A. and Meunier-Prest, R.: The reduction mechanism of aromatic nitro compounds in aqueous medium: Part V. The reduction of nitrosobenzene between pH 0.4 and 13, Journal of Electroanalytical Chemistry, **379** (1994), no. 1, pp. 427–435.

[67] Lacasse, R.; Meunier-Prest, R.; Laviron, E. and Vallat, A.: The reduction mechanism of aromatic nitro compounds in aqueous medium Part 3. The reduction of 4-nitropyridine-N-oxide between H0 = −6 and pH 9, Journal of Electroanalytical Chemistry, **359** (1993), no. 1, pp. 223–239.

[68] Laviron, E.; Meunier-Prest, R. and Lacasse, R.: The reduction mechanism of aromatic nitro compounds in aqueous medium. Part IV. The reduction of p-nitrobenzophenone between H0 = −5 and pH 14, Journal of Electroanalytical Chemistry, **375** (1994), no. 1, pp. 263–274.

[69] Siswana, M.P.; Ozoemena, K.I. and Nyokong, T.: Electrocatalysis of asulam on cobalt phthalocyanine modified multi-walled carbon nanotubes immobilized on a basal plane pyrolytic graphite electrode, Electrochimica Acta, **52** (2006), no. 1, pp. 114–122.

[70] Salimi, A.; Banks, C.E. and Compton, R.G.: Abrasive immobilization of carbon nanotubes on a basal plane pyrolytic graphite electrode: application to the detection of epinephrine, Analyst, **129** (2004), no. 3, pp. 225–228.

[71] Salimi, A.; Miranzadeh, L. and Hallaj, R.: Amperometric and voltammetric detection of hydrazine using glassy carbon electrodes modified with carbon nanotubes and catechol derivatives, Talanta, **75** (2008), no. 1, pp. 147–156.

[72] Ye, J.-S.; Wen, Y.; De Zhang, W.; Cui, H.F.; Xu, G.Q. and Sheu, F.-S.: Electrochemical Biosensing Platforms Using Phthalocyanine-Functionalized Carbon Nanotube Electrode, Electroanalysis, **17** (2005), no. 1, pp. 89–96.

[73] Anu Prathap, M.U.; Anuraj, V.; Satpati, B. and Srivastava, R.: Facile preparation of Ni(OH)2–MnO2 hybrid material and its application in the electrocatalytic oxidation of hydrazine, Journal of Hazardous Materials, **262** (2013), pp. 766–774.

[74] Barker, G.C.: E. Galus, Fundamentals of Electrochemical Analysis, Ellis Horwood Ltd., Chichester (1976), 520+ xviii pp.,\pounds 23.501977.

[75] Rastakhiz, N.; Beitollahi, H.; Kariminik, A. and Karimi, F.: Voltammetric determination of carbidopa in the presence of uric acid and folic acid using a modified carbon nanotube paste electrode, Journal of Molecular Liquids, **172** (2012), pp. 66–70.

[76] Kavian, S.; Azizi, S.N. and Ghasemi, S.: Electrocatalytic detection of hydrazine on synthesized nanozeolite-supported Ag nanoparticle-modified carbon paste electrode at a negative potential in an alkaline medium, Journal of Molecular Liquids, **218** (2016), pp. 663–669.

[77] Skoog, D.A.; Holler, F.J. and Crouch, S.R.: Principles of Instrumental Analysis, Cengage Learning, 2017.

[78] Guzsvány, V.J.; Gaál, F.F.; Bjelica, L.J. and Ökrész, S.N.: Voltammetric determination of imidacloprid and thiamethoxam, Journal of the Serbian Chemical Society, **70** (2005), no. 5, pp. 735–743.

[79] Paula, S.A.; Ferreira, O.A.E. and César, P.A.: Determination of Imidacloprid Based on the Development of a Glassy Carbon Electrode Modified with Reduced Graphene Oxide and Manganese (II) Phthalocyanine, Electroanalysis, **32** (2020), no. 1, pp. 86–94.

Chapter IV

Chitosan-stabilized silver nanoparticles for the detection of thiamethoxam in plant tissues

I. Introduction

Nanomaterials (NMs) have sizes in the range of 1–100 nm, which have become one of the most fascinating materials in the past ten years [1–3]. They possess strong size- and shape-dependence chemical and physical properties, which are quite different from those of their corresponding bulk materials, mainly because of quantum effect [4]. The past decade have witnessed progressive advances in the synthesis, characterization, and application of a variety of NMs, including gold nanoparticles (Au NPs) [5], gold nanodots (Au NDs) [6, 7], quantum dots (QDs) such as CdSe and CdTe [8, 9], magnetic nanoparticles (MNPs) [10, 11], titanium dioxide nanoparticles (TiO2 NPs) [12], silica nanoparticles (Si NPs) [13], carbon quantum dots (C–dots) [14, 15], graphene [16, 17], metal nanoclusters (NCs) [18], and so on. The as-synthesized NMs have been widely employed in many fields because of their unique size- and shape-dependence optical (e.g., surface plasmon resonance (SPR), surface enhanced Raman scattering (SERS), and fluorescence), electronic, magnetic, and catalytic properties, which make them ideal candidates as signaling elements for being sensitive biosensors [19–21]. In general, most NMs are prepared through bottom-up or top-down approaches; "bottom-up" approaches involve the self-assembly of small sized structures into larger structures and "top-down" approaches are production of nanoscale structures from large materials [22].

Among the NMs, nanoparticles (NPs) have attracted a great attention because of the incredible electrical, magnetic, thermal, and catalytic characteristics that are generated when their particle size is miniaturized [23]. Their contributions to health, electronics, manufacturing, environment, agriculture, and different biomedical industries have been reported [24, 25]. They can be generally divided into metal-based, metal oxide-based, and carbon-based NPs. Recently, metal nanoparticles are the main scientific interest and play an important role in many different aspects, including catalysis [26], sensing [27], biomedicine [28] optics [29] and electronics [30]. Particularly, silver nanoparticles (Ag-NPs) have been used to improve the performance of a variety of instruments due to their considerable physicochemical features [26, 31]. As well as, because of their low cost and better conductivity than noble metals (e.g., Pd, Au, and Pt), Ag-NPs are a promising candidate for various electrochemical sensors to detect nitro-aromatic chemicals[32–34]. In addition, Ag-NPs behaved as a nanoelectrocatalyst, resulting for a more effective electron-transfer mechanism during electrocatalysis. They are a well-known electrocatalyst for nitro-aromatic compound reduction [35, 36]. Electrochemical sensors, such as AgNP-based electrochemical sensors, are considered promising for detecting organic pollutants with sufficient sensitivity and selectivity compared with optical sensors.65 Additionally, they are less time-consuming and easier to set up. The direct detection of targeted

analytes makes electrochemical sensors feasible for in situ studies. Moreover, electrochemical sensors can monitor changes in analyte concentration with time.

AgNPs could be incorporated into electrodes through different in situ and ex situ approaches (Figure 1). The in-situ approach depends on the electrochemical deposition of AgNPs at electrode surfaces through the electrochemical reduction of Ag^+ ion with subsequent nucleation, aggregation and coalescence of metallic particles (Figure 1A). Electrochemical deposition is considered the most frequently used method for electrode modification [37, 38]. The ex situ approaches include drop casting, spin coating, sticking, transfer sticking, and carbon paste modification. The drop casting technique depends on the placement of AgNPs directly on electrode surfaces with subsequent drying for solvent evaporation.[39] (Figure 1B). In the spin coating technique (Figure 1C), AgNPs are directly placed on the surface of a stirring electrode attached to the centre of the spin coater via a vacuum system [40]. In the sticking technique (Figure 1D), the electrode is dipped in an AgNP suspension mixed with electrolytes for a certain time[39]. Similarly, the transfer sticking technique is accomplished by dipping the electrode in an AgNP suspension only, which is then transferred to the electrolyte for the stripping process (Figure 1E). The modified electrode could be prepared by incorporating a paste, formed using AgNPs, paraffin oil, and graphite, into the electrode [41]. Notably, gold, glassy carbon, and graphite electrodes were mainly used for electrode modification with AgNPs.

This chapter described a direct chemical reduction method for the synthesis of silver nanoparticles and their catalytic effect toward electroreduction of TMX insecticide was investigated. The silver ions Ag+ are stabilized by chitosan so the nanoparticles could be kept from agglomerating during the synthesis and reduced by NaBH4. The electrochemical characterisation of modified electrode was performed using cyclic voltammetry (CV), and electrochemical impedance spectroscopy (EIS). Finally, the electroanalytic activity of synthesis material was investigated against the electroreduction of TMX insecticide using square wave voltammetry (SWV).

II. Experimental section

1) Chemicals and instruments

The britton-robinson buffer (RB) pH 10.4 was used as the supporting electrolyte for electrochemical studies. It was prepared from phosphoric acid, boric acid, acetic acid and sodium hydroxide, whose were provided by Riedel de Haen (Seelze, Germany), Fluka (St. Gallen, Switzerland) and Merck (Darmstadt, Germany) with analytical reagent grade.
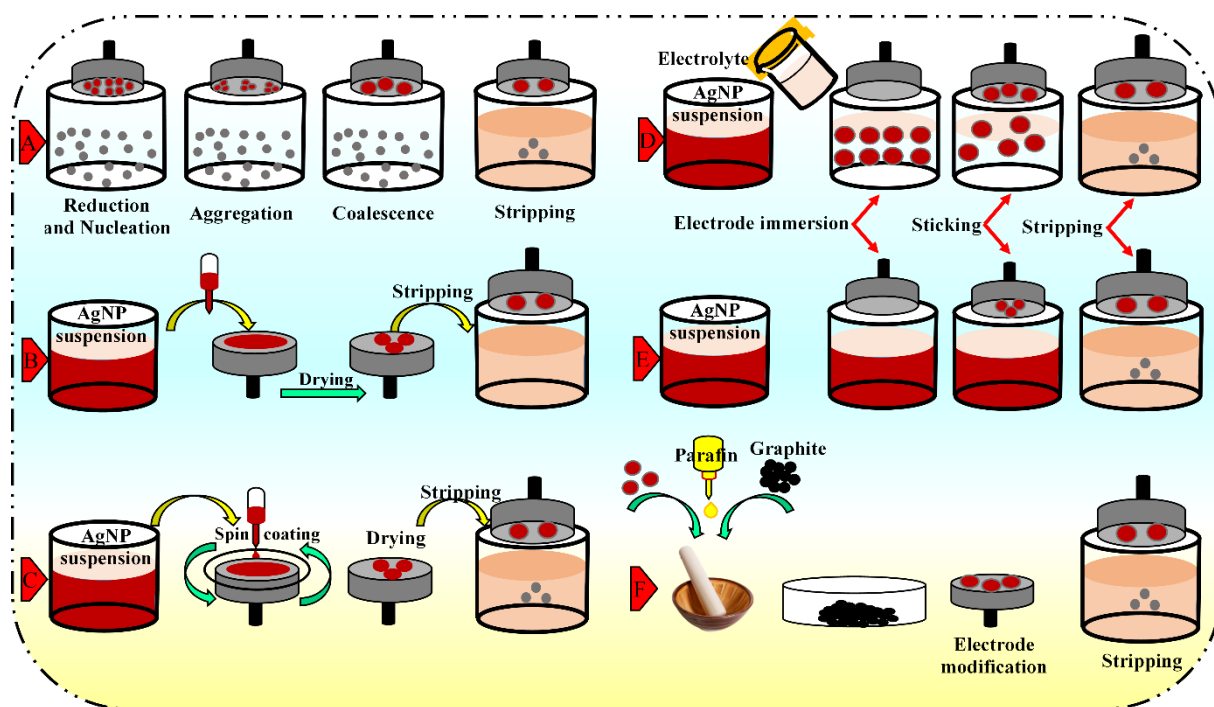
Figure 1: Electrode modification using AgNPs through electrochemical deposition (A), drop casting (B), spin coating (C), sticking (D), transfer sticking (E), and carbon paste (F), with subsequent AgNP stripping.

All electrochemical measurements were performed in a classic three-electrode cell using an analyser potentiostat voltalab (model PGZ 100, Eco Chemie B.V, Utrecht, The Netherlands) equipped with voltamaster 4. software. A carbon paste electrode (CPE) modified with chitosan-AgNPs was utilised as the working electrode, an Ag/AgCl (KCl, 3 M) electrode as the reference electrode, and Pt wire as the counter electrode.

2) Analytical procedure

i) Synthesis of silver-chitosan nanoparticles

The suspension of AgNPs-chitosan material was prepared as reported in our previous work [42]: 0.10 g of chitosan was dissolved in 10 mL of 2% acetic acid and the mixture was stirred overnight to obtain a homogeneous solution. Next, 10 mL of this solution, 1 mL of 10 mmol L^{-1} $AgNO_3$ and 0.8 mg of $NaBH_4$ were mixed and slowly stirred at this temperature for 1 hour. The colour change in the solution (from colourless to yellow) indicates the formation of silver nanoparticles.

ii) Preparation of electrode

The carbon paste electrode was immersed in the as-prepared colloidal solution of chitosan-nano silver for an optimized accumulation time about 12 min under slight stirring. The as-modified electrode was rinsed with distilled water and then exposed under dark condition with standard temperature around (20 ± 2).

iii) Plant samples preparation

Thiamethoxam was extracted from 2 g of tissue (roots and leaves) of Zea mays and bean Phaseolus vulgaris L. plants by grinding with 100 mL of ultra-pure water.

The resulting residue was sonicated (3 kHz ×40 min) and centrifuged (1792 ×g ×10 min). After three extractions (100, 100, and 50 mL), the water was removed via rotary evaporation at 80 °C, to about 5 mL of water [43]. The concentrated volume was brought to 25 mL with water. The pH of the solution was controlled by adding Britton–Robinson pH 10.4 buffer components. The solution was transferred to the electrochemical cell for TMX analysis using SWV.

iv) Electrochemical measurements

Cyclic voltammetry (CV) measurements were carried out in 0.1 mol L^{-1} B-R (pH 10.4) containing 1.0×10^{-3} mol L^{-1} TMX with the potential range between -0.40 V and -1.40 V. For square wave voltammetry (SWV) measurements, experimental parameters were as follows: the scan range was from -0.40 V to -1.40 V, the scan rate, pulse amplitude, step and duration were 10 mV s^{-1}, 50 mV, 10 mV, and 1s, respectively. For impedance spectroscopy a sinusoidal AC potential with 5 mV was applied in a frequency range between 0.1–100 kHz. All experiment results in this study were the average of three parallel experiments unless otherwise stated.

III. Results and discussion

1) Characterization of synthesis nanoparticles

According to our previous research [42], the chitosan stabilized silver-nanoparticles material was a subject of many characterisation technics including UV–vis spectroscopy (UV–vis) and XRD, SEM and FT-IR. The finding demonstrates that the synthesis of colloidal chitosan-AgNPs with particle sizes between (35–45 nm). A typical XRD pattern of the synthesized chitosan-Ag NPs was found to possess a face-centered cubic (FCC) lattice. The presence of Ag NPs was confirmed by four Bragg reflections at 2 = 37.36, 44.47, 64.80, and 77.44, which correspond to the (111), (200), (220), and (311) plans, respectively. In addition, the SEM image illustrated that the nanoparticles are relatively uniform and seemed like quasi-spheres.

Furthermore, infrared spectrometry is used to confirm the interaction between silver and chitosan.

2) Electrochemical responses of synthesis nanoparticles

Cyclic voltammetry (CV) was recorded for three electrodes in 5.0×10^{-3} mol L^{-1} $[Fe(CN)_6]^{4-}$/$[Fe(CN)_6]^{3-}$ prepared with 0.1 mol L^{-1} of KCl in a range of potential from -0.2V to 0.6 V (Figure 2A). The significance of this study was to explore the best electrode with enhanced electron transfer properties. all electrodes present cathodic and anodic peaks. In terms of reversibility, the peak-to-peak separation potential (ΔEp) were calculated to be 156 mV, 186.1 mV and 258.42 mV for CHI-AgNPs / CPE, CHI / CPE and CPE respectively. The $[Fe(CN)_6]^{4-}$ / $[Fe(CN)_6]^{3-}$ redox couple seemed reversible at the CHI-AgNPs / CPE electrode, with a peak currents ratio of I_{pa}/I_{pc}= 0.99 or nearly 1.0 for a reversible process, and a peak separation of 156 mV indicating fast electron transfer at electrode.

In addition, in term the nano-silver modified electrode shows an enhancement in term of current response a potential shift of 60 mV compared to unmodified (graphite) electrode. In other hand, the obtained results indicate good electron transfer and large surface area formed by silver nanoparticles stabilised with chitosan for easy diffusion of electrolytes to the active site of the electrode, and easy flow of electron due to the redox reaction of the Ag nanoparticles at the electrode.

The electroactive surface area (ESA) has been estimated using cyclic voltammetry of at different scan rates (ν) ranging from 0.005 V s^{-1} to 0.1 V s^{-1} according to Randles-Sevcik Eq. (1):

$$Ip = 2.69105n^{3/2}AD^{1/2}C\nu^{1/2} \qquad (1)$$

Both the peak currents (Ip) of the CHI-AgNPs / CPE, CHI / CPE and CPE were proportional to the square root of scan rate (not shown). Considering $D = 7.6 \ 10^{-6}$ cm^2 s^1 and n = 1 for a 5.0 $\times 10^{-3}$ mol L^{-1} of $[Fe(CN)6]^{3-/4-}$ and from the slopes values of the straight lines. The ESA of CHI-AgNPs / CPE, CHI / CPE and CPE were obtained are 3.24×10^{-4} cm^2, 2.42×10^{-4} cm^2 and 2.25×10^{-4} cm^2 respectively. When compared to CPE, the electroactive surface area of CHI-AgNPs / CPE enhanced by about 30.55 %, exhibiting the improved conductivity of modified electrode.

119
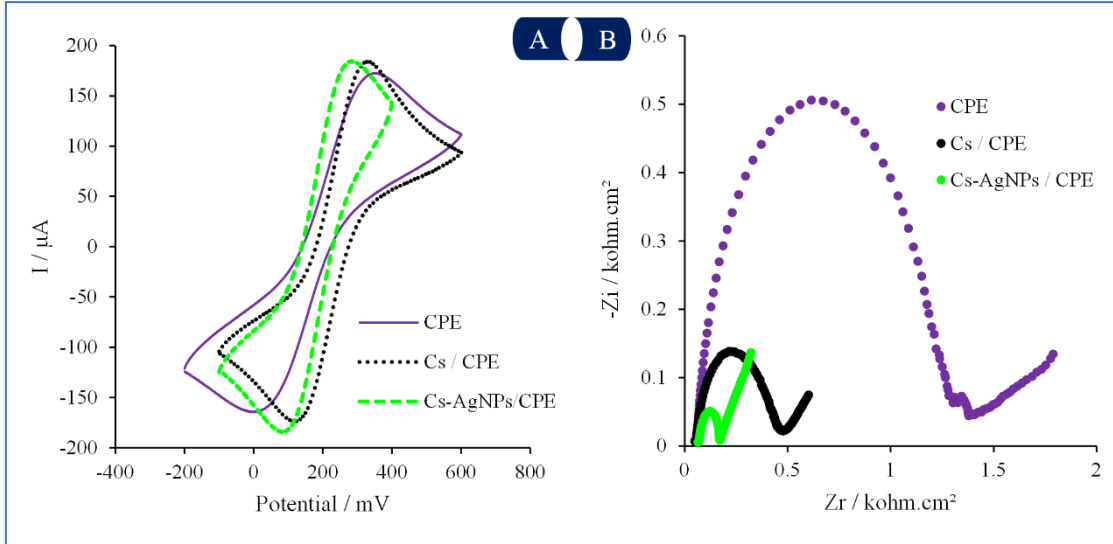
Figure 2: (A) cyclic voltammograms obtained at scan rate of 10 mV/s⁻¹ (B) Nyquist plots of CPE, CHI/CPE, and CHI-AgNPs/CPE in a 0.1 M KCl solution containing the redox couples of 5 mM [Fe(CN)6]⁴⁻/[Fe(CN)6]³⁻.

For investigating the performance of electrode materials in electrochemistry, the determination of the heterogeneous electron transfers rate constant $k°$, is crucial. The rate constant indicates the speed of electron transfer between an electroactive species and an electrode surface, as well as whether the electrode material influences the overall rate of the electrochemical reaction. It can also be used to estimate the allotrope of the material in question [44]. The procedure of Nicholson [45] can be used to determine $k°$ by using a working curve Ψ-($\Delta E_p \times n$) accompanied by an Ψ-$v^{1/2}$ plot (Eq. 2) in a quasi-reversible system, where Electron transfer rate is comparable with diffusion rate, results in a ΔEp rise with scan rate (v) [45]:

$$\Psi = K°[RT/\pi nFD]^{0.5}\, v^{-0.5} \tag{2}$$

Where Ψ is the dimensionless kinetic parameter, ν the scan rate, D is the diffusion coefficient, F faradic constant n is number of electrons transferred, R the gas constant, and T the temperature of solution. from the ΔEp of the cyclic voltammogram for one electron transfer, the empirically determined working function [46] , was used to calculate ψ for a given ΔEp:

$$\Psi = (-0.628 + 0.021\Delta Ep)/(1 - 0.0071\Delta Ep) \tag{3}$$

The Nicholson approach is only applicable for assessing quasi-reversible reaction with $\Delta Ep <$ 220 mV. Hence, an explicit expression for k°, Eq. (4) demonstrated by Klingler and Kochi [47] was used for larger ΔEp.

$$K° = 2.18[D\beta nvF/RT]^{1/2}\exp[-(\beta^2 nF/RT) \Delta Ep] \qquad (4)$$

Equation 4 was rearranged in the following form:

$$\Psi = 2.18[\beta/\pi]^{0.5}\exp[-(\beta^2 F/RT)\Delta Ep] \qquad (5)$$

The *Eq. 4* and *5* were used together to estimate values from the ΔEp experimental data, regardless of the scan rate used. From the slope of the plot Ψ- $[\pi DnF/(RT)]^{-1/2}$ $v^{-1/2}$, the kinetic parameter k° could be easily assessed.

The ET rate k was estimated to correspond to 4.77×10^{-4} cm s^{-1}, 4.12×10^{-4} cm s^{-1} and 2.00×10^{-4} cm s^{-1} for CHI-AgNPs / CPE, CHI / CPE and CPE electrodes respectively. The results suggesting that the electron transfer reaction was easily transferred on the surface modified silver nanoparticles. Furthermore, the nanomaterial components provide an abundance of active sites and faster electronic transduction to electroactive species across the surface of the developed sensing platform.

For a fundamental understanding of the charge transfer mechanism, the immobilisation growth and the impedance changes at the electrode/analyte interfacial surfaces, EIS was carried. Figure 2B shows the Nyquist plots obtained for the CPE and CHI / CPE and CHI-AgNPs / CPE electrodes in 5.0×10^{-3} mol L^{-1} [Fe(CN)6]$^{4-}$ / [Fe(CN)6]$^{3-}$ prepared with 1.0 mol L^{-1} of KCl electrolyte. The large semi-circle indicates a relatively high charge transfer resistance (R_{ct}) caused by the insulating properties of the electrode-electrolyte interface. The values of the equivalent circuit elements are mentioned in table 1. The R_{ct} value of the CPE was ≈1220 Ohm cm^2, and the R_{ct} values of the CHI / CPE and CHI-AgNPs / CPE electrodes decreased with surface modification and were equal to 407.4, and 102.5 Ohm cm^2, respectively, indicating a higher electron transfer rate for the redox probe at CPE decorated silver nanoparticles surface in comparison to unmodified electrode.

Table 1: *Impedance data acquired for CPE and chitosan – nanosilver modified electrodes in 5 mM [Fe(CN)6]4-/[Fe(CN)6]3- at a stable potential of 1.0 V (vs Ag|AgCl).*

Electrode	Rs / Ohm cm^2	R_{ct} / Ohm cm^2	C / nF cm^{-2}
CPE	53.52	1220	232.1
Cs / CPE	47.1	407.4	437.5
Cs-AgNPs / CPE	69.46	102.5	347.6

It can be concluded from CV and EIS data that the silver nanoparticles are successfully immobilized to CPE which offers a large electroactive surface area, excessive binding groups/sites that promote adsorption of target analyte species, and efficient charge transfer features.

3) Electrochemical behaviour of thiamethoxam

The SWV method was used to examine electrochemical behaviour of TMX at CPE, CHI / CPE and CHI-AgNPs / CPE in 0.1 B-R (pH = 10.4). In figure 3, a reduction peak of TMX appeared around -1.15V, -1.10V and -1.04V at CPE, CHI /CPE and CHI-AgNPs / CPE respectively.
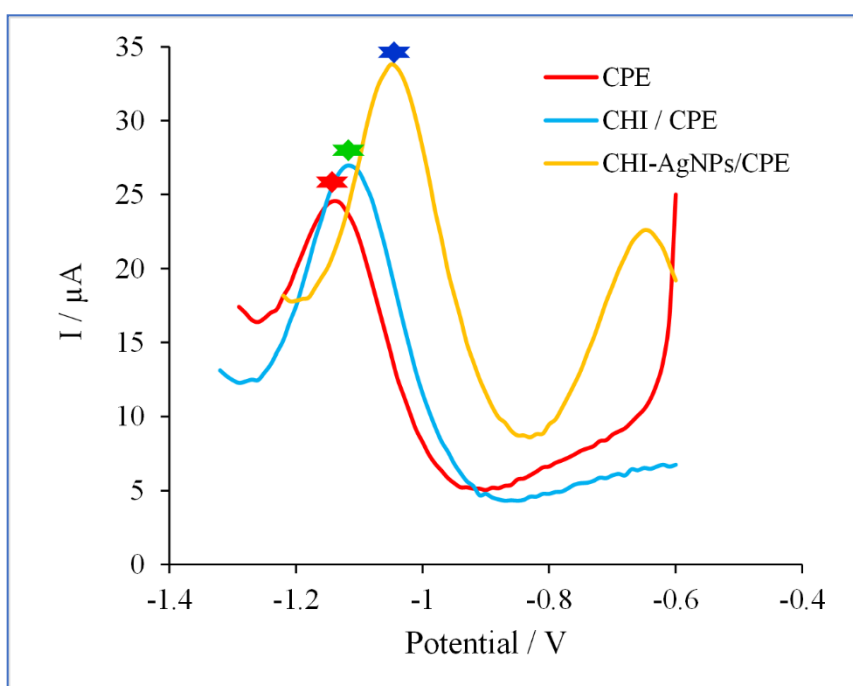
Figure 3: Square wave voltammetric response of 1.0×10^{-3} mol L^{-1} TMX respectively at CHI-AgNP/CPE, CHI/CPE and CPE in R–B buffer pH 10.4.

A clear shift in potential at the silver nanoparticles modified electrode (with 75mV) suggests an electrocatalytic activity of silver nanoparticles towards electroreduction of nitro group compound TMX. In addition, in terms of current density, the CHI-AgNPs / CPE electrode showed a significant improvement in the sensing of our analyte. These results can be explained not only because of the electrocatalytic capacity of silver but also because of the large electroactive specific surface area which was enhanced by the surface modification with chitosan, as well as the synergistic effect between chitosan and silver nanoparticles enable the composite material have tremendous benefits in electroanalysis and electrocatalysis.

122

Cyclic voltammetry was used to evaluate the effect of scan rate on the reduction of 1.0×10^{-3} mol L^{-1} thiamethoxam at CHI-AgNPs / CPE. Figure 4A illustrates the correlation of scan rate with the peak currents (I_p) and potential peak (E_p) of TMX, which probed by varying scan rates from 5 to 100 Mv s^{-1}. As the scan rate raised, the cathodic peak potential (E_p) shifted to more negative values, which is characteristic of an irreversible process.
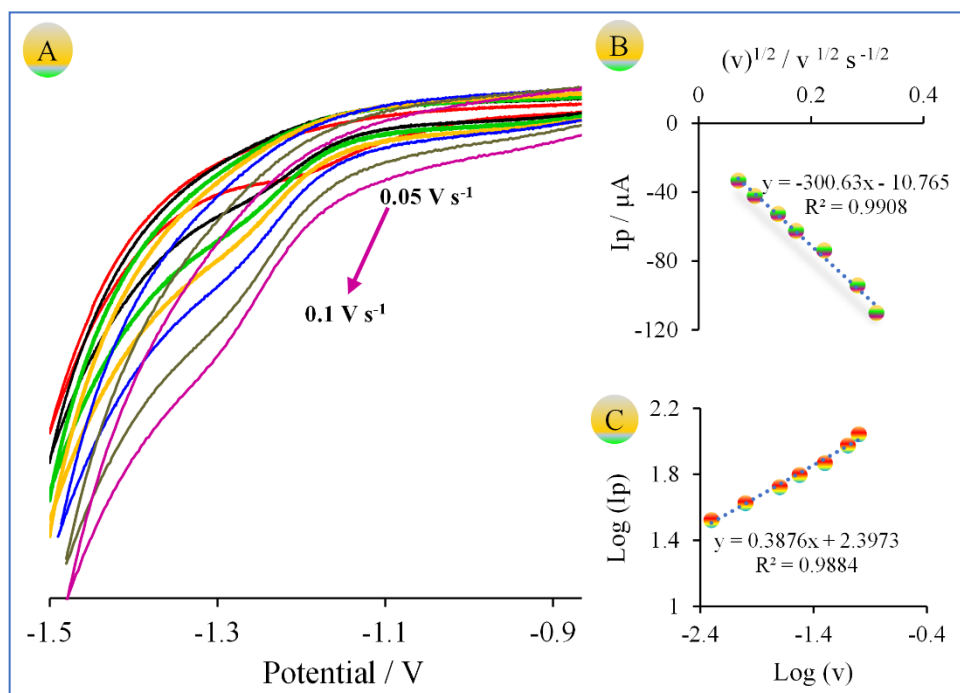
Figure 4: (A) Cyclic voltammograms recorded at different scan rates using the CHI-AgNP/CPE in B-R buffer at pH 10.4 containing 1.0×10^{-3} mol L^{-1} TMX, (B) graphs of cathodic peak currents vs the square root of scan rate, (C) graphs of log(I) vs log(v).

The plot of the cathodic peak current versus square root of scan rate (v) was established, yielding a linear regression with a correlation factor of $R^2 = 0.991$ that suggest the likelihood of the diffusion-control process (Figure 4B.). However, the slope value of log (I_p) versus log (v) was found to be 0.388, (Figure 4C), suggesting that the reduction process is governed by diffusion. This conclusion was supported by recording successive cycles of the cyclic voltammogram (instead of just one). The I_p value remained relatively steady for the second and subsequent cycles, showing that the electrode surface was not covered by adsorption.

The number of electrons (n) transferred during the electrochemical reduction of TMX was estimated using Laviron's equation, that describes irreversible electrode processes [48]. The value of αn can be deduced from the slope of the E_p vs. log v curve and was calculated to be

0.8. for n= 1.60 and α= 0.5, where n is stoichiometric number of the electron involved in the electrode reaction and α is the transfer coefficient.

The influence of pH on cathodic peak current (I_p) and cathodic peak potential (E_p) in B-R buffer containing 1.0×10^{-3} mol L^{-1} of TMX was studied using SWV (Figure 5A). The peak positions are clearly influenced by pH, as they shifted to more negative values as pH increased. This behavior indicates that protons are involved in the electrochemical reaction of TMX [49].
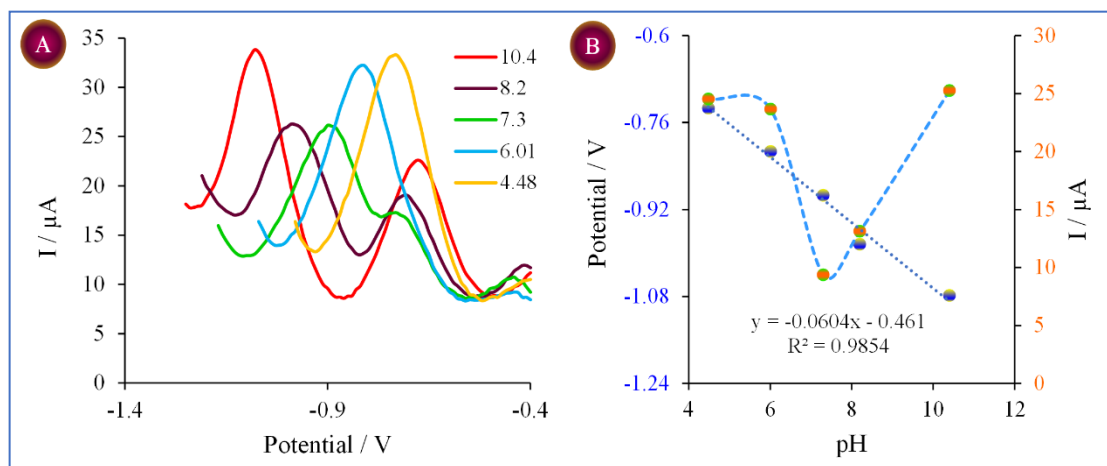
Figure 5: SWVs of CHI-AgNPs modified CPE electrode in B-R buffer solutions with different pH values, in the presence of 1.0×10^{-3} mol L^{-1}.

The relationship between E_p and pH can be expressed as E_p (V) = -0.0604 pH – 0.601 (R2 = 0.985) (Figure 5B). The slope was close to the theoretical value (-0.059 V / pH), indicating that the electroreduction of THM on CHI-AgNPs / CPE involved an equal number of electrons and protons [50]. The electron transfers number (n) is computed as 2, implying that two electrons and two protons are involved in the TMX reduction on the modified electrode.

To the best of our knowledge, the reduction of the nitro group typically occurs in two steps; through the reduction of the nitro group to hydroxylamine (Eq. (6)), followed by the reduction of the hydroxylamine to amine (Eq.(7)) [51]:

$$R\_NO_2 + 4e^- + 4H^+ \leftrightarrow R\_NHOH^- \tag{6}$$

$$R\_NHOH + 2e^- + 2H^+ \leftrightarrow R\_NH_2 + H_2O \tag{7}$$
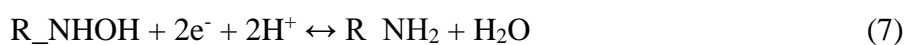
In this case, the analyzing peak corresponds to the second step of nitro group TMX electro-reduction at CHI-AgNPs / CPE, which involves two electrons and two protons.

Furthermore, chronoamperometric measurements were performed by setting the working electrode potential at -1000 mV for various concentration of thiamethoxam. For an electroactive compound TMX with a diffusion coefficient of D, the current observed for the electrochemical reaction at the mass transport limited condition is described by the Cottrell equation [52].
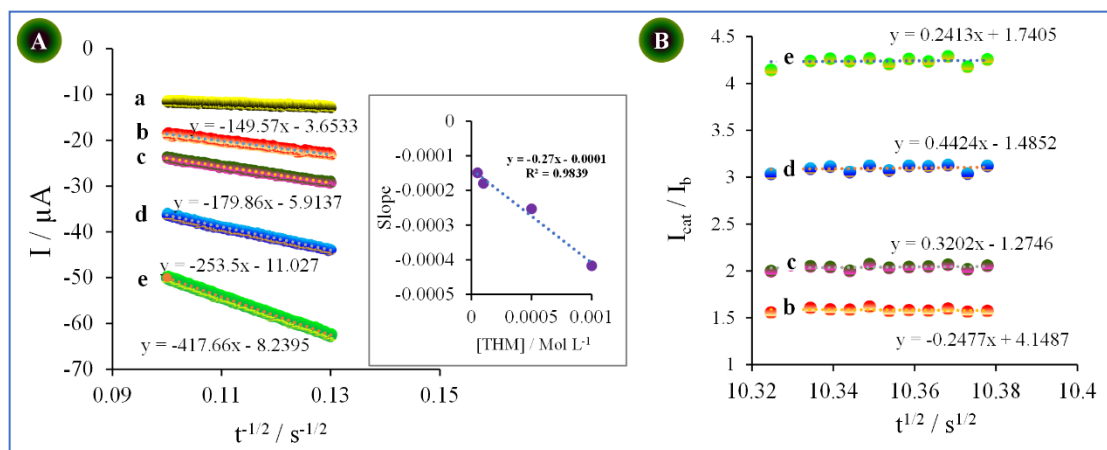
Figure 6: *(A) The plots of I_c vs. $t^{-1/2}$ ($s^{-1/2}$) obtained from chronoamperograms of TMX concentrations (a) blank, (b) 5.0×10^{-5}, (c) 1.0×10^{-4}, (d) 5.0×10^{-4} and (e) 1.0×10^{-3} mol L^{-1} with a potential step at -1000 mV in B-R buffer (pH 10.4), inset the plot of the slopes of the straight lines against the TMX concentrations, and (B) The plots of I_{cat}/I_b vs. $t^{1/2}$ ($s^{1/2}$).*

Figure 6A illustrates the experimental plots of I_p versus $t^{-1/2}$ with the best fits for different concentrations of TMX employed. The slopes of the resulting straight lines were then plotted versus the TMX concentration (inset of figure 6A), from whose slope and Cottrell equation, TMX's D value was estimated to be 5.94×10^{-6} cm^2 s^{-1}. In the electrochemical detection of TMX, the D value reflects the amount of TMX flowing through the electrode's surface. the high D value indicates that more TMX may flow across the electrode surface per unit of time, resulting in a greater reduction current and an improved electrochemical signal.

According to the Galus approach [53], chronoamperometry may be used to determine the catalytic rate constant (k) for the reaction between TMX and CHI-AgNPs / CPE. In this approach, there is an estimation relating the ratio of catalytic and limited current (I_{cat}/I_L) and the catalytic rate constant (k) as Eq. 8:

$$I_{cat}/I_L = \pi^{1/2}(kC_b t)^{1/2} \tag{8}$$

where *Icat* is the catalytic current of TMX at CHI-AgNPs / CPE, I_L is the limited current in the absence of TMX, C_b is the bulk concentration of TMX and *t* is the time elapsed. The plots of I_{cat}/I_L versus $t^{1/2}$ were constructed (Figure 6B) and from the values of slopes, the average value of k was found to be 2.15×10^2 M^{-1} s^{-1}. The *D* and *k* values determined by chronoamperometry show that the CHI-AgNPs/CPE surface has high catalytic performance for TMX.

4) Calibration plots, limit of detection and interference study

The TMX determination was realized at modified electrode CHI-AgNPs / CPE in the under the optimal conditions using SWV technique. Figure 7 shows the SWV responses of TMX with the series of different concentrations, illustrating an increase in the current response of TMX reduction with increasing concentrations in B-R. buffer (pH 10.4).

The CHI-AgNPs / CPE appeared sensitive, up to micromolar concentrations of TMX. This might be due to the large surface area of the nanoscale Ag NPs and the matrix's good conductivity. Additionally, Nitro ($-NO_2$), as a powerful electron withdrawing group, leads aromatic ring of nitro-group compounds to electron deficiency. Consequently, the H-bonding is susceptible to form between OH of chitosan-AgNPs and NO_2 of TMX due to the high electronegativity of oxygen atom of NO_2 [54, 55]. Furthermore, the Ag NPs provided larger surface area with surface electronic interaction of exposed Ag (111) facet with analyte molecules resulting in enhanced electron-transfer kinetics and improvement in the reduction current of molecule target. The plot of peak current versus TMX concentration consisted of two linear segments with slopes of 51274 and 5371 µA Mol L^{-1} in the concentration ranges of 4.0 to 1.0×10^2 µMol L^{-1} and 1.0×10^2 to 1.0×10^3 µMol L^{-1}, respectively (inset figure 7). Kinetic limitation is perhaps most likely to attribute for the decrease in sensitivity (slope) of the second linear segment.

The limits of detection (LOD) and quantification (LOQ) were calculated using the equations 3σ/b and 10σ/b, respectively, where σ is the standard deviation of the curve intercept and b is the slope of the analytical curve. The values obtained for the LOD and LOQ were 9.32×10^{-7} mol L^{-1} and 3.10×10^{-6} mol L^{-1}, respectively. The analytical performance of the CHI-AgNPs / CPE was compared to others advanced materials and nanomaterials-based electrodes previously published, as shown in table 2. So, our proposed sensor demonstrated the advantage in terms of simplicity of synthesis, a relatively low LOD and a wide linear range which can be a benefit for future practical application in development portable devices.
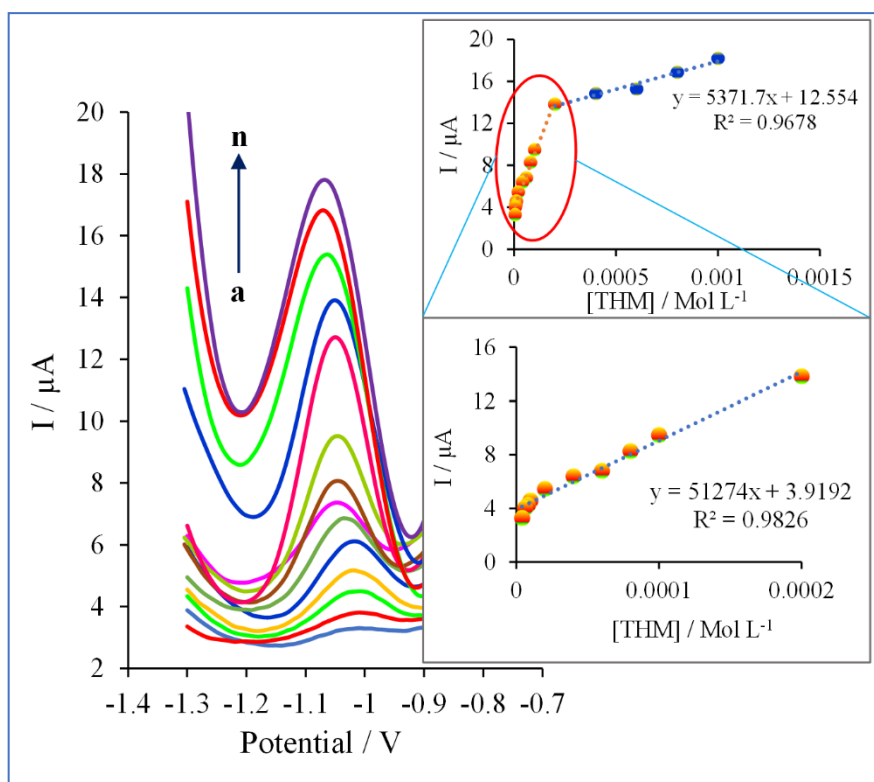
Figure 7: SWV voltammograms of TMX recorded with the CHI-AgNP/CPE at different levels of concentrations in B-R buffer at pH 10.4: a) 4.0×10^{-6} mol L^{-1}; b) 6.0×10^{-6} mol L^{-1}; c) 8.0×10^{-6} mol L^{-1}; d) 1.0×10^{-5} mol L^{-1}; e) 2.0×10^{-5} mol L^{-1}; f) 4.0×10^{-5} mol L^{-1}, g) 6.0×10^{-5} mol L^{-1}, h) 8.0×10^{-5} mol L^{-1}, i) 1.0×10^{-4} mol L^{-1}, j) 2.0×10^{-4} mol L^{-1}, k) 4.0×10^{-4} mol L^{-1}, l) 6.0×10^{-4} mol L^{-1}, m) 8.0×10^{-4} mol L^{-1}, n) 1.0×10^{-3} mol L^{-1}. Inset calibration curves for TMX constructed using the CHI-AgNP/CPE. Results for n = 3 measurements.

The selectivity of the modified electrode CHI-AgNPs / CPE was investigated by analysing the thiamethoxam with different doses of several nitro-aromatic compounds, such as 4-nitrophenol, 4-nitroaniline, 2-nitroanailine, simultaneously electrolyte (Figure 8). Compared with the current intensity of thiamethoxam, decrease in response signal with estimated relative standard deviation of 5% was observed thus confirming an acceptable selectivity of AgNPS modified electrode toward TMX. Finally, the reproducibility of proposed sensor was estimated at eight different electrodes and the relative standard deviation (RSD) of 1.5% showing good electrode-to-electrode reproducibility.

Table 2: Recovery test of TMX insecticide in extracts tissues of zea mays and bean Phaseolus vulgaris.

Plant	Tissue	Add concentration (mol L^{-1})	Found concentration (mol L^{-1})	Recovery (n=3)
Zea maize	Roots	1.0×10^{-4}	6.5×10^{-5}	65.46%
		5.0×10^{-4}	3.1×10^{-4}	62.70%
	leaves	1.0×10^{-4}	8.3×10^{-5}	82.76%
		5.0×10^{-4}	4.2×10^{-4}	84.85%
Bean Phaseolus vulgaris L.	Roots	1.0×10^{-4}	7.0×10^{-5}	70.35%
		5.0×10^{-4}	2.7×10^{-4}	54.06%
	Leaves	1.0×10^{-4}	8.7×10^{-5}	86.98%
		5.0×10^{-4}	4.0×10^{-4}	80.33%
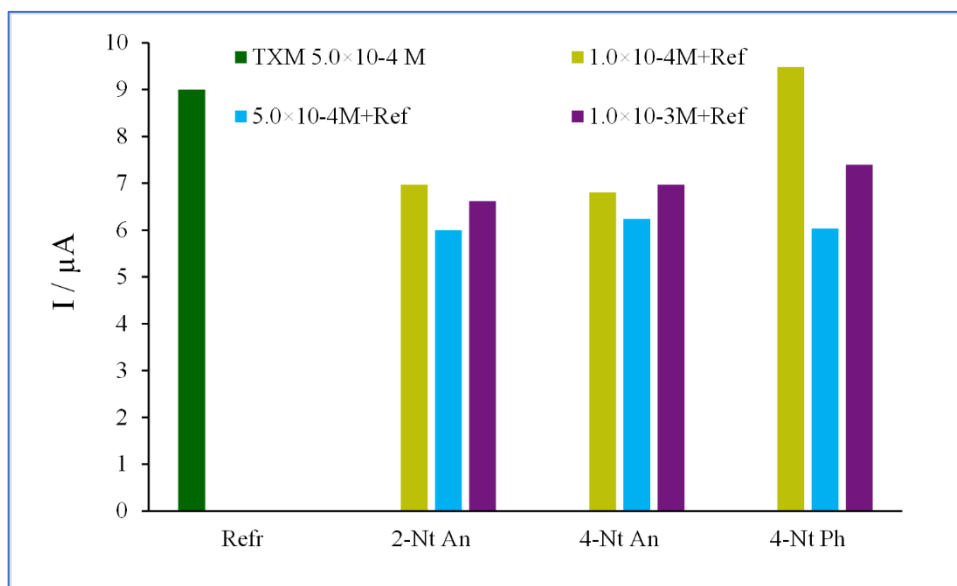
Figure 8: Interference's study of different concentrations of nitro-organic species (1.0×10^{-5}, 1.0×10^{-4} and 5.0×10^{-4} mol L^{-1}), such as 4-nitrophenol, 4-nitroanailine, and 2-nitroaniline on the electroreduction signal of 5.0×10^{-4} mol L^{-1} TMX.

5- Thiamethoxam analysis in *Zea mays* and bean *phaseolus vulgaris L.*

To evaluate the applicability of the proposed method, it was employed to determine TMX insecticide in plant tissues (roots, leaves) extracts of two plant species including *Zea mays* and

bean *phaseolus vulgaris L.* The extracts were analysed by SWV. The calibration curve of each tissue was established by adding known amounts of TMX insecticide to control extract (samples preparation was mentioned in the experimental section). The recovery percent obtained revealed the capability of our sensors for detection of TMX insecticide directly in different tissues of plants. The obtained results are shown in table 3.

Table 3: *Comparison of the sensing performance for TMX of various electrodes.*

Electrochemical techniques	Electrodes	Limit of detection (µmol L^{-1})	Limit of quantification (µmol L^{-1})	Linear range (µmol L^{-1})	Refs
DPV CV Amperometry	Nanosilver/SDS /GCE	0.100 4.700 0.880	0.40 15.91 0.88	0.10 - 9	[56]
SWV	Graphen Oxide Galssy Carbon Electrode GO/GCE	8.300	-	10 - 200	[57]
SWV	GCE/rGO/β-CD	7.450	-	-	[58]
LSV	MIP-GN/GCE	0.040	-	0.50 - 20	[59]
LSV	β-CD-rGO/GCE	0.270	-	-	[60]
FFTCAV	CHI-MWCNT/AuNP/RGNS/CILE	6.2×10^{-6}	-	0.05×10^{-3} – 35×10^{-3}	[61]
SWV	CHI-AgNPs / CPE	0.932	3.10	$4-1.0\times10^{3}$	This work

FFTCAV: Fast Fourier Transform Coulometric Admittance Voltammetry

GCE/rGO/β-CD: glassy carbon electrode modified with reduced graphene oxide and cyclodextrin

Nanosilver/SDS /GCE: nanosilver/SDS modified glassy carbon electrode.

DM-BC/GCE: carbonate minerals dolomite - moso bamboo glassy carbon electrode.

MIP-GN/GCE: molecularly imprinted polymers-based graphene

CHI-MWCNT/AuNP/RGNS/CILE: chitosan, multi-walled carbon nanotube, reduced graphene nanosheets and gold nanoparticles on a carbon paste ionic liquid electrode

.

IV. Conclusion

We presented here, for the first time, the use of silver nanoparticles stabilised chitosan for the electroanalysis determination of TMX insecticide. Compared with graphite and chitosan modified graphite electrodes the proposed electrode exhibited improved electrochemical performance. Our developed voltammetric approach was based on the irreversible electrochemical reduction of TMX on the CHI-AgNPs / CPE electrode surface. In addition, the electrochemical behavior of TMX was investigated and the mechanism for its electrochemical reduction was postulated. In the wide concentration range studied, TMX insecticide demonstrated good linearity over the surface of the CHI-AgNP / CPE. Compared with others sensors-based nanomaterials the proposed electrode presents an acceptable LOD and a wide linear range which can be a benefit for future practical application in development portable devices. Furthermore, the analytical performance of present electrochemical method for real applications was successfully investigated through the detection of TMX in plant tissues extracts. Therefore, it can be concluded that the present electrode and the electrochemical method proposed here can be considered as an effective, sensitive and environment friendly device for TMX insecticide determination in real environmental samples.

References

[1] Talapin, D.V.; Lee, J.-S.; Kovalenko, M.V. and Shevchenko, E.V.: Prospects of Colloidal Nanocrystals for Electronic and Optoelectronic Applications, Chemical Reviews, **110** (2010), no. 1, pp. 389–458.

[2] Ray, P.C.: Size and Shape Dependent Second Order Nonlinear Optical Properties of Nanomaterials and Their Application in Biological and Chemical Sensing, Chemical Reviews, **110** (2010), no. 9, pp. 5332–5365.

[3] Roduner, E.: Size matters: why nanomaterials are different, Chemical Society Reviews, **35** (2006), no. 7, pp. 583–592.

[4] Daniel, M.-C. and Astruc, D.: Gold Nanoparticles: Assembly, Supramolecular Chemistry, Quantum-Size-Related Properties, and Applications toward Biology, Catalysis, and Nanotechnology, Chemical Reviews, **104** (2004), no. 1, pp. 293–346.

[5] Saha, K.; Agasti, S.S.; Kim, C.; Li, X. and Rotello, V.M.: Gold Nanoparticles in Chemical and Biological Sensing, Chemical Reviews, **112** (2012), no. 5, pp. 2739–2779.

[6] Yuan, Z.; Peng, M.; He, Y. and Yeung, E.S.: Functionalized fluorescent gold nanodots: synthesis and application for Pb2+ sensing, Chemical Communications, **47** (2011), no. 43, pp. 11981–11983.

[7] Furube, A.; Du, L.; Hara, K.; Katoh, R. and Tachiya, M.: Ultrafast Plasmon-Induced Electron Transfer from Gold Nanodots into TiO2 Nanoparticles, Journal of the American Chemical Society, **129** (2007), no. 48, pp. 14852–14853.

[8] L. Medintz, I. and Mattoussi, H.: Quantum dot -based resonance energy transfer and its growing application in biology, Physical Chemistry Chemical Physics, **11** (2009), no. 1, pp. 17–45.

[9] Medintz, I.L.; Uyeda, H.T.; Goldman, E.R. and Mattoussi, H.: Quantum dot bioconjugates for imaging, labelling and sensing, Nature Materials, **4** (2005), no. 6, pp. 435–446.

[10] Lu, A.-H.; Salabas, E.L. and Schüth, F.: Magnetic Nanoparticles: Synthesis, Protection, Functionalization, and Application, Angewandte Chemie International Edition, **46** (2007), no. 8, pp. 1222–1244.

[11] Ho, D.; Sun, X. and Sun, S.: Monodisperse Magnetic Nanoparticles for Theranostic Applications, Accounts of Chemical Research, **44** (2011), no. 10, pp. 875–882.

[12] Markowska-Szczupak, A.; Ulfig, K. and Morawski, A.W.: The application of titanium dioxide for deactivation of bioparticulates: An overview, Catalysis Today, **169** (2011), no. 1, pp. 249–257.

[13] Zou, H.; Wu, S. and Shen, J.: Polymer/Silica Nanocomposites: Preparation, Characterization, Properties, and Applications, Chemical Reviews, **108** (2008), no. 9, pp. 3893–3957.

[14] Baker, S.N. and Baker, G.A.: Luminescent Carbon Nanodots: Emergent Nanolights, Angewandte Chemie International Edition, **49** (2010), no. 38, pp. 6726–6744.

[15] Hsu, P.-C.; Shih, Z.-Y.; Lee, C.-H. and Chang, H.-T.: Synthesis and analytical applications of photoluminescent carbon nanodots, Green Chemistry, **14** (2012), no. 4, pp. 917–920.

[16] Castro Neto, A.H.; Guinea, F.; Peres, N.M.R.; Novoselov, K.S. and Geim, A.K.: The electronic properties of graphene, Reviews of Modern Physics, **81** (2009), no. 1, pp. 109–162.

[17] Rao, C.N.R.; Sood, A.K.; Subrahmanyam, K.S. and Govindaraj, A.: Graphene: The New Two-Dimensional Nanomaterial, Angewandte Chemie International Edition, **48** (2009), no. 42, pp. 7752–7777.

[18] Díez, I. and Ras, R.H.A.: Fluorescent silver nanoclusters, Nanoscale, **3** (2011), no. 5, pp. 1963–1970.

[19] Lu, Y. and Liu, J.: Smart Nanomaterials Inspired by Biology: Dynamic Assembly of Error-Free Nanomaterials in Response to Multiple Chemical and Biological Stimuli, Accounts of Chemical Research, **40** (2007), no. 5, pp. 315–323.

[20] Baron, R.; Willner, B. and Willner, I.: Biomolecule–nanoparticle hybrids as functional units for nanobiotechnology, Chemical Communications, (2007), no. 4, pp. 323–332.

[21] Wang, Z. and Lu, Y.: Functional DNA directed assembly of nanomaterials for biosensing, Journal of Materials Chemistry, **19** (2009), no. 13, pp. 1788–1798.

[22] Chen, W.-Y.; Shiang, Y.-C.; Li, C.-L.; Periasamy, A.P. and Chang, H.-T.: DNA Functional Gold and Silver Nanomaterials for Bioanalysis, Functional Nanoparticles for Bioanalysis, Nanomedicine, and Bioelectronic Devices Volume 2, American Chemical Society, 2012, pp. 287–322.

[23] Santhosh, A.; Theertha, V.; Prakash, P. and Smitha Chandran, S.: From waste to a value added product: Green synthesis of silver nanoparticles from onion peels together with its diverse applications, Materials Today: Proceedings, **46** (2021), pp. 4460–4463.

[24] Shankar, A.; Kumar, V.; Kaushik, N.K.; Kumar, A.; Malik, V.; Singh, D. and Singh, B.: Sporotrichum thermophile culture extract-mediated greener synthesis of silver nanoparticles: Eco-friendly functional group transformation and anti-bacterial study, Current Research in Green and Sustainable Chemistry, **3** (2020), p. 100029.

[25] Mollarasouli, F.; Zor, E.; Ozcelikay, G. and Ozkan, S.A.: Magnetic nanoparticles in developing electrochemical sensors for pharmaceutical and biomedical applications, Talanta, **226** (2021), p. 122108.

[26] Njoki, P.N.; Roots, M.E.D. and Maye, M.M.: The Surface Composition of Au/Ag Core/Alloy Nanoparticles Influences the Methanol Oxidation Reaction, ACS Applied Nano Materials, **1** (2018), no. 10, pp. 5640–5645.

[27] Anker, J.N.; Hall, W.P.; Lyandres, O.; Shah, N.C.; Zhao, J. and Van Duyne, R.P.: Biosensing with plasmonic nanosensors, Nanoscience and Technology, Co-Published with Macmillan Publishers Ltd, UK, 2009, pp. 308–319.

[28] Arvizo, R.R.; Bhattacharyya, S.; Kudgus, R.A.; Giri, K.; Bhattacharya, R. and Mukherjee, P.: Intrinsic therapeutic applications of noble metal nanoparticles: past, present and future, Chemical Society Reviews, **41** (2012), no. 7, pp. 2943–2970.

[29] Kelly, K.L.; Coronado, E.; Zhao, L.L. and Schatz, G.C.: The Optical Properties of Metal Nanoparticles: The Influence of Size, Shape, and Dielectric Environment, The Journal of Physical Chemistry B, **107** (2003), no. 3, pp. 668–677.

[30] Chen, D.; Qiao, X.; Qiu, X. and Chen, J.: Synthesis and electrical properties of uniform silver nanoparticles for electronic applications, Journal of Materials Science, **44** (2009), no. 4, pp. 1076–1081.

[31] Maity, M.; Bera, K.; Pal, U.; Khamaru, K. and Maiti, N.C.: Sensing of Iron(III) Ion via Modulation of Redox Potential on Biliverdin Protected Silver Nanosurface, ACS Applied Nano Materials, **1** (2018), no. 11, pp. 6099–6111.

[32] Gupta, V.K.; Atar, N.; Yola, M.L.; Darcan, C.; İdil, Ö.; Üstündağ, Z.; and Suhas: Biosynthesis of silver nanoparticles using chitosan immobilized Bacillus cereus: Nanocatalytic studies, Journal of Molecular Liquids, **188** (2013), pp. 81–88.

[33] Ikhsan, N.I.; Rameshkumar, P. and Huang, N.M.: Controlled synthesis of reduced graphene oxide supported silver nanoparticles for selective and sensitive electrochemical detection of 4-nitrophenol, Electrochimica Acta, **192** (2016), pp. 392–399.

[34] Zhang, P.; Shao, C.; Zhang, Z.; Zhang, M.; Mu, J.; Guo, Z. and Liu, Y.: In situ assembly of well-dispersed Ag nanoparticles (AgNPs) on electrospun carbon nanofibers (CNFs) for catalytic reduction of 4-nitrophenol, Nanoscale, **3** (2011), no. 8, pp. 3357–3363.

[35] Maduraiveeran, G. and Ramaraj, R.: Potential Sensing Platform of Silver Nanoparticles Embedded in Functionalized Silicate Shell for Nitroaromatic Compounds, Analytical Chemistry, **81** (2009), no. 18, pp. 7552–7560.

[36] de Lima, C.A.; da Silva, P.S. and Spinelli, A.: Chitosan-stabilized silver nanoparticles for voltammetric detection of nitrocompounds, Sensors and Actuators B: Chemical, **196** (2014), pp. 39–45.

[37] Jiang, L.; Santiago, I. and Foord, J.: High-Yield Electrochemical Synthesis of Silver Nanoparticles by Enzyme-Modified Boron-Doped Diamond Electrodes, Langmuir, **36** (2020), no. 22, pp. 6089–6094.

[38] Lemineur, J.-F.; Noël, J.-M.; Combellas, C. and Kanoufi, F.: Optical monitoring of the electrochemical nucleation and growth of silver nanoparticles on electrode: From single to ensemble nanoparticles inspection, Journal of Electroanalytical Chemistry, **872** (2020), p. 114043.

[39] Zahran, M.; Khalifa, Z.; Zahran, M.A.-H. and Abdel Azzem, M.: Dissolved Organic Matter-Capped Silver Nanoparticles for Electrochemical Aggregation Sensing of Atrazine in Aqueous Systems, ACS Applied Nano Materials, **3** (2020), no. 4, pp. 3868–3875.

[40] Torres-Rivero, K.; Torralba-Cadena, L.; Espriu-Gascon, A.; Casas, I.; Bastos-Arrieta, J. and Florido, A.: Strategies for Surface Modification with Ag-Shaped Nanoparticles: Electrocatalytic Enhancement of Screen-Printed Electrodes for the Detection of Heavy Metals, Sensors, **19** (2019), no. 19, p. 4249.

[41] Fekry, A.M.; Abdel-Gawad, S.A.; Tammam, R.H. and Zayed, M.A.: An electrochemical sensor for creatinine based on carbon nanotubes/folic acid /silver nanoparticles modified electrode, Measurement, **163** (2020), p. 107958.

[42] Laghrib, F.; Ajermoun, N.; Bakasse, M.; Lahrich, S. and El Mhammedi, M.A.: Synthesis of silver nanoparticles assisted by chitosan and its application to catalyze the reduction of 4-nitroaniline, International Journal of Biological Macromolecules, **135** (2019), pp. 752–759.

[43] Claudine, G. da R.; Francis, H.R.F. and Claudia, A.L.C.: Quantification of Thiamethoxam in Rhizomes and Leaves of the *Hedychium coronarium* and Water and Soil by High-Pressure Liquid Chromatography, American Journal of Analytical Chemistry, **2012** (2012).

[44] Randviir, E.P.; Brownson, D.A.C. and Banks, C.E.: A decade of graphene research: production, applications and outlook, Materials Today, **17** (2014), no. 9, pp. 426–432.

[45] Nicholson, R.S.: Theory and Application of Cyclic Voltammetry for Measurement of Electrode Reaction Kinetics., Analytical Chemistry, **37** (1965), no. 11, pp. 1351–1355.

[46] Lavagnini, I.; Antiochia, R. and Magno, F.: An Extended Method for the Practical Evaluation of the Standard Rate Constant from Cyclic Voltammetric Data, Electroanalysis, **16** (2004), no. 6, pp. 505–506.

[47] Klingler, R.J. and Kochi, J.K.: Electron-transfer kinetics from cyclic voltammetry. Quantitative description of electrochemical reversibility, The Journal of Physical Chemistry, **85** (1981), no. 12, pp. 1731–1741.

[48] Laviron, E.: Adsorption, autoinhibition and autocatalysis in polarography and in linear potential sweep voltammetry, Journal of Electroanalytical Chemistry and Interfacial Electrochemistry, **52** (1974), no. 3, pp. 355–393.

[49] Siara, L.R.; de Lima, F.; Cardoso, C.A.L. and Arruda, G.J.: Electrochemically pretreated zeolite-modified carbon-paste electrodes for determination of linuron in an agricultural formulation and water, Electrochimica Acta, **151** (2015), pp. 609–618.

[50] Filip, J. and Tkac, J.: The pH dependence of the cathodic peak potential of the active sites in bilirubin oxidase, Bioelectrochemistry, **96** (2014), pp. 14–20.

[51] Junqueira, J.R.C.; de Araujo, W.R.; Salles, M.O. and Paixão, T.R.L.C.: Flow injection analysis of picric acid explosive using a copper electrode as electrochemical detector, Talanta, **104** (2013), pp. 162–168.

[52] Bard, A.J. and Faulkner, L.R.: Fundamentals and applications, Electrochemical methods, **2** (2001), no. 482, pp. 580–632.

[53] Barker, G.C.: E. Galus, Fundamentals of Electrochemical Analysis, Ellis Horwood Ltd., Chichester (1976), 520+ xviii pp.,\pounds 23.501977.

[54] Yang, R.; Wei, Y.; Yu, Y.; Gao, C.; Wang, L.; Liu, J.-H. and Huang, X.-J.: Make it different: The plasma treated multi-walled carbon nanotubes improve electrochemical performances toward nitroaromatic compounds, Electrochimica Acta, **76** (2012), pp. 354–362.

[55] Pan, S.; Wang, L.; Chen, X.; Tang, Y.; Chen, Y.; Sun, Y.; Yang, X. and Wan, P.: Enhanced electrochemical sensing of nitroaromatic compounds based on hydroxyl modified carbon submicroparticles, Electrochimica Acta, **203** (2016), pp. 301–308.

[56] Kumaravel, A. and Chandrasekaran, M.: Nanosilver/surfactant modified glassy carbon electrode for the sensing of thiamethoxam, Sensors and Actuators B: Chemical, **174** (2012), pp. 380–388.

[57] Urbanová, V.; Bakandritsos, A.; Jakubec, P.; Szambó, T. and Zbořil, R.: A facile graphene oxide based sensor for electrochemical detection of neonicotinoids, Biosensors and Bioelectronics, **89** (2017), pp. 532–537.

[58] Oliveira, A.E.F.; Bettio, G.B. and Pereira, A.C.: An Electrochemical Sensor Based on Electropolymerization of ß-Cyclodextrin and Reduced Graphene Oxide on a Glassy Carbon Electrode for Determination of Neonicotinoids, Electroanalysis, **30** (2018), no. 9, pp. 1918–1928.

[59] Xie, T.; Zhang, M.; Chen, P.; Zhao, H.; Yang, X.; Yao, L.; Zhang, H.; Dong, A.; Wang, J. and Wang, Z.: A facile molecularly imprinted electrochemical sensor based on graphene: application to the selective determination of thiamethoxam in grain, RSC Advances, **7** (2017), no. 62, pp. 38884–38894.

[60] Zhai, X.; Zhang, H.; Zhang, M.; Yang, X.; Gu, C.; Zhou, G.; Zhao, H.; Wang, Z.; Dong, A. and Wang, J.: A rapid electrochemical monitoring platform for sensitive determination of thiamethoxam based on β–cyclodextrin-graphene composite, Environmental Toxicology and Chemistry, **36** (2017), no. 8, pp. 1991–1997.

[61] Norouzi, P.; Ghaheri, N.; Aghazadeh, M.; Mofidi, Z. and Larijani, B.: Sensitive Electrochemical Measurement of Thiamethoxam on Nanocomposite Coated Carbon Paste Using FFT Coulometric Admittance Voltammetry and Flow Injection Analysis, Int. J. Electrochem. Sci, **12** (2017), pp. 8847–8859.

Chapter V

Phytotoxic effect of the insecticide imidacloprid in plant *of Phaseolus vulgaris L.*

I. Introduction

Common bean (*Phaseolus vulgaris* L.) considered one of the most important legumes and food sources in the world [1]. It is a major source of calories, fibres, lipids and proteins in many developing countries throughout the world [2]. In Eastern Africa and Latin America, this plant accounts for 65% of total protein consumption and 32% of energy intake [3]. In addition, it is estimated that about 26 million tons of beans were produced worldwide in 2016 [4], which is an economically, nutritionally, and socially important crop in developing countries [5]. One of the major factors affecting the production of common bean in the world is that a wide range of destructive pathogens attack the crop and result in severe damage. One of these is a geminivirus spread by whitefly (*bemisia tabaci*) called bean golden mosaic virus (BGMV). This pathogen produces serious foliar yellow mosaic symptoms, retarded growth, seeds and pods deformation and flowers abortion. Therefore, an annual loss ranging between 90,000 and 280,000 tons of grain [6]. Generally, due to pest and disease attack the yield of any agricultural harvest can be severely reduced [7]. In order, to minimize the loss of culture yield and to satisfy the global food demand, the application of insecticides has become a common agricultural practice and preferred to control the insect pest, due to their ease to use, less cost and enhanced effectiveness [8]. Imidacloprid is considered one of the most active neonicotinoid insecticides applied against the insect pests [9], such as whiteflies, aphids, leafhoppers, scale insects and some members of Diptera, Coleoptera and Lepidoptera [10, 11]. It is mostly used in foliar spray, seed treatment and soil application [12–14]. However, the non-rational and injudicious utilization of insecticides causes its persistence for several months or even years in soil, water and plant matter [15]. On the other hand, the residues of imidacloprid destruct the fertility of the soil [16, 17]. cause toxicity to plants which led to retarded growth, reduced photosynthetic pigments [18, 19], physiological activities [20], whereas, increase the risk to non-target plants, vertebrates and invertebrate [21, 22]. The studies noted that IMD with high doses could cause oxidative stress, lower photosynthetic efficiency and active enzymatic and non-enzymatic antioxidants and resulting in bioaccumulation of residues of IMD in plant tissues [23–25]. In the same context, many researchers reported that pesticides can adversely affect the growth of non-target host plants by inducing the accumulation of reactive oxygen species (ROS) [26–29]. The RSO has been found to decrease plant growth and membrane stability, eventually trigger plant cell death [30]. However, in relation to its accumulation, distribution and toxicological effect in the environment and non-target organisms, IMD as a worldwide used insecticide raises environmental and human health concerns. Ge and co-works investigated the accumulation and dissipation behaviour of imidacloprid in rice. They reported that IMD could be uptake by rice

from soil and easily translocated into shoots from roots [31]. IMD could be translocated into other tissues (stems, leaves and fruits …) after root uptake, through the xylem [32]. Bonmatin et al. summarized the exposure and environmental fate of IMD in soil, sediment and plants [15]. Juraske and co-authors studied the IMD uptake and persistence using soil irrigation and foliar spray way in tomato plants [33]. The uptake and accumulation of IMD in various plants, including maize, tomato, apple tree, sunflower grapevine and grape grown have been documented [31–35]. The results noted that IMD appears to be readily absorbed and subsequently accumulated in the aerial part of the plants. However, the effect of IMD on the growth of plants as well as its accumulation and translocation behavior in plant tissues remain unclear.

Therefore, there is a requirement to develop an easy, fast, highly sensitive and selective method, which should be suitable for on-site sensing of IMD. At present, several analytical techniques have been developed and used for very low-level detection of IMD, including HPLC High-pressure liquid chromatography (HPLC) [36–39], gas chromatographic–mass spectrometric (GC-MS) [40] liquid chromatography–mass spectrometry (LC-MS) [37, 41–43]. However, these analytical methods are time consuming and expensive, require professional operators, and the availability of these expensive instruments in laboratories is limited. Electrochemical detection is one of the most promising alternatives to the conventional methods, with many advantages such as low cost, straight-forward, fast response, high selectivity, great sensitivity, and less expensive equipment [44–48]. Bulk materials and nanomaterials are widely used for the development of user-friendly electrochemical sensors, due to their features such as high electrical conductivity, electrocatalytic properties, and good chemical and thermal stability [49–51].

Considering the above-mentioned problems related to the application of imidacloprid insecticide in the cultivation of common bean. The present study was therefore intended to examine the toxicological effect of the IMD insecticide on seed germination, seed vigour, plant growth, and photosynthetic pigment contents of the common bean. The bioaccumulation and translocation of the IMD in the common bean tissues was followed by square wave voltammetry using metallic silver electrode. The analytical and calibration parameters (Slope, correlation coefficient, linear range, detection limit and relative standard deviation) were calculated.

II. Experimental section

1) Reagents and materials

All chemicals used were of analytical reagent grade, sodium hydroxide (98%), phosphoric acid (85%), acetic (99.8%) and boric (99.5%) acids were purchased from Merck (Darmstadt, Germany), Fluka (St Gallen, Switzerland), and Riedel de Haen (Seelze, Germany). Common bean (*Phaseolus vulgaris* L Family Fabaceae) seeds were purchased from the local market in Khouribga City, Morocco. The commercial formulation of imidacloprid pesticide (Granular) was purchased from (Bayer CropScience (China) Co., Ltd, Hangzhou, China) and its detailed information was illustrated in table 1. The electrochemical measurements were performed using a potentiostat (model PGZ 100, Eco Chemie BV, Utrecht, The Netherlands) electrochemical analyzer operated using Voltamaster 4 software, equipped with a three electrodes cell comprising a metallic silver electrode (MSE) as a working electrode, Ag/AgCl (saturated KCl) and platinum wire as **a** reference and auxiliary electrodes respectively.

Table 1: *The main physico-chemical characteristics of imidacloprid insecticide.*

Active ingredient	Imidacloprid
Chemical name	1-[(6-chloro-3-pyridinyl)-methyl]-N-nitro-2-imidazolidinimine)
Chemical class	Neonicotinoids
Formulation	Granule
Octanol-water partition coefficient (log Kow)	0.57
Dissociation constant (pKa) at 25°C	No dissociation
Water solubility (g/L)	0.61
Recommended dose (mg/ml)	500

2) Germination and toxicity test

The seed germination test was carried out in an incubator ($22 \pm 2 \, ^\circ C$) under sterile conditions in darkness. After seeds were disinfected with sodium hypochlorite solution 10% (v/v) for 5 min and washed thoroughly with distilled water. The treated and untreated seeds by IMD were drained out and kept for germination during 6 days. Twenty seeds were kept between two layers of filter paper in each petri dish (diameter: 9.0 cm) and regularly soaked with adequate treatment solutions during the experiment time. The experiments were done in three replicates for each treatment. The number of germinated seeds was counted and the seeds were considered germinated when the radical protruding through the seed coat or least 2mm in length [52].

In order to evaluate the toxicological effect and insecticide efficiency. The definitive test helps in determining the effect measures, concentration-response curve, and effective concentration (EC50) value with a 95% confidence interval and standard error. The seeds were treated with five concentrations of imidacloprid (5.0×10^{-3}, 3.4×10^{-2}, 4.0×10^{-2}, 4.5×10^{-2}, 5.0×10^{-2} mol L^{-1}). Control without insecticide was kept. The number of germinated seeds was counted and the EC50 value was also calculated using a non-linear regression dose-response [53].

3) Monitoring of seedling growth

The seeds germinated were taken to grow in the controlled conditions for 21 days in the plastic pots (diameter 9.5 cm) containing a mixture of peat and 40% sand. The growth of seedlings was then followed. The experiment was carried out in a greenhouse condition (11h photoperiod / 13h dark cycle). The average temperatures were 28.5 and 20.0 °C for day and night, respectively. At the end of the experiment (21 days), IMD bioaccumulation and biometric parameters were measured: root and plant lengths and number of leaves and nods were counted. In addition, the Vigour index of seed was calculated according to the equation [54].

$$SVI = \text{germination percentage} \times Plant\ total\ length$$

4) IMD Extraction and quantification in plant

IMD was extracted by grinding with 100 ml of ultra-pure water 2g of vegetable tissues (roots, stems and leaves) [55]. The obtained homogenous extract was sonicated for 40 min at 3kHz and centrifuged for 10 min at 1792 g. The extraction was repeated three times (100, 100, and 50 mL), and the obtained supernatant was concentrated to about 5 mL using a rotary evaporator at 80 °C. The concentrated volume was brought to 25 mL with water. To ensure the best conditions for the IMD analysis, the pH of the solution was controlled by adding Britton–Robinson pH 11.4 buffer. The solution was transferred to the electrochemical cell. The IMD detection in different tissues of the bean plant was performed after extraction on the metallic silver electrode using square wave voltammetry.

5) Chlorophyll measurement

The chlorophyll analysis was done by the determination of chlorophyll-a and chlorophyll-b and total chlorophyll contents, following the method proposed by Arnon 1949 [56]. Fresh leaves (1g) were extracted in 4 mL of 80% (v/v) acetone. The obtained homogenous samples were then centrifuged for 30 min at 1500 g and 4 °C. After centrifugation, the supernatant was

transferred to a cuvette. The absorbance of the supernatant was measured at 645 nm and 663 nm using a UV–Vis spectrophotometer. The contents of Chlorophyll a, b and total chlorophyll were calculated according to Jeffrey and Humphrey method as follow:

$$Chl_a = 12.7 \ OD_{663} - 2.69 \ OD_{645},$$
$$Chl_b = 22.9 \ OD_{645} - 4.68 \ OD_{663},$$
$$Chl_t = Chl_a + Chl_b = 20.22 \ OD_{645} + 8.02 \ OD_{663}.$$

Were Chl_a and Chl_b are the contents of chlorophyll-a and chlorophyll-b respectively, Chl_t is the content of total chlorophyll.

6) Statistical analysis

All the data were analyzed using GraphPad Prism 8 software (GraphPad Software Inc., USA) to generate analysis of variance (ANOVA) and significant differences among treatment means were identified by Tukey's HSD (honest significant difference) test at the significance level of 5%. All values were presented as mean ± SE of three replicate experiments (n=3) of each treatment.

III. Results and discussion

1) Electrochemical behaviour of IMD on MSE

i) Electrocatalytic performance testing

The electrochemical behavior of imidacloprid was investigated in a BR buffer (pH 11.6) using glassy carbon electrode (GCE), carbon paste electrode (CPE) and metallic silver electrode (MSE). The cyclic voltammetric responses (Figure 1) shows the presence of a reduction peak of imidacloprid on the three used electrodes. No oxidation peak was present, indicating that the reaction was irreversible. In addition, a reduction peak shift of imidacloprid to -1130 mV was observed only at silver electrode. This explains the catalytic effect of silver in catalyzing the reduction of the imidacloprid compared to others electrodes. Silver is more easily coordinated with oxygen atoms than with carbon unsaturation. With these systems, they form covalent bonds and demonstrate a significant σ-Lewis acid character. When silver metal complexes coordinate with the π system of unsaturation, they reduce the electron density. This helps to increase the electrophile character of the unsaturation. The systems thus activated become more sensitive and the activation energy of this transformation is decreased [57].
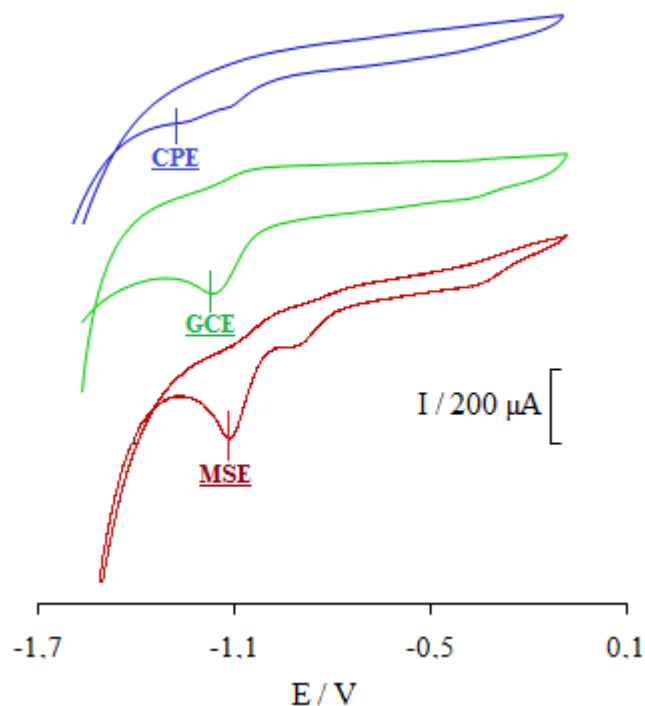
Figure 1: *Cyclic voltammograms of the various electrodes in the potential range 00 to −1600 mV vs Ag/AgCl electrode with a scan rate of 20 mV s-1, 1.0×10−3 mol L−1 of imidacloprid in BR buffer (pH 11.60).*

To evaluate this catalytic effect of silver with respect to the reduction of imidacloprid, a chronoamperometry study is also started under the same conditions. Figure 2 represents the current-time profiles recorded at the three used electrodes, by applying a potential of -1000 mV. This potential is selected from the voltammograms already recorded at MSE, CPE and GCE. As seen, the higher cathodic current of the imidacloprid reduction was reached on metallic silver electrode in comparison with that measured on carbon paste and glassy carbon electrode. As previously reported by cyclic voltammetric measurements, the chronoamperometric results confirm that silver surface exhibited greater catalytic activity to reduction of imidacloprid. Indeed, the performance of the metallic silver electrode towards imidacloprid reduction reached 80 % compared to carbon paste and glassy electrodes.

In addition, the electrochemical impedance spectroscopy was used to evaluate the catalytical properties of metallic silver in catalyzing the reduction of imidacloprid. These measurements are made in a BR buffer (pH 11.6) containing $5.0×10^{-4}$ mol L^{-1} of imidacloprid. The charge transfer resistance of the MSE (7.50 kohm cm^2) is obviously smaller than that obtained with CPE (8.07 kohm cm^2) and GCE (10.70 kohm cm^2), which suggests a faster charge-transfer of metallic silver electrode during the process of the reduction of imidacloprid. The Bode-phase angle plots clearly show that the minimum phase angle was observed at metallic silver electrode

compared with the two others electrodes. From the Bode plot (θ (phase angle) vs log f (frequency)), it is shown that on MSE, relaxation process shifts to different phase angles and at higher frequencies. This result indicates the facility to reduce imidacloprid at silver surface [58].
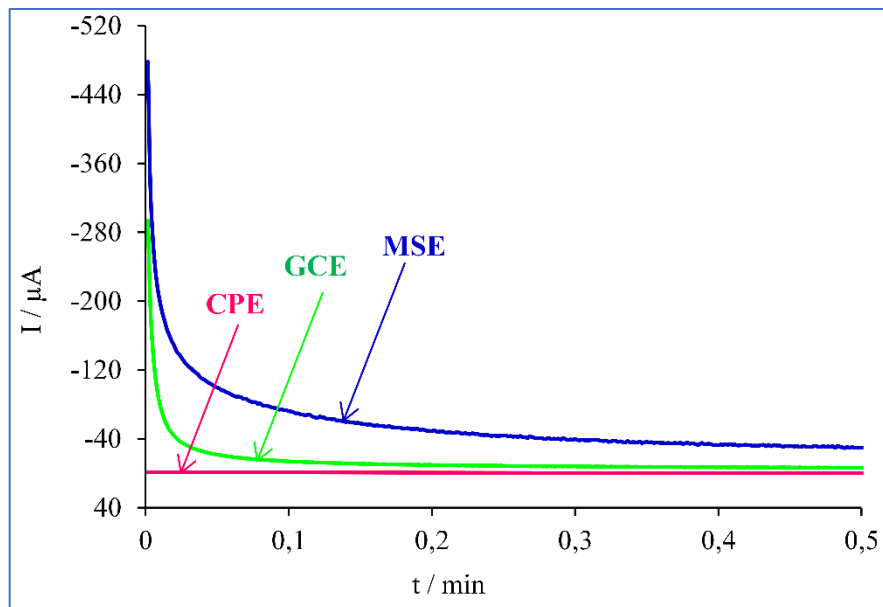
Figure 2: Chronoamperograms obtained of imidacloprid at potential step of −1000 mV, 1.0 ×10−3 mol L−1 of imidacloprid in BR buffer (pH 11.60).

ii) Reduction process of imidacloprid at metallic silver electrode

As we know, the reduction of imidacloprid is based on its nitro group. Generally, the electrochemical reduction of nitro compounds in alkaline media is done through two stages [59]. The electroactive nitro group of the imidacloprid captures four electrons in the first step to give the corresponding hydroxylamine derivative and two electrons in the second reduction step in order to be transformed in the corresponding amine according to the following mechanism:

145
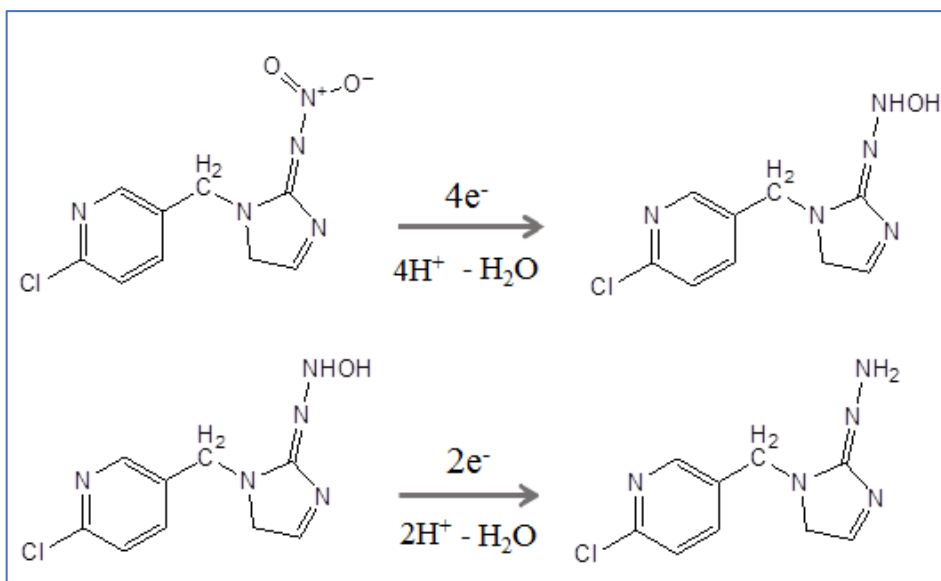
Scheme 2: The stage mechanism for reduction of imidacloprid

In this work, the interaction between imidacloprid and silver surface was recorded using various parameters extracted from cyclic voltammetry and chronoamperommetry techniques.

iii) Cyclic voltammetric study

The influence of pH on the cathodic peak potential of imidacloprid is studied using cyclic voltammetry. Indeed, for pH values below 11 (pKa of imidacloprid), we observe a linear variation of imidacloprid reduction potential as a function of the pH according to the equation: E_{pc} = -0.0388 pH – 0.7698, with a coefficient of determination of R^2 = -0.9364. While for pH higher than 11, the peak potential remains constant. This result indicates that the reduction of imidacloprid undergoes an equal number of electron and proton transfer process. The results show that the intensity of the cathodic current of imidacloprid increases linearly as a function of the pH, where it reaches the maximum in BR buffer (pH 11.60).

The effect of the scan rate on the cathodic peak current and potential of the reduction of imidacloprid was investigated at MSE in the range from 20 to 600 mV s^{-1} (Figure 3a). The cathodic peak potentials, as well as the corresponding peak currents, vary with the scan rate. Almost a linear variation of peak currents with scan rates is observed suggesting that the reduction process is adsorption controlled. The non-zero intercept can be also explained by non-neglected diffusion process after adsorption to the electrode surface. In addition, figure 3b depict Log sweep rate (Logυ) versus the Log of cathodic peak current (Log I_{pc}) curves for the reduction of imidacloprid, where i_p being the peak current expressed in µA and υ being the potential sweep rate in V s^{-1}. From the slope (0.4026) found is lower nearly to the theoretically obtained value of 1.0. Therefore, the reduction of imidacloprid is controlled also by diffusion

[60, 61]. This study indicates that the electro-catalytic behavior of imidacloprid at metallic silver electrode was controlled by the charge transfer kinetics.
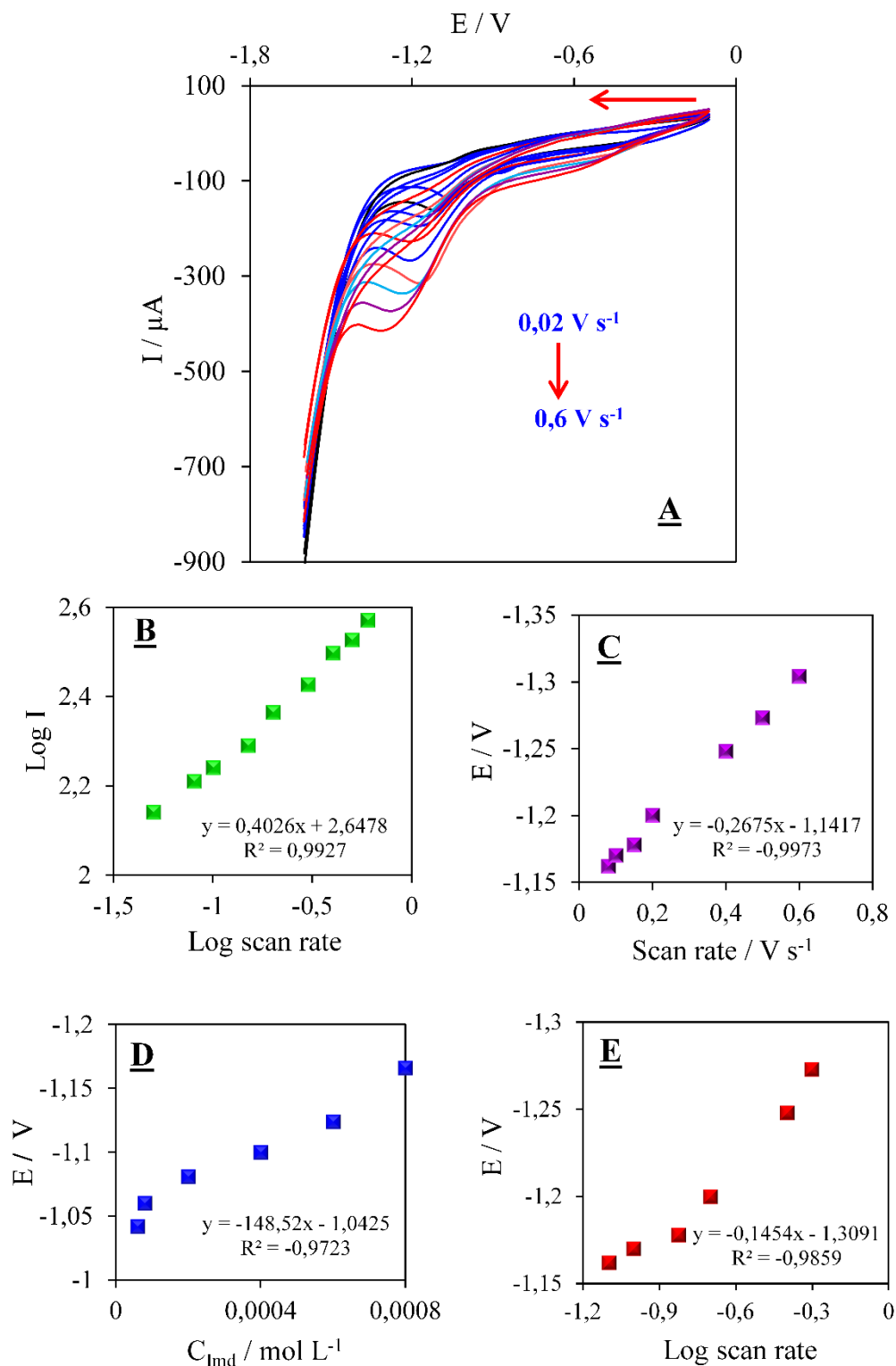
Figure 3: *Electrocatalytic reduction of 1.0×10−3 mol L−1 imidacloprid in BR buffer (pH 11.60) at various scan rates using metallic silver electrode. (A) CVs of (MSE) in BR buffer at pH 11.60. Inset: (B) (log Ip) against (log v), (C) Ep (V) versus v (V/s), (D) Ep (V) versus imidacloprid concentration C_{Imd} (mol.L^{-1}) and (E) plot of peak potential (Epc) vs log scan rate (log(v)) for the reduction of imidacloprid.*

147

On the other hand, figure 3c shows the peak potential shifted towards the negative potential with the increase of scan rate according to the following equation (Equation 1): Ep (V) = -1.1417 – 0.2675v, R^2 = -0.997, which confirms the irreversibility of the electrode process [62]. The linear relationship between the peak potentials and the concentrations were found in the range from 4.0×10^{-5} mol L^{-1} to 1.0×10^{-3} mol L^{-1} of imidacloprid (Figure 3d). The slight negative shift in the peak potential with the increase in concentration is due to the imidacloprid adsorption on metallic silver surface [63]. This effect was more pronounced for a higher imidacloprid concentration. In all cases, the difference in the value of |Ep − Ep/2| is much higher than the value required for a reversible process (59/n mV at 373 K) [64], indicating, in the range of the working conditions used in this work, that the imidacloprid reduction is controlled by both diffusion and charge transfer kinetics.

The transfer coefficient (α) and number of electrons transferred in the rate determining step (n) were determined using the Tafel slope (b) was obtained from the plot of peak potential (Epc) vs log scan rate (log υ) using the following equation [65].

$$Ep_c/AgCl = (b/2) \log υ + constant \tag{2}$$

The reduction peak potential of imidacloprid is linearly proportional to log υ with a slope value of -0.1454 V/AgCl as shown in (Figure 3e). Based on equation (2), the calculated Tafel slope value (b) is -0.2908 V. From the slope value (b), the transfer coefficient (α) and a number of electron transferred in the rate determining step (na) are estimated using the equation (3) [66].

$$y = 2.303 \ RT/ \ α \ n_aF \tag{3}$$

where y is Tafel slope (b), α is transfer coefficient, n is number of electrons transferred in the rate determining step and R, T, F are gas constant, temperature, and Faraday constant respectively. A value of -0.2054 for $αn_c$ is calculated using the above equation indicative of the overall four electrons process involved for the imidacloprid reduction and the first electron transfer is the rate determining step.

Under these conditions, the electrochemical process consists of a mixture of diffusion and adsorption-controlled processes, depending on the scan rate [67–70]. In addition, from the slope of the linear plot of Ip versus scan rate υ the surface concentration of the electroactive species (Γ) can be calculated to be about -1.0785×10^{-3} mol cm^{-2} according to the following equation [71].

$$Ip = n^2F^2A\Gamma v/4RT \tag{4}$$

iv) Chronoamperometric study

The catalytic performance of the metal silver electrode, toward the reactivity of imidacloprid, was also studied by chronoamperometry. The kinetics of the imidacloprid reduction was evaluated using the following Galus (Eq. 5) and Cottrell (Eq. 6) equations [72–74]. In Galus equation, $I_{cathodic}$ is the catalytic current of the imidacloprid reduction at metallic silver electrode and I_{blank} is the limited current in the analytical witness.

$$I_{cathodic}/I_{blank} = \pi^{1/2} (k.C.t)^{1/2} \tag{5}$$
$$I = n.F.A.D^{1/2}.C.\pi^{-1/2}.t^{-1/2} \tag{6}$$

The slops of the linear curves of $I_{cathodic}/I_{blank}$ vs. $t^{1/2}$ and I vs. $t^{-1/2}$, obtained from the chronoamperograms for different imidacloprid concentrations recorded at -1000 mV, were employed for the calculation of the kinetics parameters. From Galus equation, the mean value of catalytic rate constant (k) was obtained to be approximately 5.9×10^3 mol L^{-1} s^{-1}. By the Cottrell equation, the diffusion coefficient was obtained about 7.2×10^{-6} cm^2 s^{-1} for the diffusion of imidacloprid on metallic silver electrode.

2) Effect on seeds germination

The effect of the IMD concentration on the germination rate of *Phaseolus vulgaris* seeds was studied. The control shows a very high germination rate with a value of 95%. In the treated samples, the results clearly show that the germination rate is inversely proportional to the concentration of pesticide in the medium (Figure. 4A). Consequently, the concentrations 0.5×10^{-2}, 3.4×10^{-2} and 5.0×10^{-2} mol L^{-1} significantly induced a reduction of this rate to 35.00 %, 36.66 % and 66.66 % respectively. In addition, the seed vigour index was also affected (Figure 4B), with a decrease of 52.00 %, 55.26 % and 88.53 %, respectively. High concentrations of IMD exerted an inhibitory effect on the germination process. Indeed, the effective concentration (EC50) obtained for a good yield is 7.82×10^{-3} mol L^{-1}. This result can be explained on the one hand by the increasing sensitivity - decreasing tolerance of Phaseolus vulgaris to toxic chemical compounds [75]. On the other hand, the systemic nature of IMD and its bioaccumulation in tissues.
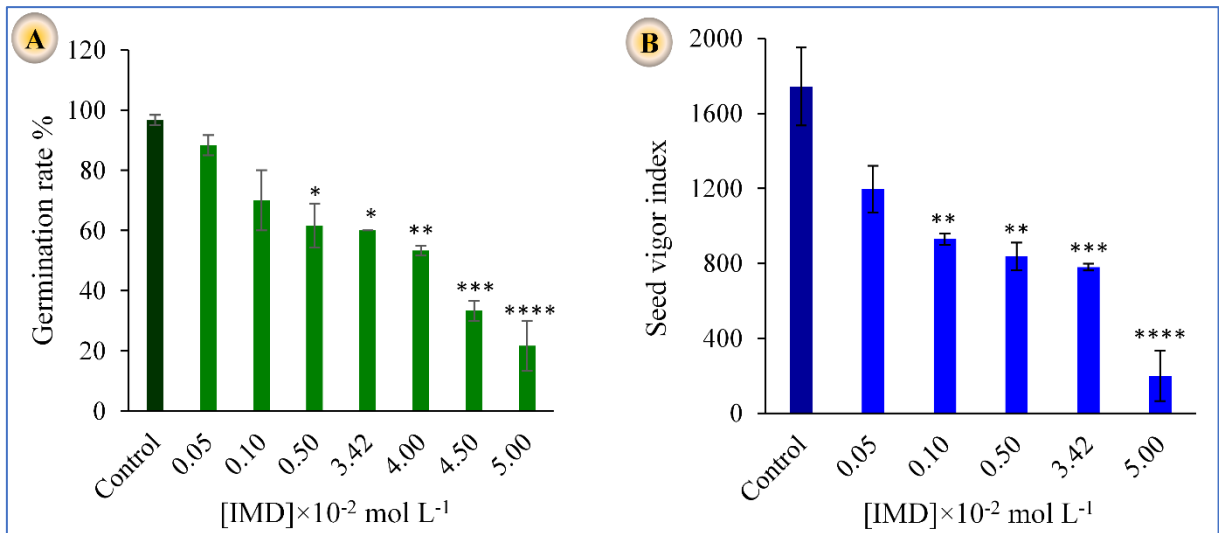
Figure 4: Toxic effect of imidacloprid on seeds germination of Phaseolus vilgarus, (A) indicate the germination rate, (B) represents the seedling vigor index. (*) indicate significant difference (p ≤ 0.05) as compared to the control.

Our results are in agreement with previous studies that have reported that imidacloprid insecticide adversely affects the germination and early growth of various cultures, for example, sweet corn [76], leek [77], and white cabbage [78]. Recently, Fioresi. V. S. et *al.* reported that the high dose of imidacloprid significantly reduced ($p \leq 0.01$) the seed germination and root growth of onion [79]. On the other hand, Neonicotinoids, such as imidacloprid, have an electronegative pharmacophore (N-nitroimine substituent $=NNO_2$), located in their nitroguanidine moiety. therefore, many studies considered imidacloprid as clastogen [80–83] and its genotoxic action has been principally ascribed to the induction of chromosomal adhesion and micronuclei. In addition, the IMD effects may also vary from one plant species to another.

3) Effect on plant morphology

At the end of the treatment, the highest IMD concentrations 0.1×10^{-2}, 0.5×10^{-2}, 3.4×10^{-2} and 5.0×10^{-2} mol L^{-1} significantly ($p \leq 0.05$) affected all the biometric parameters of the plant, namely; seedling length, number of leaves and number of nodes (Figure 5). Therefore, the results obtained proved that there is a significant inhibition of the growth and development of the bean plant. this negative effect could be explained by the reduction in the capacity of the plant to exploit the medium and obtain the nutrients necessary for normal growth, which led to various symptoms of phytotoxicity, such as the inhibition of the apical growth of the plant (Figure 5C), followed by a drop in biometric parameters, in particular in the highest concentrations, due to the reduced availability of iron, magnesium, potassium and sodium under

IMD toxicity [84]. Similar results were obtained by Sharma et al. studying the insecticide IMD against the plant *Brassica juncea L.* [85].

Our results are also consistent with all the studies cited and reported in the literature, suggesting the toxicity of IMD accumulation residues at higher doses for plant species, taking into account the situation of non-target organisms. Similar behaviour of pesticide application reported by many studies on the physiology and yield of other agricultural plants, such as tomato treated with abamectin and cartap [86], *Picea sitchensis* exposed to dimethoate, malathion and with primicarb [87]. In addition, higher doses of various pesticides inhibited the overall growth of different plant species, such as zea maize [88–90], soybeans [91], tomatoes [92] and chickpeas [93].
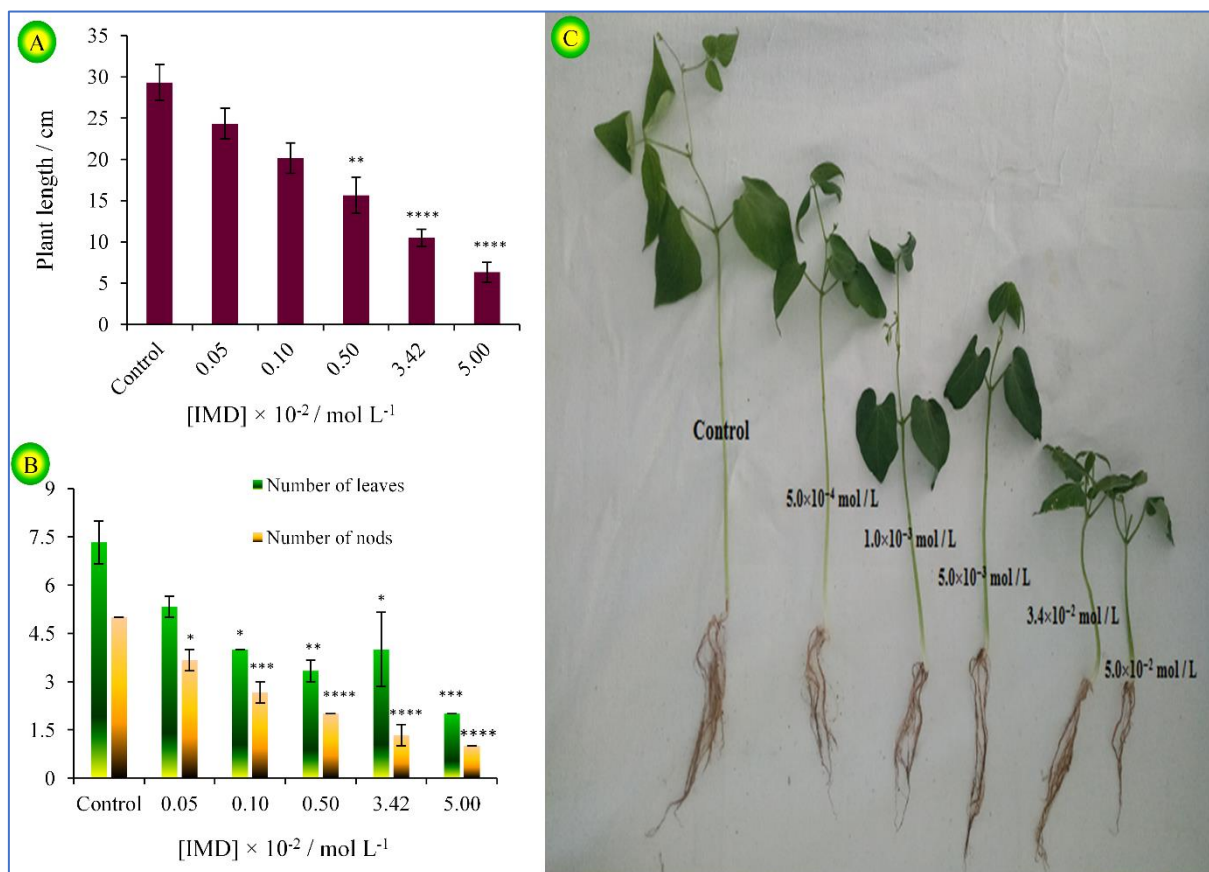

Figure 5: Morphological measurements of plants exposed to different doses of IMD. (A) plant length and (B) number of leaves. Asterisk (*) indicates significant difference *p ≤ 0.03, ** p ≤ 0.002 *** p ≤ 0.0002 **** p ≤ 0.0001 as compared to the control.

4) Effect on plant physiology

The content of photosynthetic pigments (chlorophyll) plays a crucial role in the production of organic molecules such as proteins and carbohydrates and promoting growth through the natural photosynthesis process [94, 95].

The effect of imidacloprid on total chlorophyll was examined in leaves of *Phaseolus vulgaris L.* seedlings (Table 2). A constant decrease in photosynthetic pigments was observed with increasing insecticide dose (especially Chl_a). The weakest answer in terms of Chl_a was observed at 5.0×10^{-2} mol L^{-1} of IMD, while the contents of Chl_b and total chlorophyll show similar paterns to that of Chl_a. In fact, at a high dose of IMD, Chl_a, Chl_b and total chlorophyll were reduced to percentages of 95.26 %, 80.44 % and 82.15 %, respectively, relative to the control.

The effect of imidacloprid on total chlorophyll was examined in leaves of *Phaseolus vulgaris L.* seedlings (Table 2). A constant decrease in photosynthetic pigments was observed with increasing insecticide dose (especially chl_a). The weakest answer in terms of Chl_a was observed at 5.0×10^{-2} mol L^{-1} of IMD, while the contents of Chl_b and total chlorophyll show values similar to that of Chl_t. This decline in chlorophyll under imidacloprid stress could be due to the increased enzyme chlorophyllase activity which resulted in chlorophyll degradation associated whit a disruption of chloroplast structure [96–98]. In subsequent studies, it has been shown that chemicals, in general, such as pesticides negatively affect metabolic enzymes involved in the formation of photosynthetic pigments [99].

Table 2: Concentration of chlorophyll a, b and total chlorophyll in Phaseolus vilgarus leaves after exposure to different doses of IMD. Each value is the mean of three replications ± standard error.

Concentration ($\times 10^{-2}$ mol L^{-1})	Chlorophyll a ± SE (n=3)	Chlorophyll b ± SE (n=3)	Total chlorophyll ± SE (n=3)
Control	0.0422 ± 0.0117	0.0312 ± 0.0085	0.0734 ± 0.0202
0.05	0.0193 ± 0.0036	0.0146 ± 0.0015	0.0339 ± 0.0088
0.10	0.0198 ± 0.00003	0.0072 ± 0.0006	0.0270 ± 0.0006
0.50	0.0071 ± 0.0003	0.0077 ± 0.0011	0.0149 ± 0.0032
3.42	0.0085 ± 0.0039	0.0061 ± 0.0052	0.0146 ± 0.0013
5.00	0.0020 ± 0.0002	0.011 ± 0.0001	0.0131 ± 0.0003

5) Apoptosis induction

The toxicity of IMD was assessed in the common bean plant *Phaseolus vulgaris L*, by epidermal infiltration of the insecticide into the leaves. Image software J was used to visualize the

hypersensitive response (HR). The results obtained show that from the second day of infiltration (2 dpi), the IMD treatment induced necrotic lesions on the leaves which increase in size as a function of time and concentration, it is the phenomenon of programmed cell death (PCD). Control leaves inoculated with distilled water did not show necrosis (Figure 6). 4 days post infiltration (4 dpi), the damaged area (necrotic area) increased to 3.36%, 9.16% and 10.58% of the total leaf area with an infiltrated concentration of 0.5×10^{-2}, 3.4×10^{-2} and 5.0×10^{-2} mol L^{-1} respectively, while the rest of the leaf is unaffected. PCD is a process whose activity is genetically controlled and in which cells that have become unnecessary are specifically eliminated from the body. It is essential for maintaining homeostasis and occurs naturally in all multicellular organisms, during embryogenesis, development and in response to biotic or abiotic stresses, thus making it possible to eliminate infected cells or damaged. This so-called hypersensitive cell death thus leads to rapid and localized death of the cells surrounding the site of infection by an avirulent pathogen [100]. The hypersensitive response is usually accompanied by the generation of oxidizing agents and the activation of plant defence responses.

The macroscopic changes related to hypersensitive cell death were most pronounced in fully developed leaves, leading to the interconnection between plant development and defence [101]. Recent advances in plant immunity research have led to a better understanding of the involvement of plant growth regulators such as ABA, auxins, gibberellins, cytokinin and brassinosteroids. These plant regulators coordinate agonistic and antagonistic links between defence and development pathways [102, 103].

Concentration (Mol L^{-1})	Control	0.5×10^{-2}	3.4×10^{-2}	5.0×10^{-2}
Two days post infiltration				
Damage area (cm^2)	0.009	0.085	0.741	0.498
Tree days post infiltration				
Damage area (cm^2)	0.01	0.11	0.83	0.53
Four days post infiltration				
Damage area (cm^2)	0.01	0.191	1.33	0.86

Figure 6: Induction of necrosis and cell death in Phaseolus vulgaris leaves at different doses of imidacloprid, infiltration observed under bright field at two days post infiltration (dpi), 3 dpi and 4 dpi.

6) Uptake and Translocation of imidacloprid in plant tissues

The detection and the quantification of IMD bioaccumulated by the common bean *Phaseolus vilgarus L.* were carried out by electrochemical method. The calibration curves were presented in figure 7. The current intensity increases linearly with the increase of the IMD bioaccumulated in the different plant tissues the common bean *Phaseolus vilgarus L.* The analytical and calibration parameters are presented in table 3.
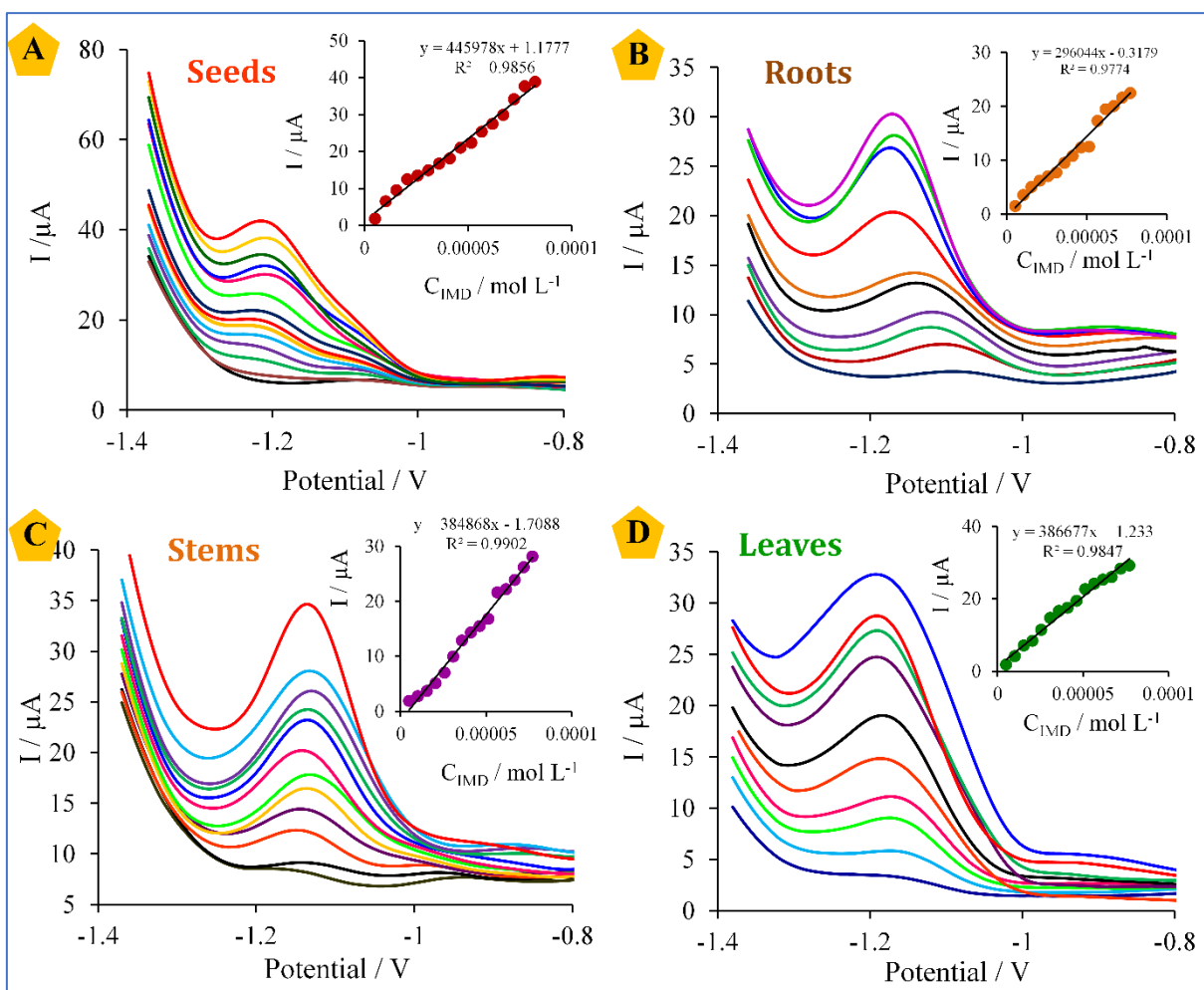
Figure 7: *(A-D) The calibration curves of the IMD in vegetable tissues (seeds, roots, stem, and leaves) of common bean plant.*

The analysis consists in applying a square wave voltammetry with a metallic silver electrode. The mean recovery (n = 3) for five different concentrations of plant samples spiked with IMD is obtained from various plant tissues (Table 4). The results revealed that IMD is detected in the roots, stem and leaves. This shows that the insecticide can be absorbed from the soil and transferred to the aerial parts of the treated plant via a translocation process. The concentrations detected in the plant are proportional to the concentrations of the treatment.

Table 3: Calibration and analytical parameters for various concentration of IMD in vegetable tissues (seeds, roots, stem, and leaves) of common bean plant.

	Calibration parameters			Analytical parameters		
	Slope ($L.\mu mol^{-1}$)	Intercept	R^2	Limit of detection ($\mu mol. L^{-1}$)	Linear range ($\mu mol\ L^{-1}$)	RSD (%)
Seeds	1.1777	445978	0.985	1.62	5.00 to 500	2
Roots	-0.2939	299543	0.986	3.76	5.00 to 500	3.38
stems	-1.7088	384868	0.990	1.68	5.00 to 500	4.56
leaves	1.233	386677	0.984	1.27	5.00 to 500	3.17

However, they vary depending on the organs and tissues. Indeed, the translocation factor (TF) was applied to accurately compare the ability of the plant to transfer pesticide to parts of the plant [104]. It is calculated as follows [105]:

$$TF_{stems} = C_{stems} / C_{roots} \quad \text{and} \quad TF_{leaves} = C_{leaves} / C_{roots}.$$

Figure 8 presents the translocation factor (TF) variation with IMD's concentration applied to bean plant samples. The TF of the stems were larger than one (>1) for low doses of IMD, demonstrating the high capability of the bean to translocate IMD from roots to stems. In contrast, for the applied dose of 5.00×10^{-3} mol L^{-1}, a decrease in the (TF_{stems}) (<1) with increasing IMD concentration was observed (from 0.81 to 0.53), indicating the poor translocation ability of the high concentration of the IMD from roots to stems (Figure 8A). At low applied concentrations (Figure 8B), the translocation of IMD from roots to leaves (TF_{leaves}) is similar to the translocate IMD from roots to stems.

Generally, the pesticide uptake, accumulation and translocation behaviour in vegetables are related to their physicochemical characteristics [106]. IMD ($logK_{ow} = 0.57$ and water solubility of 0.61 g L^{-1}) is absorbed by plant roots and significantly accumulated into the shoots system then translocated acropetally via the xylem sap [15], starting by its absorption through the root hair from the soil with the water uptake system, to be next passed via the cortex, the root epidermis and endodermis to the root xylem [107].
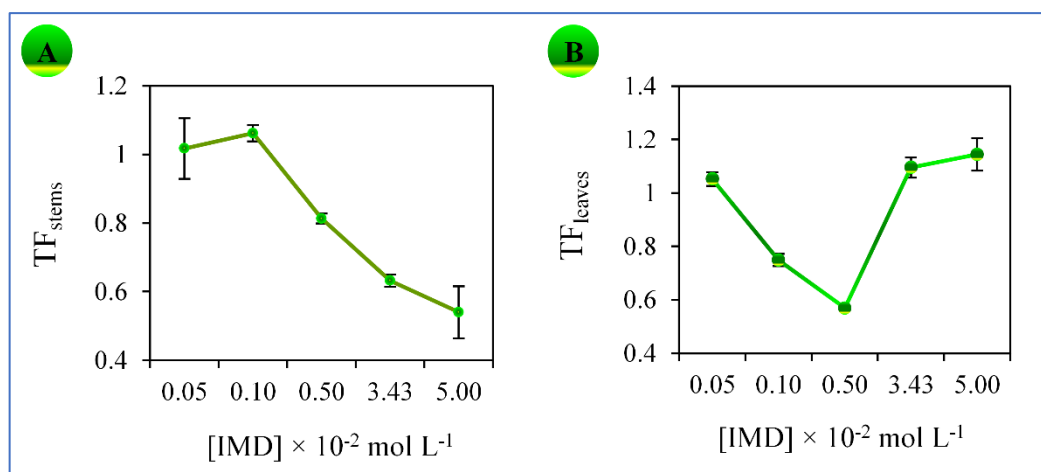
Figure 8: Translocation of IMD in Phaseolus vulgaris plant expressed by translocation factor (TF). (A) TFstems and (B) TFleaves.

Table 4: IMD insecticide content in vegetable tissues (seeds, roots, stem, and leaves) of phaseolus vilgarus after exposed to various concentrations (0.05–5.00) ×10−2 mol L−1.

Concentration ($\times 10^{-2}$ mol L^{-1})	Imidacloprid concentration in vegetable tissues $\pm$ SE ($\times 10^{-2} \pm \times 10^{-4}$ mol L^{-1}) (n=3)			
	seeds	roots	stems	leaves
0.05	0.0017±0.006	0.0011±0.004	0.0011±0.003	0.0011±0.005
0.10	0.0019±0.005	0.0018±0.002	0.0018±0.003	0.0013±0.002
0.50	0.0021±0.015	0.0029±0.001	0.0023±0.001	0.0016±0.001
3.40	0.0028±0.010	0.0045±0.010	0.0028±0.004	0.0049±0.015
5.00	0.0044±0.005	0.0054±0.190	0.0029±0.006	0.0061±0.008

The IMD uptake results and translocation pattern obtained in this research is consistent with that of maize [15], cabbage [108], rice [31] and other compounds of neonicotinoid insecticides (thiamethoxam in zea maize and rice) [15, 31, 87]. According to our results, we can suggest that the bioaccumulation of pesticides by plants could have a negative effect both on the quality of agricultural products and on the health of consumers following their consumption.

IV. Conclusion

The metallic silver electrode was used as a sensing electrode for the determination of imidacloprid. The chosen sensor demonstrates good electro-catalytic activity towards the imidacloprid reduction. The reduction potential of the selected neonicotinoid insecticide is lower on metallic silver electrode compared to

the glassy carbon electrode (GCE) and carbon paste electrode (CPE). Cyclic voltammetry (CV), chronoamperometry, electrochemical impedance spectroscopy techniques were used for study some kinetic parameters of the process. The fundamental electrochemical parameters including the electroactive surface coverage (Γ), the transfer coefficient (α), the catalytic rate constant (k) and the diffusion coefficient (D) have been determined. Moreover, square wave voltammetry was used in detecting imidacloprid at MSE electrode. Under optimum conditions, this electrode presented good linear relationship from 1.0×10^{-5} mol L^{-1} to 1.0×10^{-3} mol L^{-1} of IMD. Meanwhile, detection limit and quantification limit were found to be 6.9×10^{-6} mol L^{-1} and 2.3×10^{-5} mol L^{-1} respectively. The analytical utility of the proposed method was tested in tomato and orange samples with satisfactory results.

Imidacloprid effect on seed germination, growth and photosynthetic pigments in common bean (*Phaseolus vulgaris L.*) was studied. The utilization of imidacloprid with high doses can inhibit bean (*Phaseolus vulgaris L.*) growth, affect pigments synthesis, promote oxidative stress and disrupt antioxidant enzymes for bean development.

However, the length of roots, plant, the number of leaves and nods were reduced significantly at high applied concentration. Furthermore, IMD bioaccumulation and subsequent translocation in bean were investigated. The results show that imidacloprid can be taken up by the plant roots from contaminated soil and subsequently translocated to other vegetable tissues (stems, leaves).

V. References

[1] Myers, J.R. and Kmiecik, K.: Common bean: Economic importance and relevance to biological science research, The common bean genome, Springer, 2017, pp. 1–20.

[2] Campos-Vega, R.; Loarca-Piña, G. and Oomah, B.D.: Minor components of pulses and their potential impact on human health, Food research international, **43** (2010), no. 2, pp. 461–482.

[3] Petry, N.; Boy, E.; Wirth, J.P. and Hurrell, R.F.: The potential of the common bean (Phaseolus vulgaris) as a vehicle for iron biofortification, Nutrients, **7** (2015), no. 2, pp. 1144–1173.

[4] Nakai, J.: Food and Agriculture Organization of the United Nations and the sustainable development goals, Sustainable Development, **22** (2018).

[5] McConnell, M.; Mamidi, S.; Lee, R.; Chikara, S.; Rossi, M.; Papa, R. and McClean, P.: Syntenic relationships among legumes revealed using a gene-based genetic linkage map of common bean (Phaseolus vulgaris L.), Theoretical and Applied Genetics, **121** (2010), no. 6, pp. 1103–1116.

[6] Melo, L.C.; Del Peloso, M.J.; Faria, J. de; Yokoyama, M.; Rosaria, L.; Brondani, R.P.V.; Brondani, C. and Faria, L. de: Controle genético da reação do feijoeiro comum ao vírus do mosaico dourado, Embrapa Arroz e Feijão Santo Antônio de Goiás, 2005.

[7] Abrol, D.P.; Ramamurthy, V.V. and Srivastava, K.: Bean gall weevil and blister beetle as new pests on red kidney bean (Phaseolus vulgaris L.) in India, Journal of Asia-Pacific Entomology, **9** (2006), no. 4, pp. 317–320.

[8] Rabbinge, R. and Van Oijen, M.: Scenario studies for future agriculture and crop protection, European Journal of Plant Pathology, **103** (1997), no. 3, pp. 197–201.

[9] Ko, A.-Y.; Rahman, M.M.; Abd El-Aty, A.M.; Jang, J.; Park, J.-H.; Cho, S.-K. and Shim, J.-H.: Development of a simple extraction and oxidation procedure for the residue analysis of imidacloprid and its metabolites in lettuce using gas chromatography, Food chemistry, **148** (2014), pp. 402–409.

[10] Lashkari, M.R.; Sahragard, A. and Ghadamyari, M.: Sublethal effects of imidacloprid and pymetrozine on population growth parameters of cabbage aphid, Brevicoryne brassicae on rapeseed, Brassica napus L., Insect Science, **14** (2007), no. 3, pp. 207–212.

[11] Smith, S.F. and Krischik, V.A.: Effects of systemic imidacloprid on Coleomegilla maculata (Coleoptera: Coccinellidae), Environmental Entomology, **28** (1999), no. 6, pp. 1189–1195.

[12] Leiva, J.A.; Nkedi-Kizza, P.; Borejsza-Wysocki, W.S.; Bauder, V.S. and Morgan, K.T.: Imidacloprid extraction from citrus leaves and analysis by liquid chromatography–mass spectrometry (HPLC–MS/MS), Bulletin of environmental contamination and toxicology, **96** (2016), no. 5, pp. 671–677.

[13] Sharma, A.; Yuan, H.; Kumar, V.; Ramakrishnan, M.; Kohli, S.K.; Kaur, R.; Thukral, A.K.; Bhardwaj, R. and Zheng, B.: Castasterone attenuates insecticide induced phytotoxicity in mustard, Ecotoxicology and Environmental Safety, **179** (2019), pp. 50–61.

[14] Stevens, M.M.; Reinke, R.F.; Coombes, N.E.; Helliwell, S. and Mo, J.: Influence of imidacloprid seed treatments on rice germination and early seedling growth, Pest Management Science: Formerly Pesticide Science, **64** (2008), no. 3, pp. 215–222.

[15] Bonmatin, J.-M.; Giorio, C.; Girolami, V.; Goulson, D.; Kreutzweiser, D.P.; Krupke, C.; Liess, M.; Long, E.; Marzaro, M.; Mitchell, E.A.D.; Noome, D.A.; Simon-Delso, N. and Tapparo, A.: Environmental fate and exposure; neonicotinoids and fipronil, Environmental Science and Pollution Research, **22** (2015), no. 1, pp. 35–67.

[16] Mukherjee, S.; Tripathi, S.; Mukherjee, A.K.; Bhattacharyya, A. and Chakrabarti, K.: Persistence of the herbicides florasulam and halauxifen-methyl in alluvial and saline alluvial soils, and their effects on microbial indicators of soil quality, European Journal of Soil Biology, **73** (2016), pp. 93–99.

[17] Shahid, M.; Zaidi, A.; Khan, M.; Rizvi, A.; Saif, S. and Ahmed, B.: Recent advances in management strategies of vegetable diseases, Microbial strategies for vegetable production, (2017), pp. 197–226.

[18] Huiyun, P.A.N.; Xiaolu, L.I.; Xiaohua, X.U. and Shixiang, G.A.O.: Phytotoxicity of four herbicides on Ceratophyllum demersum, Vallisneria natans and Elodea nuttallii, Journal of Environmental Sciences, **21** (2009), no. 3, pp. 307–312.

[19] Singh, H.; Singh, N.B.; Singh, A.; Hussain, I. and Yadav, V.: Physiological and biochemical effects of salicylic acid on Pisum sativum exposed to isoproturon, Archives of Agronomy and Soil Science, **62** (2016), no. 10, pp. 1425–1436.

[20] Zaller, J.G.; König, N.; Tiefenbacher, A.; Muraoka, Y.; Querner, P.; Ratzenböck, A.; Bonkowski, M. and Koller, R.: Pesticide seed dressings can affect the activity of various soil organisms and reduce decomposition of plant material, BMC ecology, **16** (2016), no. 1, pp. 1–11.

[21] Byrne, F.J. and Toscano, N.C.: Uptake and persistence of imidacloprid in grapevines treated by chemigation, Crop Protection, **25** (2006), no. 8, pp. 831–834.

[22] Tomizawa, M. and Casida, J.E.: NEONICOTINOID INSECTICIDE TOXICOLOGY: Mechanisms of Selective Action, Annual Review of Pharmacology and Toxicology, **45** (2005), no. 1, pp. 247–268.

[23] Sharma, A.; Yerra, V.G. and Kumar, A.: Emerging role of Hippo signalling in pancreatic biology: YAP re-expression and plausible link to islet cell apoptosis and replication, Biochimie, **133** (2017), pp. 56–65.

[24] Sharma, A.; Kumar, V.; Thukral, A.K. and Bhardwaj, R.: Epibrassinolide-imidacloprid interaction enhances non-enzymatic antioxidants in Brassica juncea L., Indian Journal of Plant Physiology, **21** (2016), no. 1, pp. 70–75.

[25] Sharma, A.; Kumar, V.; Singh, R.; Thukral, A.K. and Bhardwaj, R.: Effect of seed pre-soaking with 24-epibrassinolide on growth and photosynthetic parameters of Brassica juncea L. in imidacloprid soil, Ecotoxicology and Environmental Safety, **133** (2016), pp. 195–201.

[26] Parween, T.; Jan, S.; Mahmooduzzafar, S.; Fatma, T. and Siddiqui, Z.H.: Selective effect of pesticides on plant—A review, Critical reviews in food science and nutrition, **56** (2016), no. 1, pp. 160–179.

[27] Shakir, S.K.; Irfan, S.; Akhtar, B.; Daud, M.K.; Taimur, N. and Azizullah, A.: Pesticide-induced oxidative stress and antioxidant responses in tomato (Solanum lycopersicum) seedlings, Ecotoxicology, **27** (2018), no. 7, pp. 919–935.

[28] Soares, C.; Pereira, R.; Spormann, S. and Fidalgo, F.: Is soil contamination by a glyphosate commercial formulation truly harmless to non-target plants?–Evaluation of oxidative damage and antioxidant responses in tomato, Environmental Pollution, **247** (2019), pp. 256–265.

[29] Soares, C.; Spormann, S. and Fidalgo, F.: Salicylic acid improves the performance of the enzymatic antioxidant system of barley exposed to glyphosate, Free Radical Biology and Medicine, **120** (2018), p. S157.

[30] Ahmed, B.; Shahid, M.; Khan, M.S. and Musarrat, J.: Chromosomal aberrations, cell suppression and oxidative stress generation induced by metal oxide nanoparticles in onion (Allium cepa) bulb, Metallomics, **10** (2018), no. 9, pp. 1315–1327.

[31] Ge, J.; Cui, K.; Yan, H.; Li, Y.; Chai, Y.; Liu, X.; Cheng, J. and Yu, X.: Uptake and translocation of imidacloprid, thiamethoxam and difenoconazole in rice plants, Environmental Pollution, **226** (2017), pp. 479–485.

[32] Sur, R. and Stork, A.: Uptake, translocation and metabolism of imidacloprid in plants, Bulletin of insectology, **56** (2003), pp. 35–40.

[33] Juraske, R.; Castells, F.; Vijay, A.; Muñoz, P. and Antón, A.: Uptake and persistence of pesticides in plants: measurements and model estimates for imidacloprid after foliar and soil application, Journal of hazardous materials, **165** (2009), nos. 1–3, pp. 683–689.

[34] Bonmatin, J.M.; Marchand, P.A.; Charvet, R.; Moineau, I.; Bengsch, E.R. and Colin, M.E.: Quantification of imidacloprid uptake in maize crops, Journal of agricultural and food chemistry, **53** (2005), no. 13, pp. 5336–5341.

[35] Weichel, L. and Nauen, R.: Uptake, translocation and bioavailability of imidacloprid in several hop varieties, Pest Management Science: Formerly Pesticide Science, **60** (2004), no. 5, pp. 440–446.

[36] Baskaran, S.; Kookana, R.S. and Naidu, R.: Determination of the insecticide imidacloprid in water and soil using high-performance liquid chromatography, Journal of Chromatography. A, **787** (1997), nos. 1–2, pp. 271–275.

[37] Di Muccio, A.; Fidente, P.; Barbini, D.A.; Dommarco, R.; Seccia, S. and Morrica, P.: Application of solid-phase extraction and liquid chromatography–mass spectrometry to the determination of neonicotinoid pesticide residues in fruit and vegetables, Journal of Chromatography A, **1108** (2006), no. 1, pp. 1–6.

[38] Liu, H.; Song, J.; Zhang, S.; Qu, L.; Zhao, Y.; Wu, Y. and Liu, H.: Analysis of residues of imidacloprid in tobacco by high-performance liquid chromatography with liquid–liquid partition cleanup, Pest Management Science: formerly Pesticide Science, **61** (2005), no. 5, pp. 511–514.

[39] Obana, H.; Okihashi, M.; Akutsu, K.; Kitagawa, Y. and Hori, S.: Determination of acetamiprid, imidacloprid, and nitenpyram residues in vegetables and fruits by high-performance liquid chromatography with diode-array detection, Journal of agricultural and food chemistry, **50** (2002), no. 16, pp. 4464–4467.

[40] Navalón, A.; González-Casado, A.; El-Khattabi, R.; Vilchez, J.L. and Fernández-Alba, A.R.: Determination of Imidacloprid in Vegetable Samples by Gas Chromatography–Mass Spectrometry, Analyst, **122** (1997), no. 6, pp. 579–581.

[41] Blasco, C.; Font, G. and Picó, Y.: Comparison of microextraction procedures to determine pesticides in oranges by liquid chromatography–mass spectrometry, Journal of Chromatography A, **970** (2002), no. 1, pp. 201–212.

[42] Bonmatin, J.M.; Moineau, I.; Charvet, R.; Fleche, C.; Colin, M.E. and Bengsch, E.R.: A LC/APCI-MS/MS method for analysis of imidacloprid in soils, in plants, and in pollens, Analytical Chemistry, **75** (2003), no. 9, pp. 2027–2033.

[43] Fidente, P.; Seccia, S.; Vanni, F. and Morrica, P.: Analysis of nicotinoid insecticides residues in honey by solid matrix partition clean-up and liquid chromatography–electrospray mass spectrometry, Journal of Chromatography A, **1094** (2005), no. 1, pp. 175–178.

[44] Ghalkhani, M.; Zare, N.; Karimi, F.; Karaman, C.; Alizadeh, M. and Vasseghian, Y.: Recent advances in Ponceau dyes monitoring as food colorant substances by electrochemical sensors and developed procedures for their removal from real samples, Food and Chemical Toxicology, **161** (2022), p. 112830.

[45] Karimi-Maleh, H.; Karimi, F.; Fu, L.; Sanati, A.L.; Alizadeh, M.; Karaman, C. and Orooji, Y.: Cyanazine herbicide monitoring as a hazardous substance by a DNA nanostructure biosensor, Journal of Hazardous Materials, **423** (2022), p. 127058.

[46] Karimi-Maleh, H.; Khataee, A.; Karimi, F.; Baghayeri, M.; Fu, L.; Rouhi, J.; Karaman, C.; Karaman, O. and Boukherroub, R.: A green and sensitive guanine-based DNA biosensor for idarubicin anticancer monitoring in biological samples: A simple and fast strategy for control of health quality in chemotherapy procedure confirmed by docking investigation, Chemosphere, **291** (2022), p. 132928.

[47] Karimi-Maleh, H.; Darabi, R.; Shabani-Nooshabadi, M.; Baghayeri, M.; Karimi, F.; Rouhi, J.; Alizadeh, M.; Karaman, O.; Vasseghian, Y. and Karaman, C.: Determination of D&C Red 33 and Patent Blue V Azo dyes using an impressive electrochemical sensor based on carbon paste electrode modified with ZIF-8/g-C3N4/Co and ionic liquid in mouthwash and toothpaste as real samples, Food and Chemical Toxicology, **162** (2022), p. 112907.

[48] Karimi-Maleh, H.; Beitollahi, H.; Senthil Kumar, P.; Tajik, S.; Mohammadzadeh Jahani, P.; Karimi, F.; Karaman, C.; Vasseghian, Y.; Baghayeri, M.; Rouhi, J.; Show, P.L.; Rajendran, S.; Fu, L. and Zare, N.: Recent advances in carbon nanomaterials-based electrochemical sensors for food azo dyes detection, Food and Chemical Toxicology, **164** (2022), p. 112961.

[49] Akça, A.; Karaman, O. and Karaman, C.: Mechanistic Insights into Catalytic Reduction of N$\less$sub$\greater$2$\less$/sub$\greater$O by CO over Cu-Embedded Graphene: A Density Functional Theory Perspective, ECS Journal of Solid State Science and Technology, **10** (2021), no. 4, p. 041003.

[50] Karaman, C.: Orange Peel Derived-Nitrogen and Sulfur Co-doped Carbon Dots: a Nano-booster for Enhancing ORR Electrocatalytic Performance of 3D Graphene Networks, Electroanalysis, **33** (2021), no. 5, pp. 1356–1369.

[51] Karimi-Maleh, H.; Karaman, C.; Karaman, O.; Karimi, F.; Vasseghian, Y.; Fu, L.; Baghayeri, M.; Rouhi, J.; Senthil Kumar, P.; Show, P.-L.; Rajendran, S.; Sanati, A.L. and Mirabi, A.: Nanochemistry approach for the fabrication of Fe and N co-decorated biomass-derived activated carbon frameworks: a promising oxygen reduction reaction electrocatalyst in neutral media, Journal of Nanostructure in Chemistry, (2022).

[52] Ishibashi, Y.; Koda, Y.; Zheng, S.-H.; Yuasa, T. and Iwaya-Inoue, M.: Regulation of soybean seed germination through ethylene production in response to reactive oxygen species, Annals of Botany, **111** (2013), no. 1, pp. 95–102.

[53] Vanewijk, P.H. and Hoekstra, J.A.: Calculation of the EC50 and Its Confidence Interval When Subtoxic Stimulus Is Present, Ecotoxicology and Environmental Safety, **25** (1993), no. 1, pp. 25–32.

[54] Abdul-Baki, A.A. and Anderson, J.D.: Vigor Determination in Soybean Seed by Multiple Criteria1, Crop Science, **13** (1973), no. 6, p. cropsci1973.0011183X001300060013x.

[55] Claudine, G. da R.; Francis, H.R.F. and Claudia, A.L.C.: Quantification of Thiamethoxam in Rhizomes and Leaves of the *Hedychium coronarium* and Water and Soil by High-Pressure Liquid Chromatography, American Journal of Analytical Chemistry, **2012** (2012).

[56] Arnon, D.I.: COPPER ENZYMES IN ISOLATED CHLOROPLASTS. POLYPHENOLOXIDASE IN BETA VULGARIS, Plant Physiology, **24** (1949), no. 1, pp. 1–15.

[57] Gronnier, C. and Gagosz, F.: Développement de nouvelles réactions catalysées par l'or, l'argent ou le cuivre pour la synthèse de molécules hétérocycliques2013.

[58] Farahi, A.; Bentiss, F.; Jama, C.; El Mhammedi, M.A. and Bakasse, M.: A new approach in modifying ethylene glycol methacrylate phosphate coating formulation by adding sodium montmorillonite to increase corrosion resistance properties, Journal of Alloys and Compounds, **723** (2017), pp. 1032–1038.

[59] Alvarez-Lueje, A.F.; Bastías, M.; Bollo, S.; Núñez-Vergara, L.J. and Squella, J.A.: Electrochemical Behavior and Polarographic Assay of Nitroxynil, Journal of AOAC INTERNATIONAL, **78** (1995), no. 3, pp. 637–641.

[60] Kumar, M.; Swamy, B.E.K.; Chandra, U. and Gebisa, A.W.: Co3O4/CuO composite nanopowder/sodium dodecyl sulphate modified carbon paste electrode based voltammetric sensors for detection of dopamine, International Journal of Nanotechnology, **14** (2017), nos. 9–11, pp. 930–944.

[61] Kumar, M.; Swamy, B.E.K.; Asif, M.H.M. and Viswanath, C.C.: Preparation of alanine and tyrosine functionalized graphene oxide nanoflakes and their modified carbon paste electrodes for the determination of dopamine, Applied Surface Science, **399** (2017), pp. 411–419.

[62] Mafatle, T. and Nyokong, T.: Use of cobalt (II) phthalocyanine to improve the sensitivity and stability of glassy carbon electrodes for the detection of cresols, chlorophenols and phenol, Analytica Chimica Acta, **354** (1997), nos. 1–3, pp. 307–314.

[63] Du, D.; Ye, X.; Zhang, J. and liu, D.: Cathodic electrochemical analysis of methyl parathion at bismuth-film-modified glassy carbon electrode, Electrochimica Acta, **53** (2008), no. 13, pp. 4478–4484.

[64] Bard, A.J. and Faulkner, L.R.: Electrochemical methods: fundamentals and applications, 2nd ed ed., Wiley, New York, 2001.

[65] Raoof, J.B.; Ojani, R. and Mohammadpour, Z.: Electrocatalytic oxidation and voltammetric determination of hydrazine by 1, 1-ferrocenedicarboxylic acid at glassy carbon electrode, International Journal of Electrochemical Science, **5** (2010), no. 2, pp. 177–88.

[66] Banks, C.E.; Davies, T.J.; Wildgoose, G.G. and Compton, R.G.: Electrocatalysis at graphite and carbon nanotube modified electrodes: edge-plane sites and tube ends are the reactive sites, Chemical Communications, (2005), no. 7, pp. 829–841.

[67] Siswana, M.P.; Ozoemena, K.I. and Nyokong, T.: Electrocatalysis of asulam on cobalt phthalocyanine modified multi-walled carbon nanotubes immobilized on a basal plane pyrolytic graphite electrode, Electrochimica acta, **52** (2006), no. 1, pp. 114–122.

[68] Salimi, A.; Banks, C.E. and Compton, R.G.: Abrasive immobilization of carbon nanotubes on a basal plane pyrolytic graphite electrode: application to the detection of epinephrine, Analyst, **129** (2004), no. 3, pp. 225–228.

[69] Salimi, A.; Miranzadeh, L. and Hallaj, R.: Amperometric and voltammetric detection of hydrazine using glassy carbon electrodes modified with carbon nanotubes and catechol derivatives, Talanta, **75** (2008), no. 1, pp. 147–156.

[70] Ye, J.-S.; Wen, Y.; De Zhang, W.; Cui, H.F.; Xu, G.Q. and Sheu, F.-S.: Electrochemical Biosensing Platforms Using Phthalocyanine-Functionalized Carbon Nanotube Electrode, Electroanalysis, **17** (2005), no. 1, pp. 89–96.

[71] Sharp, M.; Petersson, M. and Edstrom, K.: General expression of the linear potential sweep voltammogram for a surface redox reaction with interactions between the

adsorbed molecules: applications to modified electrodes, J Electroanal Chem, **95** (1979), p. 123.

[72] Barker, G.C.: E. Galus, Fundamentals of Electrochemical Analysis, Ellis Horwood Ltd., Chichester (1976), 520+ xviii pp.,\pounds 23.501977.

[73] Rastakhiz, N.; Beitollahi, H.; Kariminik, A. and Karimi, F.: Voltammetric determination of carbidopa in the presence of uric acid and folic acid using a modified carbon nanotube paste electrode, Journal of Molecular Liquids, **172** (2012), pp. 66–70.

[74] Kavian, S.; Azizi, S.N. and Ghasemi, S.: Electrocatalytic detection of hydrazine on synthesized nanozeolite-supported Ag nanoparticle-modified carbon paste electrode at a negative potential in an alkaline medium, Journal of Molecular Liquids, **218** (2016), pp. 663–669.

[75] Calvelo Pereira, R.; Monterroso, C. and Macías, F.: Phytotoxicity of hexachlorocyclohexane: Effect on germination and early growth of different plant species, Chemosphere, **79** (2010), no. 3, pp. 326–333.

[76] Kuhar, T.P.; Stivers-Young, L.J.; Hoffmann, M.P. and Taylor, A.G.: Control of corn flea beetle and Stewart's wilt in sweet corn with imidacloprid and thiamethoxam seed treatments, Crop Protection, **21** (2002), no. 1, pp. 25–31.

[77] Ester, A.; de Vogel, R. and Bouma, E.: Controlling Thrips tabaci (Lind.) in leek by film-coating seeds with insecticides, Crop Protection, **16** (1997), no. 7, pp. 673–677.

[78] Ester, A.; de Putter, H. and van Bilsen, J.G.P.M.: Filmcoating the seed of cabbage (Brassica oleracea L. convar. Capitata L.) and cauliflower (Brassica oleracea L. var. Botrytis L.) with imidacloprid and spinosad to control insect pests, Crop Protection, **22** (2003), no. 5, pp. 761–768.

[79] Fioresi, V.S.; de Cássia Ribeiro Vieira, B.; de Campos, J.M.S. and da Silva Souza, T.: Cytogenotoxic activity of the pesticides imidacloprid and iprodione on Allium cepa root meristem, Environmental Science and Pollution Research, **27** (2020), no. 22, pp. 28066–28076.

[80] Bianchi, J.; Cabral-de-Mello, D.C. and Marin-Morales, M.A.: Toxicogenetic effects of low concentrations of the pesticides imidacloprid and sulfentrazone individually and in combination in in vitro tests with HepG2 cells and Salmonella typhimurium, Ecotoxicology and Environmental Safety, **120** (2015), pp. 174–183.

[81] Demsia, G.; Vlastos, D.; Goumenou, M. and Matthopoulos, D.P.: Assessment of the genotoxicity of imidacloprid and metalaxyl in cultured human lymphocytes and rat bone-

marrow, Mutation Research/Genetic Toxicology and Environmental Mutagenesis, **634** (2007), no. 1, pp. 32–39.

[82] Iturburu, F.G.; Simoniello, M.F.; Medici, S.; Panzeri, A.M. and Menone, M.L.: Imidacloprid Causes DNA Damage in Fish: Clastogenesis as a Mechanism of Genotoxicity, Bulletin of Environmental Contamination and Toxicology, **100** (2018), no. 6, pp. 760–764.

[83] Karabay, N.U. and Oguz, M.G.: Cytogenetic and genotoxic effects of the insecticides, imidacloprid and methamidophos, Genetics and Molecular Research, (2005), p. 10.

[84] Azzam, S.; Yang, F.; Wu, J.-C.; Geng, J. and Yang, G.-Q.: Imidacloprid-induced transference effect on some elements in rice plants and the brown planthopper Nilaparvata lugens (Hemiptera: Delphacidae), Insect Science, **18** (2011), no. 3, pp. 289–297.

[85] Sharma, A.; Kumar, V.; Yuan, H.; Kanwar, M.K.; Bhardwaj, R.; Thukral, A.K. and Zheng, B.: Jasmonic Acid Seed Treatment Stimulates Insecticide Detoxification in Brassica juncea L., Frontiers in Plant Science, **9** (2018).

[86] Picanço, M.; Leite, G.L.D.; Guedes, R.N.C. and Silva, E.A.: Yield loss in trellised tomato affected by insecticidal sprays and plant spacing, Crop Protection, **17** (1998), no. 5, pp. 447–452.

[87] Straw, N.A.; Fielding, N.J. and Waters, A.: Phytotoxicity of insecticides used to control aphids on Sitka spruce, Picea sitchensis (Bong.) Carr., Crop Protection, **15** (1996), no. 5, pp. 451–459.

[88] Ajermoun, N.; Lahrich, S.; Bouarab, L.; Bakasse, M.; Saqrane, S. and El Mhammedi, M.A.: Physiological effects of thiamethoxam on Zea mays and its electrochemical detection using a silver electrode, Journal of the Science of Food and Agriculture, **100** (2020), no. 5, pp. 2090–2098.

[89] Coskun, Y.; Kilic, S. and Duran, R.E.: THE EFFECTS OF THE INSECTICIDE PYRIPROXYFEN ON GERMINATION, DEVELOPMENT AND GROWTH RESPONSES OF MAIZE SEEDLINGS, Fresenius Environmental Bulletin, **24** (2015), no. 1, p. 8.

[90] Kilic, S.; Duran, R.E. and Coskun, Y.: Morphological and Physiological Responses of Maize (Zea mays L.) Seeds Grown under Increasing Concentrations of Chlorantraniliprole Insecticide, Polish Journal of Environmental Studies, **24** (2015), no. 3, pp. 1069–1075.

[91] Siddiqui, Z.S. and Ahmed, S.: Combined effects of pesticide on growth and nutritive composition of soybean plants, Pakistan Journal of Botany (Pakistan), (2006).

[92] Chahid, K.: Effect of Alpha-Cypremethrin on Morphological Parameters in Tomato Plants (Lycopersiconesculentum Mill.), American Journal of Environmental Protection, **2** (2013), no. 6, p. 149.

[93] Tiyagi, S.A.; Ajaz, S. and Azam, M.F.: Effect of some pesticides on plant growth, root nodulation and chlorophyll content of chickpea, Archives of Agronomy and Soil Science, **50** (2004), no. 6, pp. 529–533.

[94] Guidi, L.; Tattini, M. and Landi, M.: How Does Chloroplast Protect Chlorophyll Against Excessive Light?, IntechOpen, 2017.

[95] Krause, G.H. and Weis, E.: Chlorophyll Fluorescence and Photosynthesis: The Basics, Annual Review of Plant Physiology and Plant Molecular Biology, **42** (1991), no. 1, pp. 313–349.

[96] Harpaz-Saad, S.; Azoulay, T.; Arazi, T.; Ben-Yaakov, E.; Mett, A.; Shiboleth, Y.M.; Hörtensteiner, S.; Gidoni, D.; Gal-On, A.; Goldschmidt, E.E. and Eyal, Y.: Chlorophyllase Is a Rate-Limiting Enzyme in Chlorophyll Catabolism and Is Posttranslationally Regulated, The Plant Cell, **19** (2007), no. 3, pp. 1007–1022.

[97] Kato, M. and Shimizu, S.: Chlorophyll Metabolism in Higher Plants VI. Involvement of Peroxidase in Chlorophyll Degradation, Plant and Cell Physiology, **26** (1985), no. 7, pp. 1291–1301.

[98] Parida, A.; Das, A.B. and Das, P.: NaCl stress causes changes in photosynthetic pigments, proteins, and other metabolic components in the leaves of a true mangrove,Bruguiera parviflora, in hydroponic cultures, Journal of Plant Biology, **45** (2002), no. 1, pp. 28–36.

[99] Sankar, B. and Karthishwaran, K.: Photosynthetic pigment content alterations in Arachis hypogaea L. in relation to varied irrigation levels with growth hormone and triazoles, Journal of Ecobiotechnology, (2016).

[100] Cheng, Y.; Dong, Y.; Yan, H.; Ge, W.; Shen, C.; Guan, J.; Liu, L. and Zhang, Y.: Effects of 1-MCP on chlorophyll degradation pathway-associated genes expression and chloroplast ultrastructure during the peel yellowing of Chinese pear fruits in storage, Food Chemistry, **135** (2012), no. 2, pp. 415–422.

[101] Chung, K.-M.; Igari, K.; Uchida, N. and Tasaka, M.: New perspectives on plant defense responses through modulation of developmental pathways, Molecules and Cells, **26** (2008), no. 2, pp. 107–112.

[102] Bari, R. and Jones, J.D.G.: Role of plant hormones in plant defence responses, Plant Molecular Biology, **69** (2009), no. 4, pp. 473–488.

[103] Vlot, A.C.; Dempsey, D.A. and Klessig, D.F.: Salicylic Acid, a multifaceted hormone to combat disease, Annual Review of Phytopathology, **47** (2009), pp. 177–206.

[104] Wang, S.; Zhang, S.; Huang, H.; Zhao, M. and Lv, J.: Uptake, translocation and metabolism of polybrominated diphenyl ethers (PBDEs) and polychlorinated biphenyls (PCBs) in maize (Zea mays L.), Chemosphere, **85** (2011), no. 3, pp. 379–385.

[105] Ge, J.; Lu, M.; Wang, D.; Zhang, Z.; Liu, X. and Yu, X.: Dissipation and distribution of chlorpyrifos in selected vegetables through foliage and root uptake, Chemosphere, **144** (2016), pp. 201–206.

[106] Agatz, A.; Ashauer, R. and Brown, C.D.: Imidacloprid perturbs feeding of Gammarus pulex at environmentally relevant concentrations, Environmental Toxicology and Chemistry, **33** (2014), no. 3, pp. 648–653.

[107] Tanoue, R.; Sato, Y.; Motoyama, M.; Nakagawa, S.; Shinohara, R. and Nomiyama, K.: Plant uptake of pharmaceutical chemicals detected in recycled organic manure and reclaimed wastewater, Journal of Agricultural and Food Chemistry, **60** (2012), no. 41, pp. 10203–10211.

[108] Buchholz, A. and Nauen, R.: Translocation and translaminar bioavailability of two neonicotinoid insecticides after foliar application to cabbage and cotton, Pest Management Science, **58** (2002), no. 1, pp. 10–16.

GENERAL CONCLUSION

The use of pesticides, with the aim of protecting crops from various threats to alter their nutritional quality but also agricultural yields, makes it necessary to monitor pesticide residue levels in consumer products, plants and the environment in a general way. Thus, due to the low levels of pesticides authorized by the regulations, analytical techniques allowing the determination and quantification of pesticides at very low concentration levels are necessary to study their ecotoxicity.

The work presented in this thesis focuses on two insecticides from the neonicotinoids family: thiamethoxam and imidacloprid. They are widely used in Morocco for the protection of plants and by individuals or companies to fight against insects harmful to human and animal health. However, these products are not released unexpectedly on the market, they are governed by a marketing authorization, resulting from ten years of research in toxicology and ecotoxicology. These researches make it possible to define a maximum dose of use for a product, supposed to guarantee food safety for the consumer, and a lower risk related to their use for the applicator.

The work presented in this thesis has two objectives: The first objective concerns the study of the effect of thiamethoxam and imidacloprid on the growth of *Zea mays* and *Phaseolus vulgaris L.* bean plants, while the second objective is dedicated to the development of electrochemical sensors for the determination and quantification of thiamethoxam and imidacloprid bioaccumulated in *Zea mays* and *Phaseolus vulgaris L.* bean plants and also in waters and foods. The effect of thiamethoxam and imidacloprid on the growth of *Zea mays* and bean *Phaseolus vulgaris L.* plants respectively was operated under laboratory conditions. The study focuses on the effect on germination, stem length and leaf size and colour after exposure to the insecticide. In addition, histological tests were performed to appreciate the abnormalities observed.

The second aim of this work concerns the development of a method for analyzing thiamethoxam and imidacloprid residues in water, food and plants after an extraction step. This purpose was relatively ambitious insofar as it was initially necessary to develop an electrochemical analysis method and to characterize the device at the metrological level for the analysis of the insecticides in question. To do this, electrochemical sensors based on metallic silver have been developed by solid reaction, electrochemical deposition and colloidal methods in the presence of the chitosan. These sensors have the advantage of being able to be miniaturized and therefore of allowing portability which, for such precise detection techniques, is rarely possible.

The present study is devoted to a first step to study the electro-catalytic performance of the silver electrode in reducing thiamethoxam and imidacloprid using cyclic voltammetry, and square wave voltammetry.

In order to improve the analytical and catalytic efficiency of silver, we have thought of minimizing the dimensions of silver by impregnating it on the surface of the graphite electrode. Indeed, the deposition of silver particles was operated by two voices, in particular by dry process and by electrodeposition.

The electrodeposition disperses the silver on the active sites of the graphite in the form of microparticles. Indeed, the heterogeneity of the surface allows the sensor to adsorb more of the insecticides studied and promote their analysis at less negative potential. While the impregnation by the solid way under nitrogen atmosphere forms a heterogeneous surface containing a phase of silver nanocrystallites and another amorphous phase. The sensor obtained is not sufficiently sensitive but it has catalytic properties in terms of the reduction of thiamethoxam and imidacloprid.

Furthermore, we opted for the synthesis of silver nanoparticles stabilized by a chitosan gel in order to better miniaturize the size of silver on the surface of the graphite electrode. The size of the nanoparticles formed is assessed by spectroscopy. The elaborate sensor intervenes doubly; as a catalyst due to the presence of silver nanoparticles and as an amplifier due to the presence of chitosan which promotes the chemisorption of a greater quantity of molecules on the surface of the sensor. This allows to amplify the electrical signal and therefore offers high sensitivity for the determination of thiamethoxam and imidacloprid.

In order to complete this thesis work, it would be necessary to test the method developed on a cereal matrix. These tests will make it possible to validate the overall analytical protocol, or on the contrary, to highlight the need to continue the optimization study. Indeed, the electrochemical sensors have shown their analytical performance after the optimization of the experimental conditions, namely the accumulation time, the pH and the parameters of the square wave voltammetry. These and other conditions together will allow the sensor to achieve the primary objective, namely, to use this method for the analysis of thiamethoxam and imidacloprid residues in waters and foods and also for the study and monitoring of their bioaccumulation in tissues of *Zea* mays and bean *Phaseolus vulgaris L.*